Investigation of Light Inputs into Plant Circadian Clocks

Laura E. Dixon

Doctor of Philosophy

Institute of Molecular Plant Sciences

And

Centre for Systems Biology at Edinburgh

The University of Edinburgh

February 2011

Contents

Acknowledgements

I am forever indebted to my wonderful family. Neil and Kathy, as always, provide a beautiful perspective and endless support and love. Nicola, thanks for the support and paving the way.

To my friends, this adventure would simply not be possible without you. I value and treasure all of your support and kindness over the years – long may it continue! And to the friends I have made during this adventure, well simply you have made it worthwhile.

To the members of the lab thank-you for your time and guidance, I have learnt so many lessons from you all. A few special mentions are required here, I am truly grateful to have had the opportunity to work with and be guided by these people;
John, my Darwin buddy, thanks for looking out for me. Gerben, you are absolutely wonderful, not only as a lab colleague but also, and more importantly, as a friend. Ozgur you are everyone's hero! Sarah, thank-you for your cool, collected approach and kindness. David, thank-you for high-fiving it out, the laughter and listening. Kirsten, ta for travelling with me in Japan- that was great, and your positive mental attitude. Oxana and Treenut, thank-you for demonstrating there is a way through this maze. To Bene and Martin, thank-you for the laughs. This is also extended to many wonderful people from the departments of CSBE and IMPS, thank-you for the smiles and joy.

A PhD is simply not possible without the supervisors; Andrew, thank-you for enabling me to work on such a diversity of topics and for your guidance throughout the PhD. Also, thank-you for providing the opportunity to meet so many wonderful scientists. To Kevin and Chris, many thanks for your support throughout my PhD. Finally to Natasha, what can I say? Simply your perspective and approach to science is an inspiration and I wish that all good things come your way.

Declarations

This thesis composes of original work based on the following published and submitted manuscripts:

- O. Sorokina, A. Kapus, K. Terecskei, **L. E. Dixon**, L. Kozma-Bognar, F. Nagy, A. J. Millar. (2009). A switchable light-input, light-output system modelled and constructed in yeast. Journal of Biological Engineering 3, 15
- J. S. O'Neill*, G. van Ooijen*, **L. E. Dixon**, C. Troein, F. Corellou, F. Bouget, A. B. Reddy, A. J. Millar. (2011). Circadian rhythms persist without transcription in a eukaryote. Nature 469, 554-558
- **L. E. Dixon***, K. Knox*, L. Kozma-Bognar, M. M. Southern, A. Pokhilko, A. J. Millar. (2011). Temporal repression of Core Circadian Genes is Mediated through EARLY FLOWERING 3 in Arabidopsis. Current Biology 21, 120-125
- C. Troein*, F. Corellou*, **L. E. Dixon**, G. Van Ooijen, J. S. O'Neill, F.-Y. Bouget, A. J. Millar. (2011). Multiple light inputs to a simple clock circuit allow complex biological rhythms. Plant Journal, Accepted
- G. van Ooijen*, **L. E. Dixon*,** C. Troein, A. J. Millar (2011). Proteosome function is required to generate a post-translational circadian rhythm. Current Biology, Accepted
- **L. E. Dixon** and A. J. Millar. (2011). A Suite of Blue-Light Photoreceptors for Synthetic Biology Applications. In preparation

* indicates joint first authorships

I hereby declare that this thesis is my own work except where explicitly stated. No part of this thesis has been submitted for a professional qualification or a degree at the University of Edinburgh or any other university.

Laura E. Dixon
February, 2011

Abstract

Circadian clocks are biological signalling networks which have a period of ~24 hours under constant environmental conditions. They have been identified in a wide range of organisms, from cyanobacteria to mammals and through the temporal co-ordination of biological processes are believed to increase individual fitness. The mechanisms which generate these self-sustained rhythms, the pathways of entrainment and the target outputs of the clock are all areas of great interest to circadian biologists.

The plant circadian clock is believed to comprise of interlocking feedback loops of transcription and translation. The morning MYB-transcription factors CIRCADIAN CLOCK ASSOCIATED 1 (CCA1) and LATE ELONGATED HYPOCOTYL (LHY) bind to the promoter of *TIMING OF CAB2 1* (*TOC1*) and repress its expression, as well as their own. As levels of CCA1 and LHY fall, *TOC1* is expressed and activates the expression of its repressors. This is a simplified version of the known clock components and the current model contains this core loop as well as an interlocked morning and evening loop, which also incorporates some post-translational modification (Chapter 1).

Understanding the plant circadian network and its entrainment are the topics of this thesis. The study has focused on two plant species, the land plant *Arabidopsis thaliana* and the picoeukaryotic marine algae *Ostreococcus tauri.* In both of these species light-mediated entrainment of the clock has been investigated (Chapter 8), as well as the core circadian mechanism. In *A. thaliana* the role of a circadian associated gene, EARLY FLOWERING 3 has been a particular focus for investigation, through both experimentation and mathematical models (Chapters 4 and 5). In *O. tauri* the responses to light signals have been tested, as have the circadian responses to pharmacological manipulation (Chapters 6, 7 and 8).

The work presented identifies a role for ELF3 in the repression of circadian genes and also links it with the regulation of protein stability. Likewise, in *O. tauri* the regulation of protein stability is identified to be a key mechanism for sustaining circadian rhythms.

As well as investigating the clock in plants, certain photoreceptors have been characterised in *S. cerevisiae* with the aim of linking them to a synthetic oscillator.

Together the work presented in this thesis provides evidence for the circadian community to aid with the understanding of circadian rhythms in plants, and possibly other organisms.

List of Figures

List of Tables

Chapter 1

Introduction

1.1 What is a circadian oscillator?

A circadian oscillator is a regulatory network which has an innate period under constant environmental conditions, of approximately 24 hours. These oscillations have been observed in a wide range of organisms from cyanobacteria (*Synechococcus elongatus)*, to plants and animals [1]. In plants circadian rhythms were first observed in 1729 through the rhythmic movement of leaves [2]. Subsequent study has added to the list of physiological, behavioural and molecular processes which the clock network directly controls or influences. These include; hypocotyl elongation and growth rates [3, 4], flowering time [5], gene expression [6, 7, 8, 9], protein stability [10, 11], stomatal regulation [12], tropisms [13], cell division [14], defence against pathogens [15], hormone regulation [16, 17, 18, 19, 20] and chromatin stability [21]. The clock is believed to be cell autonomous [22] but its function can be observed at every level of the plant, from whole organism to subcellular (Figure 1.1). Furthermore, the plant clock, like its animal counterparts, shows organ specificity [23]. In mammals the suprachiasmatic nucleus (SCN) in the brain is the central oscillator which entrains peripheral oscillators in other organs [1]. In plants, the leaves may form the driving oscillator that entrains a reduced clock network in dark-grown roots, possibly through photosynthetic output [23].

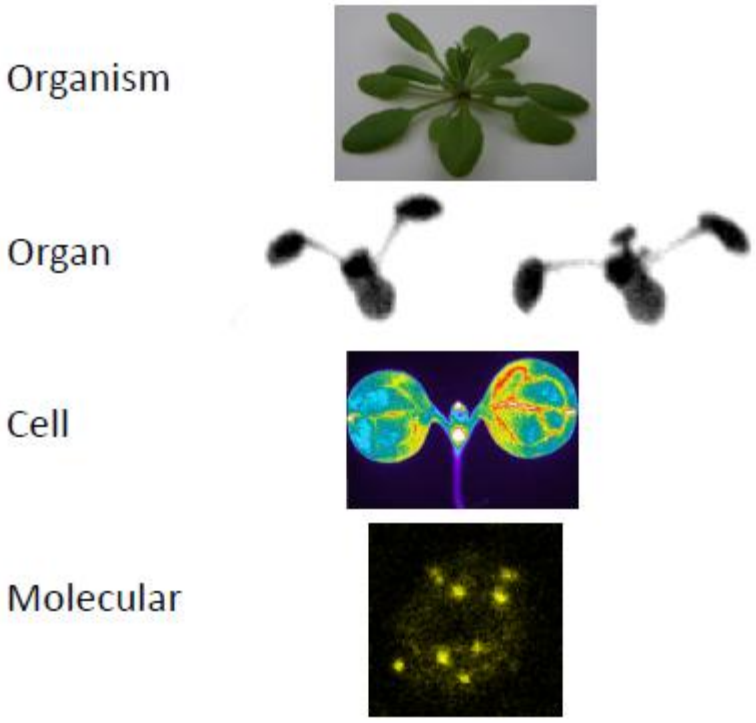

Figure 1.1: Circadian clocks affect all levels of plant physiology
Schematic representing four biological levels which the circadian clock influences of; whole organism (circadian regulation in growth and flowering) [24], organs (leaf movement occurs with an approximately 24 hour rhythmicity), cellular (differential expression patterns (Chapter 5)) and molecular (nuclear speckling of clock component ELF3 tagged with YFP (Chapter 5)).

The circadian oscillator forms part of a signalling network which has environmental signals as inputs and then, as described, a variety of outputs which link certain biological functions to specific phases. However, the pathway is not linear as components can be both inputs and outputs of the clock and therefore feedback to the clocks regulation (Figure 1.2). This is illustrated in plant clocks through the effects of Calcium [25]. Sensing environmental cues and adjusting accordingly is an essential aspect of the clock and is referred to as entrainment [26]. The components of the innate oscillator and the mechanism of entrainment are the topic of this thesis.

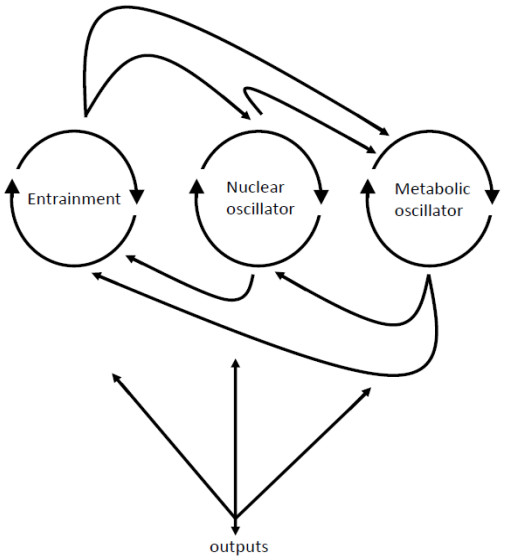

Figure 1.2: Generalised scheme for circadian networks
The multiple levels of signalling feedback in the circadian system are represented through arrows. Entrainment refers to the external entraining signals, including light, temperature and nutrients, as well as the pathways required to link these stimuli to the oscillator mechanism. The oscillator mechanism is depicted as two separate loops of nuclear and metabolic oscillators.

Circadian oscillators have been classified to meet three particular specifications; they must have an innate rhythm, with a period of approximately 24 hours which persists in the absence of environmental stimuli, they must be entrainable to environmental stimuli and they must be temperature compensated across a biological temperature range [27]. Colin Pittendrigh, whose work focused on the study of *Drosophila pseudoobscura*, posed five questions which the wider field of circadian biology has ultimately been trying to answer for over 40 years. These questions were "(1) What is the nature of the driving oscillation? (2) What is the mechanism of entrainment by environmental cycles? (3) How is it coupled to the peripheral subsystems which it drives? (4) What functions does the oscillation serve in the economy of the total system (cell or organism)? (5) Are the circadian oscillations in diverse organisms alike and historically related, or are their similarities the product of evolutionary convergence?" [28] Although a lot of progress has been made, not a single question has been fully answered in, and across, all organisms. A summary of the progress made in answering each of these questions is outlined

below, with a particular focus on the plant circadian clock.

1.1.1 What is the nature of the driving oscillation?

The characterised structure of circadian oscillators, in all organisms studied show a mechanism involving regulatory feedback loops [1]. These loops are based on transcriptional and translational processes with the pace of the oscillator being, at least in part, regulated through post-translational modifications [29]. All of the feedback mechanisms identified have both positive and negative elements (as shown in Figure 1.3). In mammals, Figure 1.3A, the bHLH-PAS transcription factors BMAL1 and CLOCK (which also has histone acetyltransferase (HAT) activity) form heterodimers which positively regulate the expression of their own negative regulators, PERIOD (PER1 and 2) and CRYPTOCHROME (CRY1 and 2). *BMAL1* is also regulated positively by RORA and negatively by Rev-Erbα, which are orphan nuclear receptors. The activity of BMAL1 and CLOCK are central to the mammalian clock as they target a number of output genes [reviewed in 29]. The BMAL/CLOCK heterodimer mediates regulation through modification to the chromatin state, with activation being associated with methylation of histone 3 and repression with histone acetylation [30, 31]. As Figure 1.3A shows phosphorylation is important in the regulation of protein stability. The core network is very similar in *Drosophila melanogaster* with bHLH-PAS transcription factors CLOCK (CLK) and CYCLE (CYC) forming the positive regulating heterodimer which activates the expression of their own repressor PERIOD (PER) and TIMELESS (TIM), (Figure 1.3C) [reviewed in 29]. The stability of both PER and TIM is regulated through phosphorylation [32]. In the fungus, *Neurospora crassa* (Figure 1.3D) a complex between the PAS domain transcription factors WHITE COLLAR 1 and 2 (WC1 and 2) which form an active white collar complex (WCC) activates transcription of FREQUENCY (FRQ) and VIVID (VVD). VVD and WCC form a complex and

WC1 and WC2 expression is repressed ([33] and reviewed in [29]). In plants, Figure 1.3B, TIMING OF CAB2 1 (TOC1) is the positive regulator of the MYB-transcription factors *CIRCADIAN CLOCK ASSOCIATED 1* (*CCA1*) and *LATE ELONGATED HYPOCOTYL* (*LHY*). CCA1 and LHY repress the expression of evening-phased clock genes, including *TOC1* as well as other core clock genes such as *GIGANTEA* (*GI*), *EARLY FLOWERING 3* and *4* (*ELF3* and *4*) and *LUX ARRYTHMO* (*LUX*). *CCA1* and *LHY* expression is also repressed by the PSEUDO RESPONSE REGULATORS 7 and 9 (PRR7 and 9) (reviewed in [26]). The regulation of CCA1's association with DNA is mediated through phosphorylation [10]. The stability of TOC1 is mediated through association with a putative blue-light photoreceptor and F-box protein, ZEITLUPE (ZTL) [11]. Further details of the plant circadian clock are provided in section 1.2.1.

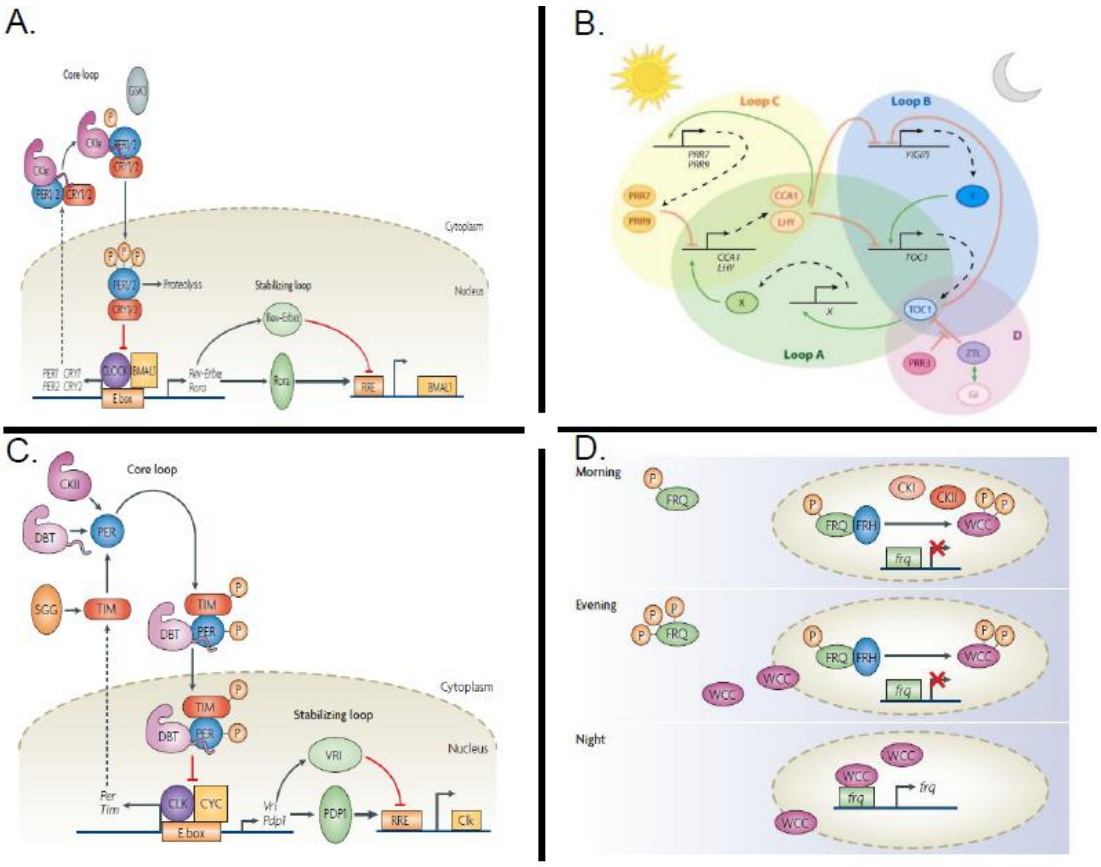

Figure 1.3: Schemes outlining the signalling networks for mammalian, plant, fly and fungi circadian clocks.

A. A simplified mammalian circadian network comprises of CLOCK and BMAL form a heterodimer which activates the transcription of PERIOD (PER1/2) and CRYPTOCHROME (CRY1/2), the proteins of which are phosphorylated by casein kinase Iε (CKIε) and glycogen synthase kinase 3 (GSK3) and go on to repress CLOCK and BMAL function. B. A simplified *Arabidopsis* circadian network comprising of a core loop (Loop A) of CIRCADIAN CLOCK ASSOCIATED 1/ LATE ELONGATED HYPOCOTYL (CCA1/LHY) repression of evening genes, specifically TIMING OF CAB2 EXPRESSION 1 (*TOC1)* and GIGANTEA (*GI)/Y* in the evening loop (LoopB). TOC1 is degraded through its interaction ZEITLUPE (ZTL), an interaction which is antagonised by PSEUDO RESPONSE REGULATOR 3 (PRR3), (Loop D). *CCA1/LHY* expression is repressed through PSEUDO RESPONSE REGULATORS 9 and 7 (PRR9 and 7) in the morning loop (Loop C).C. In a simplified representation of the *Drosophila* clock, CLOCK and CYCLE activate the transcription of PERIOD (PER) and TIMELESS (TIM) which are phosphorylated by shaggy (SGG), double-time (DBT) and casein kinase II (CKII) and go on to repress CLOCK and CYCLE function. D. In a simplified scheme of the *Neurospora* clock network WHITE COLLAR COMPLEX (WCC) activates FREQUENCY (FRQ) transcription. FRQ protein either represses WCC (morning) via binding with RNA helicase (FRH) and casein kinase phosphorylation (CKI and CKII) or stabilises WCC (evening) through hyperphosphorylation of FRQ. Recent evidence has identified an important role for the VIVID protein which is discussed in the text. P, phosphorylation. Schemes A, C and D are taken from [29] and scheme B from [26].

The co-regulation of the components within these transcriptional/translational feedback loops (TTFL's) is sufficient to drive circadian oscillations. This is verified through mutant and over-expresser phenotypes. In both mammals and flies certain mutations in the CLOCK gene, *clock*^{irk} in *Drosophila* and *Clock*$^{\Delta 19/\Delta 19}$ in mice, cause a period lengthening [34, 35] as does a mutation in the DNA-binding domain of WC2 in *Neurospora* [36]. Interestingly, regarding the CLK null mouse the effects of its mutation are tissue specific. In the SCN the CLK mutant is believed to be compensated for by the closely related factor NPAS2; this however, does not occur in the peripheral organs where CLK is required for rhythmicity [37, 38, 39]. In all cases, the mutations affect the DNA binding and transcriptional activity of the proteins and therefore regulation of the TTFL [40]. In *Neurospora* the constitutive expression of FRQ stops the majority of circadian oscillations [41]. In *Arabidopsis* the TTFL captures many of the observed circadian phenotypes. The constitutive expression of *CCA1* causes clock arrhythmia [42] demonstrating the important role CCA1 plays in regulating both morning transcription (through regulation of its own promoter) and evening transcription (through its direct binding to evening-elements) [43]. The *toc1-1* mutant is short period, again linking this gene to the regulation of the oscillator [44]. Furthermore, through the modelling of the TTFL, specifically in *Arabidopsis*, it is clear that TTFL regulation is sufficient to capture a lot of experimental data and through this modelling method even make predictions about what is required, such as an evening Y component to allow regulation on TOC1 and the requirement for a protein which directly binds to the promoter of *CCA1/LHY* to activate expression [45, 46, 47, 48]. Recent work is also incorporating the roles of LUX/ELF3/ELF4 [49] to the clock, which in *Arabidopsis*, are the only two genes (LUX and ELF4) which have mutant arrhythmic phenotypes [50, 51] and therefore must be part of a core clock mechanism. Protein interactions and stability are also important in the TTFL's, with the most recent *Arabidopsis* model including the putative blue-light

photoreceptor ZTL regulating TOC1 stability [48, 11]. In mice mutations in Fbx13, a protein which mediates ubiquitination of other proteins (specifically Cry1 and Cry2) via recruiting them to SCF ubiquitin E3-ligase complex, show a lengthening in circadian period [52].

However, it is also becoming apparent, as more multiple genetic mutations are generated and the molecular tools develop, that a wider array of biochemical mechanisms contributes to circadian regulation. These include kinase and phosphotase activity, histone acetylation and methylation, sumoylation, redox regulation, metabolic inputs and light-dependent protein stability [53 (Appendix A), 54, 55, 56, 57]. In particular, it seems that the post-translational modifications provide a mechanism to add more than just delay into the TTFL's. Further to this it is has been demonstrated that rhythmic transcription of clock associated genes is not required for circadian clocks to maintain rhythmicity. In flies, constitutive over-expression of *CLK* or expression which pushes CLK protein to its antiphase still permits normal clock function [58]. In both mammals and flies constant expression of the *PER* does not affect circadian rhythms [59, 60]. Also, the over-expression of CLK/BMAL [40] or CRY1 [61] does not cause arrhythmia in mouse fibroblasts. In plants, oscillations can still be measured in TOC1 and CCA1/LHY mutants [45, 46, 47]. In *Neurospora* there is a wide array of oscillations measured without FRQ expression [62, 63]. The global inhibition of transcription in mouse fibroblasts only had a very minor effect on the circadian network [64], an observation which was also seen in the picoeukaryotic alga *Ostreococcus tauri* ([53] (Appendix A)). This data supports the now classical observations from the single-celled marina alga *Acetabularia* where circadian rhythmicity continues in enucleated cells [65]. These results suggest that the TTFL can not completely account for cellular circadian rhythmicity as in the TTFL the timing of both gene expression and protein degradation is essential to maintain rhythms. In combination, it highlights that our understanding of the circadian mechanism needs to become more integrated with knowledge of the cellular physiology [63]. This is particularly supported through a set of

experiments in the cyanobacteria *Synechococcus elongatus* where the circadian regulation can be reconstructed in a test-tube with the three central proteins KaiA, KaiB and KaiC and adenosine triphosphate (ATP). KaiC has both autophosphorylation and autodephosphorylation activity with the autophosphorylation being enhanced by KaiA and KaiA's effects inhibited by KaiB. Through assaying KaiC phosphorylation self-sustained, 24 hour, temperature-compensated rhythms were measured [66, 67]. This demonstrated that a three protein system, with ATP, could generate circadian rhythms, without rhythmic input [68].

Therefore, currently the mechanism which creates a circadian rhythm remains unclear in most organisms. The original TTFL's now need to be incorporated and merged with the increasing number of physiological results to form a clock network which is sensitive to the cells and organisms physiology [1].

1.1.2 What is the mechanism of entrainment by environmental cycles?

In most species studied more than one interlocking loop has been identified to form part of the circadian network [1], (Figure 1.3). These multiple loops are thought to exist to enable the oscillator mechanism to be flexible and responsive to entrainment signals [69]. This allows the phase of components within the oscillator to change, or entrain, relative to environmental input. The ability of the oscillator to respond to environmental signals, and regulate when this response occurs (gating), is what makes the oscillator mechanism biologically relevant [70]. Entrainment signals differ slightly between organisms but light and temperature are the dominant ones. Defining the mechanism of entrainment is hampered by its close proximity to the potential central oscillator and because the effects of entrainment often feedback to the entrainment mechanism itself. Therefore, it is technically and conceptually difficult to separate entrainment and many of the clock inputs and outputs from the oscillator mechanism [70]. In fact, it may not

be possible or meaningful to do so in organisms which are largely dependent on light signalling for physiological requirements, most notably plants.

In *A. thaliana* plants bearing single mutations in clock components show light signalling phenotypes, as light and clock responses are very closely linked. Light entrainment to the plant clock is through at least three types of photoreceptor [71, 72, 73, 74] as well as potentially through the photosynthetic chain, as observed in *Synechococcus elongatus* [75]. The photoreceptors are the red/ far-red-light sensing phytochromes (phyA-E) with phyA and phyB playing the predominant role in circadian entrainment [71]. The blue-light sensing cryptochromes (CRY1-3) [76], the role of *A. thaliana* CRY3 has yet to be investigated but it is localised to the mitochondria and chloroplasts, and the blue-light sensing LOV (Light Oxygen Voltage) domain proteins ZTL, FLAVIN-BINDING, KELCH REPEAT, F-BOX 1 (FKF1) and LOV KELCH PROTEIN 2 (LKP2) (notably not the phototropins) [74, 77, 78, 79]. These photoreceptors relay light-signalling to the clock through a variety of methods, from direct interaction to modulating secondary messenger levels. These routes of entrainment will be discussed below.

Members of each of these photoreceptors families have direct interactions with circadian components. PhyB has been shown to have a direct interaction with ELF3 [80] and TOC1 [70], GI has been shown to interact with ZTL [81], FKF1 [82] and PhyA [83], TOC1 and PRR5 also interact with ZTL [11, 84] and finally through COP1 interaction, ELF3 and GI are regulated by the CRYs [85, 86]. Not all of these interactions have been shown to affect the clocks entrainment [83] but the potential remains. The LOV domain proteins, ZTL, LKP2 and FKF1 are believed to function by similar mechanisms and in a redundant fashion [87]. For ZTL, it has been shown that under blue-light the protein is more stable and therefore its light-interactions with other proteins increases their stability [11, 81], whilst the dark interaction enables targeting of the proteins for degradation, as ZTL also contains an F-box domain [88]. These direct

interactions offer an immediate mechanism for entrainment of the circadian clock. Furthermore, the clock regulates the levels of Phytochromes and Cryptochromes as they all exhibit circadian regulation at the transcriptional level [89, 90]. However, only PHYA, PHYB and PHYC have shown oscillations at the protein level in constant conditions [91]. The protein levels of ZTL are believed to be reciprocally regulated through its interaction with clock components [11, 81].

A number of light-signalling intermediates have also been identified to be involved with entrainment. These include the PHYTOCHROME INTERACTING FACTORS (PIF's) which are bHLH transcription factors shown to bind light signalling domains (G-boxes) in gene promoters [92]. Following light perception it is known that PhyB translocates to the nucleus where it can interact with PIFs which are bound to the promoters of light responsive genes [93, 94], including *CCA1* and *LHY*. A number of reports show that photo-activated Phytochromes target PIF's for degradation [95, 96, 97]. Likewise PIF's also regulate the stability of Phytochromes [98]. Through this mutual regulation the proportion of light signalling is relayed to light-responsive promoters, activating expression of *CCA1* [42], *LHY* [94], *PRR9* [47, 99, 100] and *GI* transcripts [45]. This is important for clock entrainment but also light-signalling responses, such as photomorphogenesis [101, 102]. This however, is not the only method of light activation of *CCA1* and *LHY* [103]. Entrainment redundancy to clock is particularly apparent when considering the PIF3 null mutant has no effect on the clock [104]. Other proteins which have been shown to be involved with entrainment include FAR RED ELONGATED HYPOCOTYLS 3 (FHY3) and ELF3 [105, 106]. Beyond this SENSITIVITY TO RED LIGHT REDUCED (SRR1) is also implicated in light signalling to the clock. It is required for full phyB function as the *srr1* mutant has long hypocotyls in red light. SRR1 may actually be very close to the core circadian network as *srr1* has a short period in white light [107]. CONSTITUTIVELY PHOTOMORPHOGENIC 1 (COP1) is also a light-signalling intermediate to the entrainment of

the clock. COP1's interaction with the Cryptochromes, which reciprocally mediate protein stability [86], has been linked with the protein regulation of ELF3 and GI [85] (further discussed in Chapter 5).

The examples above show how light signalling links to transcriptional regulation and protein stability, still there are a number of other points of entry to the clock mechanism. These include translational regulation observed for LHY [108], as well as LHY's light responsive targeted degradation by DET1 [109] and the regulation of CCA1 mRNA stability [110]. Also there is the potential for light regulation to the clock through miRNA's [111]. Other light signalling intermediates such as calcium/calmodulin and cGMP have also been linked with entrainment and clock regulation [112]. Therefore the specific points of entry of light signals to the circadian mechanism are numerous and the phenotype responses from clock mutants to different light fluence rates and wavelengths often very involved, ELF3 and GI in particular show an array of different light-dependent phenotypes [80, 113, 114, 83]. In the current TTFL model [48] not a single component is uninfluenced by light signalling at some point, a feature which has as much to do with the interlocking loops as acute light response.

Mutants in photoreceptors which entrain the circadian clock can be expected to have a long circadian period; this is in accordance with Aschoff's Rule, which links perceived light intensity and clock period. In diurnal organisms higher light intensity causes the clock to run faster, as observed in *A. thaliana* [115]. The phytochrome single and multiple mutants all show long periods, with *phyA phyB phy D* and *phyA phyB phyE* showing longer periods than the *phyA phyB* double mutants, which indicates that both PHYD and E are involved with circadian entrainment, but the effects are largely additive [71, 116]. Entrainment mediated by PHYA and PHYB appears to be over different fluence ranges with PHYA, a light-labile phytochrome, having a stronger mutant phenotype at red-light fluence rates below 5 $\mu E/m^2$, whilst PHYB, a light-stable phytochrome, mutants had a stronger effect above 5 $\mu E/m^2$ [71]. Cryptochrome mutants also

have long period phenotypes, again with the *cry1 cry2* mutant showing a longer period than either of the single mutants [72]. Interestingly the *cry2* mutant alone has only a very small effect on period. Both *cry1* and *cry2* have phenotypes in red light conditions. Under low fluence rates of red and blue light *cry2* shows a small period shortening [72]. In low fluence red-light alone *cry1* shows a period lengthening [71]. Protein-protein interactions have been identified between CRY1/PHYA and CRY2/PHYB [117, 118] which may suggest a mechanism for the mixed light phenotypes. Interestingly, the quadruple mutant of *phyA phyB cry1 cry2* does not have any effect on leaf movement rhythms [119] and the quintet *phyA phyB phyC phyD phyE* mutant can still entrain [120]. This highlights that other entrainment pathways must also be able to set the circadian phase. Like the phytochromes and cryptochromes, *ZTL* mutants also have a long period. *ZTL* over-expression causes arrhythmia, probably through causing a very short period, long hypocotyls in red light and delayed flowering [121, 77]. The over-expression of LKP2 also results in similar phenotypes [78]. The data presented shows that the phytochromes, cryptochromes and LOV domain F-box proteins have a role in entrainment. It also highlights that other factors are involved in the light entrainment of the clock, possibly through the photosynthetic chain and secondary metabolism [122].

Light signals are not the only entrainment cue to circadian clocks; temperature signalling is also important [123]. Interestingly, temperature input to clock has been linked with PSEUDO RESPONSE REGULATORS 7 and 9 (PRR7 and 9), which are also points for light entrainment to the clock [124, 125]. Mammalian oscillators have been shown to also be entrained by feeding times [1]. Nutrients also have a role in plant circadian entrainment [126, 127], with sucrose being involved, with circadian regulation, in the regulation of diurnal gene expression [127]. The role of nutrients is investigated in Chapters 6 and 8.

1.1.3 How is the oscillator coupled to the peripheral oscillator subsystems which it drives?

The plant circadian oscillator, like its animal counterparts, is believed to have an oscillator mechanism in every cell and the oscillator regulation differs at the level of organs. Through split entrainment of leaves on the same plant the existence of a cell autonomous oscillator can be inferred [22]. Single and detached leaf imaging has indicated that there may be some kind of communication between cells but also shows that there is cell type specificity in the plant clock [128]. The imaging work indicated that the rhythms of the vein preceded the rhythms in the blade of a leaf [128]. Further to this it has been observed that *CAB2* promoter activity and $[Ca^{2+}]_{cyt}$ levels run with different, approximately circadian, periods when measured in whole seedlings [129] and two oscillators can be distinguished through differences in temperature sensitivity [130]. This observation may suggest either different tissues have different clocks or that certain cells contain two clocks with slightly different periods. The latter has been observed for *Lingulodinium polyedra* (was *Gonyaulax polyedra*) which has been identified to contain two distinct oscillators within the same cell, both with an approximately circadian period [131, 132]. Work by James *et al* [23] showed that the plant clock differed significantly between shoots and dark-grown roots. In shoots a multiple interlocking loop mechanism existed (Figure 1.3 and section 1.2.1) whereas in the root a single morning loop appeared to function. This single loop regulated a significantly reduced number of transcripts, as observed in dark-grown seedlings [133], but was sufficient to sustain oscillations. Oscillations in the evening components (Figure 1.3 and section 1.2.1) could be observed under diurnal conditions or with the addition of sucrose suggesting that the root clock is entrained via a metabolic signal from the shoots. Furthermore, this entrainment response was disrupted by the photosynthetic inhibitor DCMU which blocks the plastoquinone binding site on photosystem II, suggesting that the role of sucrose and possibly redox is important in entraining the root clock [23]. Such an idea has

parallels with the mechanism of entrainment identified for the *S. elongatus* clock which is not entrained through proteins with a specific photoreceptor function but through the state of the quinone pool, which is controlled through the photosynthetic apparatus [75].

Other work is beginning to show the close link between plant hormones and the clock network [134]. Hormone signals, the levels of which are also closely linked to the metabolic state of the cell, would offer one mechanism for coupling and entrainment of different oscillators between plant cells [135]. Such regulation would also link with circadian regulation of plant-pathogen defence [15].

1.1.4 What functions does the oscillation serve in the economy of the total system (cell or organism)?

Circadian oscillators have been identified in eukaryotes and prokaryotes and seem to form a fundamental part of signalling control for these organisms. In plants the oscillator controls a huge range of biological processes, outlined above, and co-ordination of this innate 24 hour period with the environment has been shown to increase the plants overall fitness [136, 137]. The effects of clock mutations, which can cause either long or short periods of the innate oscillator, can be overcome through growing the plants in the respective long or short period photoperiods [136]. The oscillator mechanism could also enable the temporal separation of incompatible biochemical events along with the most advantageous phasing of biological processes, relative to the environmental signals. This includes DNA replication, hormone production and starch regulation [122]. No allele of an *A. thaliana* clock mutant identified shows a lethal phenotype, this may simply be because lethal and semi-lethal clock mutants are not selected for genetic analysis. However, the known mutations in clock components do seriously affect the biomass of plants. A number of mutations such as *toc1-1* and *ztl* cause dwarf phenotypes, whilst *gi-11* plants have a much greater biomass at flowering. Some of the clock

mutations also affect the flowering regulation in plants, with EARLY FLOWERING 3 (ELF3), EARLY FLOWERING 4 (ELF4) and LUX ARRYTHMO (LUX) being early flowering and GIGANTEA (GI) and PSEUDO RESPONSE REGULATOR (PRR7) being late flowering [138, reviewed in 26]. Such mutations will affect the plants viability, especially if they are diclinous. Furthermore, photosynthesis is under circadian regulation. Rhythms in stomatal conductance, net carbon assimilation and thylakoid membrane assembly have all been recorded [136, 139]. This shows that one of the most important mechanisms in life, carbon fixation and the production of oxygen is under circadian regulation. Therefore, understanding how this regulation is achieved will be very powerful in future developments in agriculture.

As the oscillator affects so many biological processes understanding its basic structure and the mechanism of entrainment may lead to advances in understanding how plants co-ordinate these processes. This understanding could be used in a number of practical applications including the application of disease resistance compounds and the movement of species or varieties between latitudes. Understanding the circadian mechanism is also highly relevant to understanding and ultimately manipulating flowering regulation. The combination of internal and external coincidence already identified to regulate CONSTANS (CO) levels, as well as the differential regulation at the transcriptional and translational level, gives some indication of the complexity of this process [82]. Through temporal regulation the timing of flowering onset could be adjusted, which has significant agricultural implications.

Furthermore, the identification of a possible common aspect to the circadian mechanism [53 (Appendix A) and 140] makes the study of the clock network in plants relevant to understanding the mammalian clock. In particular, a number of genetic and long-term experiments are possible in plants which are not possible in mammals. Therefore insights from plant research will remain directly applicable to the mammalian clock, as has previously been demonstrated through the identification of the Cryptochromes [141].

1.1.5 Are the circadian oscillations in diverse organisms alike and historically related, or are their similarities the product of evolutionary convergence?

Since the first molecular components of circadian oscillators were identified it seemed clear that although the structure of the oscillator, the transcriptional/ translational feedback loops (TTFL's), was conserved the components of the oscillator showed very little conservation between organisms. This suggested that the circadian oscillator was a product of convergent evolution [reviewed in 142 and 143]. In trying to address whether the circadian clock mechanism is a product of convergent evolution the similarities at protein level both within and between taxonomic groups needs to be considered. The three protein clock of *Synechococcus elongatus*, which if it is true to its first form must be the earliest circadian mechanism, is also observed in Archaea [144, 145, 146] but putative *Kai C* genes have not been identified in land plants. This does not mean that the *Kai C* genes do not exist in these species; it could be that the genomic sequence is now very divergent and so is not detected through homology searches but the catalytic or other relevant domains are conserved at the level of protein structure. However, first analysis suggests that the cyanobacterial clock was not inherited by land plants. Some of the kinases and phosphatases involved in circadian regulation are conserved in plants, flies, fungi and mammals ([29], [53] and Appendix A). In particular, Casein Kinase II is involved with clock function, either protein stability or affinity to bind DNA, in mammals, *Drosophila*, *Neurospora* and *Arabidopsis* [29] and the protein phosphatase PP2A is also involved in clock regulation in mammals, *Drosophila* and *Neurospora* [29]. However, the identified canonical clock proteins (section 1.1.1) are not always observed within different species of the same taxonomic group, for example LUX is only found in *A. thaliana* and rice [147]. This may suggest that the core genes being compared are not actually central to the evolved mechanism. The common recruitment of the kinases and phosphatases starts to suggest that there could be a conserved aspect to the clock mechanism. Some components do show some similarity between species such as *tej* [148],

JMJD5 [149] and FIO1 [150] (see section 1.2.1 for details) but these proteins have only been linked to the clock in one species *Arabidopsis* and notably mostly have a biochemical function. It has been observed that the circadian mechanism in plants enhances plant fitness, and therefore would suggest that there should be a relatively strong evolutionary pressure to maintain the clock network. The two genes to form the first identified loop in the *A. thaliana* circadian clock, *CCA1* and *TOC1,* are quite well conserved and have been identified to be functioning in the same manner from the picoeukaryotic alga (*Ostreococcus tauri*, more details section 1.2.2) through to Popular trees [151]. Yet, between different plant species some of the core clock components do not appear to be strongly conserved. *LUX*, *ELF3*, *ELF4* and *ZTL* have only been identified in a few other plant species and often have different circadian phenotypes, in fact *LUX* in rice, lacks a circadian phenotype [151]. Such a level of continual convergent evolution seems incredible, but not impossible. It is possible that the TTFL may be part of the circadian mechanism which was recruited to a more cytosolic or metabolic oscillator network. Therefore, a level of divergence, particularly between the plastic and polyploid genomes of many plant species does not seem so incredible.

Recent work, in *Ostreococcus tauri* (section 1.2.2) has shown that another common aspect to the clock mechanism could be based on redox regulation ([53] (Appendix A)). This is supported through the measurement of peroxiredoxin suphonilation rhythms in mature red blood cells, which are naturally anucleate [140]. The identification of a conserved rhythmic post-translational marker in two eukaryotic lineages, plants and mammals removes some of the focus from a TTFL mechanism to one which incorporates cytosolic and metabolic events [1]. If this common aspect of circadian clocks can be identified it will combine the metabolic and genetic aspects already studied and offer functional insights between clock mechanisms. Of interest to evolutionary biologists would be how the peripheral oscillators were recruited, possibly including TTFL's, as well as gaining more understanding of the early endosymbiotic events.

However, much more work is required to detail the mechanism of this aspect of the oscillator.

1.2 Green circadian networks

1.2.1 Arabidopsis thaliana

Arabidopsis thaliana has been the model research plant species for around 20 years, over this time its genome has been sequenced and a wealth of bioinformatic and experimental tools developed. By virtue of these tools many components involved with the *Arabidopsis* clock have been identified. Most of the components were first identified through either genetic screens for changes in flowering time (such as EARLY FLOWERING 3, (ELF3), LATE ELONGATED HYPOCOTYL (LHY) and EARLY FLOWERING 4 (ELF4) [5]) or through changes in *CAB*::LUC expression, a promoter fragment for the Chlorophyll A and B binding protein which is rhythmically expressed (such as TIMING OF CAB2 EXPRESSION 1(TOC1), ZEITLUPE (ZTL), TIME FOR COFFEE (TIC) and *tej* [9]). TOC1 has homology to the bacterial response regulators but lacks the vital aspartate required for phospho-transfer [44]. CIRCADIAN CLOCK ASSOCIATED 1 (CCA1) is a MYB-related transcription factor which is expressed early in the day and believed to be part of the central clock [42] as is LHY [4]. The REVEILLE (RVE1-8) [26] family members show close homology to CCA1 and LHY with a number of them being involved with clock regulation and linking the clock to hormone pathways [20, 134]. With the anti-phase expression patterns of *CCA1/LHY* and *TOC1*, the low levels of CCA1 in *toc1-1* and high levels of TOC1 in *cca1-11* mutants and the direct binding of CCA1 to the *TOC1* promoter, a minimal clock network was developed [43]. In this single loop, CCA1/LHY represses the expression of *TOC1* and TOC1 indirectly activates the expression of *CCA1/LHY* [43], Figure1.3B. This single TTFL could reproduce oscillations (confirmed through mathematical modelling [45]) and capture the correct phases of the included components. However, it was not

sufficient to capture all of the known phenotypes associated with mutant and over-expresser plants of CCA1 and TOC1. Most notably in a single loop network removal of any of the clock components would result in arrhythmia. This is not observed experimentally with the *lhy-21 cca1-11* and *toc1-1* mutants showing a short period phenotype [152, 44]. More of the experimental phenotypes have been captured through the addition of other components to the network; these include GIGANTEA (GI), ZEITLUPE (ZTL) and the PSEUDO RESPONSE REGULATORS (PRR9, PRR7 and PRR5) as well as two hypothetical components X and Y [45, 46, 47, 48]. More recent work has identified a link to the network for EARLY FLOWERING 3 (ELF3) ([153] Appendix B and Chapter 4), EARLY FLOWERING 4 (ELF4) and LUX ARRHYTHMO (LUX) ([154] and [49]), (Figure 1.4). The most recent modelled version of the network shown in Figure 1.4 [48] can not only capture the correct phase of the clock components and a large number of the mutant phenotypes but understanding is now also being gained regarding light-pulse responses and entrainment to skeleton photoperiods. Therefore, the modelled TTFL are certainly complex enough to allow for most of the clocks behaviour.

Through the experimental characterisation of double and triple mutants, in clock components which show a high level of redundancy, specifically the PSEUDO RESPONSE REGULATORS (PRR's) mechanistic understanding is being gained. The PRR's appear to act as repressors to the clock network [155] and possibly provide timing information through their sequential phosphorylation [156]. *PRR9* is the first to be expressed and therefore protein product phosphorylated, followed by *PRR7, PRR5, PRR3* and finally *PRR1* or *TOC1* [157]. Through a variety of double mutant analysis it is clear that the PRR's are partially redundant but also that they have a non-trivial relationship with light-signalling, flowering control and circadian regulation [138].

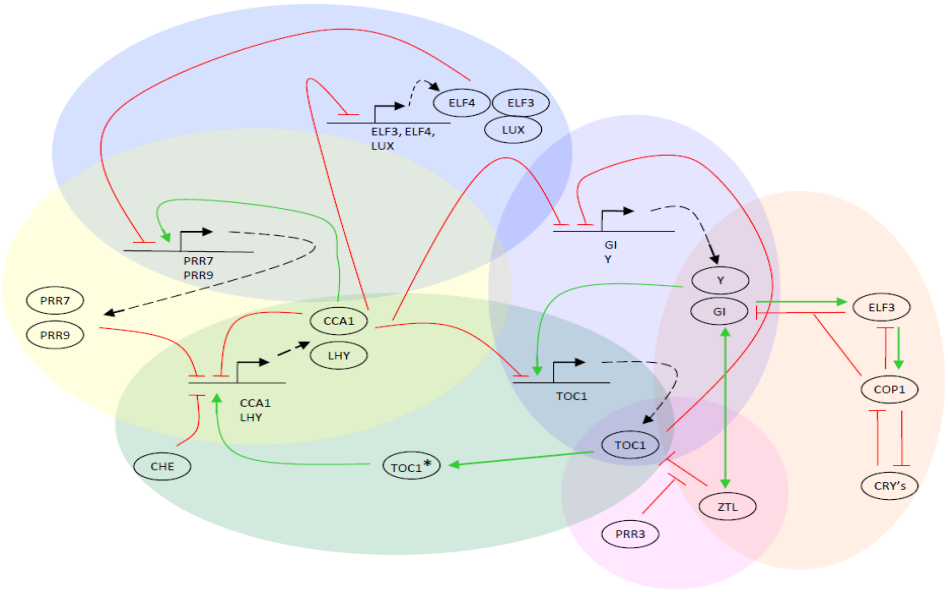

Figure 1.4: A representation of the *Arabidopsis thaliana* circadian clock network
Current experimental evidence shows that part of the *A. thaliana* circadian clock network is formed of transcription, translational and post-translational feedback loops. First identified was the repression by CIRCADIAN CLOCK ASSOCIATED 1 (CCA1) and LATE ELONGATED HYPOCOTYL (LHY) MYB-domain transcription factors of the pseudo response regulator *TIMING OF CAB 1 (TOC1)* and its activation, most probably indirect (represented as a modified form of TOC1 protein, TOC1*) of *CCA1* and *LHY* expression. This interaction is now believed to be antagonised by the TCP-domain transcription factor CCA1 HIKING EXPEDITION (CHE). Subsequently it was identified that CCA1 and LHY were repressing the expression of a number of evening expressed genes, including GIGANTEA (GI), EARLY FLOWERING 3 (ELF3), EARLY FLOWERING 4 (ELF4) and LUX ARRHYTHMO (LUX). In turn GI and another potential clock component (denoted Y [46]) acted to activate *TOC1* expression, forming an evening loop. Additionally, *CCA1* and *LHY* are believed to activate the expression of *PSEUDO RESPONSE REGULATORS 9* and *7* (*PRR9* and *PRR7*) which then function to repress the expression of *CCA1* and *LHY*, forming a morning loop. From work presented in this thesis ([153] and Chapter 4) and through other publications [154, 49] an additional loop involving the formation of an ELF3, ELF4, LUX complex which represses *PRR9* and *PRR7* has been included. Further to this two post-translational regulatory loops have been included. The first is blue-light dependent stabilisation of GI by ZEITLUPE (ZTL) and ZTL dependent degradation of TOC1, which is antagonised by PSEUDO RESPONSE REGULATOR 3 (PRR3). The second post-translational loop (Chapter 5) involved the regulation of protein stability via the dark-activated E3-ligase CONSTITUTIVELY PHOTOMORPHOGENIC 1 (COP1) of ELF3 and GI and the dependence of GI interaction with ELF3 for COP1 interaction [85]. It also includes negative regulation of COP1 by the blue-light photoreceptors CRYPTOCHROME 1 and 2 (CRY1 and CRY2). In this diagram translation is represented through black dashed arrows, activation through solid green arrows and inhibition through solid red arrows. Background colours identify the separate loops identified in the narrative. Light signalling directly or indirectly affects all of the species. Figure in style of [26].

Still a number of genes known to affect circadian function are not linked, at a specific point, to the TTFL clock network. These include the poly(ADP-ribose) glycohydrolase *tej* [148], TIME FOR COFFEE (TIC) [152], PESUDO RESPONSE REGULATOR 3 (PRR3) [158], a DUF890 domain protein with similarity to methyltransferases, FIONA (FIO1) [150], the TCP21 transcription factor, CCA1 HIKING EXPEDITION (CHE) [159], the small GTPase LIGHT INSENSITIVE PERIOD 1 (LIP1) [160] as well as a number of close homologues to circadian components which show redundant phenotypes (FKF1, LKP2) [78, 79]. A number of these genes, *tej*, TIC, FIO1 and LIP1, have links either with metabolism (TIC [152], LIP1 [160] and *tej* [148]) or biochemical processes which are not currently included in the plant clock mechanism (LIP1 and FIO1). As such they provide an indication that further regulation at the metabolic level may be very important in circadian regulation. Furthermore, linking with other observations that histone acetylation and dimethylation at the *CCA1*, *LHY*, *GI* and *TOC1* promoters positively links with expression levels [21, 3], and through drawing parallels with the animal clocks, understanding chromatin modification and regulation will also become more fundamental in deciphering circadian timing.

Further to this the mechanisms of post-transcriptional and post-translational regulation are largely not included, none of the circadian associated kinases and phosphatases are normally depicted in current clock models but this level of regulation is essential for correct clock function. Two kinases have been directly linked with the regulation of the *Arabidopsis* network. Casein kinase II has already been discussed in section 1.1.1. Its specific modification to CCA1 and not LHY is essential to enable CCA1 to bind DNA. The second kinase linked with the clock network is WITH NO LYSINES 1 (WNK1) [161]. WNK kinases are putative Ser/Thr kinases which have similarity to MAPKKKs and the WNK kinases of man and rat [162]. In plants the WNK family contains 9 members, with WNK1, 2, 4 and 6 having circadian regulated transcripts.

WNK1 has been identified to associated with and phosphorylate PRR3 [161]. Of the other WNK kinase family members only WNK4 was shown to also interact with a clock protein, PRR5 [163]. Other members of this kinase family could also be associated with regulation of the clock. Figure 1.4 includes two post-translational loops both relating to proteasome mediated protein degradation. One loop relates to the regulation of TOC1 abundance through its blue-light dependent interaction with ZTL. This interaction is antagonised, in vasculature tissues, through the action of PSEUDO RESPONSE REGULATOR 3 (PRR3) [158]. The second post-translational loop depicted in Figure 1.4 is the blue-light dependent stabilisation of GI through interaction again with ZTL but also ELF3 and the ubiquitin E3-ligase CONSTITUTIVELY PHOTOMORPHOGENIC 1 (COP1) [85]. However, a number of other clock components are also known to be regulated by the proteosome including; LHY [109], CKB4 [20], ZTL [121], GI [164], PRR5 [156], PRR7 [165] and PRR9 [166] and protein degradation is essential for sustained clock function (Chapter 6, detailed in *O. tauri*). Recent studies have added more substance to the existence of a redox-associated oscillator which will also need to be incorporated in to our current understanding [53, 140].

Beyond the structure and mechanism of the central circadian oscillator our understanding of its applications and functions to plant physiology has also undergone dramatic changes in recent years. As a TTFL the clock network was identified to have direct outputs on the regulation of gene expression, such as the *CAB2* gene which was used to identify clock components. More systematic approaches identified that a large proportion of gene expression was under circadian regulation and that the processes being controlled were extremely diverse [7]. Notably, it was not just regulatory components such as transcription factors but also proteins involved in hormone regulation and plant-pathogen defence [167]. Subsequent analysis has identified the number of transcripts which are under circadian control with an enhancer trap analysis with ~36% of transcripts to show rhythmic expression [6], this will also include micro and other non-

coding but regulatory RNAs - the significance of which remains largely unknown [111, 167]. The physiological role of the plant circadian clock has also been studied and shown to increase plant fitness [136, 137], regulate growth [3] and plant defence [15]. Combined with the known regulation of photosynthesis [136] all of the key processes for plant survival are under circadian regulation.

1.2.2 Ostreococcus tauri

The circadian clocks importance for plant survival is becoming increasingly apparent and yet the phenotypes of most of the clock mutants are quite weak, with only ELF3, ELF4 and LUX showing single mutation arrhythmia. This could be due to at least two reasons firstly, other loops of the clock (identified or otherwise) can take the role of the mutant gene or secondly close homologues of the mutant gene can assume their function. Therefore, understanding the circadian network in *Arabidopsis thaliana* is hampered through redundancy. To try and minimise this problem the single-celled alga *Ostreococcus tauri* (*O. tauri*) (Figure 1.5A) has been used in this study (Chapter 6, 7 and 8).

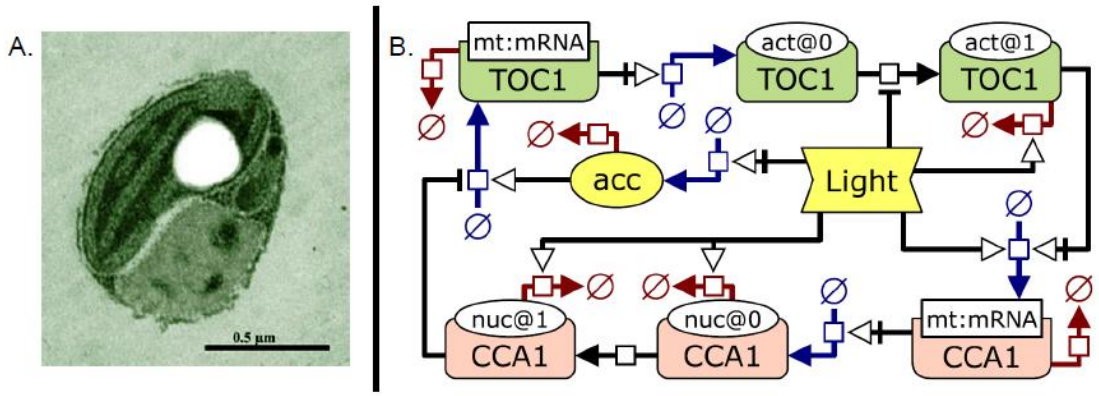

Figure 1.5: Ostreococcus tauri and a representation of its circadian network
Ostreococcus tauri is a picoeukaryotic alga (image from http://genome.jgi-psf.org/Ostta4/Ostta4.home.html) (A) which contains a reduced plant circadian network (B). The network is represented in Systems Biology Graphical Notation (SBGN). TOC1 (green boxes) and CCA1 (pink boxes) are connected through arrows in blue for synthesis, red for degradation and black for conversion or transport. TOC1 exists in two states, with light-regulated conversion from (act@0) to active (act@1). Degradation of TOC1 is light-induced and only acts on the active form. CCA1 protein exists in the cytosol (nuc@0) and the nucleus (nuc@1), and is subject to light-induced degradation at the same rate in both compartments. The light accumulator which regulates *TOC1* transcription links the overall gene expression levels to the amount of light received by the organism (yellow acc) ([168], Appendix C).

O. tauri is the smallest known eukaryote cell and is naturally found in sea-water environments; as such it plays an important role as a primary carbon producer [169]. *O. tauri's* genome was sequenced in 2005 and through comparison with *A. thaliana's* sequence some TTFL clock components have been identified. Notably, all of the clock components found existed in a single copy, removing one of the redundancy issues experienced with *A. thaliana* (Table 1.1). Work by Corellou *et al* established *O. tauri* as another model plant species for the study of the circadian clock through the development of transgenic methods in this alga [170]. In particular transcriptional and translational luciferase tagged lines were developed for the components in the first minimal loop identified in *A. thaliana*, TOC1 and CCA1. In *O. tauri* the interaction between CCA1 and TOC1 appears to be the same as in *A. thaliana* but analysis of this loop suggests that it is not sufficient for the observed oscillations [170]. Mathematical modelling of the network has proposed a mechanism through which this loop could maintain circadian time

[168]. This model requires another protein form (denoted modified TOC1) and 5 light inputs, including a light accumulator function to provide the correct delay between *CCA1* and *TOC1* expression (Figure 1.5B). A second model of the *O. tauri* network has been developed but this focuses on the robustness of oscillations under varying light intensities [171].

Gene Family Members	*Arabidopsis thaliana*	*Ostreococcus tauri*
CRY	3	1
PHY	5	0
PRR/TOC1	5	1
LHY/CCA1	15	1
ELF4	4	0
bHLH TF's	~154	1
ELF3	2	0

Table 1.1: Comparison of numbers of members of gene families between *A. thaliana* and *O. tauri*

The translational lines are particularly powerful to investigate the circadian network as no translational luciferase lines exist for plant clock components, only florescent or tag markers which do not easily allow real-time continual monitoring of protein abundance. Its ease of genetic manipulation and compact genome make *O. tauri* a more appealing organism for study of the fundamentals of circadian biology than the more complex alga *Chlamydomonas reinhardtii*. *C. reinhardtii* has a larger genome, of ~120 Mbp compared to the ~12.5 Mbp of *O. tauri* and is also a larger cell with a ~10 μM diameter versus the tiny ~ 0.8 μM diameter of an *O. tauri* cell [169, 13]. However, currently more is known about *C. reinhardtii*, it has two flagella which enable cell motility and a number of genetic mutants have been characterised. Notably the Channel Rhodopsin proteins (ChR1 and ChR2) are from *C. reinhardtii* (Chapter 3) and ChR2 in particular has proven to be very useful in controlling neuron networks [172]. Furthermore, the similarities *C. reinhardtii* has with both animals and plants will make it a very

useful organism for understanding common aspects of the circadian network [13]. Apart from *C. reinhardtii* studies of circadian rhythms in algae has largely used physiological markers. Most of this work has focused on *Lingulodinium polyedra* which has been identified to contain two distinct oscillators within the same cell, both with an approximately circadian period [131]. This raises the question as to whether the components identified which form the plant circadian oscillator are indeed forming a single oscillator or if they form multiple oscillators which are tissue or biochemically specific.

Through use of the transcriptional and translational markers a comparison can be made, under different photoperiodic conditions, to try and identify the importance of post-translational mechanisms to the circadian clock. This analysis can also enable a comparison between the single-loop *O. tauri* clock and the multi-loop *A. thaliana* clock to add to understanding about flexibility and robustness of the clock structure (Chapter 7). Cell based assays, such as the pharmacological studies used in mammalian cells can be used to start to identify mechanisms for the post-translational and cytosolic aspect of the clock (Table 2, Chapter 6 and 8). Furthermore, the ability to test large numbers of compounds simultaneously offers a quick way to identify possible target mechanisms in circadian regulation. Such an approach was used in [53] and has been continued in Chapters 6 and 8.

Putative *O. tauri* drug target	Accession	Closest H. sapiens homologue	Accession	Sequence Identity (%)	Sequence Similarity (%)	E-value (NCBI Blast, BLOSSUM 62)
DNA topoisomerase II	CAL56339	DNA topoisomerase II	AAA61209.1	54	70	0
HSP90	CAL56087	HSP90	NP_005339.3	67	85	6.00E-170
PP2A	CAL51458.1	PP2A	NP_060931.2	51	62	4.00E-127
CK1	CAL52491	CK1	NP_001884.2	72	82	2.00E-126
GSK3	CAL51449.1	GSK3	NP_001139628.1	60	74	6.00E-125
MAPK	CAL55559	p38 MAPK	NP_620407.1	54	71	6.00E-103
CK2	CAL52182	CK2	CAI18393.2	58	71	1.00E-62
Proteasome beta subunit	CAL50436	Proteasome subunit	NP_002786.2	50	67	8.00E-51
MAP Kinase	CAL55559.1	JNK	NP_620635	54	71	3.00E-17
Adenylyl cyclase	CAL54153	No relevant hits*	-	-	-	-

Table 1.2: Sequence similarity between *O. tauri* and *H. sapiens* for components involved with circadian regulation.
The * regarding Adenylyl cyclase is because *O. tauri* contains two proteins (CAL50189.1 and CAL54153.1) which are annotated as members of the class III nucleotidyl cyclase superfamily but they show very little sequence similarity with mammalian adenylyl cyclases (also class III), further details in [53] and Appendix A.

1.3 Simplification of circadian oscillators

Circadian rhythms were first observed through physiological outputs, such as fly eclosion, plant leaf movement and rodents sleep/wake cycles. These outputs are robust and led to the identification of the circadian rhythm and the formalisation of its properties; that is the rhythm must continue under constant conditions, be entrainable to stimuli and be temperature compensated (within a biological range). With the development of molecular tools the components at a cellular level started to be identified and linked to form the TTFL's which are now common in circadian biology. With the identification of the transcriptional components the importance of their regulation, and not just the circadian regulation of transcription, became apparent. Phosphorylation and small metabolites started to be incorporated into some of the clock models [173, 174, 29] and the complexity of all systems seemed to be continually expanding. However, two different approaches to circadian biology identified that this highly complex multiple interlocking network may not be required for the generation of circadian

rhythms. This does not suggest that TTFL's are not required or important in the systems studied; animal, plant and fungi, just that other mechanisms are possible and quite probably complementary for the generation of circadian rhythms. Firstly the work conducted on *Synechococcus elongatus* identified a 3 protein clock which could, with the addition of ATP, maintain circadian rhythms in phosphorylation in a test tube [66, 67, 68]. This amazing discovery suggested that the TTFL's were not essential for circadian rhythms. Furthermore, work on *S. elongatus* identified that its entrainment via light is indirect, that is the redox state of the photosynthetic quinone pool is sensed [75]. This is distinctly different to the classical photoreceptor pathways which are believed to be involved in the entrainment of the *A. thaliana* circadian clock. This observation could also indicate that the quinone state in plants is likely to be important for the entrainment of the clock. This close link is particularly reasonable when considering the effects of nutrients, specifically carbohydrates on clock networks (Chapter 6 and 8). The second intriguing observation was made in synthetic biology. The development of synthetic oscillators, with a period much shorter than circadian oscillators, has been popular. This is mainly because these networks offer a mechanism to finely control much larger gene networks. A number of different types of oscillator networks were developed, one of which was based on metabolic regulation [175]. The metabolic oscillator showed temperature compensation, a key feature of circadian oscillators but one whose mechanism has remained largely elusive. Two recent publications have made a link between Casein kinase regulation and temperature compensation in plants and fungi [176, 177]. The observation from the synthetic network indicates that the metabolic component of circadian oscillators may be responsible for some of their key properties, specifically temperature compensation, and so have a larger role in the generation of oscillations than first thought.

1.4 Aims and outline of thesis

The work which will be presented in this thesis aims to provide further understanding of the plant circadian clock and its entrainment. To achieve this, a number of different approaches have been employed.

1.4.1 Synthetic Biology

Firstly, synthetic biology has been used to characterise a number of light-signalling components and link them to a genetic framework (Chapter 3). This work aimed to be linked with a synthetic oscillator to enable the reconstruction of entrainment and hopefully understand some of the design principles required for a network which can be robust to daily fluctuations but also entrainable to daily changes in photoperiod. A synthetic oscillator offers simplification as the number of unknowns in such a network should be greatly reduced and all of the key reactive species would be available for easy modification. Through the characterisation of both red (PHYTOCHROME A, PHYA) and blue (CRYPTOCHROME 2, CRY2, *D. melonogasta* CRYPTOCHROME, CRY, human MELANOPSIN, OPN4 and *C. reinhardtii* CHANNEL RHODOPSIN 1, ChR1) light photoreceptors a suite of photoreceptors are now available for this function.

1.4.2 Arabidopsis thaliana circadian network

In *A. thaliana* the mechanism of light input, and therefore entrainment, is highly complex. As described above, a number of photoreceptors are known to be involved and their inter-relation is quite complex and largely not understood. Furthermore, other entrainment signals such as temperature, which is normally reasonably warm in experimental set-ups and so could be considered as a constant on signal, and nutrients, again normally abundant in the experimental set-up, need to be considered. One gene which has been identified to have a constant light

arrhythmia, circadian phenotype and to be a negative regulator of light signalling [106] is EARLY FLOWERING 3 (ELF3). The role of ELF3 in the plant circadian network has been unclear as it appeared to have a positive input to the morning transcription factors *CCA1* and *LHY* but a negative input to light signalling to the clock [178]. Furthermore, its function at the protein level was unknown as it has a number of protein interacting partners each with diverse biological roles; interacting partners include GI, PHYB, COP1, SHORT VEGETATIVE PHASE (SVP) and ELF4 [80, 85, 179]. Through a combination of experimental and mathematical modelling work the role of EARLY FLOWERING 3 (ELF3) was investigated (Chapter 4 and 5). Through comparative genetic analysis of *elf3-4, cca1-11 lhy-21* and *cca1-11 lhy-21 elf3-4* ELF3 appeared to have a repressor function in the dark. As ELF3 has some structural similarity to transcription factors ChIP was conducted to see if ELF3 associated with any clock promoter regions. Through this, and an acute light signalling response experiment it suggests that ELF3 does function as a repressor, entering the clock network via *PRR9* and *PRR7* promoter regulation. This work unified the functions of ELF3 such that it now simply has a repressor role to the circadian network and in light signalling (Chapter 4). However, its function at the protein level remained unclear, as a ChIP association with promoter fragments does not mean ELF3 has transcriptional activity. To try and understand ELF3's protein function a mathematical model was developed of a sub-network of the interacting partners for ELF3 (Chapter 5). From this network, previously published material and through microscopy imaging, a role for ELF3 in the regulation of protein stability was developed. This idea is consistent with ELF3 being associated with promoter regions and having a diverse array of protein interacting partners, as if ELF3 functioned to regulate other proteins stability it could be localised to promoter fragments and interact with a number of substrates. A similar function has already been observed relating to circadian and floral regulation, with the formation of a trimer complex between GI, FKF1 and CYCLING DOF FACTOR 1 (CDF1) [82].

1.4.3 Ostreococcus tauri circadian network

The work presented in Chapter 4 and 5 proposes two entry points for the function of ELF3 in the clock network; it is also the 11th protein species to be included in this network. As such understanding phenotypes and the principles of a basic circadian system can be easily lost in the complexity. To try and minimise some of this a plant species with a naturally reduced clock has been employed (Chapter 6, 7 and 8). *O. tauri* has been used firstly to investigate the properties of circadian oscillators which are not so easily studied in a multi-cellular plant, such as nutrient and drug responses. Through this specific pathways can be investigated, such as the contribution of transcription and translation [53] and the role of proteasome mediated degradation (Chapter 6). Drug based assays have also been utilised to show that the clock in *O. tauri* responds to specific drugs in the same way as the clock of mammals, insects and fungi [53]. From this *O. tauri* has been used in a chemical screen of approximately 1,600 bioactive compounds (Chapter 7). This high-throughput approach offers the potential to identify new compounds which affect the circadian network and light-signalling mechanism in plants. *O. tauri* has also been used in a comparative study with *A. thaliana* to try and understand the contributions of multiple loops to the flexibility and robustness of the circadian network (Chapter 8). Most circadian research is conducted primarily in constant conditions, or under a single photoperiodic condition. The data presented in Chapter 8 is from luciferase imaging of *O. tauri* and *A. thaliana* from a range of changing photoperiodic conditions and shows that the links to light signalling and the circadian mechanism are extremely close. It also raises the question as to how to classify the circadian components and whether TOC1 is part of a central mechanism in *O. tauri*.

Finally, this work is drawn together and perspectives for future studies are considered in Chapter 9, Discussion. Throughout the thesis time is shown in Zeitgeber time (ZT) where 0 is the start of data collection.

Chapter 2

Materials and Methods

Unless otherwise stated all supplies and reagents were provided by Sigma, U. K.

2.1 *Arabidopsis thaliana* growth conditions

2.1.1 Growth rooms

Plants of *Arabidopsis thaliana* (*A. thaliana*) required for bulking of seed stocks and for genetic crossing were grown to maturity on soil under 100 $\mu E/m^2$ white light in 16:8 Light:Dark cycles at constant 22^oC, in temperature-controlled growth rooms. To avoid cross-contamination, plants were individually staked and bagged, following primary floral bolting in plastic baguette bags. Seeds were harvested once plants had dried.

2.1.2 Growth medium

A. thaliana plants for all assays were grown in sterile culture on solid agar media containing Murashige and Skoog (MS) salts [180] and either (a) 3% sucrose or (b) no sucrose. Lighting conditions are given for each assay type. Media batches of multiples of 400 ml were made with the MS basal salt mixture (Melford, Ipswich, Suffolk) being dissolved in dH_2O, and for 3% sucrose media, sucrose (Fisher) added , taken to pH 5.8 with addition of 1M KOH and then made up to final volume. 400 ml was dispensed into 500 ml bottles and agar powder added. The media was then autoclaved at 116^oC for 20 minutes.

2.1.3 Seed sterilisation and stratification

To minimise fungal and bacterial infection seeds were surface sterilised before use. This follows a standard protocol [181], comprising one rinse in 70% ethanol, followed by 10 minutes treatment with 10% commercial Bleach, and 8-10 washes with dH_2O. To ensure synchronised germination, seeds were stratified for 4 days at 4^oC prior to plating on solid media.

2.1.4 Entrainment conditions

The entrainment of plants for luciferase imaging and RNA time-courses was for at least 5 days under light conditions specified for each experiment. All plants were grown at constant 22^{o}C, on media detailed in (2.1.2) with specified sucrose concentrations in Petri dishes of defined size in each experiment, sealed with gas-permeable tape. If plants were required to have a change in entrainment, the new entrainment regime was applied for at least 7 days before samples were harvested. White light, for entrainment, was provided by cool white fluorescent bulbs, at 50-65 μE/m^2 measured at the level of the samples. Blue light entrainment was provided by light-emitting diode arrays (λ_{max} 450 nm), at 40-60 μE/m^2 measured at the level of the samples.

2.1.5 Selection of transgenic plants

ELF3::ELF3::YFP transgene expression was confirmed through Polymerase Chain Reaction (PCR) with amplification primers (Table 2.1) directed across the ELF3 to YFP join. Selection of homozygous, single insert line was performed on 10μg/ml DL-phosphinothricin (PPT) (Melford) MS plates (2.1.2). Under these conditions plants containing the resistance gene grow normally whilst those lacking the gene can germinate but are extremely small, have bleached cotyledons and rarely form first leaves.

Primer name	Primer pair	Primer sequence	Tm ^{o}C	Chapter
ELF3YFP F	**ELF3YFP R**	GCCACAGGGAATCTCTGGTA	55	4
ELF3YFP R	**ELF3YFP F**	GAACTCCAGCAGGACCATGT	55	4

Table 2.1: Primers used in selection of *elf3-4 ELF3*::ELF3::YFP

2.1.6 Plant lines used

The work described in this thesis relies on the use of previously published and unpublished plant lines. The plant lines are outlined in Table 2.2 along with the relevant reference and thesis chapter.

Genotype	Background	Publication	Chapter
Wild type	Ws		4, 5
ELF3::ELF3::YFP	Ws *elf3-4*	Dixon *et al*, 2011 [153, Appendix B]	4, 5
35S::ELF3::YFP	Ws *elf3-4*	Dixon *et al*, 2011 [153, Appendix B]	4, 5
35S::ELF4::YFP	Ws *elf4-1*	Dixon *et al*, 2011 [153, Appendix B]	4, 5
cca1-11 lhy-21	Ws	Hall *et al*, 2003 [152]	4
cca1-11 lhy-21 elf3-4	Ws	Dixon *et al*, 2011 [153, Appendix B]	4
ELF3::LUC	Ws	Edwards *et al*, 2010 [182]	5, 8
CCA1::LUC	Ws	Doyle *et al*, 2002 [51]	8
LHY::LUC	Ws	McWatters *et al*, 2007 [181]	5, 8
TOC1::LUC	Ws	McWatters *et al*, 2007 [181]	5, 8
PRR9::LUC	Ws	Edwards *et al*, 2010 [182]	5, 8
CAB2::LUC, *elf3-4 CAB2::LUC*	Ws	McWatters *et al*, 2000 [106]	4, 8
CCR2::LUC	Ws	Doyle *et al*, 2002 [51]	8
35S::LUC	Ws	Edwards *et al*, 2010 [182]	8
gi-11	Ws	Richardson *et al*, 1998 [183] and Fowler *et al*, 1999 [184]	4
elf3-4	Ws	Hicks *et al*, 2001 [185]	4, 5

Table 2.1: Plant genotypes used in this study

2.1.7 Luciferin, required for Luciferase assays

A number of the real time assays in both *Arabidopsis thaliana* and *Ostreococcus tauri* rely on luciferase imaging, as this allows continuous, non-destructive real-time imaging. In all cases D-Luciferin (Biosynth, A.G., Switzerland) dissolved in 0.1M triphosphate buffer (pH8.0) was used, to give a final stock concentration of D-Luciferin of 50 mM. For *Arabidopsis* imaging this stock is diluted in 0.01% Triton-X to a final concentration of 5 mM and filter sterilised (0.22µm pore size) before use. For the alga, *Ostreococcus tauri*, the luciferin stock is diluted in artificial sea water (ASW) supplemented with Keller salts (2.5.1) to a final concentration of 33µM.

2.2 Real-time assays, *A. thaliana, in vivo*

2.2.1 Luciferase imaging (time-course)

For real-time imaging of luciferase reporters in *A. thaliana*, seeds were surface-sterilised and stratified, as in (2.1.3), and grown in entrainment conditions (as described in 2.1.4) in 9 cm square tissue culture dishes (Fisher) for 6 days. Seedlings were then sprayed with 5 mM D-luciferin in 0.01% Triton-X, to ensure an even distribution of luciferin. Tissue culture dishes were re-sealed with gas-permeable tape and returned to entrainment conditions. Before the first dawn on the first day of imaging, tissue culture dishes were moved to the imaging chamber under the light conditions required for the particular assay. Images were captured by a low-light digital camera (Hamamatsu, Welwyn Garden City, U. K.) under the control of Wasabi software (Hamamatsu) with an exposure time of 30 minutes. The software controls a delay (when the chamber lights can be on) of 1.25 h between exposures. Within the imaging chamber the blue and red LED arrays (NIPHT, Edinburgh, U.K.), total 10 $\mu E/m^2$, are also controlled through the Wasabi software.

2.2.2 Delayed fluorescence imaging

200µl of solid culture media (2.1.2) was added to the wells of a white 96-well plate (Greiner Bio One) in rows 1 and 7, and 200µl of dH_20 to wells in row 2, 6 and 8, to minimise desiccation of the adjacent samples. To each well containing media, surface-sterilised and stratified (2.1.3) seeds were added (between 2 to 6 per well) and the plate was sealed with a gas permeable film. Plants were germinated and entrained under cool white light (60-70 $\mu E/m^2$) for 7 days. On the 7^{th} day the plastic lid was removed and replaced with a clear adhesive film (Topseal, Perkin Elmer). The film above each well containing a plant was pierced with a needle to allow gas exchange to the plants. Plates were then moved to continuous red and blue light (NIPHT LIMITED, Edinburgh, U.K.) for data collection in scintillation counter. Each plate was stacked between

mirror plates to allow light to reach all wells, and fluorescence was measured following no count delay, with each well being read for 2 seconds [186].

2.3 Single time-point assays, *A. thaliana*

2.3.1 Confocal imaging

Seeds were surface sterilised and stratified (2.1.3) and plated to 4.5 cm petri dishes on solid agar media (2.1.2). Plants were grown under entrainment conditions in Percival cabinets for 6 days. 3 plants were used for each timepoint. Plants were laid flat on a microscope slide and 70µl of water was added to the slide and a coverslip placed on top, ensuring no air bubbles formed. Mounted slides were kept under humid, dark conditions for transport from the laboratory to microscope. A Leica SP5 confocal microscope was used for all confocal imaging. For timecourse imaging of *ELF3*::ELF3::YFP, starting at the upper epidermis cell layer of the first true leaves, were imaged using a 63x water-immersion objective, with a 1024x1024 scanning resolution. Raw data were processed - with 8x line averaging over a depth of approximately 11µm. Illumination was provided by 20% of an argon laser and fluorescence signals were filtered monochromated for YFP (excitation band width 525-560), Chlorophyll (excitation band width 640-715).

2.3.2 High-resolution imaging of luciferase reporter lines

Promoter::Luciferase lines had been previously constructed (Table 2.2) and were used in this assay. The seeds were sterilised and stratified as (2.1.3) and grown on solid agar media (2.1.2), for 6 days in white-light 70 $\mu E/m^2$ 12:12 Light:Dark cycles. On day 5 of growth 5 mM D-Luciferin in 0.1% Triton-100 was added to the roots of the plants on agar media and the following day, at the time when maximal expression of the clock-gene promoter luciferase was expected, whole plants were removed and placed on a microscope slide. 70µl of dH_2O was added to cover the plant and a microscope coverslip was placed over the plant, taking care not to

crush the plant. The plant was imaged using a 2.5x objective of a Zeiss florescence Microscope. Correct focus in the camera rather than the eyepiece was confirmed under green light-illumination, using a 2 second exposure of the low-light sensitive cooled camera (Hamamatsu). Luciferase luminescence was collected with a 30 minutes exposure on the same camera. 3 separate plants were imaged at each time point.

2.3.3 Hypocotyl measurements

Plants were grown under Short Day (6L:18D) or Long Day (18L:6D) white-light (70-100 μE/m^2) photoperiod conditions on MS, 1% agar media, with or without 3% sucrose, for 6 days. Hypocotyls, with a centimetre ruler were imaged using a digital camera. Measurement of hypocotyl length was performed by Image J [187] with hypocotyl length being defined as from V in hypocotyls-cotyledon formation to hypocotyls-root junction.

2.4 Molecular Biology, *A. thaliana*

2.4.1 DNA extraction

The components and concentrations for DNA extraction buffer are shown in Table 2.5.

Components	[Stock solution]	Final [extraction buffer]
NaCl	5 M	0.25 M
Tris pH 7.5	1 M	0.2 M
EDTA	0.5 M	0.025 M
SDS	10%	0.5%

Table 2.2: *A. thaliana* DNA extraction buffer

For genotyping PCR's a crude DNA preparation was used. A single leaf was harvested from 20-30 day old, soil grown, *Arabidopsis thaliana* plants, into a 1.5 ml tube and ground with a mini-pestle. 200μl of extraction buffer , above, was added and mixed, samples were then centrifuged at 13.5 xg for 3 minutes and 150μl of the supernatant was transferred to a 1.5 ml tube containing

150µl of isopropanol. This solution was gently mixed by pipetting and then centrifuged at 13.5 xg for 5 minutes and the supernatant discarded. The pellet is air-dried and re-suspended in 150µl of dH_2O. From this 1µl is used in subsequent polymerase chain reactions.

2.4.2 Polymerase Chain Reaction (PCR)

Genotyping PCRs were conducted using Taq polymerase (NEB) with 10x Taq polymerase buffer (NEB) a dNTP mix was made containing ATP, TTP, GTP and CTP such that each dNTP was at 10µM, following standard protocol [188]. Amplified DNA products were visualised on 1% agarose gel with Ethidium Bromide under UV-light, using 1 Kbp or 100 bp DNA ladder (NEB) as reference.

2.4.3 RNA extraction and cDNA synthesis

Arabidopsis thaliana seeds were surface-sterilised and stratified as (2.1.3) and then plated onto MS solid media (2.1.2) in 4.5 cm petri dishes (Plastiques Gosselin). To ensure an even distribution of seeds across each plate 1 ml of water agar was added to the surface of each plate and 150µl of seeds, re-suspended following stratification, in water agar. The plates were then gently agitated left open, in a sterile flow hood, to allow the evaporation of the water agar, this is important to gain synchronised germination of the seeds. Plates were sealed using gas permeable tape and seedlings grown for 6 days under the specific experiments entrainment conditions. All plants from one plate were harvested using tweezers into 1 ml of RNAlater (Ambion) in 1.5 ml tubes at ZT's specified by the experiment. Samples were then stored for 24 hours at 4^oC. Following this total RNA was extracted using Qiagen Plant RNA extraction kit (Qiagen, 74106) with QIAshredders (Qiagen) according to manufacturer's instructions for the mini-centrifuge protocol with the following modifications. Firstly, ensuring all RNAlater is dried from the tissue sample through blotting on paper towel and secondly, an additional wash step before elution of RNA was added to ensure complete removal of ethanol from the sample.

The amount of RNA from the extraction was quantified using a 1.5 µl sample on Nanodrop (Nanodrop, ND-1000 spectrophotometer). Following this cDNA was synthesised from 1 µg of total RNA and random hexamer primers using a cDNA synthesis kit (Fermentas, K1622).

2.4.4 Q-PCR

Q-PCR primer pair sequences were either used from previous publications, *ELF3, GI, LUX, TOC1, ZTL, PRR9, PRR7, CCA1* and *LHY* [182], or were designed to be specific for cDNA through Perl Primer (http://perlprimer.sourceforge.net/) [189]. *IPP2* was identified as a gene with constant expression and has been used in [159] to normalise expression.

Primer name	**Sequence**	**Primer name**	**Sequence**	**Tm (^{o}C)**
ELF3 F	GGAAAGCCATTG CCAATCAA	ELF3 R	ATCCGGTGATGC AGCAATAAGT	60
GI F	TATTGAAGTGTC GTCTACCAG	GI R	GAGCTTTGGTTC ATGATATCAC	60
CRY1 F	GTATGATCCATTG TCTTTGGTG	CRY1 R	TTGAATGATCGA ACCGCT	60
CRY2 F	CTTATCTCAATC CTTGAAGGCTC	CRY2 R	GAAACAGGATC ATAGAGGTGG	60
COP1 F	CAGAGTCTTATG GAGTATGAAGAG	COP1 R	CCAAACTTTAA CCTTGCAGTC	60
LUX F	TGCTCATCATCT TCACAAACC	LUX R	CTTCCTCTCCC ATTTCAAACTC	60
TOC1 F	ATCTTCGCAGA GTCCCTGTGATA	TOC1 R	GCACCTAGCTTC AAGCACTTTACA	60
IPP2 F	GTATGAGTTGCTT CTCCAGCAAAG	IPP2 R	GAGGATGGCTG CAACAAGTGT	60

ZTL F	GGAGACGATGAT ACTATTACCC	ZTL R	TTGAAGATCCAA GAACAGGTC	60
PRR9 F	GATTGGTGGAAT TGACAAGC	PRR9 R	TCCTCAAATCTTG AGAAGGC	60
PRR7 F	CTTTCTCAAGGT ATAATCCAGCC	PRR7 R	ACAATCATATGC TGCTTCAGTC	60
LHY F	CAACAGCAACAA CAATGCAACTAC	LHY R	AGAGAGCCTGAA ACGCTATACGA	60
CCA1 F	CTGTGTCTGACGA GGGTCGAA	CCA1 R	ATATGTAAAACTTT GCGGCAATACCT	60

Table 2.3: Q-PCR primers used in this study

cDNA was diluted 1:5 in RNase-free dH_20 into clear 96-well skirted plates (Agilent Technologies, 401334), with the first column containing the dilution series standard, 1 to 1:10000 of cDNA taken from random samples in the experiment, and negative controls of no cDNA, no enzyme and water. The addition of reagents to Q-PCR plates (LightCycler 480 multiwell Plate 384, white, Roche) was by a Tecan Freedom EVO robot controlled by EVOware standard software. Mastermix containing Roche SYBR Green, gene-specific primers (sequences in table 2.4) at 3μM and RNase-free dH_20 was first plated followed by cDNA. Set-up plates were sealed with Roche sealing foils (supplied with 384-well plates, Roche) and centrifuged for 1 minute at 1000 rpm (Grant Bio LMC-3000) to settle the reagents. The Q-PCR was conducted in a Roche LightCycler 480 (Roche) controlled by LightCycler 480 SW1.5 software.

2.5 *Ostreococcus tauri* materials and growth conditions

2.5.1 Growth medium

Ostreococcus tauri cells were cultured in sterile 250 ml tissue culture flasks (Sarstedt) in 100 ml of supplemented artificial sea water (ASW), salinity of 30 ppm (Instant Ocean, Aquarium

Systems). Artificial sea water is supplemented with Keller salts (Sigma) and f/2 Vitamin solution (Table 2.7). The components of Keller salts [190, 191, 192, 193] are detailed in Table 2.5 and 2.6 and the f/2 vitamin solution in Table 2.7.

Component	**Stock solution**	**Quantity (ml)**	**Final concentration (M)**
$NaNO_3$	75.00g/L dH_2O	1	$8.82x10^{-4}$
NH_4Cl	2.67 g/L dH_2O	1	$5.00x10^{-5}$
Na_2b-glycerol-phosphate$6H_2O$	2.16 g/L dH_2O	1	$1.00x10^{-5}$
$Na_2SiO_3 \cdot 9H_2O$	15.35 g/L dH_2O	1	$5.04x10^{-4}$
H_2SeO_3	1.29mg/L dH_2O	1	$1.00x10^{-8}$
Tris-base (pH 7.2)	121.10 g/L dH_2O	1	$1.00x10^{-3}$
Trace metal solution	See Table 2.6	1	
Vitamin solution	See Table 2.7	0.5	

Table 2.4: Keller salts

Component	**Stock solution**	**Quantity**	**Final medium (M)**
$Na_2EDTA \cdot 2H_2O$		37.22 g	$1.00x10^{-4}$
Fe-Na-$EDTA \cdot 3H_2O$		4.93 g	$1.17x10^{-5}$
$FeCl_3 \cdot 6H_2O$		3.15 g	$1.17x10^{-5}$

$MnCl_2 \cdot 4H_2O$		0.18 g	9.00×10^{-7}
$ZnSO_4 \cdot 7H_2O$	23.00 g/L dH_2O	1 ml	8.00×10^{-8}
$CoSO_4 \cdot 7H_2O$	14.05 g/L dH_2O	1 ml	5.00×10^{-8}
$Na_2MoO_4 \cdot 2H_2O$	7.26 g/L dH_2O	1 ml	3.00×10^{-8}
$CuSO_4 \cdot 5H_2O$	2.50 g/L dH_2O	1 ml	1.00×10^{-8}

Table 2.5: Trace metal solution

f/2 vitamin solution was made separately and from this stock solution 1:2000 final dilution.

Component	Stock solution	Quantity	Final medium (M)
thiamine· HCl		200 mg	2.96×10^{-7}
biotin	0.1 g/L dH_2O	10 ml	2.05×10^{-9}
cyanocobalamin	1.0 g/L dH_2O	1 ml	3.69×10^{-10}

Table 2.6: f/2 vitamin solution

The artificial sea water also contains the antibiotics ampicillin (50 µg/ml) from 50 mg/ml stock in dH_2O, kanamycin (50 µg/ml) from 10 mg/ml stock in dH_2O and neomycin (40 µg/ml) from 40 mg/ml stock in dH_2O, to reduce bacterial infection.

As *Ostreococcus tauri* is an obligate phototroph a modified artificial sea-salt medium was used to culture and image cells which would be experiencing very low light intensity (1-2 $\mu E/m^2$) or over 24 hours of darkness. This media was supplemented with carbohydrate sources such that the final media contained 0.4% glycerol and 200 mM D-sorbitol [53 and Appendix A].

The enriched ASW and the carbohydrate-supplemented enriched ASW was filter sterilised, 0.22µM pore size (Vacuum-driven filtration, Stericup and Steritop, Millipore) and stored for a maximum of 7 days in darkness.

2.5.2 Culturing conditions

Ostreococcus tauri cells were cultured in 100 ml ASW (2.5.1) in 500 ml flasks in temperature and light controlled Sanyo incubators. Cells were grown at 20°C under white light from cool white fluorescent bulbs passed through one-layer of Ocean Blue filter (Rosco filters, UK) with a fluence rate of 10 μE/m^2. Cells were split (1:100) into fresh artificial enriched sea-water every 10 days for the maintenance of all cultures. 96-well plates were also entrained under the same conditions.

2.5.3 Transgenic *O. tauri* lines used in this study

Genotype	Background	Published	Chapter
pCCA1::LUC	*O. tauri*	Corellou *et al*, 2009 [169]	6, 7, 8
CCA1::CCA1::LUC	*O. tauri*	Corellou *et al*, 2009 [169]	6, 7, 8
pTOC1::LUC	*O. tauri*	Corellou *et al*, 2009 [169]	6, 7, 8
TOC1::TOC1::LUC	*O. tauri*	Corellou *et al*, 2009 [169]	6, 7, 8
pCAB::LUC	*O. tauri*	Corellou *et al*, 2009 [169]	6, 7, 8
pP12::LUC	*O. tauri*	Corellou *et al*, 2009 [169]	6, 7, 8
WT	*O. tauri*	Corellou *et al*, 2009 [169]	6, 7, 8

Table 2.7: *O. tauri* lines used in this study

2.6 Real-time assays, *O. tauri*

2.6.1 Scintillation counter (Topcount) assay LL

O. tauri cells are simultaneously diluted (1:5, 160 μl fresh ASW, 40 μl cells) and plated into 96-well white microplates (Greiner Bio One) and sealed with clear lids (Greiner Bio One) with gas

permeable film. These plates are entrained for 6 days (2.5.2) and on day 6 the media is refreshed and luciferin added (150 µl media removed and keller/luciferin added (2.1.8)). This is possible, as during the entrainment period the *O. tauri* cells drop to the base of the plate wells. Following refreshing media and the addition of luciferin the plates are sealed with a clear adhesive Topseal (Perkin Elmer) and returned to entrainment conditions. Imaging starts the following day under the specific light cycles required for the experiment. All Topcount (Perkin Elmar adapted microplate scintillation and luminescence counter) imaging is conducted under red and blue vertical lights (NIPHT LIMITED, Edinburgh, U.K.) with mirror plates in between each imaging plate to provide a gradient in light intensity across the plate. Within Topcount, plates are moved into a dark chamber for reading, there is a 2 minute count delay to reduce the levels of auto-florescence before total luminescence is recorded. For pharmacological assays, including the 'wedge', compounds were diluted to the required stock concentration and 20 µl added per well. Control vehicle wells were on the same plate where 20 µl of the compound solvent was added per well. The specific compound concentrations are provided with the results (Chapter 6). Data are shown as luminescence collected in cpounts per second (cps) or normalised luminescence.

2.6.2 Degradation assay (Chapter 6)

O. tauri cells were plated as described in (2.5.1) and entrained at a constant 20^{o}C, under white light from cool white fluorescent bulbs passed through one-layer of Ocean Blue filter (Rosco filters, UK) with a fluence rate of 10 µE/m^2 to the photoperiodic conditions specified in Table 2.9.

Experiment	Entrainment conditions	Assay conditions	Lines used
Continuous	12:12 L:D	LL	*TOC1*::TOC1::LUC, *CCA1*::CCA1::LUC
Short day (SD)	6:18 L:D	6:18 L:D	*TOC1*::TOC1::LUC, *CCA1*::CCA1::LUC
Long day (LD)	18:6 L:D	18:6 L:D	*TOC1*::TOC1::LUC, *CCA1*::CCA1::LUC
12:12	12:12 L:D	12:12 L:D	*TOC1*::TOC1::LUC, *CCA1*::CCA1::LUC

Table 2.8: Degradation assay entrainment and assay conditions (Chapter 6)

At each timepoint (given in Chapter 6), 5 wells had 20 µl of drug (MG132 or epoximycin) (suspended in dimethyl sulfoxide (DMSO) and diluted in keller containing luciferin (2.1.8)) added and 3 wells had the vehicle, DMSO, added. All assays were conducted under red and blue light with a two minute count delay and each well being counted for 3 seconds.

2.6.3 Photoperiod switches (Chapter 8)

O. tauri cultures of *pCCA1*::CCA1::LUC, *pCCA1*::LUC, *pTOC1*::TOC1::LUC and *pTOC1*::LUC were plated as described in (2.5.1) and assayed in the Topcount with a count delay of 2 minutes and each well being read for 3 seconds.

Experiment	Entrainment conditions	Assay conditions
HHLLHH	12:12 L:D	12:12 L:D
LLHH	12:12 L:D	12:12 L:D
SD	8:16 L:D	8:16 L:D
LD	16:8 L:D	16:8 L:D
SDLD (Dusk)	8:16 L:D	2x(8:16 L:D)4x(16:8 L:D)
LDSD (Dusk)	16:8 L:D	2x(16:8 L:D)4x(8:16 L:D)
SDLD (Dawn)	8:16 L:D	2x(8:16 L:D)t4x(16:8 L:D)
LDSD (Dawn)	16:8 L:D	2x(16:8 L:D)t4x(8:16 L:D)

Table 2.9: Photoperiod switch assays
Photoperiodic switch assay conditions, where H=High light intensity of ~10 μE/m^2 and L=Low light intensity of 1 μE/m^2. SD= Short Day, LD=Long Day and L:D refers to Light:Dark cycles, t=transient photoperiod which is inserted when the photoperiods are switched at dawn.

2.6.4 Pharmacological Screening (Chapter 7)

O. tauri cultures of *CCA1*::CCA1::LUC are plated (1:5, 80μl keller, 20μl cells) into fresh artificially enriched sea-water in 96-well white microplates (Greiner Bio One) as described in (2.5.1). Cells are entrained for 6 days in 12:12 blue Light:Dark cycles and on day 6 cells are refreshed in fresh ASW which contains 33μM luciferin. Plates are returned to entrainment conditions and on Day 7 compounds are added at 2 μM, plates are then transferred to the Topcount for data recording under one Light:Dark cycle followed by continuous light. All plating manipulations are conducted by a Tecan liquid handling robot.

2. 7 Yeast methods

2.7.1 Strains used and culturing

All yeast strains were cultured at a constant 30^{o}C. Cultures on solid media were grown for 3 days and liquid cultures overnight. Dropout media and agar required for selecting mutant strains were made following standard protocols [188] using reagents from Foremedium (Hunstanton, U.K.). Induction of galactose-inducible promoters (for OPN4 constructs) followed overnight culture in glucose-based media, the media was then changed (yeast pelleted at 3,000rpm and washed 2x in dH_20) to raffinose-based media for a further 16 hours incubation with a subsequent addition of galactose to a final concentration of 2%. With induction, samples were transferred to a temperature-controlled dark suite and all-*trans*-retinal, 1µM final concentration, dissolved in DMSO was added, light treatments and sampling started 1 hour after induction.

For the yeast-2-hybrid LexA based assays the yeast was cultured in liquid media overnight at 30^{o}C in the dark and a quantitative β-galactosidase assay (Clontech, Mountain View, U.S.A.) was conducted according to the manufactures instructions in the dark.

2.7.2 Cloning

OPN4 cDNA was received from E. Tarttellin (University of Manchester), dCRY and PER plasmids from Dr. E. Rosato (University of Leicester) [194] and CRY2 and COP1 plasmids were as described in [86]. Gateway compatible destination vectors pAG315GAL-ccdB and pAG306GAL-ccdB were purchased from the Lindquest collection [195] via Addgene (Cambridge, U.S.A.). All cloning was conducted using the Gateway technology (Invitrogen, Paisley, U.K.) to enable the construction of 2, 3 and 4 component constructs and for the efficient cloning of further constructs. All polymerase chain reactions (PCR's) were conducted using the high-fidelity polymerase Phusion (Finnzymes, NEB, Ipswich, U.S.A.) according to manufacturers' instructions. Bacterial transformations followed standard heat shock protocol

into chemically competent Mach1 or DH5α *E.coli* with cells being plated onto LB agar plates containing the appropriate selecting antibiotic. Due to the unknown toxicity level of OPN4 in *S.cerevisiae* the constructs were expressed from a weak Gal1 promoter (GalS) which contained mutations in a number of the Gal binding sites, plasmid p413 GalS (ATCC-87670). An N-terminal localisation sequence, as used in [196], was attached to the N-terminal domain of OPN4 from yeast pheromone receptor STE2 to ensure localization to the plasma-membrane. Primer sequences used in cloning are listed in Table 2.11.

Primer name	**Sequence 5'-3'**
ATTB1Gal	GGGGACAAGTTTGTACAAAAAAGCAGGCTTAACGGATTAGAAGCCGCCG
ATTB5rGal	GGGGACAACTTTTGTATACAAAGTTGTGGTTTTTTCTCCTTGACG
ATTB5Ste2	GGGGACAACTTTGTATACAAAAGTTGTGATGTCTGATGCGGCTCCT
ATTB4Ste2	GGGGACAACTTTGTATAGAAAAGTTGGGTGGAGTAACAGTACTGTTAA
ATTB4rGFP	GGGGACAACTTTTCTATACAAAGTTGCTATGAGTAAAGGAGAAGAA
ATTB3rGFP	GGGGACAACTTTATTATACAAAGTTGTTTTGTATAGTTCATCCATGCC
ATTb1Gal	GGGGACAAGTTTGTACAAAAAAGCAGGCTTAACGGATTAGAAGCCGCCG
ATTB5rGal	GGGGACAACTTTTGTATACAAAGTTGTGGTTTTTTCTCCTTGACG
ATTB2OPN4	GGGGACCACTTTGTACAAGAAAGCTGGGTAAATAACCGGTGACGTCAC
ATTB3OPN4	GGGGACAACTTTATTATACAAAGTTGTAACCGGTGACGTCACCAT

Table 2.10: Primers used in photoreceptor cloning (Chapter 3)

2.7.3 Transformation and selection

OPN4 constructs were transformed into strain BY1172 from GlaxoSmithKline (Brentford, U.K.). Yeast-2-hybrid constructs (dCRY/PER and CRY2/COP1) were transformed into LexA yeast (Kevin Hardwick, U.K.). All yeast transformations followed the standard LiOAc-PEG protocol [188] and were plated to appropriate synthetic drop-out media. Results shown are from at least 2 independent transformations.

2.7.4 Beta-galactosidase assays

For the wave-length specificity assay 5 minute light treatments were applied to yeast suspension in 1.5 ml tubes. Blue-light treatments were from a light-emitting diode source (λ_{max} 450 nm), at 40-60 $\mu E/m^2$, red-light treatment used cool white fluorescence bulbs filtered with 2 layers of red plastic film (E027 medium red, Rosco, Black Light, Edinburgh, U.K.), green-light treatment used cool white fluorescence bulbs filtered with 2 layers of green plastic film (EO90 Dark yellow/green, Rosco, Black Light, Edinburgh, U.K.), and yellow-light was provided by yellow LED's (LED module yellow 56-3044, Rapid Electronics Ltd, Colchester, U.K.). For the treatment duration assay, blue-light at the fluence rate of the photoreceptors maximum response, as given by the fluence rate assays, was applied for durations indicated and samples then taken. For the fluence rate assay, 5 minute blue-light treatments were applied to yeast suspension, (OD600=0.6) in 1.5 ml tubes at the required fluence levels. All manipulations were conducted under dim red safe-light (cool white fluorescence bulbs wrapped in 2 layers of E027 medium red, Rosco, Black Light, Edinburgh, U.K.) with a fluence rate of less than 1 $\mu E/m^2$.

2.7.5 Luciferase assays

1 ml of yeast culture was used in each luciferase assay with the addition of luciferin at a final concentration of 5 mM, diluted in dH_2O. For the opsin proteins all-*trans* retinal was also added (as in previous assays). The first image taken, on a low-light sensitive digital camera (Hamamatsu) was a dark control. Then light treatments were applied according to specific

experimental condition, using the light sources described in section 2. 8. 4. For opsin imaging a 5 minute blue-light treatment was applied and images collected with a exposure of 20 minutes, controlled through Wasabi software. For phyA-FHL imaging the light treatments are described in Figure 6, Chapter 3. The images were then analyzed using Metamorph software to remove background and gain total light intensity.

2.7.6 Protein extraction and blots

Protein extraction and gel blots followed standard protocol [188], starting from 5 ml of yeast, OD600 = 0.6 for each sample. Protein extracts were separated on 4-12% Bis-Tris SDS gels (Invitrogen, Paisley, U.K.) using the Invitrogen See Blue (C5625) as the protein weight marker. For the Melanopsin blot the primary antibody was anti-melanopsin, sc-32870 (Santa Cruz Biothechnology, Santa Cruz, U.S.A.) and the secondary antibody goat anti-rabbit peroxidase, ab6721 (Abcam, Cambridge, U.K.). The blot was developed using ECL Plus (GE Healthcare, Amersham) and detected on Biomax Light Film (Kodak, Sigma-Aldrich, cat no. Z370398).

2.8 Data analysis and processing

2.8.1 Metamorph analysis for luciferase imaging timecourses

The software package, Metamorph version 7.7.1., was used for the image processing of all luciferase images. This software enables the measurement of the total light captured for specific regions of the image over time. The pattern of emitted light from plants treated with luciferin and containing the luciferase transgene, can be collected along with background levels in the imaging chamber, or from the camera noise. This background and noise can be subtracted from the total light collected. The numerical data collected from the images in Metamorph software was then processed in Microsoft Excel. Rhythmic properties were analysed using BRASS and an imaging macro run through excel [182].

2.8.2 Metamorph for confocal imaging timecourses

For each time point, three separate plants were imaged across an approximately 11µm leaf section. All confocal image data analysis was conducted in Metamorph version 7.7.10. Each 4-D image stack was condensed to a single projection in the Z-plane. A background threshold was set to minimise background noise. The total signal intensity above threshold was then measured for a 500x400 Voxel region. The threshold was then raised to capture only fluorescence in the nuclear speckle formation and total speckle intensity was measured. This gave the amount of YFP in the nuclear speckles. These values were then averaged for each timepoint (an average of three plants) and plotted as a time series.

2.8.3 BRASS analysis

Time-course data either from Metamorph processing of plant luciferase imaging or from Topcount files was analysed using Biological Rhythm Analysis Software System (BRASS) Version 3.0 (available from www.millar.org) [182].

2.8.4 Noise analysis peak and phase value determination (Chapter 8)

Peak and trough values from noise data were determined by two independent methods; firstly using the FFT-NLLS analysis from BRASS (2.7.3) and secondly through a peak finding programme (available from http://www.billauer.co.il/peakdet.html) and used in Matlab 2008b.

2.8.5 Chemical screen data analysis (Chapter 7)

Period estimates for the control compounds went from 24 hours to 120 hours and were made via BRASS (2.9.3). This provided an indication of the variability on each plate, within and between batches. Compound period estimates were taken across the entire timecourse (0- 120 hours), due to the rapid damping in rhythms following addition of the compound. These period estimates were then paired with compound replicates and identified if the compound had a reliable effect on the period of the rhythm (either longer or shorter than the screen average). Those which had a reliable effect were then ordered by period length to identify the range of periods the

compounds produced on the cells. The specific compound for each of these consistent hits was also identified.

2.8.6 Q-PCR analysis

Q-PCR data was collected using the LightCycler 480 SW1.5 software and initial analysis of the melt curve, to check for secondary product formation or excessive primer dimerization was conducted on this software. Absolute quantification against the dilution series standards was also made in this software. Normalisation to the levels of the house-keeping gene *IPP2* was then conducted in MS Excel and this data used for subsequent work.

2. 9 Mathematical modelling

2.9.1 Forming of Ordinary Differential Equations (O.D.E.'s) and model simulations

Ordinary Differential equations were formed according to the model network. The model was written in Matlab2008b with separate files for the "Light" reactions (representing 12 hours of light) and the "Dark" reactions (representing 12 hours of dark) and the two files were combined with a script which allows the Light and Dark reactions to continuously loop after each other. The equations were solved in Matlab2008b using ODE23s.

2.9.2 Parameter fitting and constraining

Parameter values were constrained relative to each other, as much as possible, using data from the literature. However, data was not available for all of the kinetic parameters of the protein interactions, so the parameters have been constrained so rates and values are relative to each other. The parameters have then been manually fitted to experimental protein profiles, to give simulations that are close approximations of this data.

Chapter 3

Characterisation of Photoreceptors for use in Synthetic Biology

Sections of this chapter have been published in Sorokina *et al*, 2009 ([197] and Appendix D) or in preparation, Dixon and Millar, 2011

3.1 Introduction

Synthetic biology requires well-characterized components to design, model and build novel biological devices. The characterisation of these components needs to document the key features of their biological function, in a standard host, as well as to provide access to the component in a flexible and available form for practical use. Photoreceptors are one type of discrete unit which are known to link with a number of signalling systems [198]. The characterisation of a suite of photoreceptors would provide a resource from which the correct photoreceptor could be selected for specific network requirements. This chapter describes the characterisation of both blue-light, Cryptochromes and Opsins, and red-light photoreceptors, Phytochromes, for this purpose.

To characterise these photoreceptors the unicellular yeast *Saccharomyces cerevisiae* (*S. cerevisiae*) has been used as a host. *S. cerevisiae* is widely used in the yeast-2-hybrid system [199] to identify protein interactions using gene transcription as the reporter, and therefore is appropriate for recording signalling function from synthetic networks. *S. cerevisiae* is also an ideal host for the heterologous expression of membrane bound G-protein coupled receptors (GPCR). In its haploid form yeast contains only one GPCR that signals through the yeast mating pathway which is well characterised, mathematically modelled and controls an array of

transcriptional outputs [200]. This transcriptional output can enable the utilisation of a number of available reporter genes to provide both qualitative and quantitative information, such as *lacZ* [201]. As both the yeast-2-hybrid and G-protein coupled cascade result in a change in transcription these two systems lend themselves for use in synthetic biology networks.

3.1.1 Synthetic Biology

Synthetic Biology aims to use the wealth of molecule techniques which have been developed over the last 30 years to create new assemblies of biological components. This can be with the aim of gaining greater understanding of a system, such as a circadian clock network with a shorter period and so more amenable to real-time studies, or to create a new biological function, an organism which can degrade plastics. In order to create these networks in a safe and reliable fashion it is proposed that each component should be well characterised in a host, normally heterologous, organism [202]. This characterisation should be such that the biological properties of each component in this host can be used to create an accurate, predictive mathematical model when many of the components are associated [197]. With such a model the requirement to try all variations of a network and the identification of unwanted biological functions should largely be accounted for before actual biological construction of this network occurs. This study describes such a characterisation, based on the work of Shimizu-Sato [207], for photoreceptor proteins with the ultimate aim that these components could be used in the formation of a light-entrainable oscillating network in *S. cerevisiae.*

3.1.2 Red/Far-red light photoreceptors

The GAL based yeast-2-hybrid system was used in the characterisation of the *Arabidopsis thaliana* red-light photoreceptor PHYTOCHROME A (PHYA) through its light dependent interaction with FAR-RED ELONGATED HYPOCOTYL 1-LIKE (FHL) [197]. PHYA is a

member of a large family of red/far-red light absorbing photoreceptors. In *Arabidopsis thaliana* there are 5 PHY's (PHYA-E), all of which covalently bind the chromophore phytochromobilin [203]. On absorption of red-light (λ_{max}= 660 nm) the protein undergoes a conformational change to its physiologically active state (P_{fr}). In this conformation phytochromes are able to absorb far-red light (λ_{max}= 730 nm) which causes a reversal of conformation to the P_r form [203]. The balance between these forms gives a measure of the ratio of red:far-red light in a plant's environment and so signals the plant's physiological growth responses, such as shade avoidance [101]. A number of interacting signalling factors have been identified to associate with Phytochromes, in particular the transcription factors PHYTOCHROME INTERACTING FACTORS (PIF's) [204], to which FHL has similarity to [205, 206]. The interaction between Phytochromes and PIF's enables light-regulated transcriptional control and also provides a mechanism for the regulation of PHY and PIF protein stability [95, 96, 97, 98]. It is this interaction which has been used for heterologous signalling pathways [207] and subsequently to control light mediated switching of forms in more complex pathways [208]. It is also this interaction which provides the signalling mechanism described in [197] and in Figures 3.6 and 3.7 of this Chapter.

3.1.3 Blue light photoreceptors

The LexA based yeast-2-hybrid system was utilised for controlling signalling through the blue-light photoreceptors CRYPTOCHROME (CRY from *Drosphila melongasta* and CRY2 from *Arabidopsis thaliana*) interacting with PERIOD (PER) (Figure 3.2) or CONSTITUTIVELY PHOTOMORPHOGENIC 1 (COP1) (Figure 3.3) respectively. Cryptochromes were first identified in plants and show structural similarity to either of the two types of DNA photolyase [141]. In *Arabidopsis* three CRYPTOCHROMES have been identified (CRY1-3), with CRY2 containing a positively charged groove though which it could bind directly to DNA [209]. The

chromophore binding domain of CRYPTOCHROMES is similar to that found in photolyases and in *Arabidopsis* this N-terminal photolyase related (PHR) domain is known to non-covalently interact with the flavin ($FADH^-$) chromophore and possibly with a second chromophore pterin (methenyltetrahydrofolate, MTHF) [209]. CRYPTOCHROMES have a distinct 2-peak action spectrum which shows absorption of light in the UV-A (~320-400nm) and blue-light (400-500nm) regions [209]. In *Arabidopsis*, CRYPTOCHROMES are involved with photomorphogenic responses and entrainment of the circadian clock, the interacting protein COP1 is also involved in these responses [71, 210, 86]. In *Drosophilia* CRYPTOCHROMES are believed to be part of the core circadian clock network (Chapter 1), as is the interacting protein used in this study for the yeast-2-hybrid response, PERIOD (PER) [194].

For the investigation and characterisation of GPCR blue-light photoreceptors *S. cerevisiae* which lacked its GPCR (STE2, in the specific strain used in this study) and contained a humanised form of the Gα-subunit (summary diagram of the modified GPCR network [211]) was used. Human Melanopsin (OPN4) [212, 213] has been shown to have an important role in the entrainment of the mammalian circadian network [214]. OPN4 has a λ_{max} = ~480nm and is structurally similar to Rhodopsin, both contain 7-membrane spanning domains and form a classic GPCR structure. Also both bind the chromophore all-*trans* retinal which undergoes an isoform change to 13-*cis* retinal following the absorption of light. OPN4 is believed to signal through the $G\alpha_q$ subfamily of Gα subunits [215] and so the yeast stain used in this study contained a humanised Gα subunit, similar to the $G\alpha_q$ structure [216].

Two other blue-light absorbing opsins were investigated which have greater structural similarity to microbial-like opsins. These were the Channel Rhodopsin proteins CHANNEL RHODOPSIN 1 (ChR1) and CHANNEL RHODOPSIN 2 (ChR2) from *Chlamydomonas*

reinhardtii [217, 218]. The *in vivo* structure assumed by these proteins and the downstream signalling mechanism is less well characterised but they do contain 7 membrane spanning domains, like other opsins, and form non-specific cation channels which undergo blue-light induced conformational changes. The conducting state of ChR2 is twice as long as that of ChR1 and as such has been utilised in neurobiological applications [172, 219]. Like OPN4, ChR1 and ChR2 have a λ_{max} = 480nm and bind the chromophore all-*trans*-retinal which, following absorption of a photon undergoes an isoform change to 13-*cis*-retinal, and it is this change which causes conformational change in the protein structure [220]. The pathways used for the characterisation of the CRYPTOCHROMES and OPSINS are represented in schematic form in Figure 3.1.

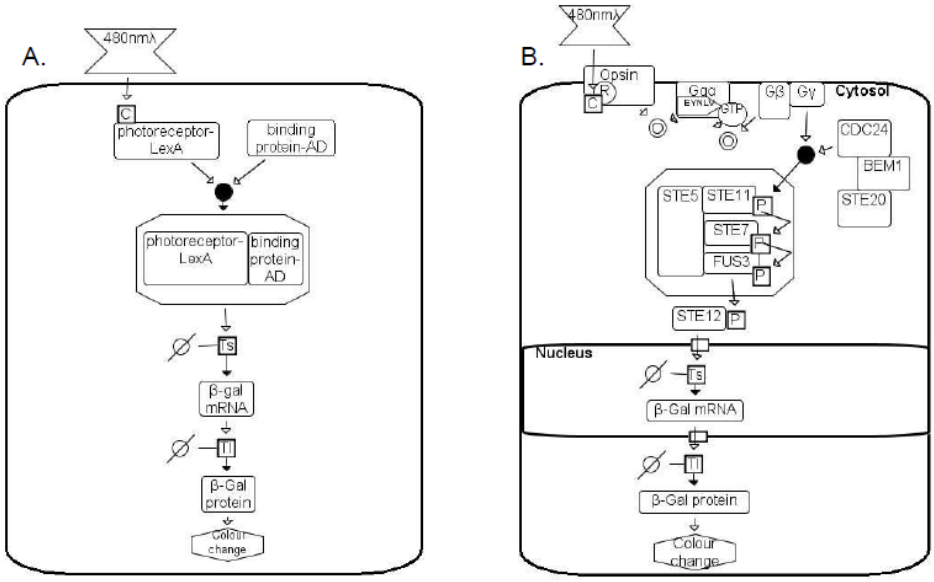

Figure 3.1: Schematic of blue-light photoreceptor signalling pathways used in this study.
Pathways represented using the Systems Biology Graphical Notation (SBGN) [221]. A) Photoreceptors in LexA yeast-2-hybrid system; represents dCRY (photoreceptor-LexA) and PER (binding protein-AD) interaction, or CRY2 (photoreceptor-LexA) with COP1 (binding protein-AD). Compartments are not shown. B) Photoreceptors linking to the yeast pheromone signalling pathway; represents OPN4 as opsin. Yeast component names as in [200]. EYNLV represents the modified (humanized) amino acid sequence of the Gα subunit used.
C = conformational change, Ts = transcription, Tl = translation, P = phosphorylation

3.2 Results

The characterisation of the photoreceptors described used three separate, genetically modified, yeast strains as described in Chapter 2. For the reporting of light-induced photoreceptor activity the LexA yeast-2-hybrid strain contained an integrated LacZ reporter, whilst the GAL4-based yeast-2-hybrid strain contained an integrated Luciferase reporter gene. Two separate strains were used for the characterisation of opsin photoreceptors, one containing an integrated *FUS1*::LacZ reporter and the other an integrated *FUS1*::Luciferase reporter. The photobiological assay results on these strains are described below, for each photoreceptor. All experimental procedures used in this section can be found in Chapter 2.

3.2.1 dCRY-PER characterisation

Protein formation and the specificity of a blue light-dependent interaction and signalling response between dCRY and PER [194] were confirmed though wavelength specific assays, Figure 3.2A. Neither dCRY or PER alone showed activation of LEXA-promoted transcription of the LacZ reporter as determined on X-gal plates, and the expression of PER protein was confirmed by protein gel blots (data not included). The signalling response shows a low background level of activation and saturation of response after a 1 minute blue light treatment, Figure 3.2C. The interaction between dCRY and PER was fluence-rate dependent with the strongest response being observed with the highest fluence rates, Figure 3.2B.

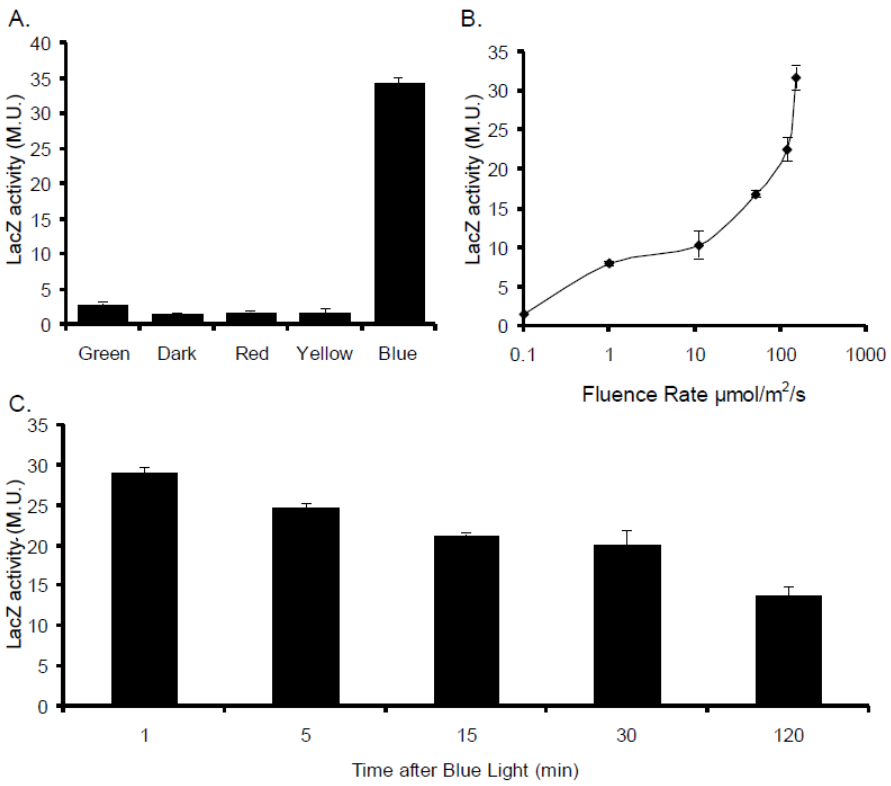

Figure 3.2: Characterisation of dCRY-PER blue-light signalling in *S. cerevisiae*.
S. cerevisiae LexA with integrated LacZ reporter was transformed with dCRY and PER constructs. The beta-galactosidase activity (Miller Units, M.U.) of liquid cultures containing the dCRY2-PER system was assayed after the light treatments shown. A) Wavelength dependence of dCRY-PER interaction, for 5 minute treatments of 100 µE/m^2 fluence rate. B) dCRY-PER fluence-rate response curve, for 5 minute treatments of blue light, with background activity subtracted. C) dCRY-PER duration response for blue light of 100 µE/m^2 fluence rate, with background activity subtracted. All results are averages from 3 biologically independent experiments with error represented as S.E.M.

3.2.2 CRY2-COP1 characterisation

Specificity of a blue light-dependent interaction between CRY2 and COP1 [86] was confirmed through wavelength specific assays, Figure 3.3A. This interaction shows a higher background level than the dCRY-PER interaction and there is a low signalling response to green and red light treatments. Single transformation of the plasmids (either CRY2 or COP1) did not show activation of LEXA-promoted transcription of LacZ, determined on X-gal plates. In contrast to

dCRY, CRY2 showed a strong low-fluence rate response this signalling reponse decreased for intermediate fluence rates, Figure 3.3B. However, at higher fluence rates the response showed variability, ranging from very low levels up to the maximal levels observed for the low fluence rate responses. Like the dCRY-PER system saturation of the response is observed after 1 minute, Figure 3.3C.

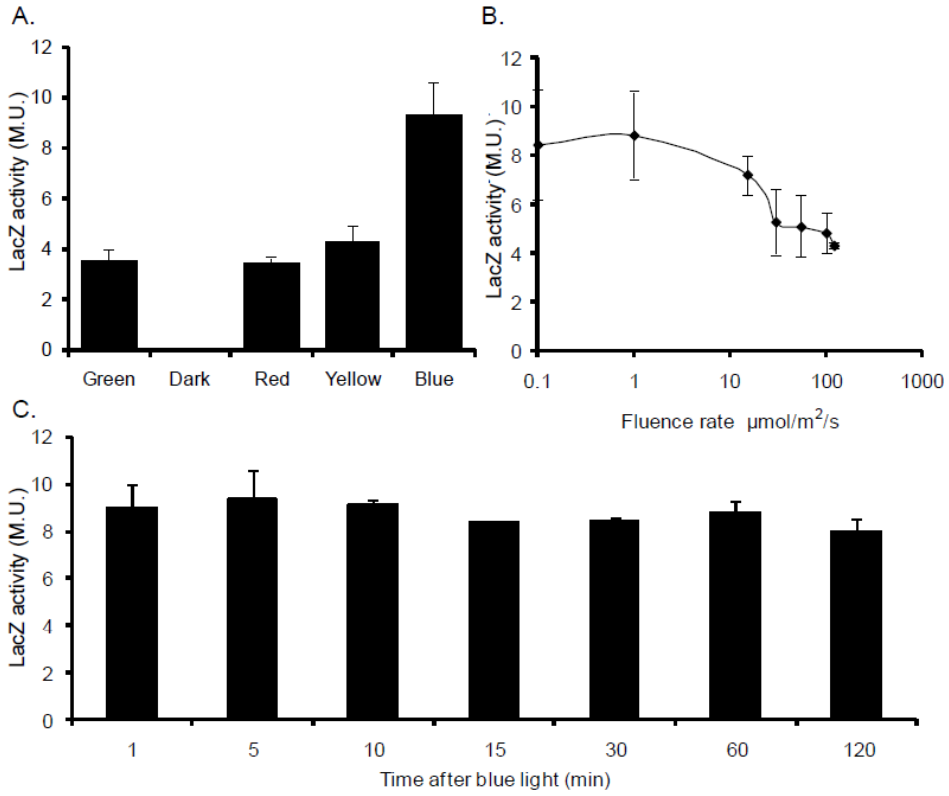

Figure 3.3: Characterisation of CRY2-COP1 blue-light signalling in *S. cerevisiae*.
S. cerevisiae containing LexA and integrated LacZ reporter was transformed with CRY2 and COP1 constructs. The beta-galactosidase activity (Miller Units, M.U.) of liquid cultures containing the dCRY2-PER system was assayed after the light treatments shown. A. Wavelength dependence of CRY-COP1 interaction, for 5 minute treatments of 10 µE/m^2 fluence rate. B. CRY-COP1 fluence-rate response curve, for 5 minute treatments of blue light, with background activity subtracted. C. CRY-COP1 duration response for blue light of 10 µE/m^2 fluence rate, with background activity subtracted. All results are averages from 3 biologically independent experiments with error represented as S.E.M.

The two cryptochrome proteins investigated here offer a major advantage over many photoreceptors as their chromophores, FAD and pterin are both naturally synthesized within the yeast cell and so no external chromophore application is required. Furthermore, their photoreceptor activity, using the described reporter system, can be assayed in both liquid and solid cultures.

3.2.3 OPN4 characterisation

Melanopsin was characterized through the utilization of yeast's pheromone signalling cascade, which was modified to activate LacZ transcription. The strain used in this study lacks the yeast pheromone receptors and contains a humanised Gα subunit, as an integrated modification to the N-terminus of the Gpa1 sequence. This modification has enabled signalling from human GPCR through the yeast pheromone pathway in a previous study [216]. The modification used made the yeast Gα subunit more similar to human Gqα, OPN4 is believed to signal through the Gqα family [215]. To avoid cell cycle arrest, which is normally activated as an output of this signalling cascade [200], the FAR1 gene was knocked out in the strain. Finally the reporter genes LACZ and HIS3 were both expressed from different integrated copies of the *FUS1* promoter.

OPN4 expression from the weak galactose promoter was confirmed through protein blot (Figure 3.4D). Assays with OPN4 were conducted from fresh yeast stocks, as prolonged culture appeared to have an effect on the proteins function regarding its blue-light signalling. This could be due to a number of individual and compounding factors, including protein toxicity and the viability of the highly modified yeast strain used. OPN4 showed a low level of background activity. A clear blue-light response was observed, Figure 3.4A, with an approximately 10-fold

change in signalling response when exposed to blue light compared with darkness. The fluence response (Figure 3.4B) of OPN4 is intermediate to that of the two cryptochromes and again shows a maximal response after 1 minute blue-light pulse, Figure 3.4C.

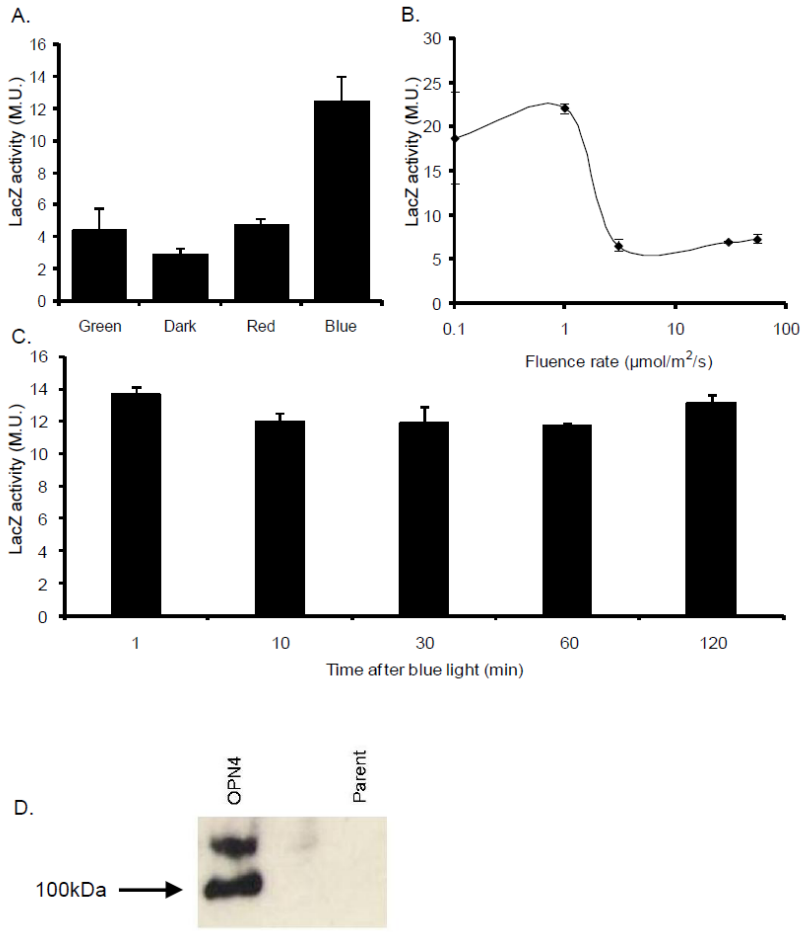

Figure 3.4: Characterisation of OPN4 blue-light signalling in *S. cerevisiae.*
S. cerevisiae harbouring humanised Gαq and lacking any GPCR's (strain BY1172) was transformed with OPN4 construct which contained an N-terminal membrane localisation domain. The beta-galactosidase activity (Miller Units, M.U.) of liquid cultures was assayed after the light treatments shown. A) Wavelength dependence of OPN4 signalling, for 5 minute treatments of 10 µE/m^2 fluence rate. B) OPN4 fluence-rate response curve, for 5 minute treatments of blue light, with background activity subtracted. C) OPN4 duration response for blue light of 10 µE/m^2 fluence rate, with background activity subtracted. All results are averages from 3 biologically independent experiments with error represented as S.E.M. D) Protein blot confirming OPN4 expression in BY1172 yeast.

3.2.4 Channel Rhodopsin 1 but not Channel Rhodopsin 2 links to the native G-protein coupled signalling mechanism in S. cerevisiae

Like OPN4 it was proposed that ChR1 and ChR2 may be characterised through coupling to the yeast pheromone G-protein coupled receptor pathway. Both Channel Rhodopsins are known to form non-specific cation channels in the plasma membrane in *Chlamydomonas reinhardtii* [217, 218] and through structure predictions [220] it is apparent that ChR1 is very similar to that of classical GPCR's. To test this hypothesis ChR1 and ChR2 constructs were transformed and expressed in the BY1172 strain used for the successful expression of OPN4. The reporter *FUS1*::LUC was used as it allows a non-destructive assay of the ChR's activity which could be utilised in a synthetic network. Reporting through the luciferase reporter in yeast was confirmed with the constitutive expression of luciferase from the ADH (ALCOHOL DEHYDROGENASE) promoter (Figure 3.5A, (*ADH*::LUC+)). The background level of expression through the GPCR activated promoter *FUS1* without a GPCR, but with luciferin, is shown in Figure 3.5A (*FUS1*::LUC+). Also, the background level of luminescence from the *FUS1*::LUC strain, with the addition of luciferin and all-trans-retinal or the vehicle for retinal, DMSO, are shown in Figure 3.5A (Gq RET and Gq DMSO respectively) and are of extremely low levels.

For three separate transformations ChR1 signals through the GPCR pathway whilst ChR2 does not (Figure 3.5B). This shows that in *S. cerevisiae* ChR1 can link to the GPCR pathway and suggests that this could be a signalling mechanism used in its native host. Furthermore, this result also indicates that signalling networks of ChR1 and ChR2 are different in *Chlamydomonas reinhardtii*. As ChR2 could not be linked to the transcriptional output associated with GPCR signalling it has no clear applicable function for use in genetic synthetic networks. However, ChR1 can be easily and reliably linked to the GPCR signalling network and therefore a transcriptional output and so could be used for blue-light dependent control of gene expression in a synthetic network. However, due to its channel properties it would not be so easy to control

levels of secondary messenger as changes in internal ion concentration are known to have significant and relevant effects on signalling pathways in yeast [222].

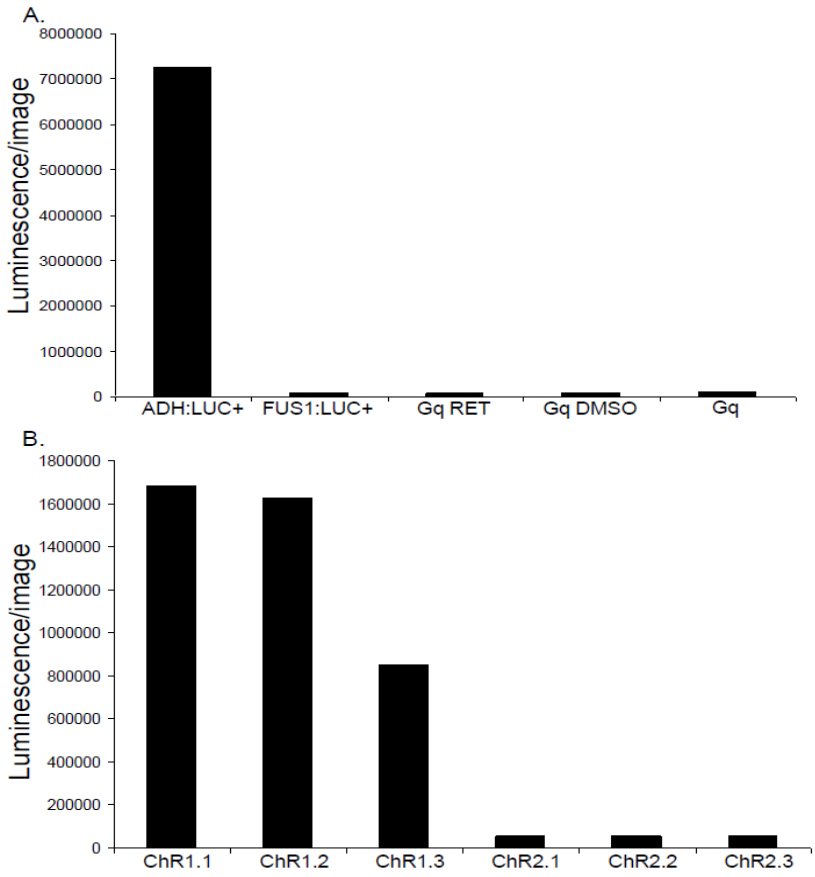

Figure 3.5: Channel Rhodopsin 1 links with the G-protein coupled signalling cascade
S. cerevisiae containing humanised $G_{\alpha q}$ and lacking any GPCR's (strain BY1172) was transformed with either ChR1 or ChR2 constructs which contained an N-terminal membrane localisation domain. The beta-galactosidase activity (Miller Units, M.U.) of liquid cultures was assayed after the light treatments shown. A) Signalling from the FUS1:LUC reporter did not occur without the presence of a GPCR (FUS1:LUC), nor was signalling detected with the addition of all-trans retinal (Gq RET) or DMSO (Gq DMSO) (vehicle for retinal). The use of luciferase as a reporter in yeast is demonstrated through luminescence from the constitutively expressed *ADH1*:LUC reporter. B) Signalling following the expression of ChR1 (with the addition of all-trans retinal) was detected in three separate transformed lines but not ChR2. Background subtracted from each strain.

3.2.5 Using red and far-red light to control Phytochromes for light switchable regulation in S. cerevisiae

Using a system constructed and developed by collaborators in Szeged, Hungary, the PHYA-FHL interaction was confirmed as red-light dependent and far-red light reversible (Figure 3.6). This light-dependent protein interaction, when linked to the yeast-2-hybrid system and with the application of various combinations of red and far-red light pulses could provide fine regulation of downstream signalling. A representative graph is shown in Figure 3.6 where yeast cultures containing the *GAL1*::LUC reporter are imaged on solid cultures. Luciferin is added 17 hours before the light treatments start as luminescence needs to reach a steady state. A 10 minute red-light pulse is given at T=17.30 hours to all cultures, then following either a 1 minute, 30 minute or 1 hour delay a 10 minute far-red light pulse is applied. The cultures exposed only to a red-light pulse show an acute induction in gene expression, and therefore luminescence read-out, and a broad-peak in expression (Figure 3.6, red squares). The cultures which are then exposed to far-red light show a clear inhibition in signalling through this pathway with the 1 minute delay between light pulses showing a much lower level of induction than the cultures with the 30 minute or 1 hour delay (Figure 3.6, filled red diamonds, triangles and crosses respectively). This indicates that the PHYA-FHL interaction is working in a very similar mechanism in yeast as to that in plants [223, 224], with phytochrome undergoing a far-red light reversion from its active form. Further to this it was confirmed that for the strain used, but with independent transformations, light-dependent signalling (originally seen in Szeged) occurred without the addition of the phytochrome chromophore, phytochromobilin [225, 226, 227]. This observation makes the system very attractive for Synthetic Biology as it offers a light-dependent switch, with real time reporting and no requirement for the addition of chromophore.

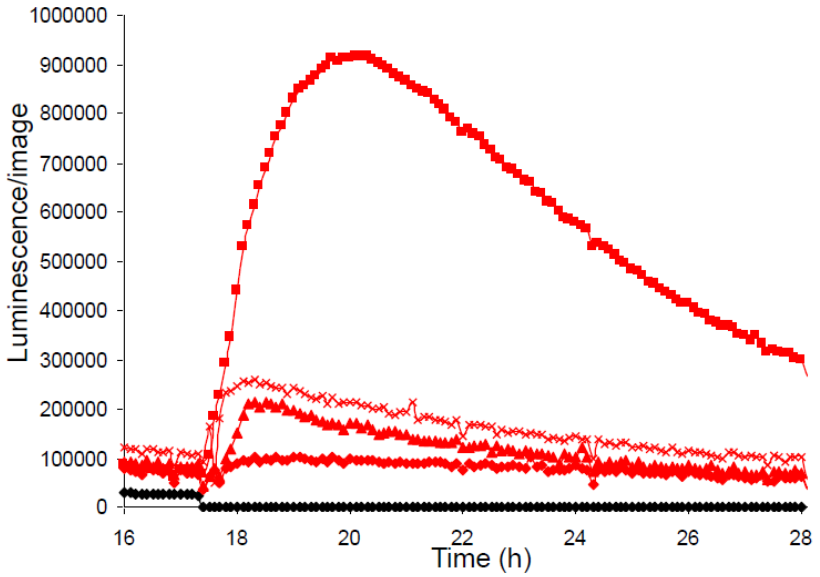

Figure 3.6: PHYA-FHL is a light switchable unit
GAL4 yeast-2-hybrid strain, containing the integrated reporter *GAL1*::LUC was transformed with PHYA and FHL constructs and the light dependent interaction measured in real-time on CCD-cameras. Luciferin was added at T=0 and a 10 minute red-light pulse were given to all strains, except the dark control (black diamonds). No further light-pulses were applied to the red-light control (red squares), and a 10 minute far-red light pulse was applied following either a 1 minute delay (red diamonds), a 30 minute delay (red triangles) or a 1 hour delay (red crosses). Images were collected every 15 minute and background subtracted.

3.2.6 Experimental constraint of parameters for the modelling of the PHYA-FHL interaction

The light switchable properties of PHYA-FHL interaction make it particularly attractive for use in synthetic biology as it provides a mechanism to control the level of induction in a spatial and temporal fashion. Therefore, this system was investigated and characterised further, with O. Sorokina constructing a mathematical model to include the PHYA-FHL signalling properties [197 and Appendix D]. The use of luciferase as the biological marker and the requirement for imaging over prolonged periods of time (potentially days) meant that the liquid culturing of cells was not optimal for this system. This is specifically due to the requirement for agitation of the cells in liquid media to ensure they do not settle on the base of the culturing vessel and enter an

anaerobic state of metabolism. Therefore, growth and imaging on agar plates was used. This experimental set-up requires an additional, experimentally measureable, parameter for the modelling of the system (please see Sorokina *et al* for the details of the model) which is the diffusion rate of the substrate for luciferase, luciferin, away from its point of application on the yeast colony.

The diffusion rate was measured through spacing yeast patches on agar plates 1 cm apart and then applying luciferin to a well in the centre of the plate (Figure 3.7). Continual imaging of the plate enabled the rate of luciferin diffusion through agar to be determined by the time taken for more distant yeast patches to start to emit light (due to luciferase activity). From this the diffusion rate was calculated to be around 3-10 mm/h [197 and Appendix D].

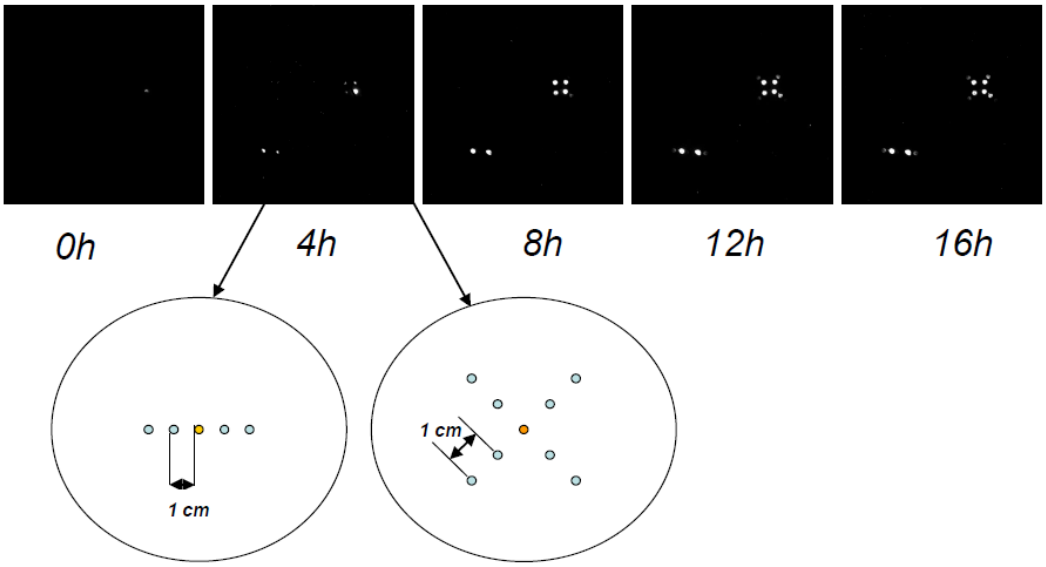

Figure 3.7: Determining parameters for biological modelling of the PHYA-FHL light switchable unit
A) The rate of luciferin diffusion through 1% agar plates was determined by measuring the time taken for *ADH1*::LUC expressing yeast patches spaced 1cm from a central luciferin source and with 1cm between each patch to emit light. Images were captured on a low-light detecting camera every 15 minute for 16 hours. Schematic below the timecourse shows the yeast patch spacing on the agar plates.

3.3 Discussion

This chapter presents the characterisation of a number of heterologously expressed photoreceptors in the eukaryote host *S. cerevisiae.* Photoreceptor activity is confirmed in *S. cerevisiae* and the properties of each photoreceptor characterised with respect to light responses and connection to a heterologous genetic network (Figures 3.2-3.7). The host, *S. cerevisiae*, was chosen as it has a number of advantages compared to prokaryote and multi-cellular eukaryotic hosts. As a single-celled eukaryote the cellular organisation and signalling mechanisms are broadly similar to that of multi-cellular eukaryotes, normally the donors of proteins being investigated, and so the folding and possible modification of proteins is more likely to occur in a similar way. Beyond this *S. cerevisiae* is amenable to genetic and biochemical manipulation and, importantly for this study, can be easily and reliably cultured on agar plates. This offers the potential for temporal and spatial regulation and has enabled the measurement of parameters for mathematically modelling the system (Figure 3.7). Furthermore, the aim for the synthetic oscillator was to build it in a eukaryotic host and therefore the photoreceptors needed to be characterised in the same host.

The characterisation presented in this chapter provides a clear basis for application to synthetic networks and the development of more accurate mathematical models. The investigation has identified a previously unknown signalling pathway used by ChR1 (Figure 3.5) as well as characterised some of the photoreceptor properties of opsins, cryptochromes and phytochrome in *S. cerevisiae*. The different properties seen between the two CRY proteins further highlights the importance of this type of characterisation to enable the development of accurate mathematical models. As the characterisation of components for a eukaryotic oscillator is very limited, most synthetic oscillators are constructed in prokaryotic hosts [228], the kinetics identified through the photoreceptor characterisation will be important for constraining models to biologically relevant parameter space.

The characterisation of the photoreceptors was intended for use in the design and construction of a synthetic oscillator based on the principles of circadian clocks (reviewed in [228]). One of the principles of circadian oscillators is that they can maintain self-sustaining oscillations under constant conditions [1]. However, for a circadian oscillator to be biologically useful it must be able to be informed or entrained by environmental conditions, most commonly via light or temperature cycles [70]. Therefore, the properties and kinetics of the photoreceptors used, in a synthetic oscillator, must be such that they enable entrainment within a biologically relevant timeframe. This timeframe would ideally be less than 24 hours for ease of experimentation, as has been observed in the prokaryotic oscillators [228]. For this aspect, in particular, an accurate and predictive model would be extremely useful. The model for PHYA-FHL interaction matches the dynamics observed experimentally very well (Figure 3.8) and has been used to identify sensitive parameters as well as predict the dynamics of the interaction [197 and Appendix D].

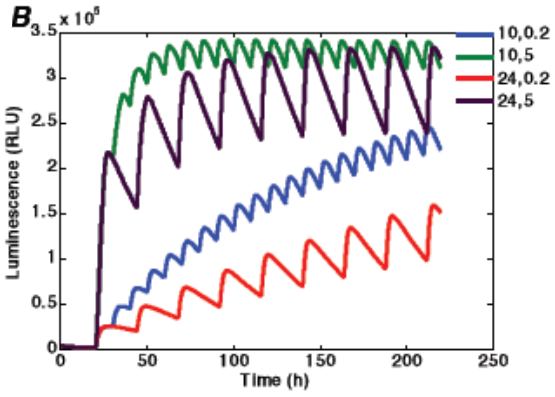

Figure 3.8: Example of model simulation and prediction
The model simulations for varying time intervals between red and far red light pulses as presented in [197]. The Green curve simulates the response for 10 hours between red light (RL) and 5 hours between far-red light (FRL) pulses, the black curve has 24 hours between RL and 5 hours between RL and FRL pulses, the blue curve has 10 hours between RL and 2 minutes between RL and FRL pulses, and the red curve has 24 hours between RL and 2 minute between RL and RHL pulses.

As such, it provides a strong basis to develop and implement an oscillator model. Known circadian oscillators, see Chapter 1 for more detailed information regarding *Arabidopsis thaliana*, are entrained through multiple light inputs, of different wavelengths. Therefore, to try and understand the relative function of these multiple light inputs to a clock network the development of a synthetic oscillator entrained by multiple light inputs would be a powerful tool. It may also aid understanding regarding the relative importance of other entraining factors in natural networks, such as nutrients [126] and possibly light entrainment through non-photoreceptor mediated pathways, as observed in the cyanobacterial circadian clock [75].

Each of the photoreceptor systems investigated has different properties to be considered before application to a synthetic network and these are summarised in Table 3.1.

Photoreceptor	**dCRY**	**CRY2**	**OPN4**	**ChR1**	**ChR2**	**PHYA**
Links to genetic network	✓	✓	✓	✓	X	✓
Low background activity	✓	X	✓	✓	✓	✓
Inducible expression	X	X	✓	✓	✓	✓
Stable expression from plate cultures	✓	✓	X	X	X	✓
Requires addition of chromophore	X	X	✓	✓	✓	X

Table 3.1: Comparison of characterised photoreceptor properties

Generally, the yeast-2-hybrid based systems were more reliably expressed, none of the photoreceptors required the addition of chromophore and there was a direct link with the genetic network. The opsin based systems did require the addition of chromophore, at a relatively high concentration, and so added a further step of manipulation. This is particularly noticeable when using luciferase as an output, as the addition of luciferin is also required. Both of these

compounds alter the pH of the media and therefore the properties of the yeast and specifically the opsin properties as the G-protein coupled cascade is known to be pH sensitive [222]. Further to this opsins are transformed into a highly modified yeast strain which may not be the most suitable platform for further synthetic networks. Whilst the yeast-2-hybrid systems require a co-transformation, these could be made as stable chromosome insertions and therefore the strain is more suitable for further genetic manipulations.

The PHYA-FHL system provides an additional level of control through the switching of PHY forms. Such regulation is attractive for the control of a synthetic oscillator as it provides the possibility of pulse experiments and unusual entrainment regimes. However, such pulse experiments would limit the properties of the synthetic oscillator as the oscillator would have to have a longer period than the switch kinetics of phytochrome in *S. cerevisiae.*

The characterisation presented in this chapter can aid the development of future synthetic networks which require control of genetic networks via light-signalling. Specifically these photoreceptors could be used in the deciphering of mechanisms and properties of entrainment to circadian networks.

Chapter 4

ELF3 has a role in the repression of circadian controlled gene expression

Parts of this work have been published in Current Biology, Dixon *et al,* 2011. The ChIP and light-pulse experiment (Figures 4.7 and 4.8) were conducted by Dr. K. Knox and the imaging experiment (Figure 4.9) by A. Thomson.

4.1 Introduction

The circadian clock mechanism provides robust, ~24 hour biological rhythms throughout the eukaryotes. This core signalling mechanism is entrained through environmental signals, most notably light and temperature (Chapter 1). The circadian clock enables the temporal division of biological processes and has been shown to increase overall plant fitness [136], [137]. The circadian gene circuit in plants is believed to comprise of interlocking transcriptional feedback loops, reviewed in [26], whereby the morning-expressed transcription factors CIRCADIAN CLOCK-ASSOCIATED 1 (CCA1) and LATE ELONGATED HYPOCOTYL (LHY) repress the expression of evening genes, notably *TIMING OF CAB EXPRESSION 1 (TOC1)*. However, in mutants of these genes circadian rhythms are maintained suggesting that this single loop is not sufficient to explain the clock network. The gene network has been expanded to include a number of the other components, including GIGANTEA (GI) and PSEUDO-RESPONSE REGULATORS 9 and 7 (PRR9 and PRR7 respectively) and is currently formed of three proposed loops [45], [46], and [47] with some post-translational regulation [48]. There are a number of other genes, not currently included in this network, the mutants of which confer a strong arrhythmic circadian phenotypes, these include *EARLY FLOWERING 3* and *4* (*ELF3* and

ELF4 respectively) [229, 51], *TIME FOR COFFEE* (*TIC*) [152] and *LUX ARRHYTHMO* (*LUX*) [50].

ELF3 encodes a plant-specific protein of unknown function which was first identified through a mutant screen for altered flowering time [5]. *elf3* plants flower early under long and short days and show arrhythmia only under constant light conditions [230], [185]. ELF3 has been identified to have a role in light signalling to the clock; it acts to repress light signalling during the evening light to dark transition and has therefore been suggested to act as a zeitnehmer [106]. This hypothesis is supported through the light-specific phenotypes *elf3* showed relating to period length and acute light signalling [113]. Furthermore, the ELF3 protein binds to the red-light photoreceptor PHYTOCHROME B (PHYB) [80]. Quantitive Trait Locus (QTL) analysis has also linked ELF3 with the shade avoidance response, an observation which connects well with the PHY based ELF3 phenotypes as it is the ratio of PHY conformations which signal shade avoidance strategies in plants [231, 232].

ELF3 has also been shown to interact with the ubiquitin E3-ligase CONSTITUTIVE PHOTOMORPHOGENIC 1 (COP1) to regulate the stability of GI [85]. Another ELF3 based pathway has been proposed which links the clock and flowering regulation through CCA1, ELF3 and a MADs-box transcription factor SHORT VEGETATIVE PHASE (SVP), signalling to the flowering activator FLOWERING LOCUS T (FT) [179]. In addition to the light and flowering phenotypes ELF3 has been shown to be required for temperature entrainment of the circadian clock, and to function as a repressor of temperature signals in this mechanism. Specifically, ELF3 is involved with the repression of *PRR7* and *PRR9* at high temperature [233]. A role for ELF3 in the thermal regulation of flowering pathways has been identified [234] which could link with ELF3's direct interaction with SVP, as SVP also has temperature and flowering associated phenotypes.

Generally this data suggests ELF3 has a role as a repressor but the expression of *CCA1* and *LHY* is greatly reduced in *elf3* backgrounds, suggesting ELF3 acts as an activator of these light-inducible genes [4], [178].

In this chapter *cca1-11 lhy-21 elf3-4* plants are used to separate the repressive function of ELF3 from its downstream targets *CCA1* and *LHY*. Through collaborative work with K. Knox we demonstrate that ELF3 associates physically with the promoter of *PSEUDO-RESPONSE REGULATOR 9 (PRR9)*, a repressor of *CCA1* and *LHY* expression, in a time-dependent fashion. The repressive function of ELF3 is thus consistent with indirect activation of *LHY* and *CCA1*, in a double-negative connection *via* a direct ELF3 target, *PRR9*. This mechanism reconciles the functions of ELF3 in the clock network during the night, and points to further effects of ELF3 during the day.

This direct link with the circadian clock has been further supported through a subsequent publication [154] and presentation [49] providing evidence for an ELF3/ELF4/LUX complex with LUX also showing association with the *PRR9* promoter by ChIP analysis [154]. The number of protein interacting partners now identified for ELF3 is the largest for any of the plant circadian proteins and strongly suggests that ELF3 is functioning at a signalling hub within this network. Furthermore, it suggests that ELF3's regulation and role in regulation at the post-translational level is of at least equal interest to its regulation by the transcriptional/ translational loops. It is the role of ELF3 at the post-translational level which is investigated in detail in Chapter 5.

4.2 Results

4.2.1 elf3-4 mutation is linked with a distinct set of circadian phenotypes

Hypocotyl growth is a circadian output and can be used as an indicator of clock function [235]. *elf3-4* seedlings show abnormally elongated hypocotyls as the clock-controlled repression of

hypocotyl growth is lost in these plants [185, 229]. To study the interaction between ELF3 and CCA1/LHY the hypocotyl length in loss of function mutant backgrounds was examined. Seedlings were grown under long day (LD) or short day (SD) conditions (18h light:6h dark or 6h light:18h dark cycles respectively) for 6 days on either no-sucrose (black bars Figure 4.1A and 4.1B) or 3% sucrose media (white bars Figure 4.1A and 4.1B) and hypocotyl length was measured on day 7. Hypocotyl lengths are much shorter under LD than SD, as hypocotyl elongation is a physiological response to low light conditions. Generally in LD the presence of sucrose in the media has no effect, the one exception to this is that the *cca1-11 lhy-21* seedlings are slightly shorter on sucrose media, consistent with previous observations on sucrose media [152]. In LD conditions *elf3-4* showed an elongated hypocotyl phenotype, as did *cca1-11 lhy-21 elf3-4* whilst the wild-type ecotype, Wassilewskija (Ws) and *cca1-11 lhy-21* showed hypocotyls of similar length. Under SD conditions this general trend was more apparent. Ws and *cca1-11 lhy-21* seedlings showed hypocotyls of similar length on no-sucrose media and *cca1-11 lhy-21 elf3-4* and *elf3-4* seedlings had very elongated hypocotyls (Figure 4.1B). The presence of sucrose had no effect on the length of *cca1-11 lhy-21* hypocotyls in SD whilst Ws hypocotyls were slightly longer. This slight increase in hypocotyl length relative to no-sucrose in the media was also observed for both the *elf3-4* and *cca1-11 lhy-21 elf3-4*. Images of example seedlings (Figure 4.1C) show the elongated hypocotyl phenotype of *elf3-4* and *cca1-11 lhy-21 elf3-4* compared to Ws and *cca1-11 lhy-21*. This data shows that CCA1 and LHY are not required for the long hypocotyl phenotype of *elf3-4*. It also shows that the effect of sucrose on hypocotyl growth is masked under conditions when seedlings do not experience low-light conditions.

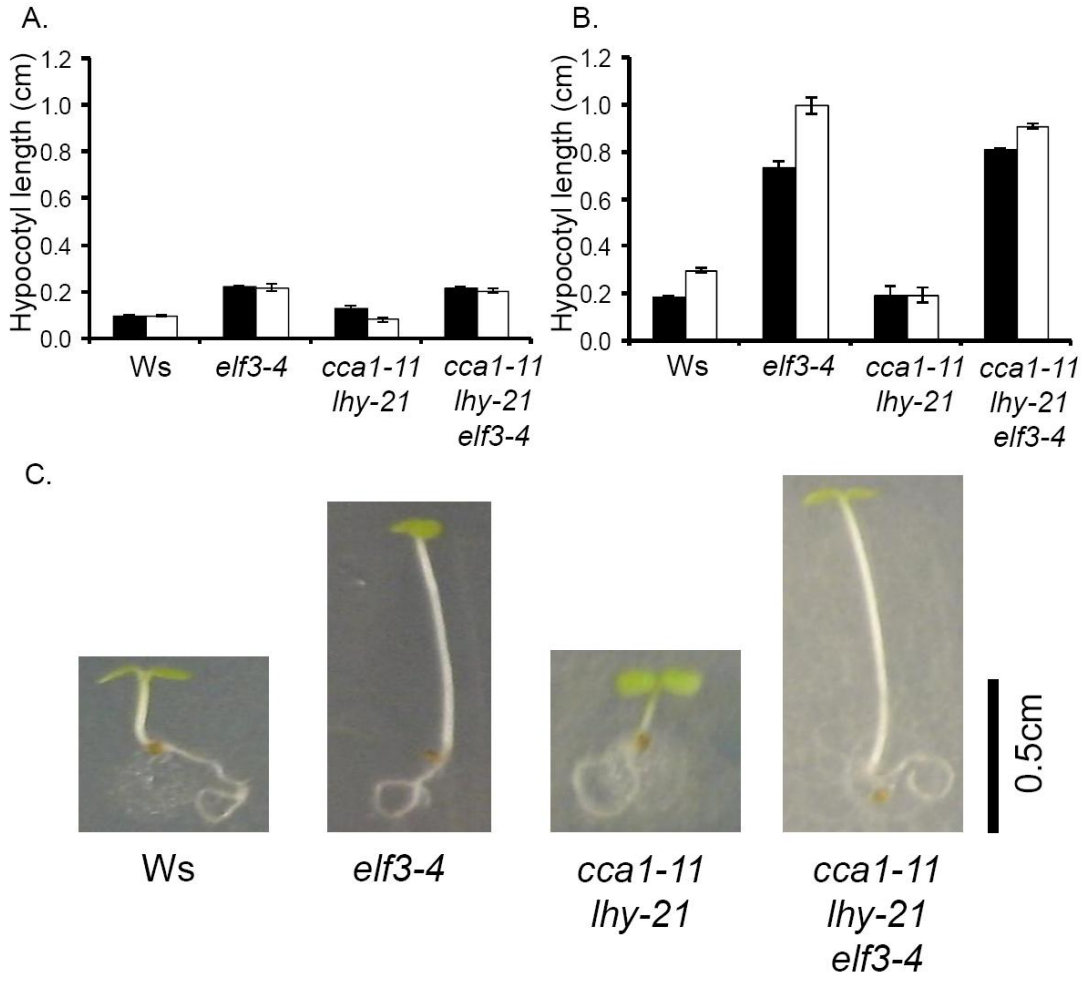

Figure 4.1: Hypocotyl phenotypes of *cca1-11 lhy-21 elf3-4* seedlings
Hypocotyl length of 7-day old seedlings was measured and is shown as an average length of the population with error being represented as SEM. A. Seedlings grown under white light Long Day (18hrs light, 6hrs dark) cycles on either MS media (black bars) Ws n= 15, *elf3-4* n= 11, *cca1-11 lhy-21* n= 18, *cca1-11 lhy-21 elf3-4* n= 12 , or MS supplemented with 3% sucrose (white bars) Ws n= 13 , *elf3-4* n= 17, *cca1-11 lhy-21* n= 15, *cca1-11 lhy-21 elf3-4* n= 15. B. Seedlings grown under white light Short Day (6hrs light, 18hrs dark) cycles on either half MS media (black bars) Ws n=12 , *elf3-4* n= 18, *cca1-11 lhy-21* n= 19, *cca1-11 lhy-21 elf3-4* n= 23 or half MS supplemented with 3% sucrose (white bars) Ws n= 16, *elf3-4* n= 16, *cca1-11 lhy-21* n= 15 , *cca1-11 lhy-21 elf3-4* n=18. C. Example images of 7-day seedlings grown under SD white light cycles on half MS media. Data is from and representative of two biologically independent experiments.

To investigate if the *elf3-4* mutation affected the core circadian network, and was not limited to just a hypocotyl growth phenotype, delayed chlorophyll fluorescence imaging in constant light was used as another circadian marker. Delayed fluorescence allows real-time, non-destructive collection of data from plants which contain no transgenic markers. The method collects the amount of delayed fluorescence light emitted from light-absorbing pigments within the seedling. This delayed fluorescence is under circadian control [236], as can be seen from the rhythmic trace from Ws (Figure 4.2A). Under constant light conditions it is known that *cca1-11 lhy-21* have a short period phenotype [46], this was confirmed through delayed fluorescence imaging (Figure 4.2A) and FFT-NLLS analysis of the traces (Figure 4.2B). The imaging confirmed that like *elf3-4* mutants, *cca1-11 lhy-21 elf3-4* plants were arrhythmic for this physiological marker in constant light (Figure 4.2A, B and C). Data has been plotted as estimated period, from FFT-NLLS, against Relative Amplitude Error (R. A. E.) as this gives an indication of the confidence in robustness of the rhythms. Ws had low R. A. E. values, and therefore robustly rhythmic and the single trace which gave a rhythm to *elf3-4* had a high R. A. E. showing that the rhythm measured is not very robust (Figure 4.2B).

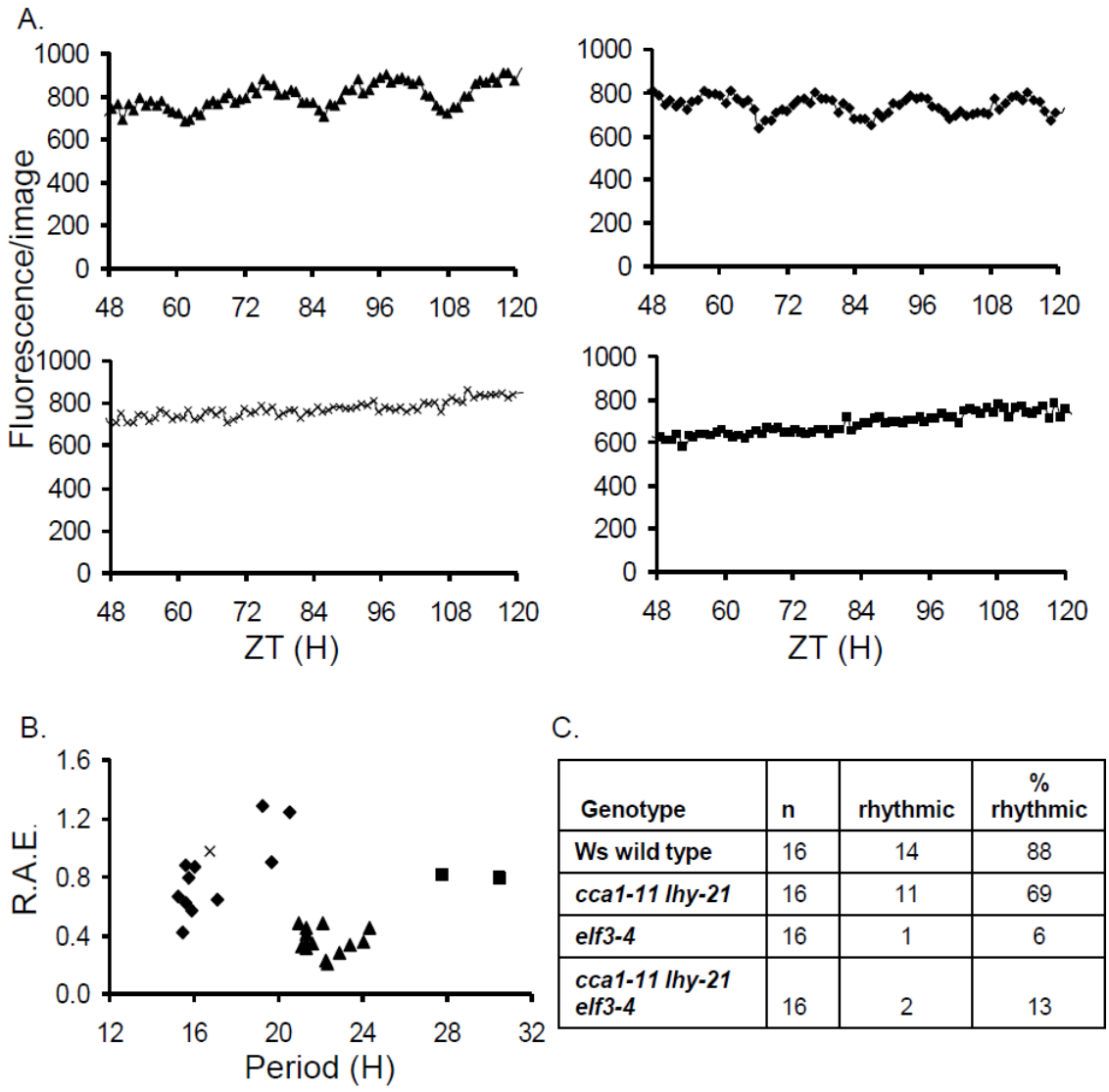

Genotype	n	rhythmic	% rhythmic
Ws wild type	16	14	88
cca1-11 lhy-21	16	11	69
elf3-4	16	1	6
cca1-11 lhy-21 elf3-4	16	2	13

Figure 4.2: Seedlings carrying the *elf3-4* mutation are arrhythmic in constant light
Delayed fluorescence imaging starting on 6-day old seedlings, entrained in 12:12 white light:dark cycles and transferred to constant red and blue light showed that plants with the *elf3-4* mutation are arrhythmic in constant light. A. Example traces of delayed florescence imaging for Ws (filled triangles), *cca1-11 lhy-21* (filled diamonds), *elf3-4* (crosses) and *cca1-11 lhy-21 elf3-4* (filled squares) following transfer to constant light at ZT0. For each genotype n=16 wells imaged, each well containing 4-8 seedlings. B. Period analysis vs relative amplitude error (R.A.E.) determined by FFT-NLLS from the Brassv3 software package from delayed florescence imaging. Ws n= (filled triangles), *cca1-11 lhy-21* n= (filled diamonds), *elf3-4* n= (cross) and *cca-11 lhy-21 elf3-4* n= (filled squares) C. Summary table showing the number and percentage of rhythmic seedlings from the delayed fluorescence imaging. Results are a combination of 2 independent experiments.

4.2.2 CCA1/LHY and ELF3 are involved in reciprocal regulation of transcription

The MYB-transcription factors CCA1 and LHY, form a core part of the current circadian transcriptional/translational network in *Arabidopsis* (Figure 4.3A). *CCA1* and *LHY* RNA expression levels were shown to be very low in *elf3* mutant seedlings, suggesting a mechanism for their arrhythmia [178]. This was confirmed through QPCR analysis on 7 day old seedlings under 12:12 white light:dark cycles (LD) (Figure 4.1), consistent with previous data on plants transferred from 12:12 red LD to constant red light (LL, [153, Appendix B]). The high amplitude of *CCA1* and *LHY* expression rhythms in wild type (100 to 1000-fold in LD, 10-fold in LL) collapsed in the *elf3-4* plants, which became arrhythmic in LL. The light-arrhythmic phenotype is supported by original observations that *elf3* was arrhythmic under constant light [185].

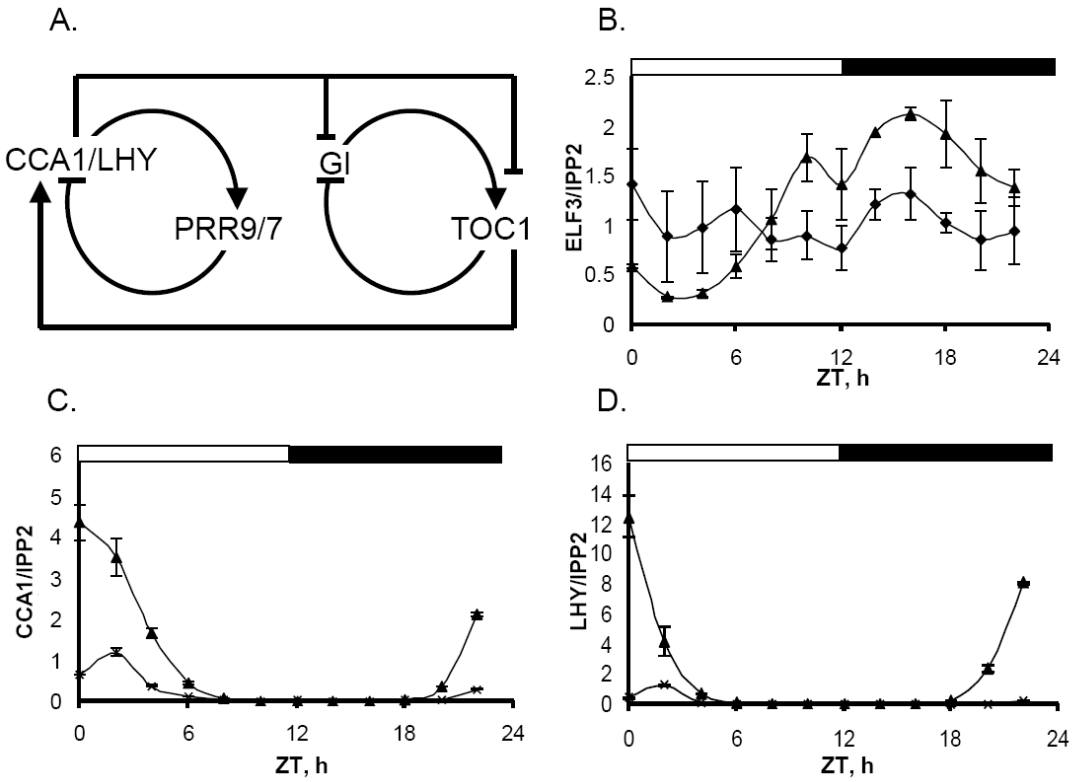

Figure 4.3: Influence of ELF3 and CCA1/LHY on reciprocal gene expression
A. Scheme showing the current hypothesis for the plant circadian network. Activation indicated by arrows, and inhibition indicated by bars. CCA1/LHY and PRR9/PRR7 make a morning loop and GI and TOC1 form an evening loop, the two are joined through CCA1/LHY repression of *TOC1* and TOC1's activation of *CCA1/LHY*. B. QPCR measurements for gene expression of *ELF3* in Ws (filled triangle) and *cca1-11 lhy-21* double mutant (filled diamond) and C. *CCA1* and D. *LHY* in Ws (filled triangle) and *elf3-4* (cross) mutant are normalised between QPCR experiments and against *IPP2* expression. Graphs are an average of two to three biologically independent experiments, with normalised data being used to generate S.E.M. error bars. Seedlings were grown in 12:12 white light:dark and samples taken every 2 hours across a 12:12 cycle starting at ZT=0.

Further to this, although clock function is impaired in the *elf3-4* background (Figure 4.1 and 4.2) this mutant was able to respond relatively normally to light entrainment (Figure 4.4). Figure 4.4 shows that under short day and long day conditions *elf3-4 CAB2*::LUC expression are very similar to Ws *CAB2*::LUC expression, with only the transient responses at changing light conditions which showed differences.

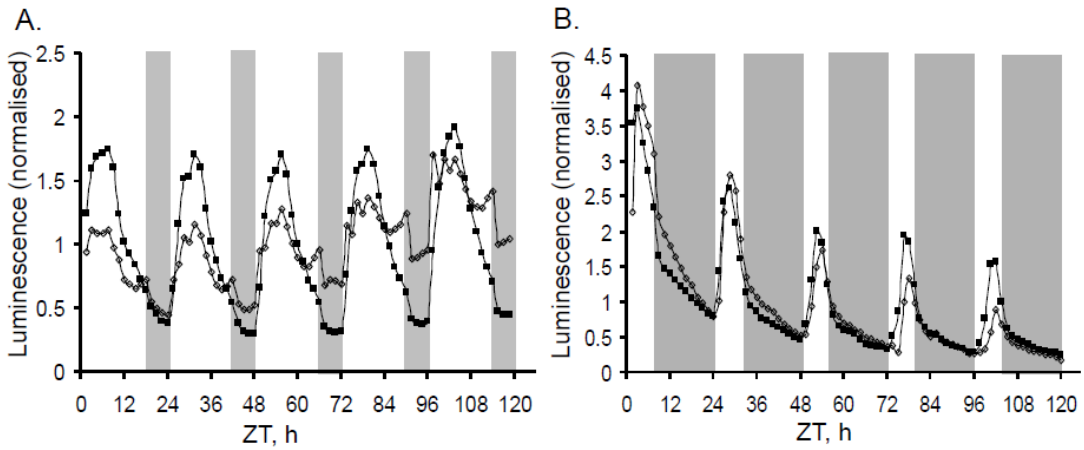

Figure 4.4: *elf3-4* plants are able to entrain to light/dark cycles.
Imaging of *CAB2*::LUC (filled squares) and *elf3-4 CAB2*::LUC (open diamonds) starting on 6-day old seedlings under either A. LD or B. SD conditions. Seedlings were grown in imaging photoperiods under white light and transferred to red and blue lights for imaging. Data has been normalised within each genotype to allow comparison of waveform between the genotypes and is an average of n= 20 (SD), n=13 (LD) seedlings for *CAB2*::LUC and n= 23 (SD), n= 12 (LD) seedlings for *elf3-4 CAB2*::LUC. Data is representative of 2 biologically independent experiments.

This luciferase imaging experiment highlighted that there is still information regarding circadian time in the *elf3-4* mutant under light:dark conditions where any impaired oscillator is being strongly driven. Therefore, transcript analysis under light:dark cycles was more informative than that in constant light conditions where the mutants lost all timing. The low-amplitude rhythm in both *CCA1* and *LHY* transcripts ([153, Appendix B]) showed that the clock's morning functions were severely impaired in the *elf3-4* mutant, though a rhythm could still be driven by the LD cycle. *ELF3* RNA levels had a lower-amplitude rhythm in the wild type (at most 10-fold in LD), whereas in *cca1-11 lhy-21* mutants *ELF3* RNA showed little or no rhythmicity under LD and arrhythmia under LL (Figure 4.1B and Appendix B). Circadian control of *ELF3* expression [178] requires the morning loop components CCA1 and LHY. ELF3 in turn regulates these clock genes, as well as gating entrainment signals [106].

4.2.3 ELF3 is involved in the dark regulation of circadian controlled genes

An evening loop, involving at least *TOC1* and *GIGANTEA* (*GI*) and possibly *LUX ARRHYTHMO (LUX)*, is proposed to generate the short-period rhythms observed in *lhy cca1* double mutants [46]. Through the comparison of clock gene expression in Ws, *elf3-4*, *cca1-11 lhy-21* and *cca1-11 lhy-21 elf3-4* plants, the role of ELF3 in this proposed evening loop was investigated. Plants were grown under 12:12 light:dark cycles for 6 days, sampled on day 7, and tested for expression of *PRR9*, *PRR7*, *GI*, *LUX* and *TOC1* (Figure 4.5). In *cca1-11 lhy-21* plants the evening genes (*TOC1*, *LUX* and *GI*) showed an early morning peak of high amplitude (Figure 4.5C, 4.5D, 4.5E). This is in agreement with previously published data [46, 237, 238] and also supports the hypothesis that CCA1 and LHY act to repress evening gene expression in the early morning. In the double mutant, *PRR9* showed a lower amplitude rhythm, probably due to loss of expression activation from CCA1 and LHY (Figure 4.3A). The *elf3-4* mutant showed a lower amplitude rhythm in gene expression for all measured genes, with notably higher levels (over ten-fold increase compared to wild type) of *PRR9*, *PRR7* and *GI* expression in the night, as reported in [184] for *GI*, as well as slightly higher night-time expression of *LUX* and *TOC1*. The aberrant gene expression continued into the early morning, when CCA1 and LHY should be active in the wild type (Figure 4.3C and 4.3D).

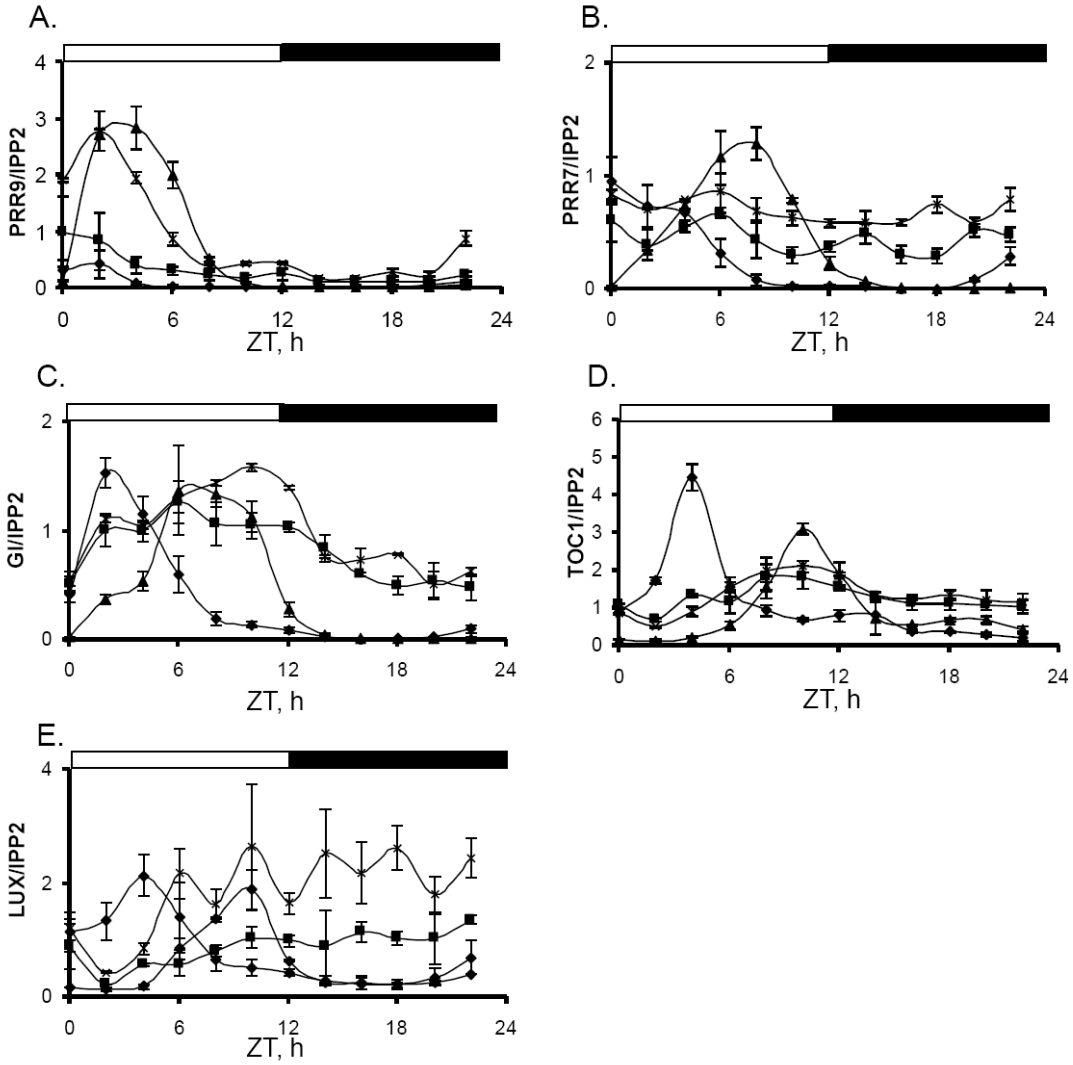

Figure 4.5: ELF3 is a regulator of the expression of core circadian genes.
QPCR measurements for A. *PRR9*, B. *PRR7*, C. *GI*, D. *TOC1*, E. *LUX* normalised between experiments and against *IPP2* in Ws (filled triangles), *elf3-4 (cross)*, *cca1-11 lhy-21* (filled diamonds) and *cca1-11 lhy-21 elf3-4* (filled squares). Graphs are an average of three biologically independent experiments each containing a triplicate of samples. Normalised data used to generate S.E.M. error bars. Seedlings were grown in 12:12 white light/dark cycles and samples were taken every 2 hours starting at ZT0 for one cycle. The Figure is shown on a logarithmic scale in Appendix B.

Such results are consistent with a combination of indirect and direct mechanisms, whereby CCA1 and LHY repress evening gene expression in the morning (Zeitgeber time (ZT) 0-4, where ZT0 is defined as the time of lights-on) and ELF3 represses many genes at night (ZT 12-

20), before *CCA1* and *LHY* are expressed. From this it could be expected that the *cca1-11 lhy-21 elf3-4* triple mutant would show high expression of certain clock genes throughout the light:dark cycle. This was not observed. Instead in the triple mutant, all genes were expressed at intermediate levels, without strong responses to the ongoing LD. *PRR9* and *PRR7* expression was higher than in *cca1-11 lhy-21,* but lower than in *elf3-4*. Evening genes (*TOC1*, *LUX* and *GI*) lost the early peak observed in *cca1-11 lhy-21*, but then had the higher night-time expression characteristic of *elf3-4*. This suggests that ELF3 influences the circadian network at more than one point and thus affects both morning and evening loops.

4.2.4 ELF3 binds in vivo to the promoter of PRR9 in the early night.

As *ELF3* shows some sequence homology with transcription factors [80] and affects gene expression, ELF3's ability to physically associate with circadian-controlled promoters was investigated. Chromatin Immunoprecipitation (ChIP) experiments were conducted using transgenic *elf3-4* plants that expressed an *ELF3::YFP* fusion protein from either the native *ELF3* promoter or from the 35S*CaMV* promoter. Period analysis, from delayed fluorescence imaging of these lines under constant light, showed that *ELF3* expression was complementing the *elf3-4* mutant phenotype and that in *35S*::ELF3::YFP over-expression did cause a slight increase in period length (Figure 4.6).

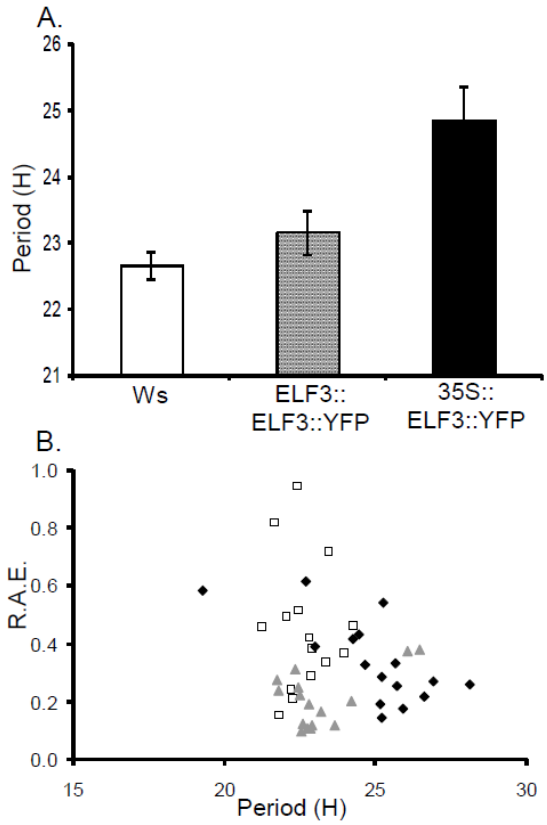

Figure 4.6: Characterisation of ELF3::YFP lines used in ChIP
A. Delayed florescence imaging of Ws, *elf3-4 ELF3*::ELF3::YFP and *elf3-4 35S*::ELF3::YFP, 6 day old seedlings entrained in 12.12 white light:dark cycles and released into constant red and blue light. Data for each genotype is from 16 wells with each well containing 4-8 seedlings. Period analysis by FFT-NLLS confirms that *elf3-4 ELF3*::ELF3::YFP has a similar period to Ws and that the *35S*::ELF3::YFP is slightly long period. B. Data rhythmicity assessed through Relative Amplitude Error (R. A. E.) plotted against period, Ws (open squares), *elf3-4 ELF3*::ELF3::YFP (grey triangles) and *elf3-4 35S*::ELF3::YFP (black diamonds). Data is an average of two biologically independent experiments and error is represented as SEM.

35S::ELF4::YFP was also used in the ChIP to investigate whether ELF3 and ELF4 act on the same promoters. *EARLY FLOWERING 4 (ELF4)* is a circadian controlled gene which shows similar gene expression patterns and clock phenotypes to ELF3 [51]. ELF3 and ELF4 were both able to associate with the *PRR9* promoter (Figure 4.7B and [153, Appendix B]). However, when ELF3 was expressed from its native promoter, it showed time-dependent affinity for the *PRR9* promoter, being bound at ZT14 but not significantly (by Students t-test) at ZT6 (Figure 4.7C). ELF3's apparently rhythmic association with the *PRR9* promoter and the increased *PRR9* expression observed in the *elf3-4* mutant suggest that ELF3 acts as one of the repressors of *PRR9* gene expression. Association of ELF3 with the *PRR7* promoter was weak, as it was detected only in the *35S*::ELF3::YFP plants (Appendix B). Association of ELF4 with *PRR7* was comparable to results for *PRR9* (Appendix B). Testing 1.3kbp of sequences upstream of the ATG codon of *CCA1* did not reveal any ELF3 or ELF4 association (data not shown), although this promoter fragment is sufficient for rhythmic transcription [181]. However, de-repression of the *PRR9* promoter is sufficient to explain low levels of *CCA1* and *LHY* expression in the *elf3-4* mutant (Figure 4.3C and 4.3D), because PRR9 is a known repressor of *CCA1* and *LHY* [106]. The promoter regions required for rhythmic expression of *PRR5*, *TOC1* and *GI* were also tested and ELF3 and ELF4 were not found to associate with these (data not shown), suggesting that ELF3 is involved in the regulation of their expression indirectly.

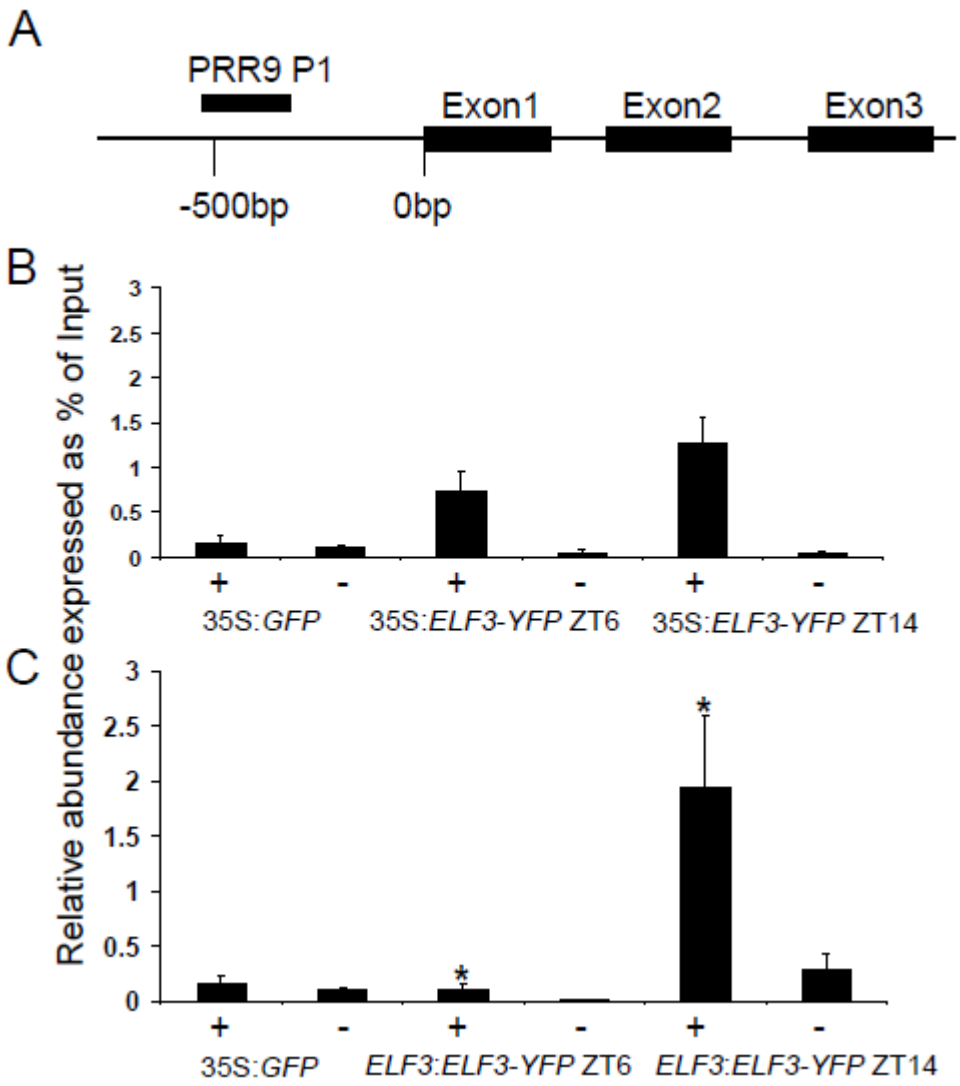

Figure 4.7: ELF3 binds in vivo to the promoter of *PRR9* in the early night but not during the day.

A. Scheme of the *PRR9* genomic region tested. The black bar indicates the position of the primers which amplified the ChIP DNA. B-C. Chromatin of 3 week old seedlings was immunoprecipitated using either no antibody (-) or anti-GFP antibody(+). Resultant DNA from *35S*::GFP (B-C), *35S*::ELF3::YFP (B) and *ELF3::*ELF3::YFP (C) was analysed by QPCR and each sample expressed as a percentage of the non-immunoprecipitated DNA (Input) extracted from the same tissue sample. Bars represent the mean of at least six samples taken from 3 independent ChIP experiments. Error bars represent the SEM. Significant differences, by Students t-test are indicated by the *.

4.2.5 A combination of repressors are required for the control of circadian regulated light responses

In order to investigate the role of ELF3, linking with its known function in light signalling, a 20 minute white-light pulse was applied to seedlings entrained in 12:12 white light:dark cycles and released into darkness. *PRR9* and *GI* were specifically investigated as they have both been implicated in light-signalling to the clock [99], [114], and showed mis-regulation of gene expression in the *elf3-4*, *cca1-11 lhy-21* and *cca1-11 lhy-21 elf3-4* mutants and represented the morning and evening loops of the circadian network. Wild-type plants showed strong light induction of *PRR9* (Figure 4.8A). In *cca1-11 lhy-21* double mutants, the expression levels of *PRR9* were very low and a clear acute response to light was observed, which was as large or larger than that in Ws during the predicted night, ZT38 (Figure 4.8A). In *elf3-4* and *cca1-11 lhy-21 elf3-4* seedlings, *PRR9* had a higher level of basal expression, consistent with Figure 4.5A. Little change in expression was observed following a light pulse at either predicted day ZT30 or night ZT38 (Figure 4.8A). Notably, the *PRR9* expression level was not maximal compared to peak levels (Figure 4.5A), suggesting that another factor is involved in the gating of light responses in the dark. *GI* expression was not light-responsive at these times in Ws, showed light induction in *cca1-11 lhy-21*, but not in *elf3-4* and the triple mutant (Figure 4.8B). This again indicates that ELF3 affects clock gene expression both in darkness and in response to light, that ELF3 still controls clock genes in *cca1-11 lhy-21* seedlings, and that some repressive functions remain in the triple mutant.

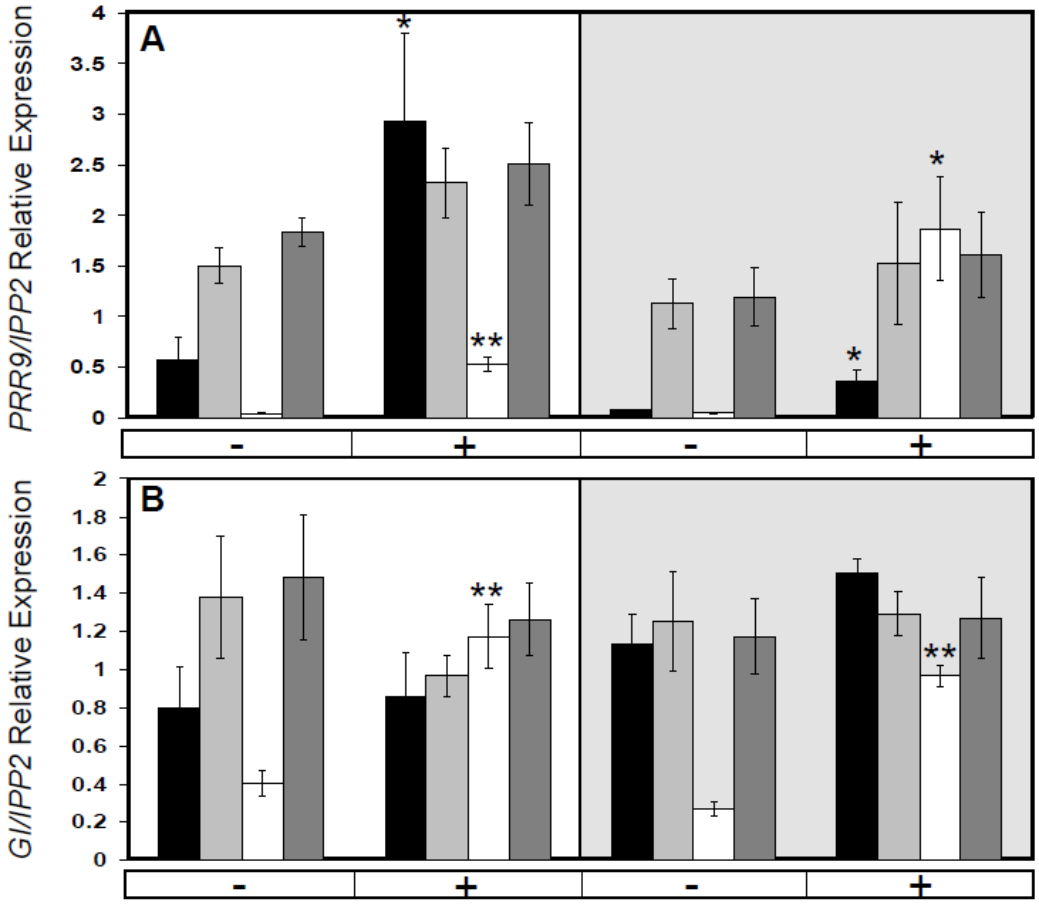

Figure 4.8: ELF3 is required for the control of circadian regulated light responses in *GI* and *PRR9*

Acute light-induction of *PRR9* (A) and *GI* (B) gene expression was measured by QPCR in Ws (black bars), *elf3-4* (light grey bars), *cca1-11 lhy-21* (white bars) and *cca1-11 lhy-21 elf3-4* (dark grey bars). Seedlings were grown for 5 days under white light 12:12 L:D cycles and released into continuous dark from ZT12 on day 5. On day 6, samples were either treated with (+) or without (-) a white light pulse (20 minute, 80 μE/m^2)1 hour before sampling in the predictive day at ZT30 (white background) and predictive night at ZT38 (grey background). Significance by Students t-test is indicated by *.

4.3 Discussion

This work aimed to further understand the role of ELF3 in the circadian network. ELF3 was known to affect *CCA1/LHY* expression and this was investigated through measuring transcript levels in *cca1-11 lhy-21 elf3-4* plants. To investigate a mechanism for this regulation, ELF3's association with canonical clock components promoters was also tested. Figures 4.3 and 4.5 showed that ELF3 has repressive effects on several clock genes. The observed activation of *CCA1* in *elf3-4* mutants can be explained consistently with ELF3's repressive function, by a double negative effect *via* PRR9, the repressor of *CCA1* and *LHY* (Figure 4.9).

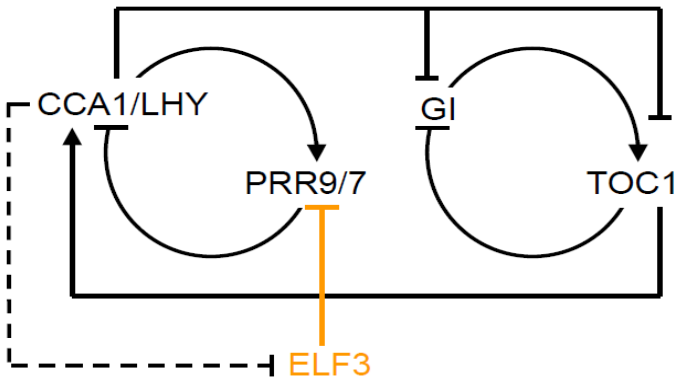

Figure 4.9: Scheme showing the current 3-loop plant circadian network with the addition of ELF3
Scheme showing a current hypothesis for the plant circadian network, activation is represented by arrows and repression by bars. CCA1/LHY and PRR9/PRR7 make a morning loop and GI and TOC1 form an evening loop and the two are joined through CCA1/LHY repression of *TOC1* and TOC1's activation of *CCA1/LHY*. From work presented in this chapter ELF3 is proposed to repress the expression of *PRR9* and possibly *PRR7* and is represented in orange.

ELF3 protein associates with the *PRR9* promoter (Figure 4.7). This finding has been supported by another recent publication [154] and presentation [49] which showed ELF3 forming a complex with EARLY FLOWERING 4 (ELF4) and LUX [49] and that LUX can associate with *PRR9* promoter [154]. In *elf3-4* the levels of *PRR9* are high and so the repression of *CCA1* and *LHY* is greater. This logic can also be applied to the observed similarity between *elf3* mutants and over-expression of CCA1. In both of these backgrounds it can be anticipated that the levels

of PRR9 are high and so the circadian mechanism becomes stalled around the same point [155, 238]. However, high *PRR9* levels are not sufficient to explain the observed arrhythmia seen in these backgrounds under constant light (Figure 4.10). The arrhythmia in these lines could conceptually be linked with the role both of the proteins have in light signalling. In CCA1-ox the light signalling path could be considered to be over-activated and in *elf3* under-repressed, resulting in the same output. This output would be the stalling of the clock through the evening phase.

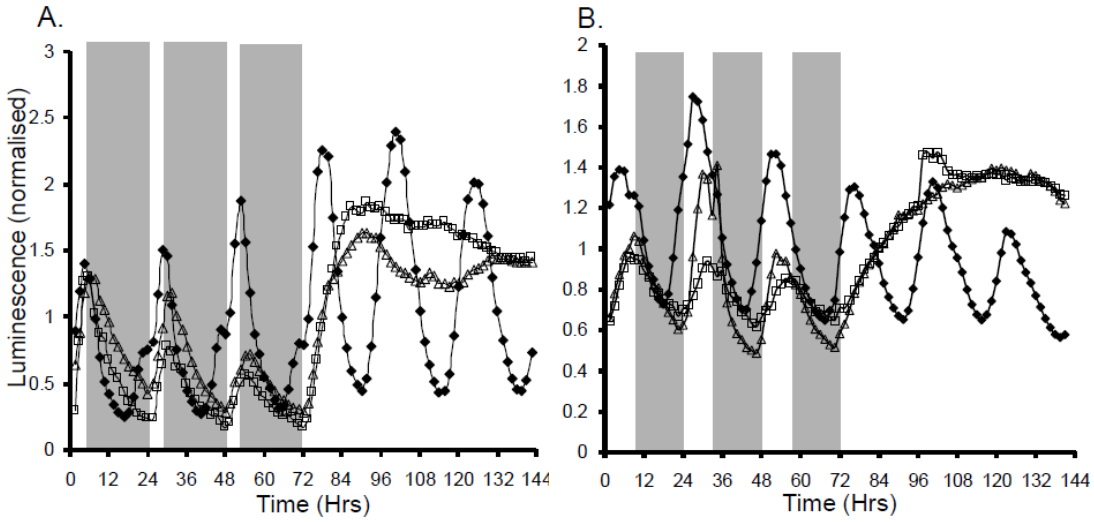

Figure 4.10: *CCA1*-overexpression and *elf3-4* have similar *CAB2*::LUC expression
7-day old seedlings entrained under the respective white light:dark cycles A. 3L:21D and B. 9L:15D were imaged under red and blue light for 3 days under photoperiod conditions before being released into constant light (LL). In A. *CAB2*::LUC (filled diamonds) n=18, *CCA1*-ox *CAB2*::LUC (open triangles) n=21 and *elf3-4 CAB2*::LUC (open squares) n= 23 and in B. *CAB2*::LUC (filled diamonds) n=23, *CCA1*-ox *CAB2*::LUC (open triangles) n=18 and *elf3-4 CAB2*::LUC (open squares) n=23. Data from experiments in Millar group database; conducted by A. Thomson.

The high expression of evening genes *GI* and *TOC1* in *elf3-4* mutants cannot simply be explained due to low levels of CCA1 and LHY, as this high baseline was not observed in *cca1-11 lhy-21* mutants.

To investigate the role of ELF3 independently of the influence of CCA1 and LHY we generated *cca1-11 lhy-21 elf3-4* plants. These plants have a growth phenotype similar to the *elf3-4* plants (Figure 4.1). *cca1-11 lhy-21 elf3-4* mutants show high basal levels of clock gene expression in the dark period of 12:12 LD cycles, as in *elf3-4*, but do not show the characteristic early peaks of *PRR7, GI, LUX* and *TOC1* expression observed in *cca1-11 lhy-21* (Figure 4.5). This high night gene expression is also observed in the acute light pulse responses (Figure 4.8). Thus through comparison of the *cca1-11 lhy-21* and *cca1-11 lhy-21 elf3-4* data it seems that ELF3 allows rhythmicity in the *cca1-11 lhy-21* double mutant. It also suggests that there maybe another, normally redundant factor which is able to take the role of CCA1/LHY in the early morning (ZT0-4) and repress the expression of circadian genes. This function is not observed in the *cca1-11 lhy-21* double mutant as the component is still being repressed by ELF3.

ELF3 is capable of binding to the *PRR9* promoter (Figure 4.7) and possibly *PRR7* promoter [153, Appendix B], and as the PRRs can function as repressors [155], proteins of this family can be considered candidates for the additional repression of *GI* and *TOC1* genes, in the *cca1-11 lhy-21 elf3-4* triple mutant.

Association with the *PRR9* promoter provides a mechanism for ELF3's direct (*PRR9*) and indirect (*CCA1/LHY*) effects on the clock network. The fact that ELF3 affects the clock network beyond the times when ELF3 is detected at the *PRR9* promoter is consistent with the known complexity of the clock circuit.

ELF3 is known to have a number of binding partners, including the red-light photoreceptor PHYB, the ubiquitin E3-ligase COP1, and clock-related proteins GI, SVP, CCA1, ELF4 and LUX suggesting that ELF3 may function in large signalling complexes. In this setting, ELF3 could participate in protein degradation [85] or transcriptional control, through transcriptional complexes or histone/chromatin modifications. Such an interpretation is supported by the mild

phenotypic effect of the ELF3-overexpressor on the clock network ([26] and Figure 4.6) compared to the severe effect of the mutant: the ELF3 protein is required for correct clock function but its level might not be so important.

This work identifies ELF3 as repressing gene expression of clock components, resulting in widespread effects on the clock gene network. Thus ELF3 is essential for the operation of the circadian transcriptional/translational feedback loops in light-grown plants, as reported in dark-grown seedlings [233]. The mechanism of ELF3 action presented here (Figure 4.9) links to ELF3's rhythmic repression of light signalling to the clock, as well as identifying ELF3's direct link to the circadian network.

Chapter 5

Investigating the structure of protein networks involved in ELF3 regulation

The work presented in this chapter has been conducted under the supervision of and in collaboration with Dr. N. S. Savage (Duke University).

5.1 Introduction

EARLY FLOWERING 3 (ELF3) was one of the first genes to be associated with plant circadian rhythms but its function has remained unclear as introduced in Chapter 4. The results from Chapter 4 aid the understanding of where ELF3 links to the circadian network and also begin to indicate possible protein functions; those associated with DNA binding, including direct transcriptional regulation, proteolysis or chromatin regulation. Understanding ELF3 protein function has been hampered by its lack of sequence homology with any known protein families and by its occurrence only in lineages of flowering plants [185]. The theronine-serine rich domain suggests a possible role as a novel type of transcription factor, but this has yet to be supported experimentally [80]. Furthermore, during the past two years a large number of publications have identified protein interacting partners with ELF3, these include proteins involved in the clock (CCA1, GI, ELF4 and LUX), flowering regulation (GI, SVP, ELF4 and LUX) and protein degradation (COP1) [179, 239, 85, 49]. Given that some of these proteins also have a large number of interacting partners, the existence of multi-protein complexes involved in the temporal regulation of gene expression is looking increasingly probable. Thus, understanding the dynamics of complex formation and separation will be essential in understanding circadian rhythms.

To try and gain understanding of ELF3's function an aspect of its interacting network has been investigated in this chapter using a dual approach of mathematical modelling and experimentation.

Mathematical modelling offers a variety of methods for investigating biological networks which are not available, or easily achievable, experimentally. Firstly, it enables the systematic investigation of a number of different networks. Such investigation, if possible in the lab, would be extremely laborious. Secondly, it enables complex networks, such as the circadian clocks interlocking negative feedback loops, to be understood at each stage through the ability to simultaneously track all of the modelled clock components as well as the behaviour of the oscillator. Modelling enables rigorous testing of ideas on a simplified representation of the organism under investigation, which, as long as the modelling assumptions are 'reasonable', can indicate at mechanisms and guide experimentation. As such, mathematical modelling provides a useful tool in the understanding of biological networks and has aided understanding of the plant circadian network [168, 45, 46, 47, 48, 240]. However, mathematical modelling does have limitations, most notably the flexibility of the network with increasing numbers of parameters and the setting of these parameters in the absence of experimental data [241].

The network developed and investigated in this chapter is based on work presented in Yu *et al*, 2008 [85] and extended to include the protein interactions from Wang *et al*, 2001 [86] and Kim *et al*, 2007 [81]. This provides a network of 6 protein species; ELF3, GI, COP1, CRYPTOCHROME 1 (CRY1), CRYPTOCHROME 2 (CRY2) and ZEITLUPE (ZTL). ELF3 has already been introduced in Chapter 4. GI is a large protein (137 kDa) of unknown function, but from genetic analysis it has a positive role in activating the photoperiodic flowering pathway and is central to the correct function of the circadian clock. GI protein levels do not simply track that of its rhythmic mRNA expression as when GI is over-expressed the GI protein is still rhythmic [164]. Evidence presented in [85] indicates that some of the rhythmicity of GI protein

levels occurs through its interaction with ELF3 and COP1. COP1 is an E3-ubiquitin ligase with RING-finger and WD-40 domains and functions to target proteins for degradation by the 26S proteasome [242]. In particular, proteins required for photomorphogenesis are targeted for degradation by COP1 [243]. CRY1 and CRY2 are blue-light photoreceptors (Chapter 3) believed to function in a partially redundant fashion in plants and are also important for flowering regulation and entrainment of the clock [71]. These photoreceptors have been shown to interact with COP1 and are believed to prevent it from functioning in the light [86]. In turn, COP1 is thought to degrade both CRY1 and CRY2 in the dark [86]. Finally, ZTL (ADO1 or LKP1) is a member of a small family of blue-light photoreceptors [74] that contain a PAS/LOV (Light Oxygen Voltage) domain which binds FMN (flavin mononucleotide) as its chromophore. ZTL also contains an F-box domain which enables function in proteasome mediated degradation via Skp/Cullin1/F-box-type E3-ligase complex, and 6 kelch repeats which are involved in protein-protein interactions [74]. ZTL has been shown to be a blue-light dependent regulator of protein stability for three circadian proteins TIMING OF CAB EXPRESSION (TOC1), PSEUDO RESPONSE REGULATOR 5 (PRR5) and GI [81, 11].

Through imaging of *ELF3*::ELF3::YFP fusion proteins and the development of a mathematical model, evidence is collected that suggests ELF3 has an important role in protein degradation. Linking this work with published data [85] suggests that ELF3-mediated protein degradation directly affects the clock mechanism.

5.2 Results

5.2.1 ELF3 is expressed throughout the plant

ELF3 expression is under clock control ([185] and Chapter 4); however, there is no information regarding *ELF3* expression localisation patterns *in planta*. Using promoter::luciferase transgenic lines the tissue-specificity of *ELF3* expression was investigated in comparison with other clock-controlled genes. As the circadian network is believed to exist in every cell it could be expected that the expression localisation patterns of the clock genes would be very similar. However, this was not observed. Luciferin was added at the roots of seedlings containing clock promoter::luciferase fusion tags and luminescence was collected for 20 minutes (Chapter 2). The intensity of luminescence is represented in a heat-map with red being high levels through to black which is low levels (Figure 5.1). The expression of *ELF3*::LUC (Figure 5.1D) is located predominately in the veins of the leaf whilst the expression of *LHY*::LUC (Figure 5.1B) is much more dispersed. *ELF3*::LUC expression is also different from *PRR9*::LUC (Figure 5.1A) which was observed to be less expressed in the leaf veins. The expression pattern of *ELF3*::LUC was similar to that of *TOC1*::LUC (Figure 5.1C) which showed very clear vein expression as well as expression in all other tissue types. The different expression patterns observed supports the future use of luciferase as a sub-cellular marker, which offers the notable advantages of being used in live plants. Expression patterns were not notably changed when plants had been grown under either blue or red light, for the resolution provided by this analysis.

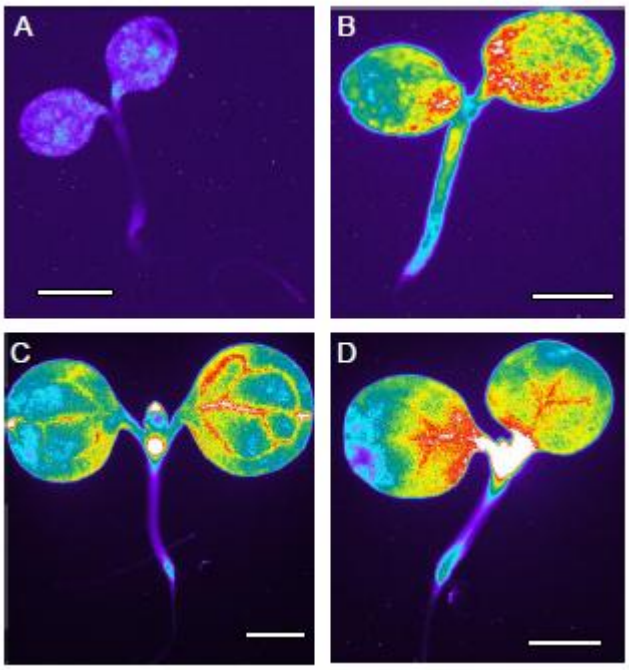

Figure 5.1: Expression patterns of clock controlled gene expression
Arabidopsis thaliana seedlings were entrained in 12:12 white light:dark cycles for 6 days and a single post-spray luminescence image was captured at times of expected peak expression for each of the following transgenic lines, A. ZT0 *LHY*::LUC, B. ZT0.30 *PRR9*::LUC, C. ZT10 *ELF3*::LUC, D. ZT12 *TOC1*::LUC on cooled CCD- camera attached to a Zeiss fluorescence microscope. 2.5x objective used for all images and scale bar is on each image, a pseudo colour map has been applied for ease of distinguishing gradients of expression ranging from purple for low expression to white for very high. Each image has at least two biologically independent repeats.

5.2.2 ELF3 protein is found in all plant tissues and forms distinct nuclear speckles

Previous protein work to measure ELF3 has required nuclei enrichment of the tissue samples and either a direct anti-ELF3 antibody [80] or incubation with the proteasome inhibitor MG132 [85]. As such, any information regarding tissue specificity of the protein or sub-cellular distribution is lost. To investigate the sub-cellular distribution of ELF3 an *elf3-4 ELF3*::ELF3::YFP transgenic line was used which allows native expression of ELF3 tagged with YFP. The lines were confirmed to have normal clock behaviour through *CCA1*::LUC imaging in constant light (Figure 5.2).

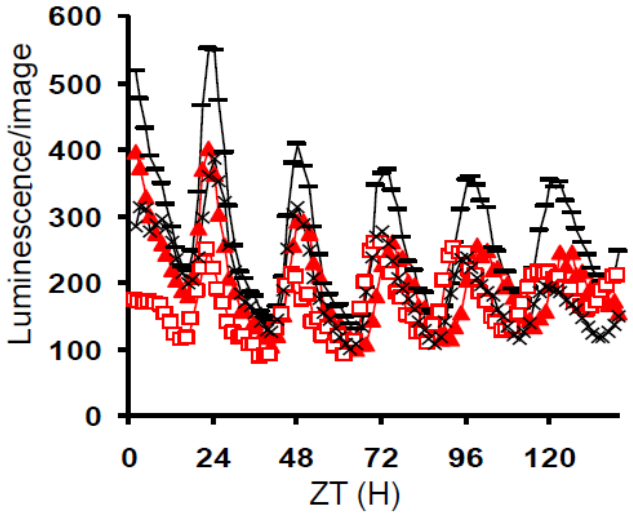

Figure 5.2: Characterisation of *ELF3*::ELF3::YFP
ELF3::ELF3::YFP lines were used to identify the protein distribution and confirm sub-cellular localisation of ELF3. The lines were confirmed to have normal clock function through *CCA1*::LUC imaging starting with 7 day old seedlings entrained under 12:12 white light:dark cycles and released into constant light at ZT0. Two independent Ws *CCA1*::LUC lines were imaged (black crosses and black dashes) and two independent Ws *elf3-4 ELF3*::ELF3::YFP *CCA1*::LUC (red filled triangles and red open squares). Graphs represent the averaging of 15-30 individual plant traces and data is from two biologically independent experiments which show similar results. Free-running period of the *elf3-4 ELF3*::ELF3::YFP line also confirmed through delayed florescence imaging (Chapter 4).

7-day old *ELF3*::ELF3::YFP seedlings, which had been entrained in 12:12 white light:dark cycles, were mounted on microscope slides with the tissue to be imaged submerged in water beneath a coverslip. Images were collected between ZT10-14, using a 63x objective with 8x line averaging. For each tissue type, three separate plants were imaged from at least three biologically independent experiments. *ELF3*::ELF3::YFP was always observed to be localised to the nucleus and mostly in distinct nuclear-localised speckles (Figure 5.3). These speckles are found in all organs imaged; hypocotyl, root and leaf as well as at different developmental stages; cotyledon and leaf. However, the intensity and number of speckles can be seen to vary (Figure 5.3).

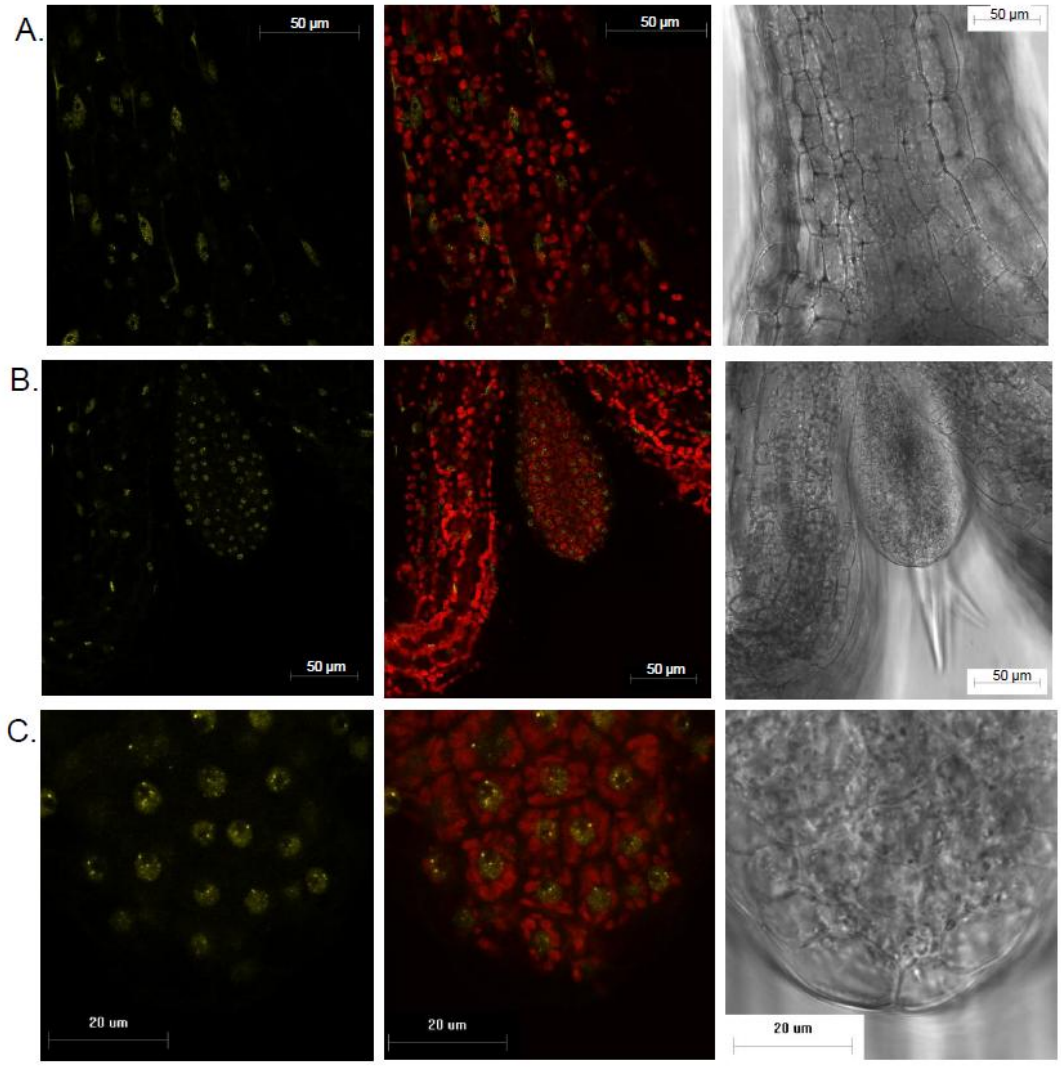
A.
50 µm
50 µm
50 µm
B.
50 µm
50 µm
50 µm
C.
20 um
20 um
20 um

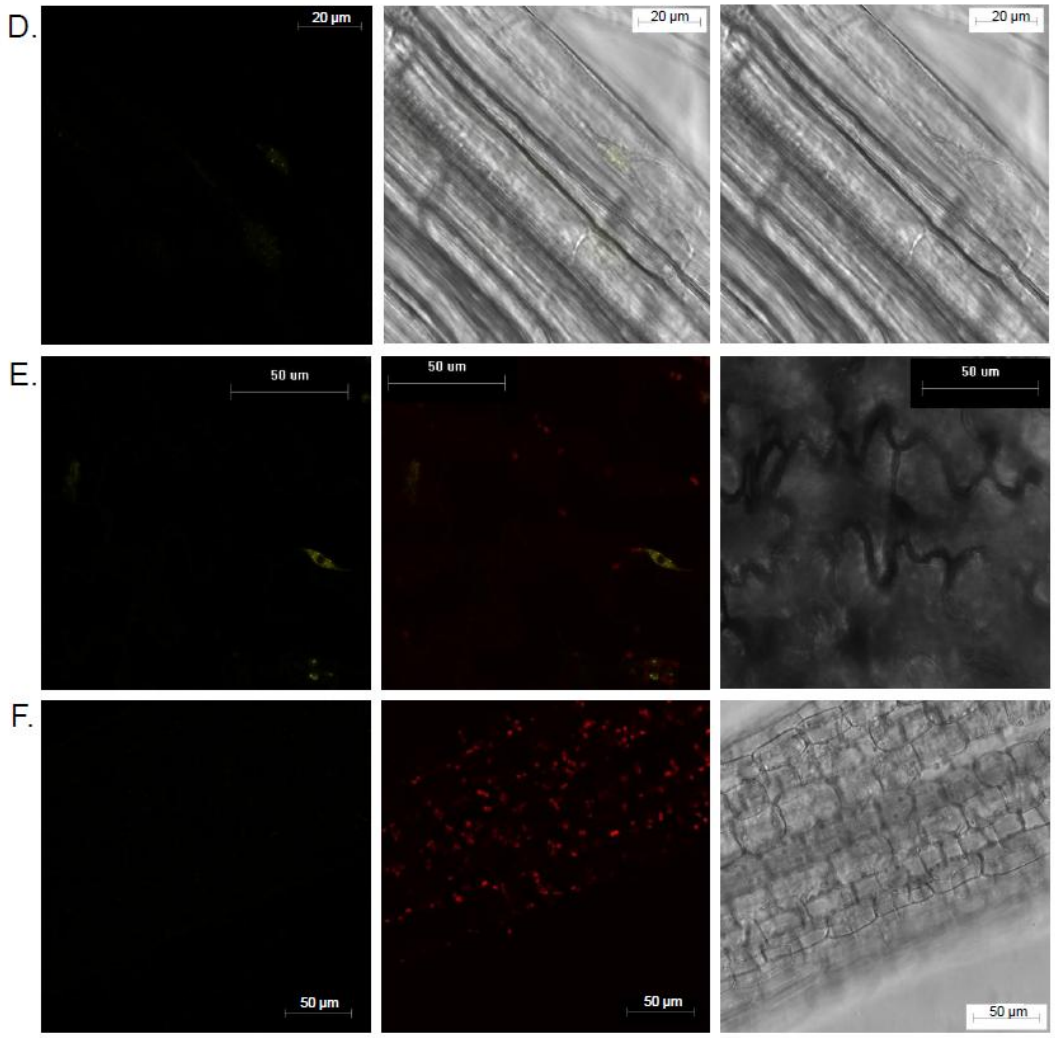

Figure 5.3: *ELF3*::ELF3::YFP localisation patterns
Localisation of *ELF3*::ELF3::YFP protein was assessed in 7 day old seedlings entrained in 12:12 white light:dark cycles and imaged between ZT10-14 by confocal microscopy. *ELF3*::ELF3::YFP shows nuclear localisation in all tissues investigated; hypocotyl (panel A), primary leaf (panel B), root (panel D) and cotyledons (panel E) but nothing in untransformed *elf3-4* parent lines (panel F). Speckle formation occurs in all tissue types, a zoom example is from the primary leaf (panel C). Each image shows YFP (excitation band width 525-560) in yellow, Chlorophyll (excitation band width 640-715) in red and the bright field in grey scale with images having 1024x1024 pixels and each line had 8x averaging.

The speckle formation in the root is particularly faint, and can not be observed in all root cells. This may be a consequence of how faint the fluorescence of *ELF3*::ELF3::YFP is in this organ, as opposed to ELF3 not localising there. The aerial tissues have a higher level of ELF3 protein than the roots. In the leaf and hypocotyl the speckles are observed in nearly every cell and are highly dynamic. This links with ELF3 having a role in light signalling [80, 113] and its association with DNA [153]. Distinct speckle formation is very similar to that of other light and stress signalling proteins, listed in Table 5.1, which is consistent with ELF3's known interacting partners [179, 239, 85, 49]. In response to stress stimulus and light signalling it is known that the transcriptome changes dramatically [244] and so it may be speculated that these speckles are involved with this. Molecularly this would suggest a role in chromatin modification, degradation or the formation of regulatory units on DNA.

Protein	**Function**	**Reference**
TOC1	Component of circadian clock network	Strayer *et al*, 2000 [245]
PHY's	Red-light/Far-red-light photoreceptors	Yamaguchi *et al*, 1999 [246], Kim *et al*, 2000 [247],Mas *et al*, 2000 [118]
PIF3	Transcription factor	Bauer *et al*, 2004 [248]
HEMERA/pTAC12	PHY interaction	Chen *et al*, 2010 [249]
COP1	Protein proteolysis	Ang, *et al*, 1998 [250], Stacey *et al*, 1999 [251]
COL3	Light signalling (B-box)	Datta *et al*, 2006 [252]
PIF7	Transcription factor	Leivar *et al*, 2008 [253]
BIT1	MYB transcription factor	Hong *et al*, 2008 [254]
CRY2	Blue-light photoreceptor	Mas *et al*, 2000 [118], Yu *et al*, 2009 [255]
STH3	B-box protein	Datta *et al*, 2008 [256]
ELF3	Light signalling and clock	This study
STH2	B-box protein	Datta *et al*, 2007 [257]
EID1	F-box protein	Marrocco *et al*, 2006 [258]
LAF1	MYB-like transcription factor	Ballesteros *et al*, 2001 [259]
SR45	Pre-mRNA splicing factor	Zhang *et al*, 2009 [260]
elF4-III	RNA helicase	Koroleva *et al*, 2009 [261]

Table 5.1: A number of light-signalling and stress-related proteins form similar nuclear speckles to those observed for ELF3

5.2.3 ELF3 protein levels vary in a temporal fashion

Using the *ELF3*::ELF3::YFP line and confocal microscopy it is possible to gain a high time resolution for imaging *ELF3*::ELF3::YFP over an extended period. 7-day old seedlings entrained in 12:12 white light:dark cycles were imaged; at each time point three separate plants were imaged over a z-stack, starting at the epidermis cell layer, of 11 μm. Protocol testing to develop a method which enabled continuous imaging of the same plant identified a number of problems. As the leaves provide the most reliable *ELF3*::ELF3::YFP signal (Figure 5.3) they were identified as the tissue to be imaged across the timeseries. However, constant submersion in water or nutrient-enriched water caused cell death. Keeping the plant hydrated without saturating the leaf tissue also caused cell death and caused the requirement for constant refocusing.

The method of imaging the primary leaf in different plants allows the real-time recording of protein levels and the identification of fluctuations which are missed in lower time-resolution protein blotting. This is of particular relevance to ELF3 as protein blotting often uses non-physiological plant growth conditions to enable detection of the protein. These protein blots [80, 85] have shown that ELF3 protein is detectable at all of the timepoints but its levels fluctuate, with a peak at ZT12 when plants have been entrained in 12:12 light:dark cycles. Figure 5.4 shows that, from quantification of microscope imaging, the protein levels fluctuate around the light to dark transition of 12:12 light:dark entrained plants and do not form a single, well-defined peak observed in protein blotting.

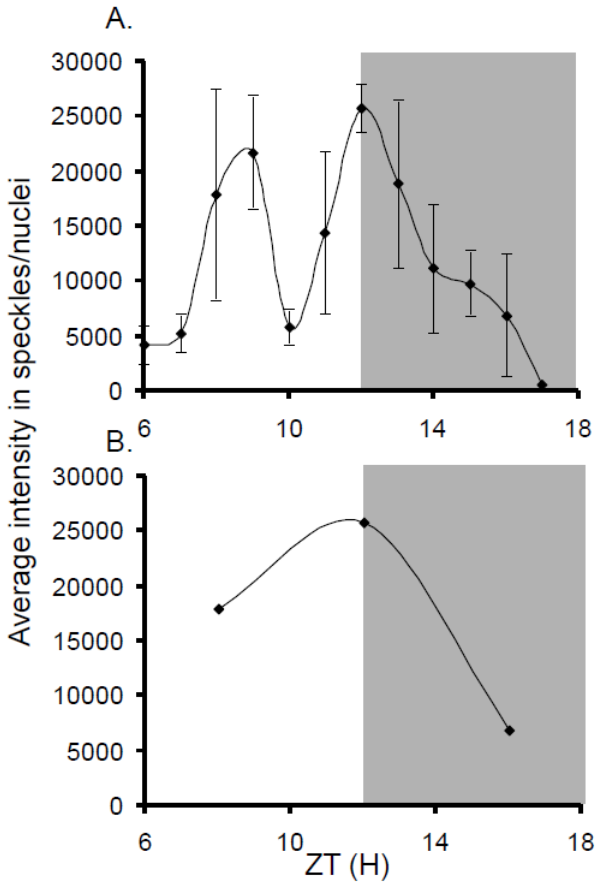

Figure 5.4: *ELF3*::ELF3::YFP microscope timecourse
High temporal resolution data was acquired through a 12 hour imaging time-course from 12:12 white light:dark entrained 7 day old seedlings, across the light to dark transition. Each hour 3 different plants were imaged once through an 11 μm z-stack in the primary leaf. Total speckle intensity was divided by the number of nuclei and an average intensity from the three plants at each timepoint was then calculated. A. A complete time-series with error being presented as SEM and B. The time-points used in previous measurements of ELF3 protein [80] which confirms at this resolution the peak level is ZT12. Data presented in A and B is from one of two biologically independent experiments with similar results.

The imaging shows a first peak at ZT8-9 followed by a clear drop at ZT10 and a second peak at ZT12, but when represented at the same time resolution as the protein blots the single ZT12 peak is observed (Figure 5.4B). The error in these measurements is large and it is unclear if this error is comparable with protein blotting error levels. The differences in the imaging data maybe a reflection of the stochastic differences which occur at this resolution; that is the data is a

combined average from three plants and the oscillations may simply be different between different plants. Therefore, a small sample size will have a large variation. In protein blots a much larger number of seedlings (70-100 seedlings) are normally used and so the variation will appear smaller. Still, the trends identified from both methods are informative as to the dynamic nature of ELF3 protein regulation. The development of an assay system which enables a full 24 hours of continuous imaging on the same plant would be extremely powerful.

5.2.4 ELF3 speckle morphology changes over time

Imaging across a 12 hour timecourse identified that the structure of the speckles varies and that the speckles are highly dynamic. Figure 5.5 shows example images from the timecourses of Figure 5.4A at ZT 6, 9, 12 and 16. These images are representative of the general speckle dynamic at each timepoint. There is biological variation in the samples, most probably relating to stochasticasity and light intensity during entrainment. The speckles are highly dynamic and through z-stack imaging there is a chance of over-representation of speckle number in each image. This is because each 11 μm z-stack takes about 5 minutes to be captured and the speckles observed in one plane could move to another during imaging. Therefore when the stack is compressed there is an over-representation. Generally, however, when the speckles appear distinct in the compressed stack they can probably be counted as individual.

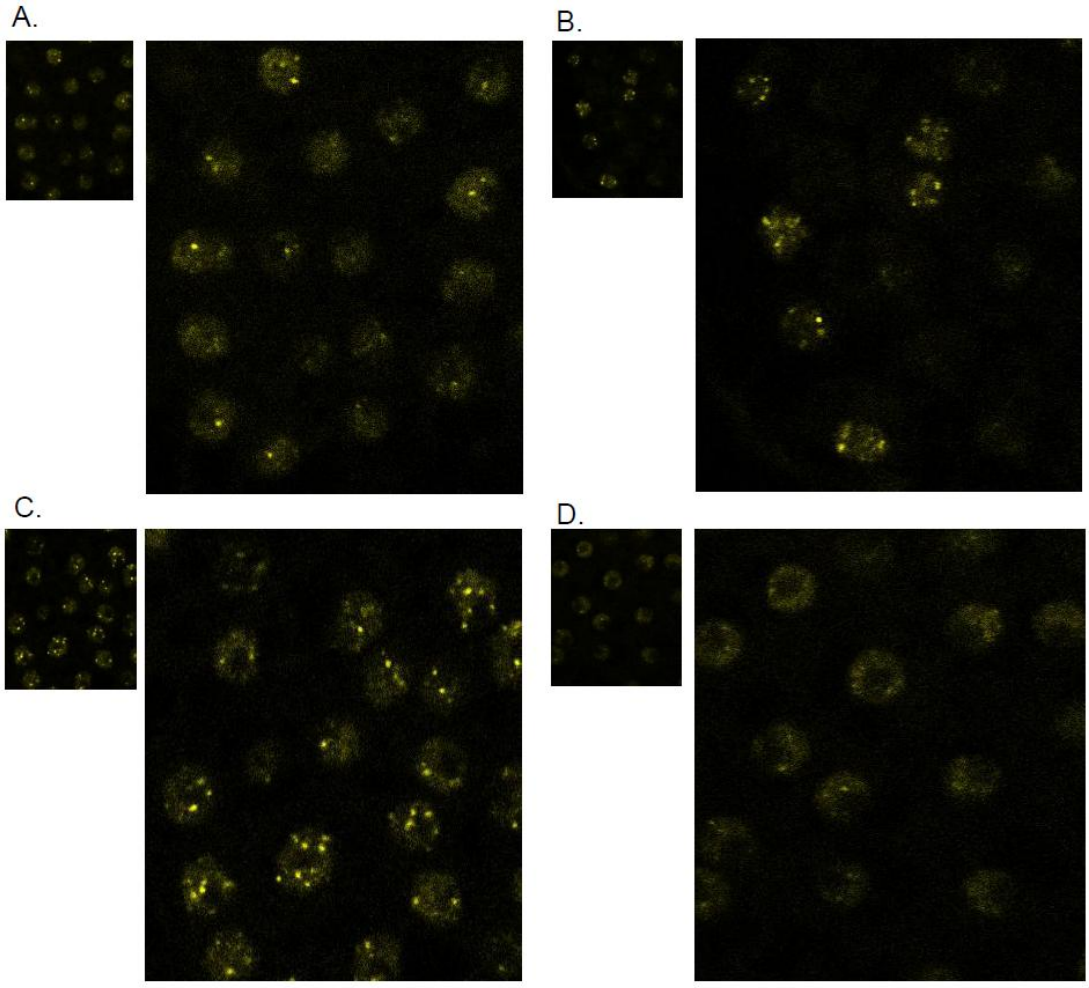

Figure 5.5: Morphology and number of ELF3 nuclear speckles changes over time
Images of the primary leaf from 7 day old *ELF3*::ELF3::YFP seedlings entrained in 12:12 white light:dark cycles with a 3x enlarged area to show the changing morphology of the ELF3 speckles over time. Images are representative of 9 plants at each timepoint from 3 biologically independent experiments. A. ZT6, B. ZT9, C. ZT12, D. ZT16.

At ZT6 speckle formation can always be seen but the number in each nucleus is low, approximately 1-4 (Figure 5.5A). At ZT9 speckle number is higher than ZT6 and the exclusion from the nucleolus region of the nucleus can be observed (Figure 5.5B). At ZT12 the peak in ELF3 speckle formation is at its highest, with multiple speckles being observed in most nuclei (Figure 5.5C). Then in the dark, speckle formation rapidly decreases and by ZT16 very few speckles are observed (Figure 5.5D). In all of the images it can be seen that not all of the

ELF3::ELF3::YFP signal forms nuclear speckles, there is diffuse YFP signal in the background of most nuclei showing speckles. This more diffuse signal may relate to dynamic movement of *ELF3*::ELF3::YFP between speckles, or if the speckle formation is linked with degradation *ELF3*::ELF3::YFP being localised for degradation.

These dynamics suggest that ELF3 speckles are linked with light signalling components and that the speckles form in response to post-transcriptional signalling or circadian events. If speckle formation correlated with ELF3 abundance, then according to transcript levels [185] it would be expected that ELF3 speckle formation would still be abundant for a large proportion of the dark period. Instead, ELF3 levels fall rapidly at night.

5.2.5 Development of a protein interaction model to aid understanding of ELF3 function

5.2.5.1 Network structure

Protein regulation is important for sustained circadian rhythmicity (Chapter 6 and [56]), furthermore protein levels do not always follow that of their mRNA (Figure 5.4 and [164]). To understand protein regulation more thoroughly key components of ELF3's regulation under blue-light have been identified and these interactions are represented symbolically in a mathematical model (Figure 5.6). The network of protein-protein interactions, centred on ELF3, was developed based on experimental evidence presented in [85], [86] and [81]. The data presented in [85] suggests ELF3 has a central role in the regulation of GI protein levels and the model investigates this observation in more detail.

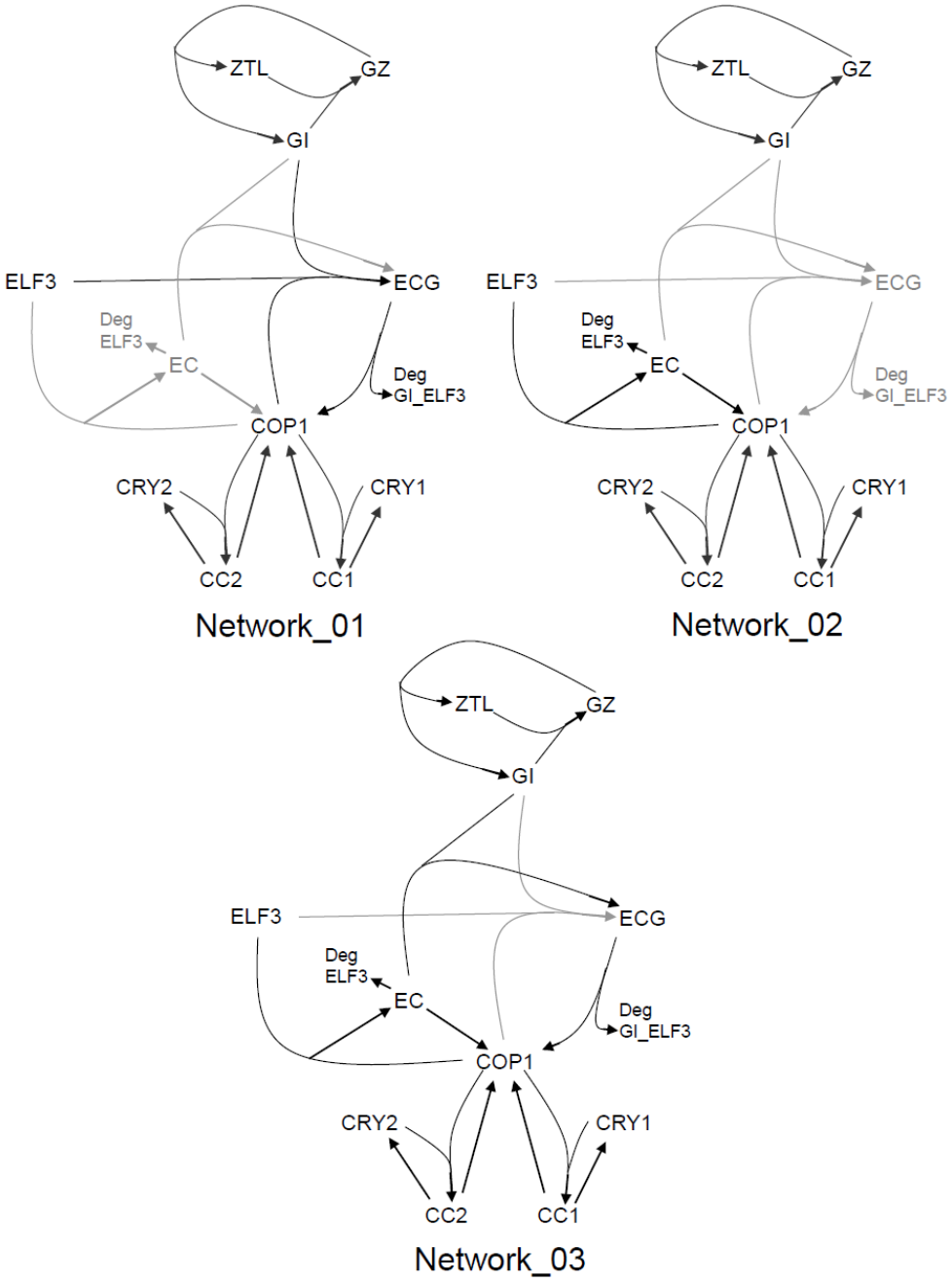

Figure 5.6: Networks investigated through model simulations
The network diagrams show possible protein-protein interactions which can occur in this network. The ELF3/GI/COP1 complex interactions which are simulated in each respective network are highlighted in black, those absent from specific model network are faded out in grey. The ZTL, CRY1 and CRY2 loops are in dark grey as the topologies of these do not change between the simulations but are included in all simulations. ECG = ELF3/COP1/GI trimer, EC = ELF3/COP1 dimer, CC2 = COP1/CRY2 dimer, CC1 = COP1/CRY1 dimer, GZ = GI/ZTL, deg = degradation.

Through investigating this network with respect to possible combinations of protein interactions it was hoped that a mechanism for ELF3 mediated GI regulation could be proposed. The mutant data presented in [85] indicates that ELF3 has a more direct role in the regulation of GI stability than the ubiquitin E3-ligase COP1. This is shown as GI accumulates throughout the 24 hour cycle in *elf3-8* mutant but only at the end of the night in the *cop1-4* background, suggesting that COP1 is possibly not GI's sole regulator.

5.2.5.2 Justification of network species

The network formed does not include all of the known protein interacting partners for the six protein species (Figure 5.7). Other components were not included in order to constrain the complexity of the interaction network, with the aim of extracting useful, mechanistic, interpretations.

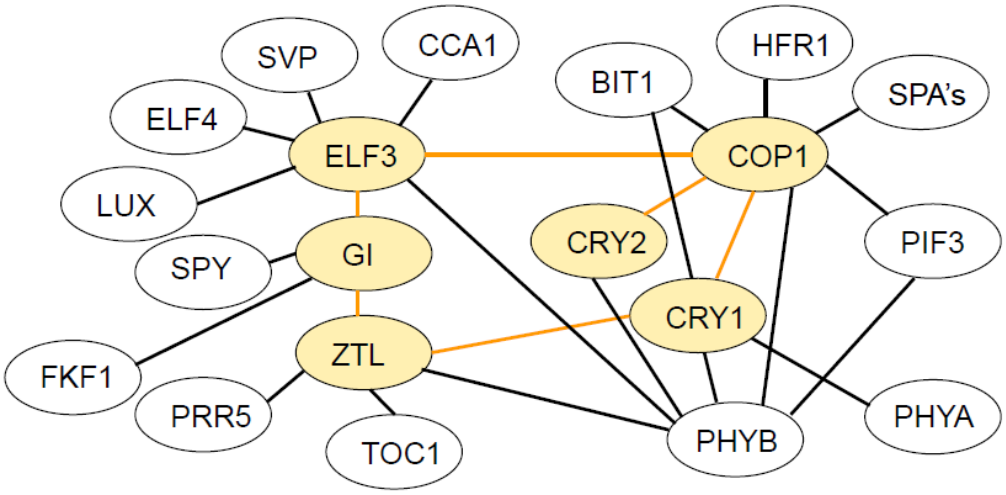

Figure 5.7: Experimentally observed protein interactions for species in model
The network shows the interacting partners, identified experimentally but not always *in vivo*, of the 6 protein species (shown in orange as are the connecting lines) investigated in the model. The interactions represented are only 1 removed from the proteins of interest to enable the network to be limited.

The first simplification step taken in the formation of the network was to limit protein interactions to those observed under blue-light. This is a sensible limitation due to a number of factors. Firstly, the central part of the model, GI/ELF3/COP1, contains COP1 which is an ubiquitin E3-ligase known to target proteins involved in photomorphogenesis for degradation [examples in 262, 263, 264, 243]. Therefore, it has a huge array of interacting partners but only the CRY's are known to regulate COP1's activity [86]. Due to this, the CRY's must be included to modulate the activity of COP1. CRY's are blue-light photoreceptors and the only kinetic data available for their function is from blue-light conditions [265]. Secondly, ELF3, CRY2 and ZTL are known to interact with the red-light photoreceptor PHYB [80, 118 and 266 respectively]. However, the PHYB/ZTL interaction could not be detected in a different assay [267]. Furthermore, the nature, timing or roles of these interactions are unknown and therefore very hard to include in the model. This is also true for the CRY1-PHYA interaction [117]. By not including the major red-light photoreceptors and associated interactions, a simpler blue-light specific network is favoured. Finally, it has been shown that GI is stabilised under blue-light conditions through its interaction with the blue-light photoreceptor and F-box protein ZTL [81]. GI has also been shown to interact with the blue-light photoreceptor FKF1 and through this interaction have an important role in regulating the stability of the transcription factor CYCLING OF DOF 1 (CDF1) and floral transition [82]. However, this interaction has not been shown to regulate GI stability [82] and therefore was not included in the model. The additional sequestering of GI through the FKF complex is accounted for via the basal degradation rate placed on the free GI protein species. Other GI protein interacting partners have not been included as the interaction does not lend itself to understanding the stability and regulation of ELF3 and GI [268]. Similarly to this, ZTL's interaction with CRY1 [117] has not been explicitly included in the model network as its function and role in protein stability is completely unknown. Finally the constraint of a blue-light network means that the PHY interacting factors

such as PIF's and SPA's can also be excluded from this particular network as no significant function has yet to be contributed to them under blue-light conditions.

5.2.5.3 Network development

With the protein species limited to six the formation of an informative model is possible. The data presented in [85] and summarised in Table 5.2 indicates that there are a number of feasible combinations of dimer and trimer interactions. Yu *et al* [85] investigated dimer interactions through *in vivo* and *in vitro* assays. The evidence presented strongly supports the formation of an ELF3/COP1 dimer with this interaction leading to the degradation of ELF3. Furthermore, through yeast-2-hybrid assays and microscope imaging (BiFC) the data suggests that GI/COP1 interaction can only occur following interaction with ELF3. As the data shows that ELF3 can interact, at the level of a dimer, with both COP1 and GI it suggests that an ELF3/GI/COP1 trimer could be formed.

Complex	**Experimental evidence**	**Experimental evidence**	**Experimental evidence**	**Experimental evidence**	**Experimental evidence**
ELF3/ COP1	Yeast-2-hybrid interaction (Fig4A)	Pull-down (Fig4C)	In vitro ubiquitin assay (Fig4D)	In *cop1-4* ELF3 accumulates (Fig5C)	BiFC COP1/ ELF3 (dark + MG132) (Fig6C)
GI/ COP1	No Yeast-2-hybrid interaction (Fig4)	Fragments of GI and COP1 can interact in yeast-2-hybrid (Fig6B)	Immunoblots with COP1, GI is degraded (Fig6D)	GI altered accumulation in *cop1-4* (Fig6F)	BiFC COP/GI when ELF3 co-infiltrated (dark+MG132) (Fig6C)
ELF3/ GI	Yeast-2-hybrid interaction (Fig6A)	Immunoblots with ELF3 GI is degraded (Fig6D)	GI accumulates in *elf3-8* (Fig6F)		BiFC ELF3/GI (dark+MG132) (Fig6C)

Table 5.2: A summary of the experimental evidence used to form the dimer and trimer networks between ELF3, GI and COP1
The table outlines the varying types of experimental evidence used to inform and develop the model network, taken from Yu *et al,* 2008 [85] with figure references referring to the figures in Yu *et al,* 2008 [85]. BiFC is bimolecular fluorescence complementation, where separate parts of a fluorescence protein is attached to either of the proteins under assay meaning fluorescence is only observed when the two proteins come into close proximity.

To investigate the possible protein interaction networks, given the data in Table 5.2, three hypothetical networks were developed, outlined in Table 5.3 and Figure 5.6.

ELF3/COP1	ECG	iECG	Network name
0	1	0	Network_01
1	0	0	Network _02
1	0	1	Network _03

Table 5.3: Summary of the networks investigated in this study
Three different protein networks were investigated and these are outlined in the Table. ECG represents direct ELF3/COP1/GI trimer formation and iECG represents indirect formation of the ELF3/COP1/GI trimer. A 0 represents none of this species and a 1 represents formation of this species. These networks are illustrated in Figure 5.6.

A main consideration in the formation of the protein interaction networks is that a direct COP1/GI dimer has not been observed. Only once GI has interacted with ELF3 can a COP1/GI dimer form. Assuming the sequential interactions resulting in the trimer, ELF3/GI/COP1, are fast, trimer formation can be estimated as a simultaneous binding of the three proteins (Network_01, Figure 5.6, Table 5.3). However, this is most probably a large assumption. As the ELF3/COP1 dimer is well verified through experimentation [85 and Table 5.2] alternative networks excluding GI/COP1 interaction could be envisaged containing a single ELF3/COP1 dimer (Network_02, Figure 5.6, Table 5.3) and its subsequent indirect trimer formation with GI (Network_03, Figure 5.6, Table 5.3

5.2.5.4 Constraining the model

To enable light-dependent regulation of protein activity, which is required for the photoreceptors CRY1, CRY2 and ZTL the model was developed so light and dark parameters could be varied independently. Specifically, the model enables simulations over 12:12 light:dark cycles. The models parameters were set in accordance to information from the literature, such that even

though none of the parameters have been empirically measured they are all set within realistic limits relative to each other. As the network is simulating the dynamics of protein interactions most of the parameters, Table 5.4, are linked with rates of protein-protein association and disassociation, the kinetics of which are not known and therefore relative setting of parameters is the best approximation.

Parameter exploration was conducted manually from what was considered to be a good starting fit and then moving around local parameter state space. Therefore, it is quite possible that other parameter sets exist which can fit the data. In order to be able to make mechanistic interpretations about the ELF3/GI/COP1 interactions, parameters not directly involved in ELF3/GI/COP1 dimer and trimer formation were set at fixed values.

In the model networks protein which is not in a complex is subject to basal degradation levels (parameter d1-7) the rate of which remains constant between simulations.

Reaction	Parameter	Supporting literature
Basal degradation		
$ELF3 \rightarrow \phi$	d_1	
$ZTL \rightarrow \phi$	d_2	
$GI \rightarrow \phi$	d_3	
$COP1 \rightarrow \phi$	d_4	
$CRY1 \rightarrow \phi$	d_5	
$CRY2 \rightarrow \phi$	d_{6L} d_{6D}	*Yu et al, 2007* [265]
GI/ZTL complex		
$GI + ZTL \rightarrow GZ$	k_{2L} k_{2D}	*Kim et al, 2007* [81]
$GZ \rightarrow GI + ZTL$	k_{-2L} k_{-2D}	*Kim et al, 2007* [81]
COP1/CRY1 complex		
$COP1 + CRY1 \rightarrow CC1$	k_3	*Wang et al, 2001* [86]
$CC1 \rightarrow CRY1$	k_{-3L} k_{-3D}	*Wang et al, 2001* [86]
$CC1 \rightarrow COP1$	k_{-4L} k_{-4D}	*Wang et al, 2001* [86]
COP1/CRY2 complex		
$COP1 + CRY2 \rightarrow CC2$	k_5	*Wang et al, 2001* [86]
$CC2 \rightarrow CRY2$	k_{-5L} k_{-5D}	*Wang et al, 2001* [86]
$CC2 \rightarrow COP1$	k_{-6L} k_{-6D}	*Wang et al, 2001* [86]
ELF3/COP1 complex		
$ELF3 + COP1 \rightarrow EC$	$k_{1.2L}$ $k_{1.2D}$	*Yu et al, 2008* [85]
$EC \rightarrow COP1$	$k_{-1.2L}$ $k_{-1.2D}$	*Yu et al, 2008* [85]
ELF3/COP1/GI complex		
$ELF3 + COP1 + GI \rightarrow ECG$	k_1	*Yu et al, 2008* [85]
$EC + GI \rightarrow ECG$	$k_{1.4L}$ $k_{1.4D}$	*Yu et al, 2008* [85]
$ECG \rightarrow COP1$	k_{-1L} k_{-1D}	*Yu et al, 2008* [85]

Table 5.4: Model parameters
Each model parameter and its corresponding biological function are shown in this table. *k* corresponds to kinetic parameters of association and dissociation (-) which may be different in light (L) and dark (D) conditions and *d* to basal degradation.

Basal degradation

With the exception of CRY2 (d_{6L}, d_{6D}) which has been shown to be light-labile [265] the basal degradation of protein, not associated in complexes, has the same rate in light and dark. The rates have been set at a level which enables the best fit of simulation data to experimental data, where available. COP1 could not be fitted due to the absence of experimental data.

GI/ZTL complex

Complex formation is based on the findings presented in [81] which show a blue-light dependent interaction between GI/ZTL that increases the stability of both of the proteins in blue-light. Therefore complex formation is higher in the light and disassociation higher in the dark. Proteins are not degraded in complexes.

CRY/COP1 complex

Complex formation occurs at the same rate in the light and the dark but the rate of disassociation is different between the two conditions. This regulation effectively means that COP1 is degraded in the light, through its interaction with the CRY's targeting it for degradation and CRY's are degraded in the dark through their interaction with COP1 [86].

COP1 mediated degradation

In the complex combinations described (Table 5.3) the parameters are set to ensure that proteins which are degraded via COP1 have always interacted with COP1 in the dark, and therefore in COP1's biologically active state [242].

5.2.5.5 Model network formation

The networks outlined in Table 5.3 were converted to a set of Ordinary Differential Equations (O. D. E.'s), given below.

$$\frac{d[ELF3]}{dt} = f_E - k_1[ELF3][COP1][GI] - k_{1.2}[ELF3][COP1] + d_1[ELF3]$$

$$\frac{d[GI]}{dt} = f_G - k_1[ELF3][COP1][GI] + k_{1.4}[ELF3/COP1][GI] + d_3[GI]$$
$$- k_2[GI][ZTL] + k_{-2}[GI/ZTL]$$

$$d\frac{[CRY1]}{dt} = f_{C1} - k_3[CRY1][COP1] + k_{-3}[COP1/CRY1] + d_5[CRY1]$$

$$\frac{d[CRY2]}{dt} = f_{C2} - k_5[CRY2][COP1] + k_{-5}[COP1/CRY2] + d_6[CRY2]$$

$$d\frac{[ZTL]}{dt} = f_Z - k_2[GI][ZTL] + k_{-2}[GI/ZTL] + d_2[ZTL]$$

$$d\frac{[COP1]}{dt} = f_{COP1} - k_1[ELF3][GI][COP1] + k_{-1}[ELF3/GI/COP1] + k_{1.2}[ELF3][COP1]$$
$$+ k_{-1.2}[ELF3/COP1] + k_3[CRY1][COP1] + k_4[COP1/CRY1] + k_5[CRY2][COP1] + k_6[COP1/CRY2]$$
$$- d_4[COP1]$$

$$d\frac{[ELF3/GI/COP1]}{dt} = k_1[ELF3][GI][COP1] + k_{-1}[ELF3/GI/COP1] + k_{1.4}[ELF3/COP1][GI]$$

$$d\frac{[COP1/CRY1]}{dt} = k_3[CRY1][COP1] + k_{-3}[COP1/CRY1] + k_{-4}[COP1/CRY1]$$

$$d\frac{[COP1/CRY2]}{dt} = k_5[CRY2][COP1] + k_{-5}[COP1/CRY2] + k_{-6}[COP1/CRY2]$$

$$d\frac{[GI/ZTL]}{dt} = k_2[GI][ZTL] + k_{-2}[GI/ZTL]$$

$$d\frac{[ELF3/COP1]}{dt} = k_{1.2}[ELF3][COP1] + k_{-1.2}[ELF3/COP1] + k_{1.4}[ELF3/COP1][GI]$$

The production terms (f_E, f_G, f_{C1}, f_{C2}, f_Z, f_{COP1}) for the input to the six protein species are experimentally measured mRNA levels. This data was collected from 12:12 white light:dark

cycles (Figure 5.8) and is an average of two independent experiments, with error not being included in the model input.

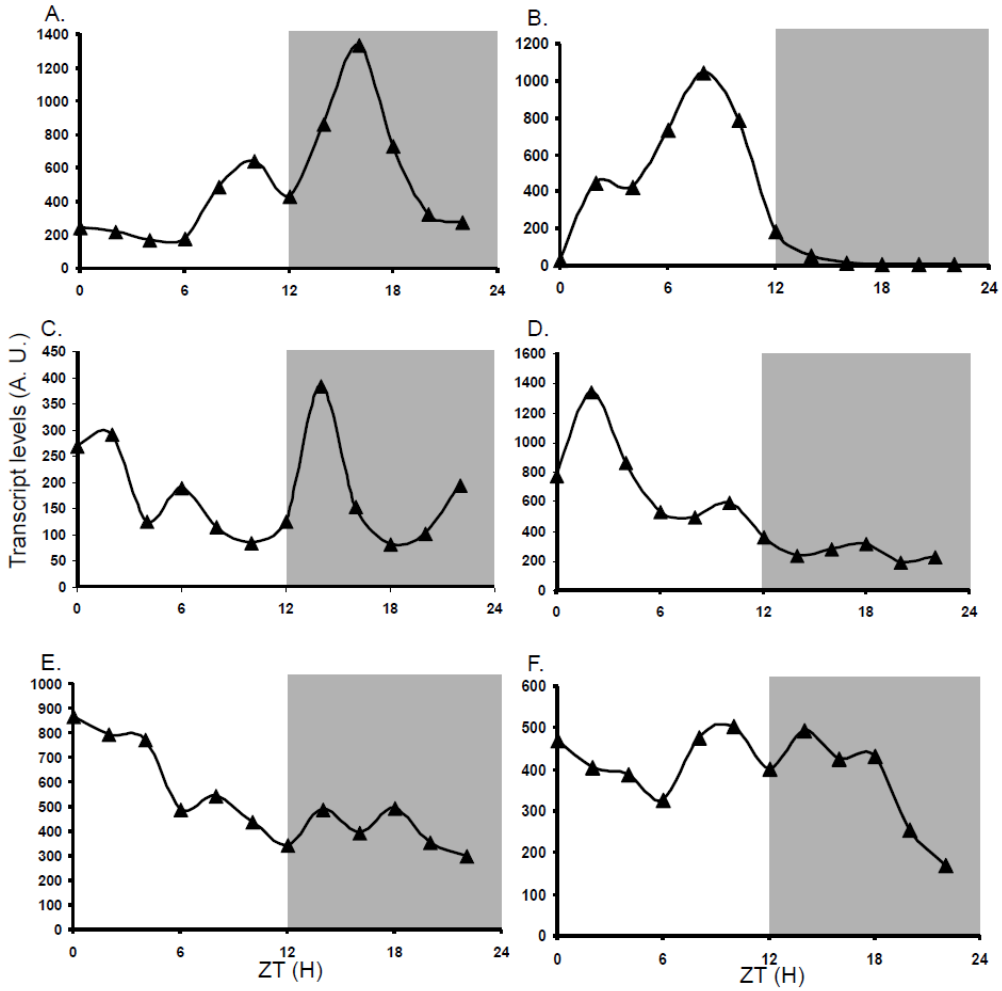

Figure 5.8: Input plots measuring mRNA levels each of the components in the model
QPCR measuring of mRNA levels in 7 day old seedlings grown in 12:12 white light:dark cycles. Samples harvested starting at ZT0 which is lights on, every 2 hours. The graphs represent an average from 2 – 4 independent experiments. A) *ELF3*, B) *GI*, C) *ZTL*, D) *COP1*, E) *CRY1*, and F) *CRY2*, with the bars above the plots representing light conditions.

The model assumes a direct and immediate conversion of mRNA to protein. The parameters controlling the rates of protein association, disassociation and degradation for each of the three networks are shown in Table 5.5. The equations are solved in Matlab ODE solver, ODE 23s.

Reaction		01a	01b	02	03
Basal degradation					
$ELF3 \rightarrow \phi$	d_1	0.2	0.2	0.2	0.2
$ZTL \rightarrow \phi$	d_2	0.4	0.4	0.4	0.4
$GI \rightarrow \phi$	d_3	0.3	0.3	0.3	0.3
$COP1 \rightarrow \phi$	d_4	0.3	0.3	0.3	0.3
$CRY1 \rightarrow \phi$	d_5	2	2	2	2
$CRY2 \rightarrow \phi$	d_{6L}	3	3	3	3
	d_{6D}	0	0	0	0
GI/ZTL complex					
$GI + ZTL \rightarrow GZ$	k_{2L}	0.1	0.1	0.1	0.1
	k_{2D}	0	0	0	0
$GZ \rightarrow GI + ZTL$	k_{-2L}	0	0	0	0
	k_{-2D}	0.1	0.1	0.1	0.1
COP1/CRY1 complex					
$COP1 + CRY1 \rightarrow CC1$	k_3	0.1	0.1	0.1	0.1
$CC1 \rightarrow CRY1$	k_{-3L}	10	10	10	10
	k_{-3D}	0	0	0	0
$CC1 \rightarrow COP1$	k_{-4L}	0	0	0	0
	k_{-4D}	1	1	1	1
COP1/CRY2 complex					
$COP1 + CRY2 \rightarrow CC2$	k_5	0.1	0.1	0.1	0.1
$CC2 \rightarrow CRY2$	k_{-5L}	10	10	10	10
	k_{-5D}	0	0	0	0
$CC2 \rightarrow COP1$	k_{-6L}	0	0	0	0
	k_{-6D}	0.1	0.1	0.1	0.1
ELF3/COP1 complex					
$ELF3 + COP1 \rightarrow EC$	$k_{1.2}$	0	0	0.7	0.7
$EC \rightarrow COP1$	$k_{-1.2L}$	0	0	0	0
	$k_{-1.2D}$	0	0	0.5	5
ELF3/COP1/GI complex					
$ELF3 + COP1 + GI \rightarrow ECG$	k_1	0.7	0.7	0	0
$EC + GI \rightarrow ECG$	$k_{1.4}$	0	0	0	0.7
$ECG \rightarrow COP1$	k_{-1L}	0	0	0	0
	k_{-1D}	0.6	0.2	0	0.2

Table 5.5: Parameters set for each network
With the development of the networks minimal parameter changes have been made between sets in order to identify any characteristics of the network which are particularly sensitive. If the species is not in the network the parameter value is denoted as 0 in light grey.

5.2.6 Model simulations

In all of the networks outlined in Table 5.3 the structure of the CRY1, CRY2, COP1 interaction and ZTL/GI interaction remain unchanged and so for clarity these loops have been coloured dark grey in all network diagrams (Figure 5.6 and 5.9-5.12). The functional ELF3/GI/COP1 interactions for each model are highlighted in black, non-functional interactions are light grey. Simulations were run over two 12:12 light:dark cycles with the second cycle plotted, allowing the model to enter its periodic state. Simulation results are plotted at the same time-points as the experimental data to enable direct comparison. The networks will be discussed in order of increasing structural complexity.

5.2.6.1 Network_01 - Direct ELF3/GI/COP1 trimer formation

A function of the ELF3/GI/COP1 trimer is to mark both GI and ELF3 for degradation. This function is represented in the model by the disassociation of the ELF3/GI/COP1 trimer which results in COP1 only, i.e. ELF3 and GI are degraded instantly when released from the trimer. Thus, the degradation of GI and ELF3 is coupled. Simulation results identify that this coupling results in the inability to capture both the ELF3 and GI protein profiles. If trimer disassociation is 'fast' the simulation captures the ELF3 protein profile (Figure 5.9 and Appendix E, Figure E1), if trimer disassociation is 'slow' the simulation captures the GI protein profile (Figure 5.10 and Appendix E, Figure E1). This remains true for the intermediate degradation rates between 0.2 and 0.6 (Appendix E, Figure E2). To capture a reasonable ELF3 profile (Figure 5.9, Network_01a) trimer disassociation (which only takes place under dark conditions) is required to be faster than that which allows a good representation of the GI profile (Figure 5.10, Network_01b). The faster disassociation causes GI protein levels to fall rapidly shifting the peak into the light period (Figure 5.9).

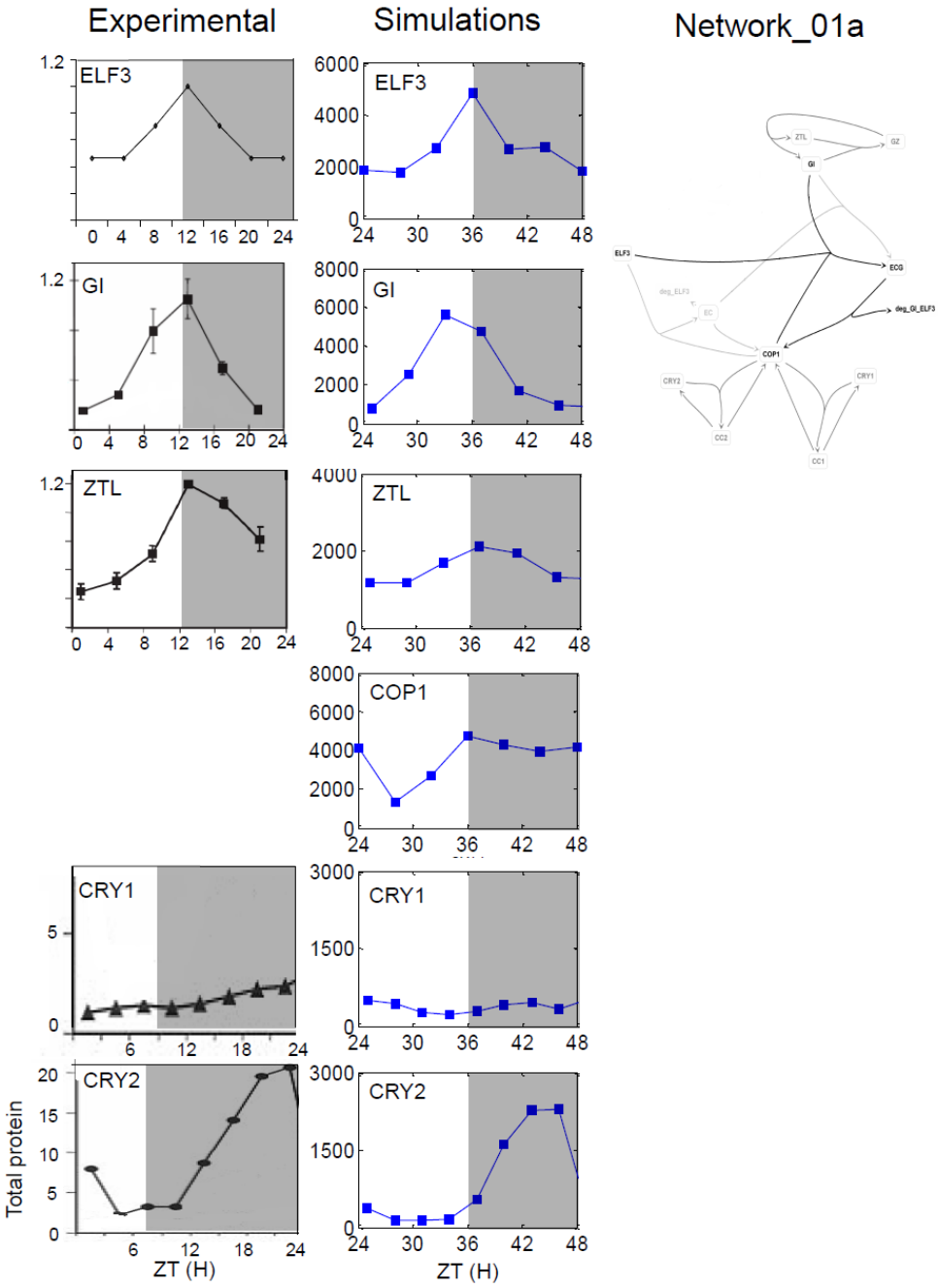

Figure 5.9: Simulations of Network_01a
Biological data, network diagram and simulation results for model network 01a. The graphs in the first column show experimental data which has been taken from published literature (ELF3 [80], GI and ZTL [81], CRY1 and CRY2 [326]). In the second column are the simulation results showing total protein levels in the system for each species. On the right is the network diagram showing the ELF3/GI/COP1 complex interactions with the ZTL, CRY1 and CRY2 loops in dark grey and the network components absent from this simulation in light grey.

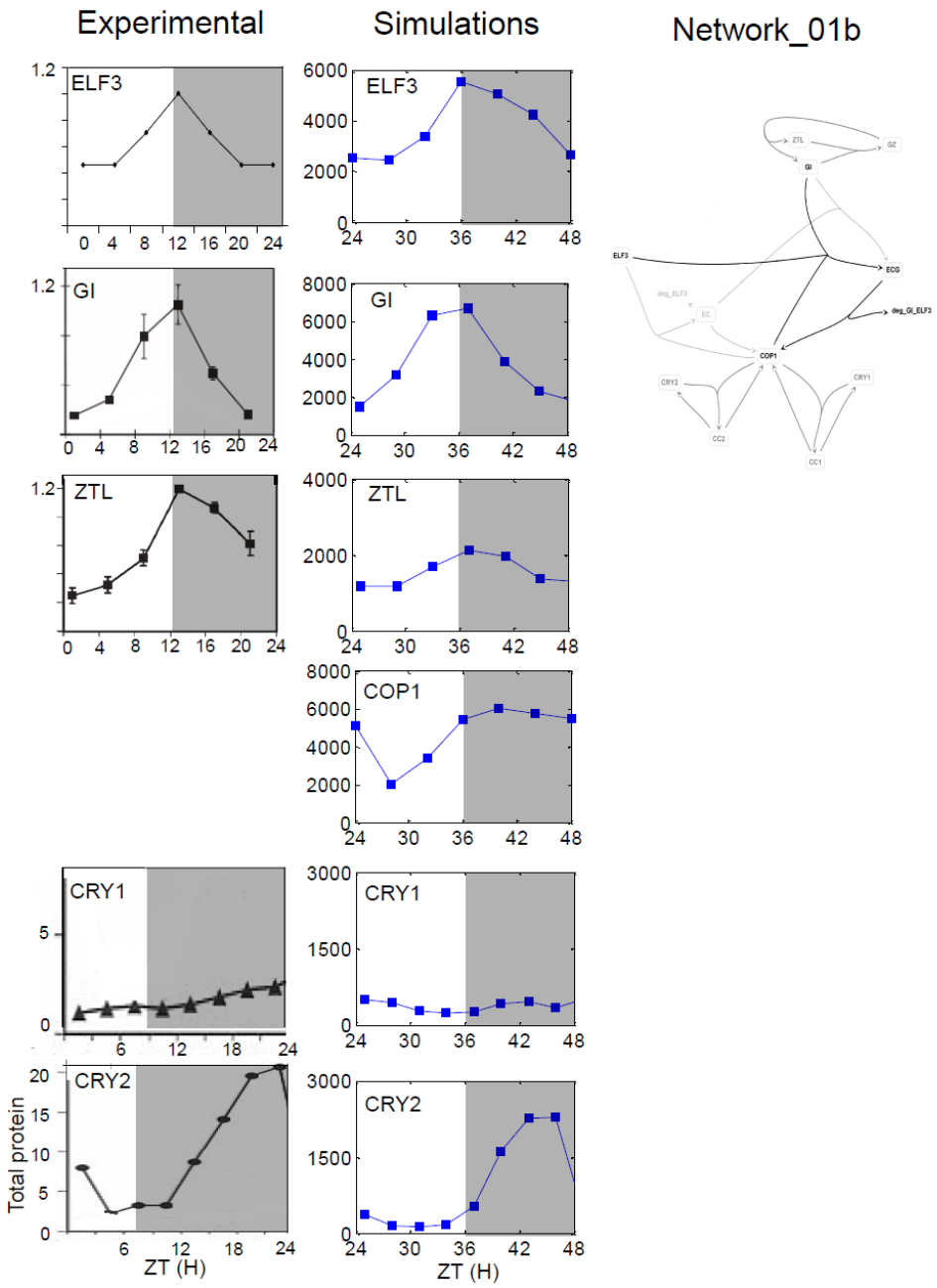

Figure 5.10: Simulations of Network_01b
Biological data, network diagram and simulation results for model network 01b. The graphs in the first column show experimental data which has been taken from published literature (ELF3 [80], GI and ZTL [81], CRY1 and CRY2 [326]). In the second column are the simulation results showing total protein levels in the system for each species. On the right is the network diagram showing the ELF3/GI/COP1 complex interactions with the ZTL, CRY1 and CRY2 loops in dark grey and the network components absent from this simulation in light grey.

This light peak is due to the frequency of data collection, which is the same as the experimental data. However, the peak actually occurs on the light to dark transition (Appendix E, Figure E1). Coupled GI, ELF3 degradation leads to too much ELF3 or too little GI, therefore to reproduce both the GI and ELF3 profiles simultaneously their degradation needs to be decoupled. Network_01 captures CRY and ZTL profiles very well.

5.2.6.2 Network_02 - ELF3/COP1 dimer formation

The formation of an ELF3/COP1 dimer which leads to ELF3 degradation is experimentally well supported (Table 5.2). In Network_02 there is no ELF3/GI/COP1 trimer so the degradation of ELF3 and GI are completely uncoupled (Figure 5.11). In the model ELF3 degrades instantly with the disassociation of the ELF3/COP1 dimer (which takes place in dark conditions) and through basal degradation. Simulation results show this network is sufficient to capture ELF3 protein profiles (Figure 5.11), as a high level of night degradation can be controlled through the ELF3/COP1 dimer. GI degradation only occurs via basal degradation, when GI is not in complex with ZTL. The GI/ZTL complex is formed in the light and disassociates in the dark. In Figure 5.11, the GI peak is in the light as there is no further dimer formation, which protects GI from degradation, and the GI transcription rate is negligible so no new protein is fed into the system.

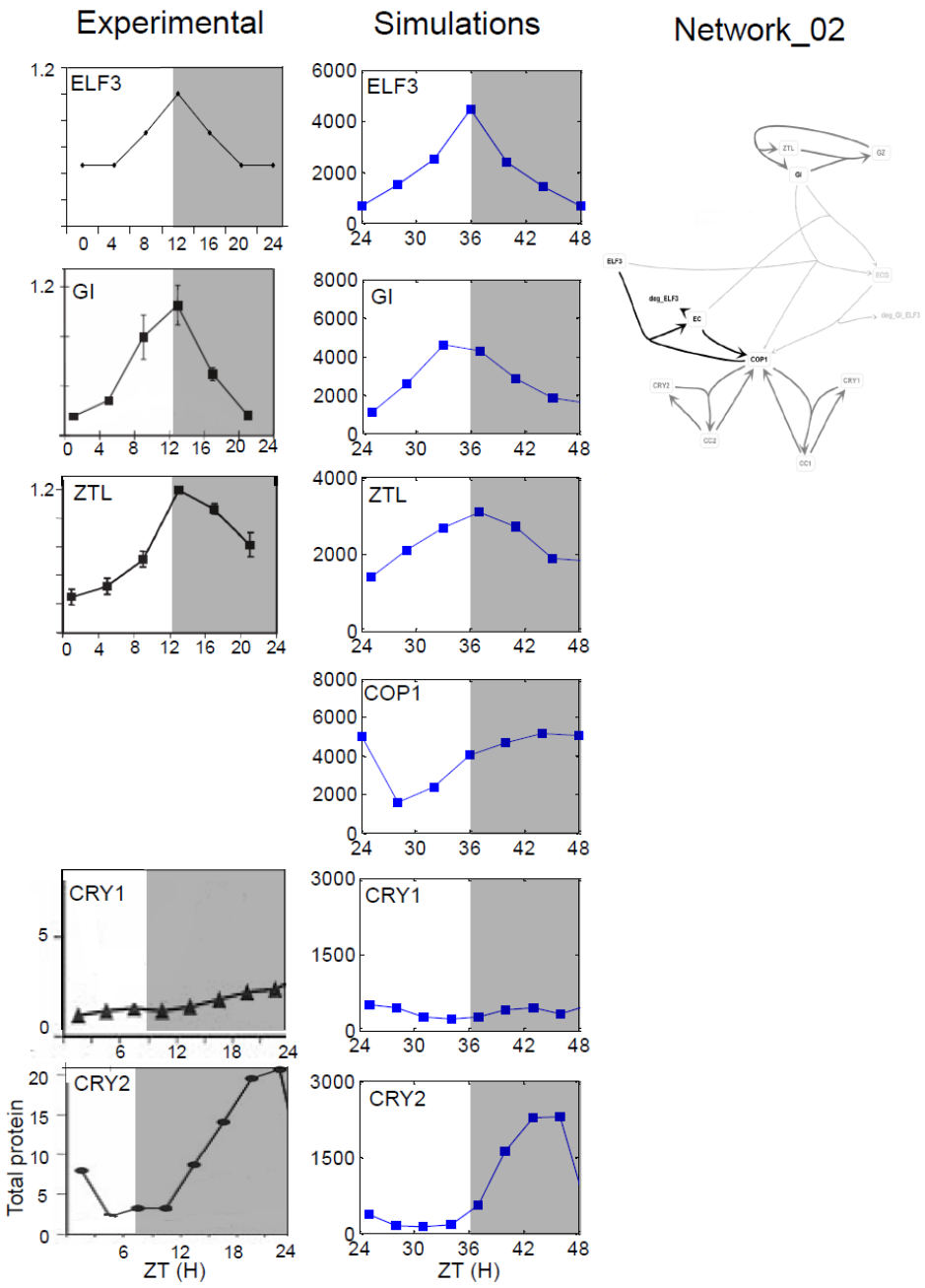

Figure 5.11: Simulations of Network_02
Biological data, network diagram and simulation results for model network 02. The graphs in the first column show experimental data which has been taken from published literature (ELF3 [80], GI and ZTL [81], CRY1 and CRY2 [326]). In the second column are the simulation results showing total protein levels in the system for each species. On the right is the network diagram showing the ELF3-GI-COP1 complex interactions with the ZTL, CRY1 and CRY2 loops in dark grey and the network components absent from this simulation in light grey.

GI/ZTL dimer alone is not sufficient for the light regulation of ZTL, simulated protein levels accumulate faster than the experimental data. When in the dimer ZTL is protected from basal degradation, as without any other binding partners all of GI in Network_02 is available to bind with ZTL, causing ZTL's accumulation. In Network_01 a proportion of GI is sequestered by binding ELF3 and COP1 during trimer formation, leaving ZTL more available to degradation and therefore reducing its light accumulation. With this, adding trimer formation to Network_02 should recapture the ZTL profile, Network_03.

5.2.6.3 Network_03 - ELF3/COP1 dimer formation and indirect trimer formation

In this network ELF3 degradation occurs via two complexes; ELF3/COP1 dimer and through ELF3/COP1 trimer formation with GI. GI degradation is now regulated through its coupling to the levels of ELF3 and COP1 through the trimer formation. This network is able to capture the correct peak times for all of the experimentally measured species (Figure 5.12). As expected the ZTL light profile is captured. In addition the GI peak is in the dark as a consequence of the continual trimer formation protecting GI from degradation. While trimer formation couples GI and ELF3 degradation, as in Network_01, its combination with the ELF3/COP1 dimer allows independent total degradation rates, resulting in the simultaneous capture of ELF3 and GI protein profiles. Therefore, the sequential formation of the ELF3/COP1/GI trimer allows the capture of the experimentally observed features.

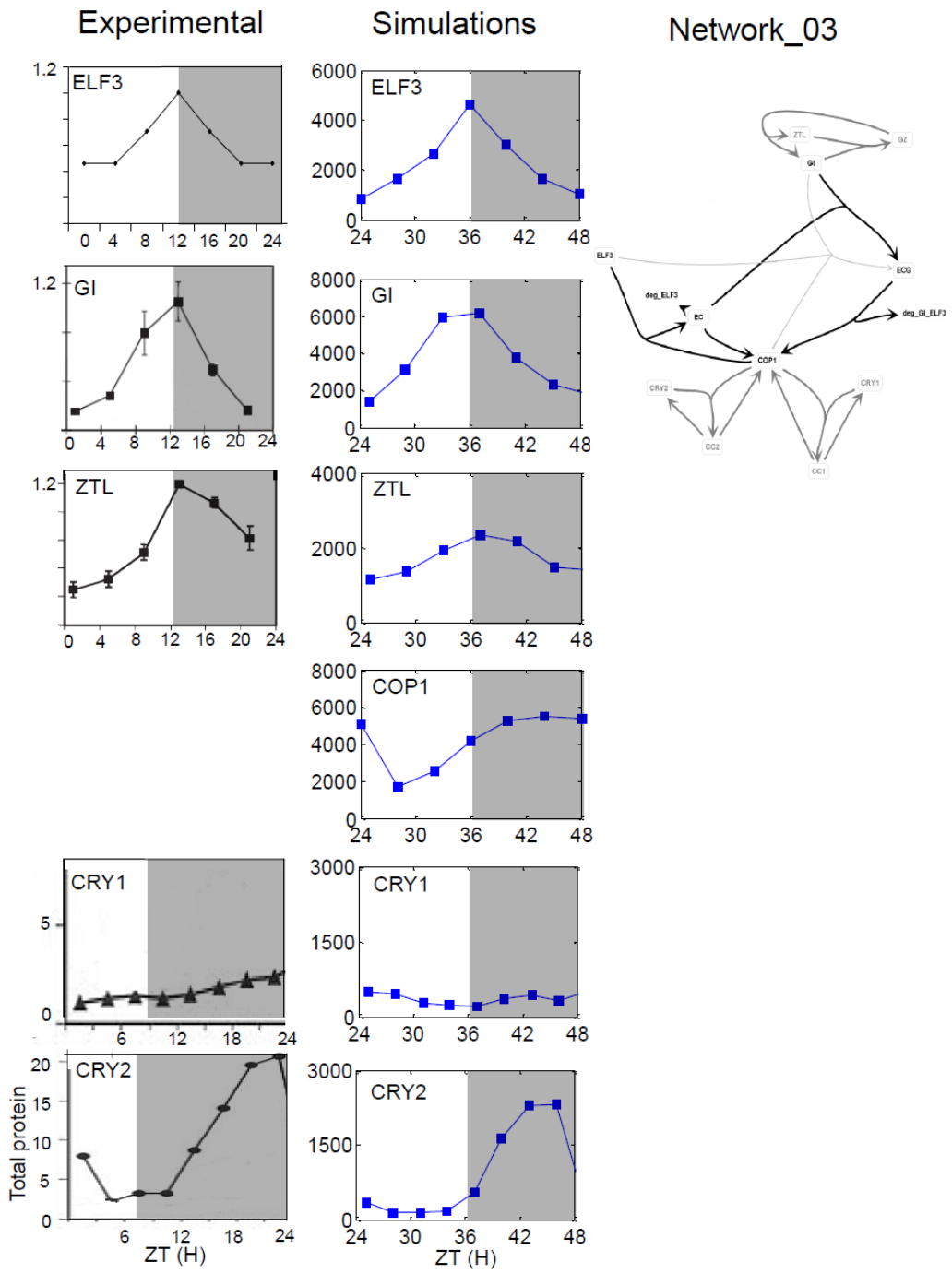

Figure 5.12: Simulations of Network_03
Biological data, network diagram and simulation results for model network 03. The graphs in the first column show experimental data which has been taken from published literature (ELF3 [80], GI and ZTL [81], CRY1 and CRY2 [326]). In the second column are the simulation results showing total protein levels in the system for each species. On the right is the network diagram showing the ELF3-GI-COP1 complex interactions with the ZTL, CRY1 and CRY2 loops in dark grey and the network components absent from this simulation in light grey.

5.2.7 Model simulations of mutant backgrounds

From the simulation results of the wild-type networks (Figures 5.9- 5.12) it suggests that the formation of the trimer enables a level of regulation which is more realistic to that observed experimentally. This is mainly due to the partial decoupling of ELF3 and GI degradation rates. Simulations were run to compare the model with mutant experimental profiles observed in Yu *et al,* 2008 [85], Figures 5.13A and 5.14A. These simulations are over 12:12 light:dark cycles. Therefore, for comparison between experimental and simulated data it is the profile shape and response after the light to dark transition that are the key features for determining the quality of fit.

In Yu *et al* the wild-type genotype (denoted Col in Figure 5.13A and 5.14A) is actually a transgenic *35S*::GI line and so *GI* transcript levels in the model were set to a constant 500, rather than the rhythmic input (Figure 5.8). This level was chosen because it is the experimentally measured mid-point in *GI* transcript. In the mutant simulations only the input mRNA of the mutant genes were altered; the *cop1-4* is a weak mutation, and so *COP1* transcript was reduced to 1:10 of its original level. It is very unlikely that in plants over-expressing *GI*, and with a *cop1-4* mutation, that the mRNA levels of the other genes will be unchanged. However, as a first approximation, this approached may uncover features of the network

5.2.7.1 Simulated mutant profiles, GI

The experimental data presented in Yu *et al* measured GI levels under short day photoperiod, (SD). Under SD conditions, in the over-expresser of *GI* (35S::GI), GI peaks with the light:dark transition and has a trough at ZT16. In the over-expresser with *cop1-4* mutation, the amplitude of the GI rhythm is greatly reduced, with a two small peaks one at ZT4 and the other at ZT16. Notably there is no peak with the light:dark transition and the profile could be approximated to be a flat line across the mid-point of 35S::GI levels. This is unexpected in a background where the protein of interest (GI) is over-expressed and its degrader (COP1) is reduced, (Figure 5.13A).

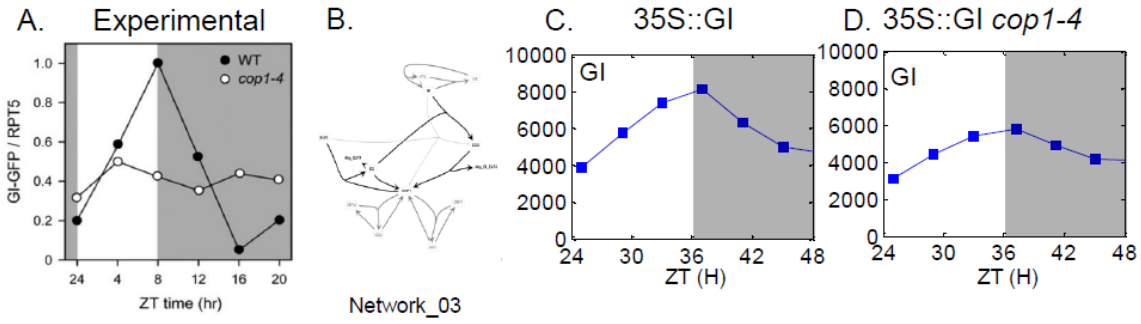

Figure 5.13: GI simulations in *35S*::GI cop1-4 background
Biological data, network diagram and simulation results for model Networks_03, 05 and 07, in *35S*::GI and *35S*::GI *cop1-4* backgrounds. A. Shows the experimental data which has been taken from [85]. B. The network diagrams which correspond to the horizontal simulations in C) *35S*::GI background and D) *35S*::GI *cop1-4* background.

For the simulated GI profiles in the 35S::GI background (Figure 5.13C) a high amplitude rhythm of GI protein is observed even when transcript is constant, as seen experimentally (Figure 5.13A). Network_03 shows a significant decrease in amplitude in the GI rhythm this supports the idea that COP1 is not GI's only regulator in degradation, ELF3 also has a function.

5.2.7.2 Simulated mutant profiles, ELF3

In the same transgenic backgrounds, *35S*::GI and *35S*::GI *cop1-4,* the levels of ELF3 have also been experimentally measured in both SD and long day (LD) conditions ([85] and Figure 5.14A). Under LD conditions the *35S*::GI (denoted Col, Figure 5.14A) shows a peak during the light period, at around ZT14. In SD the ELF3 peak is now in the dark, at between ZT14-18. However, with the addition of *cop1-4* mutation the profiles alter substantially. In LD the peak of ELF3 moves later, to around ZT18 whilst in SD it moves earlier to around ZT6. In both of these conditions the overall protein levels of ELF3 increase. These results show that photoperiod conditions do have a significant impact on the ELF3 protein profile. As such the results of the 12:12 light:dark simulations can not be expected to be exact replicates of either experimental data set as the model network is also sensitive to photoperiod.

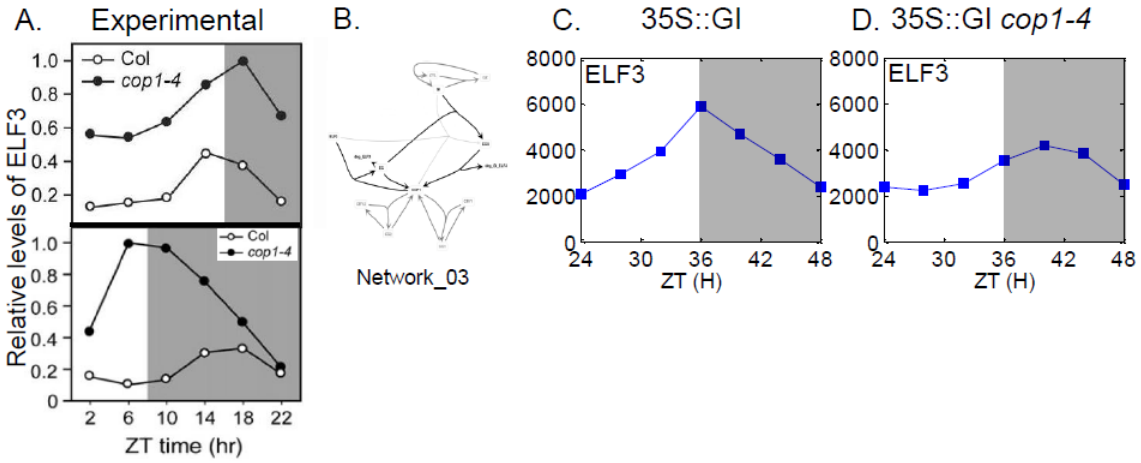

Figure 5.14: ELF3 simulations in *35S*::GI *cop1-4* background
Biological data, network diagram and simulation results for model Networks_03, 05 and 07, in *35S*::GI and *35S*::GI *cop1-4* backgrounds. A. Shows the experimental data which has been taken from [85]. B. The network diagrams which correspond to the horizontal simulations in C) *35S*::GI background and D) *35S*::GI *cop1-4* background.

The simulations for Network_03 show that in the *35S*::GI background the peak levels of GI are earlier (at the light:dark transition) than in the *35S*::GI *cop1-4* background (in the dark period). These simulations re-iterate ELF3's sensitivity to photoperiod. Furthermore, as the levels of ELF3 do not accumulate in any of the simulation profiles it suggests that ELF3 has an even higher rate of degradation than is allowed for through the partial decoupling of the ELF3 and GI degradation.

Together the simulation data indicate that the direct trimer formation is too great a simplification and that the rhythmicity of GI protein levels can be produced through mutual regulation by ZTL, ELF3 and COP1. The results support ELF3 having a function in regulating GI protein stability.

5.2.8 ELF3 function is closely linked to that of the proteasome

Combining the information from Yu *et al* and the modelling simulations it suggests that ELF3 does have a role in the regulation of protein stability. As there have been previous suggestions that the speckles formed by other light signalling components are linked to protein degradation seedlings containing the *ELF3*::ELF3::YFP were entrained in 12:12 light:dark cycles and at ZT6 seedlings were placed in a solution of either the proteasome inhibitor MG132 or its vehicle

DMSO. Following 4 hours incubation, which should be sufficient to allow infiltration of the chemicals, seedlings were imaged as previously described. These images show a general trend that with the addition of MG132 the speckle formation is dramatically reduced or abolished (Figure 5.15).

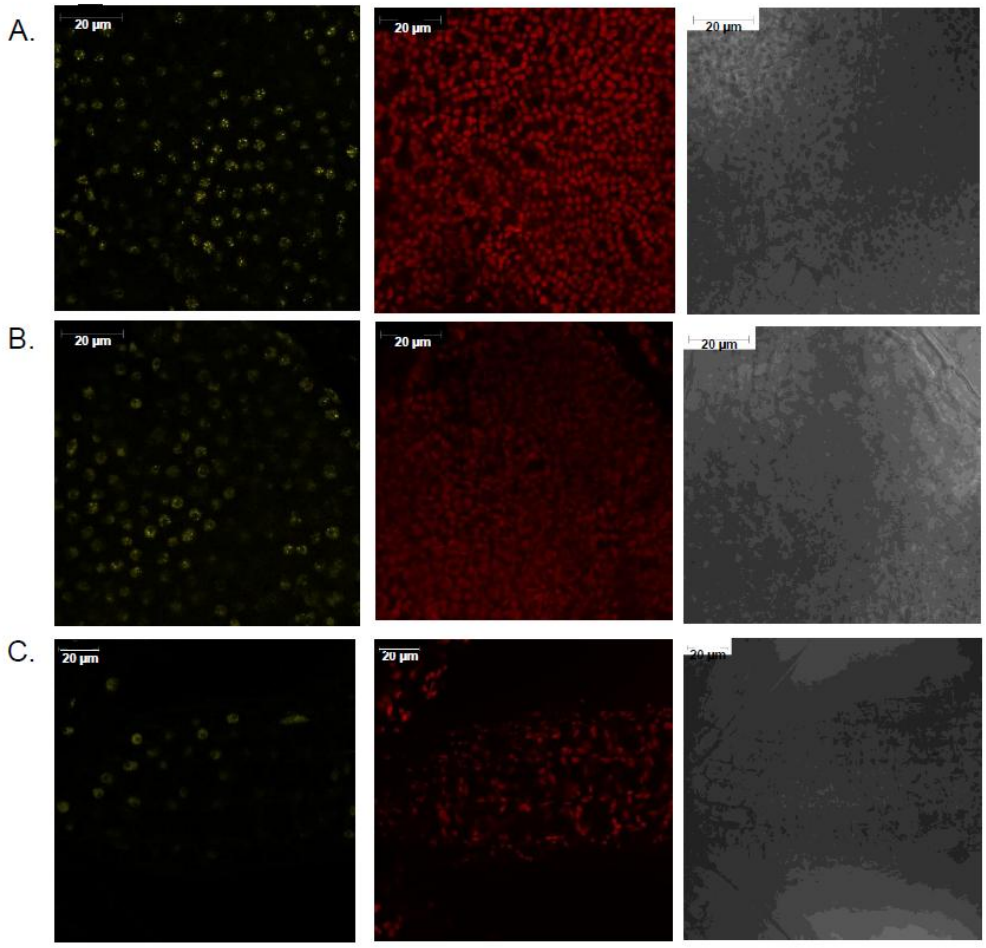

Figure 5.15: ELF3::YFP speckle formation is sensitive to proteosome function
7 day old *ELF3*::ELF3::YFP seedlings were grown in 12:12 white light:dark cycles, on day 7 at ZT 6, 5 seedlings were placed in either 0.5% DMSO (vehicle) or 100 µM MG132 in 1ml of dH_20. These seedlings then remained in entraining conditions and were imaged at ZT 10. A) An example image of DMSO control, B-C) example images of MG132 treated plants.

The images do not always show a complete loss of speckle formation, this is most likely due to the duration of incubation. In protein blot work seedlings are incubated for 16 hours in MG132

[85]. This long incubation period was not used for imaging as the power of the microscope technique used is that the plants are still alive and in relatively normal physiological conditions. The images strongly suggest that the speckle formation by ELF3 requires an active proteasome.

5.3 Discussion

The work presented in this Chapter has investigated both the position and role of ELF3 protein in the *Arabidopsis* circadian clock network. It strongly supports the idea that ELF3 has a function as a mediator of protein stability which is influenced both by circadian regulation and photoperiod. The expression and protein localisation patterns of ELF3 show that it is found in all major tissue types (Figure 5.1 and 5.3), even in the roots where ELF3 had previously been reported to have a very low expression level [23]. ELF3 localisation in the root showed faint speckle formation (Figure 5.3), identifying that there is organ specificity regarding the levels of ELF3 protein. This specificity could be linked with light signalling components and it would be interesting to observe if the speckles co-localised with any of the photoreceptors, associated with clock regulation (Chapter 1), in the shoot.

ELF3 forms nuclear speckles in all the tissue types imaged and shows distinct differences in abundance which correlate with time and light condition (Figures 5.3 to 5.5). Under light conditions the speckles are, on average, more numerous and smaller than those observed from plants which are taken from dark conditions. This is quite similar to the speckle patterns observed for the red-light photoreceptors, Phytochromes. In general the ELF3 speckles are more similar to the later, larger phytochrome speckles [118]. This observation may also be linked with *ELF3* expression patterns which also fall during the dark phase of a photoperiodic cycle. Analysis of nuclei speckle intensity over time shows that the peak levels in speckle intensity coincide with the peak levels of ELF3 measured in total protein blots (Figure 5.4B). However, the increased temporal resolution in microscope imaging shows that the single peak observed in

the protein blots may actually be a split peak, before and after the light to dark transition. This feature was also observed in some of the modelling simulations but is not presented due to the temporal resolution of the experimental data (Appendix E, Figure E1).

ELF3 is not the only protein observed to form nuclear speckles, many proteins involved in responses to a variety of stimuli, form nuclear speckles. As Table 5.1 highlights, the speckle formation is often observed in response to sudden changes in signalling pathways, and has been associated with protein degradation and chromatin re-modelling. Beyond plant responses, this type of speckle has also been observed in mammalian systems where it is linked with chromatin modification [269].

To investigate ELF3's function in protein degradation a mathematical model was developed. This network aimed to investigate if ELF3's role in protein degradation was substantial, as experimental data suggested that GI protein levels were not only regulated by COP1. The experimental results from Yu *et al* enabled a particular set of constraints on the network formation (Figure 5.6). The networks formed were able to capture a lot of the experimentally observed features, mainly through the separate regulation of light and dark conditions and the partial decoupling of ELF3 and GI degradation. This also highlights the likely importance of photoperiod control on these proteins, a feature which becomes particularly clear in the mutant simulations (Figures 5.13 and 5.14). Through comparison with experimental data in both wild type and mutant conditions a favoured network was identified. This network is the formation of an ELF3-COP1 dimer which then forms a trimer with GI (Figures 5.12, 5.13 and 5.14). This couples GI degradation tightly to ELF3 availability but ELF3 degradation is less tightly coupled to GI availability, as it can be degraded independently of GI through the ELF3-COP1 dimer. This network identifies at least two separate mechanisms of photoperiodic control on GI, directly via ZTL and indirectly via ELF3, which is reflected experimentally through GI's sensitivity to photoperiodic cycles [164]. It also indicates that the sequential formation of complexes is

important for protein regulation as this enables separate regulation at each step of the complex formation. This explains why the direct trimer formation, which completely couples ELF3 and GI degradation, does not enable the simulation of both the GI and ELF3 profiles (Figures 5.9 and 5.10). Specifically, ELF3's degradation rate must be higher than GI's.

Whilst the model Network_03 is successful in capturing a number of the experimentally observed features it does not mean that the protein interactions proposed in the model network are the definite interactions which occur *in planta*. The modelling provides an overall topology of the network and indicates at possible biological mechanisms. The network, in combination with experimental evidence from Yu *et al*, indicates that ELF3 does have a role in protein degradation. This was further tested and supported experimentally through the incubation of plants in the proteasome inhibitor MG132 (Figure 5.15). The speckle formation of ELF3 was disrupted in the presence of MG132 which highlights two main points. Firstly that the formation of the ELF3 nuclear speckle is dependent on an active proteasome and therefore that the ELF3 speckles are functional, with ELF3 degradation as a possible function. It would be of great interest to identify which other proteins are found in these speckles. The work presented in Chapter 4 has identified that both ELF3 and EARLY FLOWERING 4 (ELF4) associate with DNA, and the data in Yu *et al* shows that ELF3 binds with COP1 and GI. GI has also been shown to associate with DNA [82]. These observations, along with the many other protein interacting partners of ELF3 and the fact that the ELF3 over-expresser plants only show a very mild period lengthening (Chapter 4) suggest that ELF3 could have a role in regulating protein degradation at the promoters of clock associated genes. This would provide both clock and photoperiodic regulation to these promoters and explain why ELF3 has an abundance of protein interacting partners. The model identifies that the sequential formation of such complexes is important and this is an area which would be worth further investigation.

Chapter 6

Ostreococcus tauri as a model organism for understanding circadian rhythms

Parts of this chapter have been published in Nature in O'Neill *et al,* 2011 and submitted for publication in van Ooijen *et al*. The degradation work was conducted in collaboration with Dr. Gerben van Ooijen and I am particularly grateful to Gerben for Figure 6.9.

6.1 Introduction

Understanding the circadian network in plants has focused on the use of *Arabidopsis thaliana* (Chapter 4 and Chapter 5). For fundamental plant research this terrestrial plant offers a number of technical advantages when compared to most crop species which include, its relatively small genome size (~119Mb), short life cycle (typically around 8 weeks) and ease to grow. Circadian biologists have very successfully utilised the small and tractable genome, using screens for changes in flowering time and *pCAB2*::LUC reporter imaging to identify clock mutants (reviewed in [270] and [167]). However, such screens become saturated and are only targeting part of the cellular physiology to identify the clock mechanism. Still, an array of clock genes were identified through this and associated approaches (Chapter 1) which form a basis for any circadian homology searches in other green lineages. These homology searches in plants have identified a number of the circadian components which are conserved, mostly MYB-based transcription factors similar to CCA1/LHY, found in *Oryza sativa* (rice), *Populus nigra* (popular), *Castanea sativa, Pisum sativum* (pea), *Glycine max* (soyabean), *Phaseolus vulgaris, Lemna gibba, Lemna paucicostata, Ostreococcus tauri, Mesembryanthemum crystallinum* (common ice plant) and *Physcomitrella patens.* Also the pseudo response regulator TOC1 is well conserved and found in, rice, *Castanea sativa*, pea, soyabean, *Brassica rapa, Ostreococcus tauri* and the common ice plant (reviewed in [151]). However, a number of the clock genes are not so well conserved with ZTL only being found in rice and the common ice plant and LUX only in rice [151]. Whilst the single CCA1/LHY, TOC1 loop is known not to be sufficient to

maintain oscillations [45], the homology analysis questions what the other factors could be. Further to this the clock mechanism, regarding the canonical transcription/translation feedback loops (TTFL) does not initially show conservation across taxa as the transcriptional components seem to have diverged but the loop structure remains [167]. This observation appears counter intuitive for a signalling network which must have evolved with life and is fundamental to the temporal compartmentalisation of processes in the majority of organisms studied to date [167].

Notably, when homology searches use circadian associated modifiers of proteins, conservation is much higher. This was strikingly demonstrated with the sequencing of the algae *Chlamydomonas reinhardtii* which initially seemed to lack the majority of plant circadian components but contained all of the circadian related kinases and phosphotases as well as the dark-dependent regulator of protein degradation COP1 [13]. This is particularly interesting as a number of studies have identified these post-translational modifiers in clock networks across taxa [1, 52, 56, 271-275]. Subsequent genome analysis in *C. reinhardtii* identified proteins similar to CCA1/LHY (ROC40) and LUX (ROC15/75) [13] but no TOC/PRR homologues. The sequencing of the unicellular algae *Ostreococcus tauri* again showed that a number of the circadian components identified through genetic screens in *Arabidopsis thaliana* were absent whilst the circadian kinases and phosphotases were present [Appendix A, 53]. OtTOC1 and OtCCA1 were shown to form a signalling loop which was required, although potentially not sufficient, for circadian rhythmicity [170]. Therefore, unlike in *C. reinhardtii, O. tauri* contains a naturally reduced (minimal) plant circadian transcriptional/ translational oscillator.

This identified that *O. tauri* was an ideal model organism to understand the fundamentals of circadian biology. *O. tauri* is the smallest free-living single-celled eukaryote currently identified and is naturally found in a number of the worlds seas (Mediterranean and Sargasso Seas and the English Channel) and oceans (North Atlantic, Indian and Pacific Oceans) [169]. Most likely due to its size *O. tauri* contains a single copy of the plastid, mitochondria and golgi organelles. *O.*

tauri is easily cultured in the laboratory in enhanced artificial sea-water (ASW) and amenable to many cell-based assays, specifically as a platform for chemical biology. *O. tauri* contains a small, 12.5Mb, genome which is of comparable size to those of single-celled yeasts, *S. pombe* 12.5Mb and *S. cerevisiae* 13.5Mb. The genome, which was sequenced by Derelle *et al*, 2006, is extremely gene dense and there is little redundancy of genes. In comparison with *A. thaliana*, which has a genome size of 119Mb and ~25,000 genes only 35% exist as single copies due to genome duplication events. *O. tauri* contains a predicted 8,166 protein coding genes in its 12.5 Mb genome, making it the most gene dense eukaryote known to date [169]. This is mainly through less genetic redundancy, smaller intergenic space and gene compaction [169]. Such a reduction in redundancy means that in *O. tauri* it is may be easier to understand the functions of certain genes. This is particularly important to circadian biology where weak circadian phenotypes are often ascribed to the high level of redundancy within the gene families involved. Like *C. reinhardtii*, *O. tauri* has been shown to have circadian rhythmicity in cell division, an important physiological output for a single-celled organism [14]. *O. tauri* has also been transformed with transcriptional and translational reporter fusions to the two clock component genes (*CCA1* and *TOC1*) as well as the clock output marker *CAB* and the constitutively expressed phosphate transporter marker (*PPT*) [170]. Over-expressing and anti-sense lines were created for the two clock component genes, which were used to show that the rhythms observed in *O. tauri* are indeed endogenous oscillations [170].

For circadian research *O. tauri* offers a further advantage of being a single cell. As introduced in Chapter 1, circadian rhythms are observed at the organism, organ, cell, and molecular level in multi-cellular organisms. A single cell system offers the potential to understand some of the complexities observed in circadian responses, such as those relating to metabolism, without tissue-specific complications. Furthermore, work on a single-celled alga, which is amenable to pharmacological and genetic manipulation, offers the potential to understand some intriguing

observations in the circadian field. These include the two circadian oscillations observed in the single celled *Lingulodinium polyedra* [131] and the oscillations in *Acetabularia* which persist without nuclear input [65]. Finally, this reduced but conserved clock is the perfect system to ask how the known transcriptional/translational feedback loops link with the post-translational and metabolic mechanisms.

This chapter will outline the development of *O. tauri* as laboratory tool for use in understanding circadian biology. The work finds its foundations in the approaches used in the study of *Lingulodinium polyedra* and pharmacological approaches which have been utilised by mammalian circadian biologists.

The results presented here and in the two associated publications [Appendix A [53] and Appendix F] show that the circadian clock in *O. tauri* is very similar to that in other green lineages [26]. In *O. tauri* delayed fluorescence can be used as a circadian output (Figures 6.1 and 6.2), as seen in *A. thaliana* [236]. The rhythms in *O. tauri* were identified as nutrient sensitive (Figures 6.3 to 6.6), as are those in *Lingulodinium polyedra* [126], and a cytosolic component to the circadian network could be identified through the development of an assay which enabled *O. tauri* to remain alive in constant darkness. Following its release from darkness, where no transcription or translation was occurring, the circadian rhythms measured were not simply re-started with the transfer to light. This indicated that timing must be continuing in these near dormant cells and highlighted the possibility that part of the circadian mechanism is conserved at a more fundamental biological level than that of transcription/ translation. Testing of previously validated pharmacological compounds which are known to affect circadian rhythms in other species on *O. tauri,* identified that *O. tauri* showed the same responses (Appendix A, [53] and Chapter 7). This supported the idea of a conserved mechanism. Redox-based regulation was identified as a possible mechanism through the use of peroxiredoxin sulphonylation as a rhythmic marker for this non-transcription/translational rhythm [53, 140].

Furthermore it re-emphasises previous observations that the circadian clock is highly regulated at the level of protein function [177].

The importance of protein regulation was confirmed in *O. tauri* through the use of degradation based assays. These identified that unlike transcription and translation, although clearly required for rhythms, the degradation of proteins is fundamental for sustaining circadian rhythms (Figure 6.9). In *O. tauri* only CCA1's degradation was circadian regulated (Figure 6.7), whilst TOC1's degradation regulation occurs in response to darkness, but some circadian gating does appear to be involved (Figure 6.7). Testing the response of the more conserved oscillator through measuring peroxiredoxin sulphonylation, when protein degradation is inhibited even this rhythm is lost [Appendix F]. This highlights that protein regulation is absolutely essential for sustained circadian oscillations. It also shows that the clock components identified in *A. thaliana* may not be as central as first assumed in the *A. thaliana* or *O. tauri* clock mechanisms. Furthermore, TOC1's strong regulation by light:dark signalling indicates that the control of at least one of these core clock components is as much through photoperiodic cues as the clock itself (this idea is further explored in Chapter 8).

6.2 Results

6.2.1 Circadian markers in O. tauri

Previous reports of circadian rhythms in alga have shown that a number of aspects of their physiology are under circadian control [276]. In *Lingulodinium polyedra* oscillations in nitrate assimilation and depth in a water column are under circadian control, but the oscillator itself may be different as these two particular rhythms have a different period [131]. In *C. reinhardtii* circadian regulation of phototaxis, chemotaxis, cell division, UV sensitivity and adherence to glass have been characterized [13]. As mentioned above in *O. tauri* the circadian rhythms in cell division and of central clock components CCA1 and TOC have already been characterized [14, 170]. However, using cell division or clock genes as markers requires either extensive sampling followed by the extraction of RNA, or genetic manipulation and transformation. To avoid this requirement in *A. thaliana* delayed fluorescence can be measured [236]. This is the fluorescence collected from light harvesting pigments and has been identified to be under circadian regulation ([236] and Chapter 4). *O. tauri* also shows circadian oscillations in delayed chlorophyll fluorescence (Figure 6.1A). Delayed fluorescence was collected from cells entrained under 12:12 light:dark cycles and released into constant light. The period of the rhythms measured is slightly short of 24 hours (around 22 hours on average) (Figure 6.1B and C), as seen in *Arabidopsis* [236].

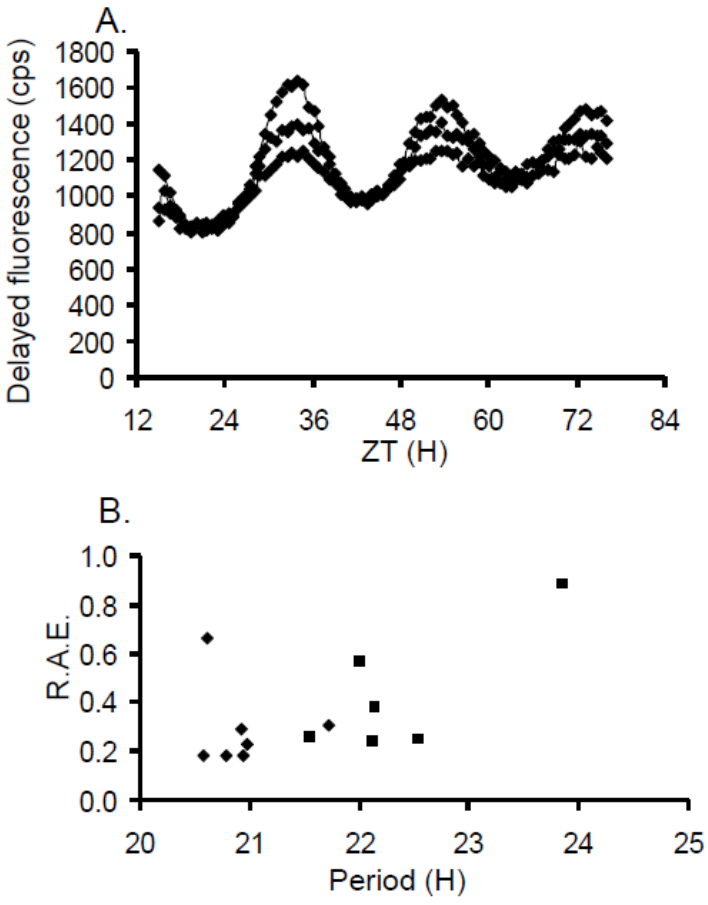

C.

	No. of wells	No. rhythmic	% rhythmic
Wild type 1	7	7	100
Wild type 2	7	6	86

Figure 6.1: Delayed fluorescence rhythms in *O. tauri* cells
O. tauri wild type (OTTH0595) cells were entrained in 12:12 blue light:dark cycles for 7 days and then transferred to constant red and blue light during data collection by the Topcount. Delayed fluorescence was measured for 2 seconds following no count delay. A. Example traces of wild type cells delayed fluorescence rhythms. B. Period vs Relative Amplitude Error (R.A.E.) analysis for two independent experiments, wild type 1 (filled diamonds) and wild type 2 (filled squares). C. The number of wells imaged and percentage rhythmic.

In the transformed lines the delayed fluorescence shows sensitivity to the additional copy of the proteins. In the protein lines CCA1 has a delayed florescence pattern very similar to that of wild type (Figure 6.2A, open squares) whilst the TOC1 line shows no observable rhythms (Figure 6.2A, black rectangles) and has few rhythmic traces following FFT-NLLS analysis (Figure 6.2B and C). This is most probably related to an output function of the TOC1 protein and chlorophyll/chloroplast regulation as the TOC1 line is still rhythmic at the level of gene expression and TOC protein [170].

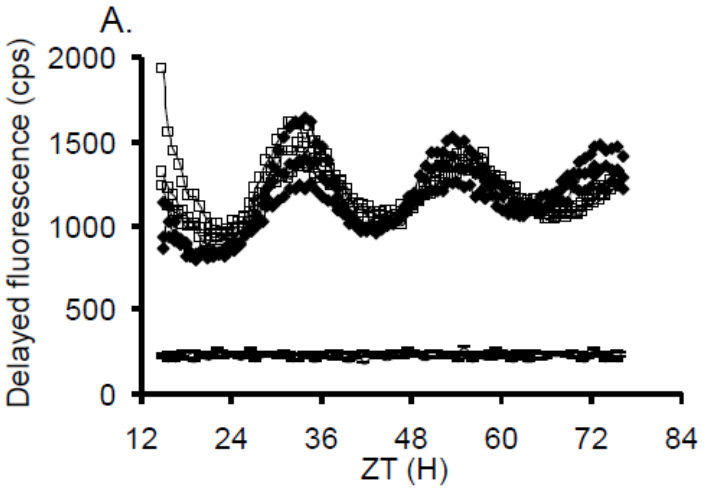

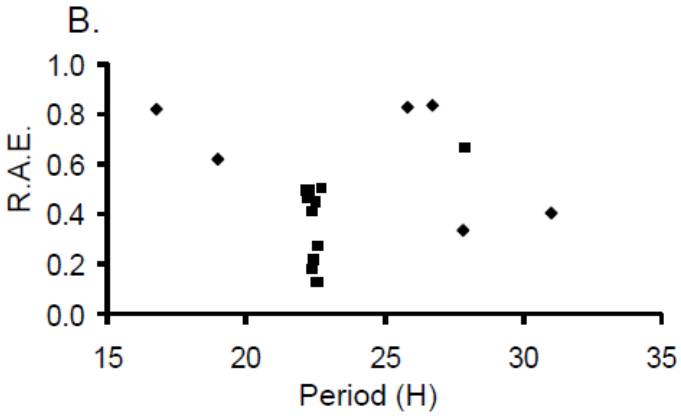

C.

	No. of wells	No. rhythmic	% rhythmic
CCA1	12	12	100
TOC	12	6	50

Figure 6.2: Delayed fluorescence rhythms in transformed *O. tauri* cells
O. tauri cells transformed with either *TOC1*::TOC1::LUC or *CCA1*::CCA1::LUC were entrained in 12:12 blue light:dark cycles for 7 days and then transferred to constant red and blue light during data collection by the Topcount. Delayed fluorescence was measured for 2 seconds following no count delay. A. Example traces of wild type cells delayed fluorescence rhythms (filled diamonds), *TOC1*::TOC1::LUC (filled rectangles) and *CCA1*::CCA1::LUC (open squares). B. Period vs R.A.E. analysis for both lines, *TOC1*::TOC1::LUC (filled diamonds) and *CCA1*::CCA1::LUC (filled squares). C. The number of wells imaged and percentage rhythmic. Data is representative of three independent experiments.

6.2.2 Metabolic contributors to circadian rhythms in O. tauri

6.2.2.1 The effects of carbohydrate levels on circadian rhythms in O. tauri

O. tauri can be cultured in either real sea water or enhanced artificial sea water (ASW). The advantage of ASW is that contamination is lower, there is no requirement to have a ready supply of sea water and the components of the sea water can be modified and regulated according to requirement. As *O. tauri* is an obligate phototroph one of the first tests was to identify a carbohydrate source which would enable *O. tauri* to survive in darkness [53]. The carbohydrate source identified was D-sorbitol and glycerol (Chapter 2). With the addition of D-sorbitol and glycerol *O. tauri* was able to remain competent for as long as 5 days in constant darkness. However, under these conditions *O. tauri* is not conducting transcription or translation [53] and therefore most probably not undergoing cellular division. *O. tauri* circadian rhythms are affected when cells are kept in this carbohydrate supplemented media. Under constant light, the oscillations in the *CCA1*::CCA1::LUC line, are not observed to damp as rapidly compared to cells in ASW (Figure 6.3A). This reduction in damping of the rhythms is not likely to be a reflection of cell count as the cells are entrained for 7-days, in the respective media, in 96-well plates. In the 96-well plates cell division is believed not to be occurring [53]. Therefore, the more robust rhythms are either a product of the increased nutrients affecting energy via the luciferase output and/or through increased or more sustained synchronisation of rhythms. The additional carbohydrate source also has a mild effect on the period length of the rhythm, showing a period lengthening of almost 1 hour (Figure 6.3A and B).

A.

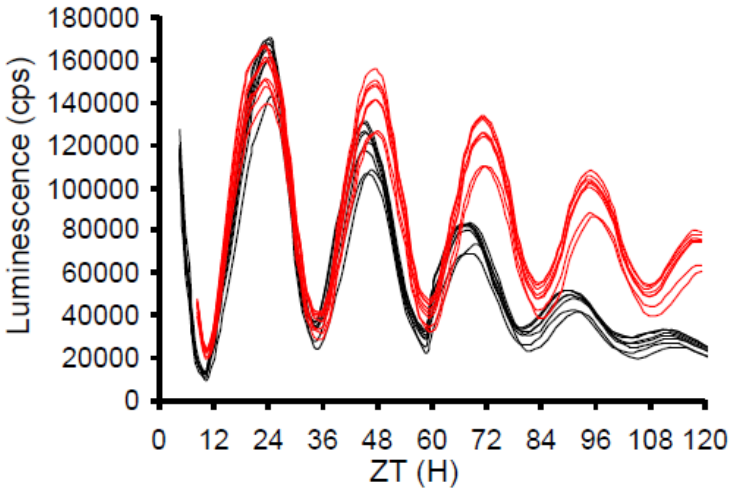

B.

	Mean period	SEM
ASW	23.67	0.10
ASW + carbohydrate	24.73	0.03

Figure 6.3: Addition of carbohydrate affects the amplitude and period of rhythms
O. tauri cells containing the *CCA1*::CCA1::LUC marker were entrained for 7 days in 12:12 blue light:dark cycles on either artificial sea water (ASW) (black lines) or ASW containing 200 mM D-sorbitol and 0.4% glycerol (red lines). Cells had 0.5% DMSO added at ZT0 and were released in to constant red and blue light during data collection by the Topcount, n=8.

In constant darkness a single peak is observed during the first 24 hours in darkness from the translational reporters (Figure 6.4A, B, C black, closed rectangles) before the cells enter a non-transcriptional/translational state. This single peak is also observed when cells are released into constant light with the photosynthetic chain inhibitor DCMU being applied at ZT0 (Figure 6.4A red crosses) but not when either transcription or translation are partially inhibited (Figure 6.4B and C respectively). The same single peak is observed for all three drugs when cells are released into constant darkness (Figure 6.4A, B, C red rectangles). DCMU functions through binding the plastoquinone (PQ) binding site on photosystem II (PSII). This will not only disrupt photosynthesis but will also causes a significant change in redox signalling from PQ. This data suggests that the photosynthetic chain, either through photosynthate or redox, is essential for the circadian oscillations in *O. tauri* as the cells are still viable to survive on the high carbohydrate media.

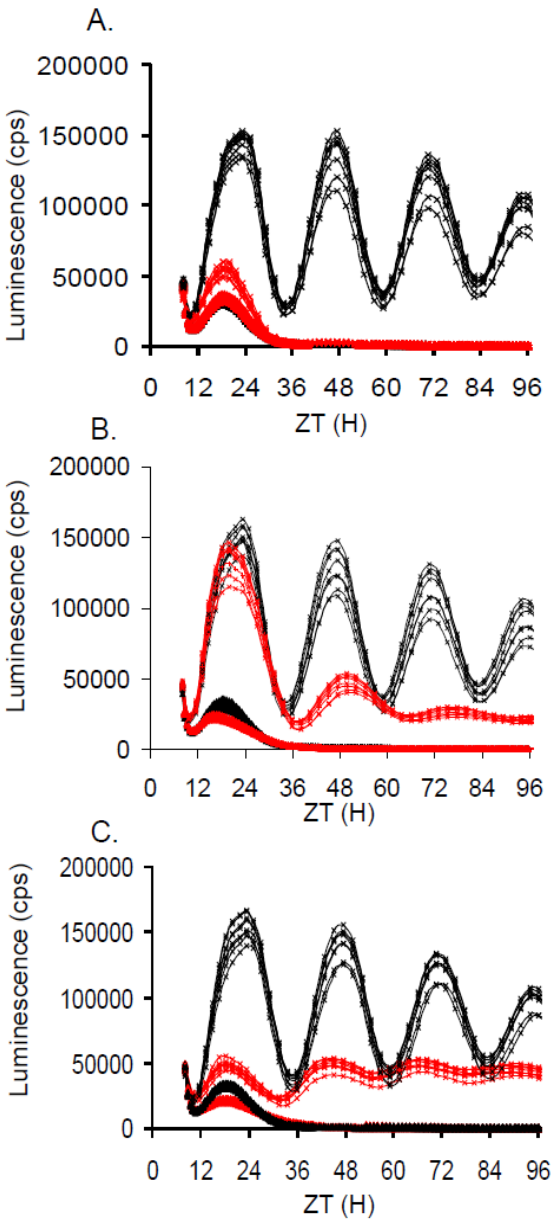

Figure 6.4: Photosynthesis is a requirement for circadian rhythms in *O. tauri*
O. tauri cells were entrained in ASW with 200 mM D-sorbitol and 0.4% glycerol for 7 days in 12:12 blue light:dark cycles. Cells were then either treated as vehicle controls (black lines) or with non-saturating drug treatments (red lines), where vehicle trace obscured by treated there is no change by treatment. Treatments DCMU (1 nM) for photosynthetic inhibition (A), cordycepin (0.5 µg/ml) for transcriptional inhibition (B) or cycloheximide (0.5 ng/ml) for translational inhibition (C). Luminescence was then collected by the Topcount under constant light (LL, crosses) or constant dark (DD, bars), n=8 for all experiments. Data is representative of two independent repeats.

6.2.2.2 The effects of nitrate levels on circadian rhythms in O. tauri

Nitrate has been identified as a non-photic entrainment signal to the circadian system in *Lingulodinium polyedra* [126]. In this system the addition of nitrate to nitrate starved cells caused phase delays. These delays, and therefore the effect of nitrate could be blocked through the dual addition of nitrate and the glutamine synthase inhibitor MSX (L- methionine sulfoximine). Glutamine synthase is the final enzyme in the pathway which converts nitrate into glutamine. Also in this pathway is nitrate reductase, an enzyme which is known to be under circadian regulation [132, 277, 278]. The study in *L. polyedra* used its physiological circadian markers of bioluminescent glow and aggregation as outputs to this response [126]. In *O. tauri* the transcriptional and translational CCA1 lines are used. In response to increasing nitrate levels being added to nitrate starved cells there is a clear dose-dependent rise in luminescence level and rhythm amplitude for both CCA1 and *pCCA1* lines (Figure 6.5A and C respectively). There is a slight phase advance in both lines but only *pCCA1* shows a change in period length (Figure 6.5C and D), notably these changes in circadian response are not dose-dependent (Figure 6.5B and D).

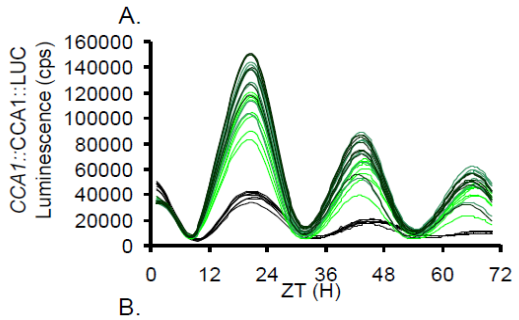

B.

	Number of wells	Mean Period (Hrs)	SEM
Low NO_3 ASW	8	24.18	0.20
Low NO_3 ASW + 300μM NO_3	8	23.96	0.08
Low NO_3 ASW + 700μM NO_3	8	23.82	0.07
Low NO_3 ASW + 1mM NO_3	8	23.79	0.08

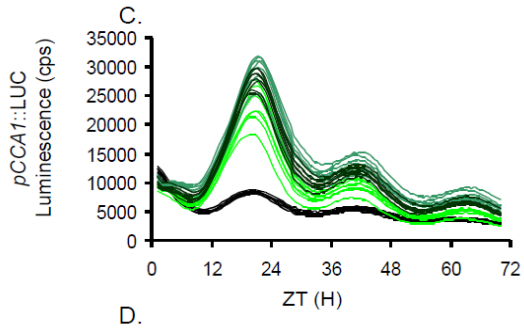

D.

	Number of wells	Mean Period (Hrs)	SEM
Low NO_3 ASW	6	21.19	0.15
Low NO_3 ASW + 300μM NO_3	8	22.39	0.37
Low NO_3 ASW + 700μM NO_3	8	22.93	0.88
Low NO_3 ASW + 1mM NO_3	8	22.23	0.07

Figure 6.5: Circadian rhythms in *O. tauri* are sensitive to the level of nitrate
O. tauri cells were cultured in a modified ASW with $2.2x10^{-4}$ M $NaNO_3$ as the only source of nitrogen and entrained in 12:12 blue light:dark cycles. All medium was refreshed the day before imaging started and cells had either no more nitrate (black), 300 μM $NaNO_3$ (light green), 700 μM $NaNO_3$ (mid-green) or 1 mM $NaNO_3$ (dark green) added to either *CCA1*::CCA1::LUC (A) or *pCCA1*::LUC (C). At ZT 0 recording of luminescence levels by the Topcount started, n=8 for all experiments. Rhythmicity was assessed by FFT-NLLS on BRASSv3 software and a summary is presented for *CCA1*::CCA1::LUC (B) and *pCCA1*::LUC (D). Data is representative of two independent repeats.

The amplitude based response shows that the *O. tauri* oscillator is sensitive to nitrate levels, this is not surprising given that nitrate is a scarce nutrient in marine environments. In response to the dual addition of nitrate and MSX *O. tauri* did not respond like *L. polyedra* as *O. tauri* does not show phase shifts with the addition of nitrate. Again only amplitude was affected. In nitrate starved cells the circadian oscillations are very low amplitude (Figures 6.5 and 6.6), the addition of nitrate recovers the amplitude of the rhythms (Figure 6.6) but they also damp or lose amplitude very quickly.

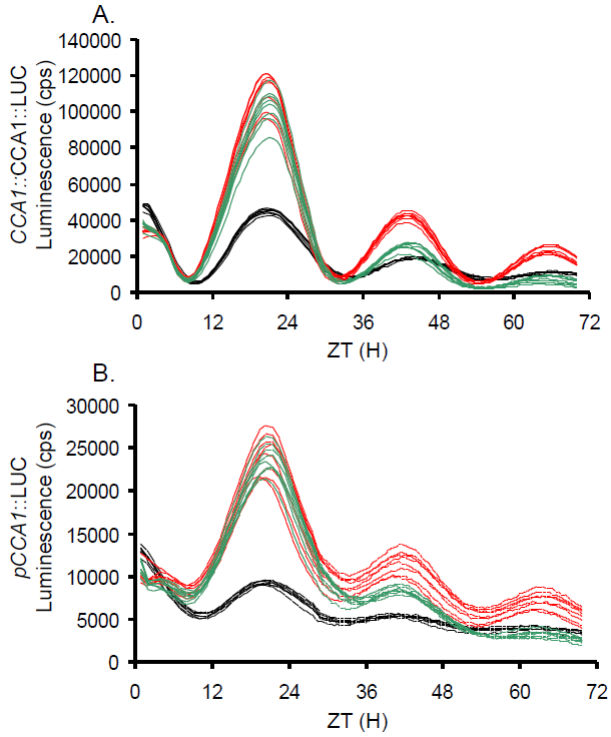

Figure 6.6: Nitrate metabolism affects the circadian waveform in *O.tauri*
O. tauri cells were cultured in a modified ASW with $2.2x10^{-4}$ $NaNO_3$ as the only source of nitrogen and entrained in 12:12 blue light:dark cycles. At ZT 0 data collection started by the Topcount and cells were either refreshed in low $NaNO_3$ (black), had 700 µM $NaNO_3$ added (green) or 700 µM $NaNO_3$ and 40 µM MSX (red) with vehicle to either *CCA1*::CCA1::LUC (A) or *pCCA1*::LUC (B), n=8. Rhythmicity was assessed by FFT-NLLS on BRASSv3 software. Data is representative of two independent repeats.

With the addition of MSX, at a non-saturating level, the amplitude damps more slowly. This indicates that nitrate is affecting circadian rhythms in *O. tauri* but not as significantly as it

affects the rhythms in *L. polyedra*, this could be because the *O. tauri* data measures gene and protein response whilst in *L. polyedra* the output was physiological. These assays, and the results from [53], identify that *O. tauri* is perfect to investigate the links between the TTFL and other factors influencing the oscillator. Developing on work from [53] the importance of protein degradation was next investigated.

6.2.3 Protein degradation of CCA1 but not TOC1 is under circadian regulation

To investigate the role of protein degradation in circadian rhythms the translational fusion lines (*CCA1*::CCA1::LUC and *TOC1*::TOC1::LUC) were used in a constant light (LL) pharmacological assay. *De novo* protein synthesis was blocked by applying saturating levels of cycloheximide (CHX) [53] at 2 hour intervals across 24 hours. From the luciferase luminescence recorded from these lines the degradation rate could be calculated through curve fitting to the initial exponential decay of these traces (analysis conducted by Dr. Carl Troein). In constant light TOC1 degradation remained relatively stable whilst CCA1 showed a clear peak in degradation around ZT6, which is the middle of the subjective day (Figure 6.7A). This strongly indicates that CCA1 protein degradation is under circadian control. As noted in Appendix F the absolute rates show slight variability between experiments but the peak rate of *CCA1*::CCA1::LUC degradation is about 2-3 times higher than that of the trough. Further to this using actual molecule numbers, measured by Gerben, the actual number of *CCA1::*CCA1::LUC molecules being degraded at the peak is around 100 molecules per cell per hour [Appendix F].

6.2.4 TOC1 protein degradation is under light:dark regulation

Whilst TOC1 protein degradation was not under circadian regulation it was clear from the *TOC1*::TOC1::LUC traces in light:dark cycles that the protein was subject to degradation control (Examples shown in Chapter 8). To investigate this further the degradation rates of TOC1 and CCA1 were measured, as in LL conditions, under photoperiodic conditions of standard 12:12, long day 18:6 and short day 6:18 light:dark cycles. Under these conditions the flat line of TOC1 degradation rate is lost, with TOC1 degradation being responsive to darkness. This is clearly seen under 18:6 (Figure 6.7A) and 12:12 conditions but is less notable under 6:18 where there is a mild increase in degradation rate after ZT 12. This indicates that whilst TOC1 degradation is not directly under circadian control, the circadian clock must regulate an aspect of the TOC1 protein degradation to ensure that TOC1 is not immediately degraded when transfer to darkness is before a certain time. Therefore, TOC1 degradation is dark and day-length dependent, inferring some circadian gating mechanism. This is particularly notable when the degradation rate is normalised (through multiplication with luminescence level from the control traces of the assay) to provide the absolute cellular degradation of CCA1 and TOC1 (Figure 6.7B). These results suggest that the timing of degradation in the *O. tauri* clock is important for the physiological phases observed for CCA1 levels.

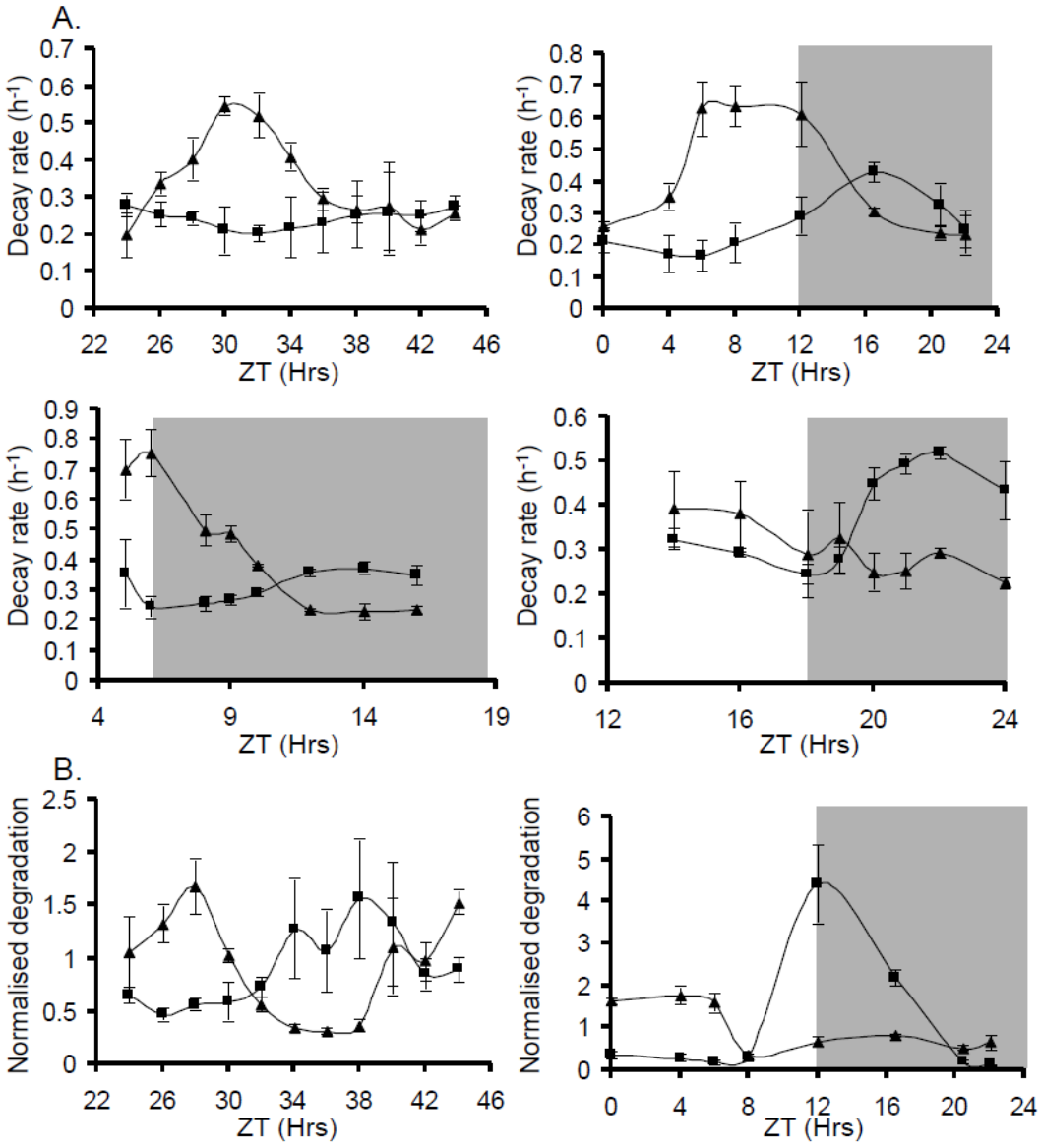

Figure 6.7: Degradation rates of CCA1 and TOC1 under different light conditions
O. tauri cells were entrained in blue light either under the imaging photoperiod condition or in 12:12 light:dark cycles before release into LL. All data collection was under red and blue light on the Topcount. A) Degradation rates of *CCA1*::CCA1::LUC (triangles) and *TOC*1::TOC1::LUC (squares) were calculated from curve fitting the exponential phase of decay following inhibition of *de novo* protein synthesis with cycloheximide at the time-points indicated. Photoperiod conditions are represented by the white (light) and grey (dark) areas. Error is SEM of n=5. B) Normalised absolute degradation of *CCA1*::CCA1::LUC (triangles) and *TOC1*::TOC1::LUC (squares) for LL and LD 12:12 conditions. Error is SEM of n=5.

6.2.5 Protein degradation is essential for sustained rhythms in the circadian clock

The results from Figure 6.7 indicate that the timing of degradation is important for the phases of the circadian components, specifically CCA1. Furthermore, the levels of protein from the molecular counts do not reach 0 (Appendix F) indicating that there is fine regulation on degradation. That is the degradation of CCA1 and TOC1 can not only be considered through substrate availability, they may also be circadian regulation on the degradation machinery. Alternatively, through sequestering of protein to complexes a proportion of TOC1 and CCA1 may not available for degradation. To investigate importance of protein degradation in circadian timing further the proteasome inhibitor MG132 was used to conduct a "wedge" experiment. The specificity of MG132 was confirmed through comparison with the known highly specific proteasome inhibitor epoximicin [Appendix F]. For a wedge experiment *O. tauri* are treated with either drug or vehicle for increasing duration (4, 8, 12, 16, 20 and 24 hours) starting from different times and the phase of the reinitiated rhythms in LL following wash-off are analysed. Therefore the drug used must be reversible such that with wash-off the pharmacological inhibition is stopped and the resultant rhythms measured show the effect the compound had on the clock mechanism. This was confirmed for MG132 for two phases of drug application (Figure 6.8). Following wash-off the clock was phase delayed by about the duration of the MG132 treatment but following a 12 hour dark period light responses occur which enabled phase changes to coincide the oscillator and photoperiod cycles.

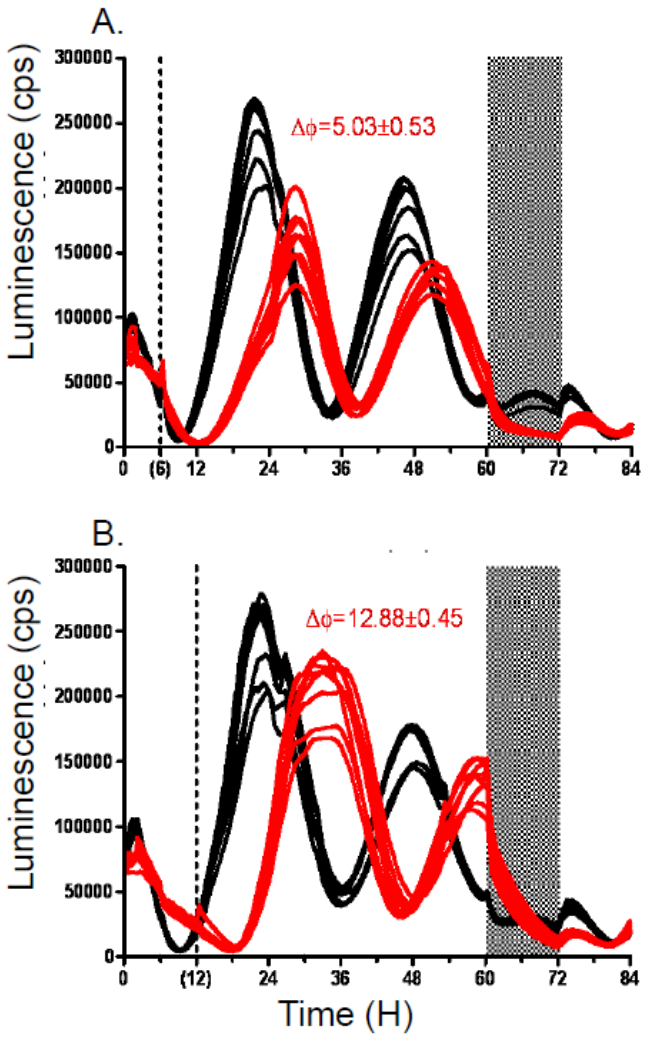

Figure 6.8: MG132 allows reversible inhibition of proteasome function
O. tauri cells containing *CCA1*::CCA1::LUC were entrained in 12:12 blue light and released in to constant red and blue light for data recording by the Topcount. MG132 (red lines) or vehicle (black lines) was applied to *O. tauri* cells at times indicated by the black dashed line and washed off after 6 (A) or 12 (B) hours. Phase change (Δφ) following wash-off is indicated. Cells were imaged in LL for 2 days followed by 12 hours of darkness to test the clocks ability to re-entrain.

This confirms that MG132 could be sufficiently washed-off to enable circadian behaviour in these cells. This pulsed inhibition allows the identification of any phases which are sensitive to proteasomal inhibition through comparison with the vehicle trace. A wedge shape in response in phase changes of the treated lines indicates that the treatment has stopped the clock and that the cell's phase has been set by drug wash-off. Alternatively the wash-off response might be similar to that of the vehicle and so the drug has not affected the circadian mechanism. The results from transcriptional and translational inhibition showed a complex mix of these two hypotheses [53]. The results of reversible MG132 inhibition showed the wedge shape, indicating complete resetting of the circadian mechanism to drug wash off (Figure 6.9A and B). This shows that post-translational mechanisms, specifically protein degradation, are essential for circadian rhythmicity, a point which is expanded on in the discussion (6. 3).

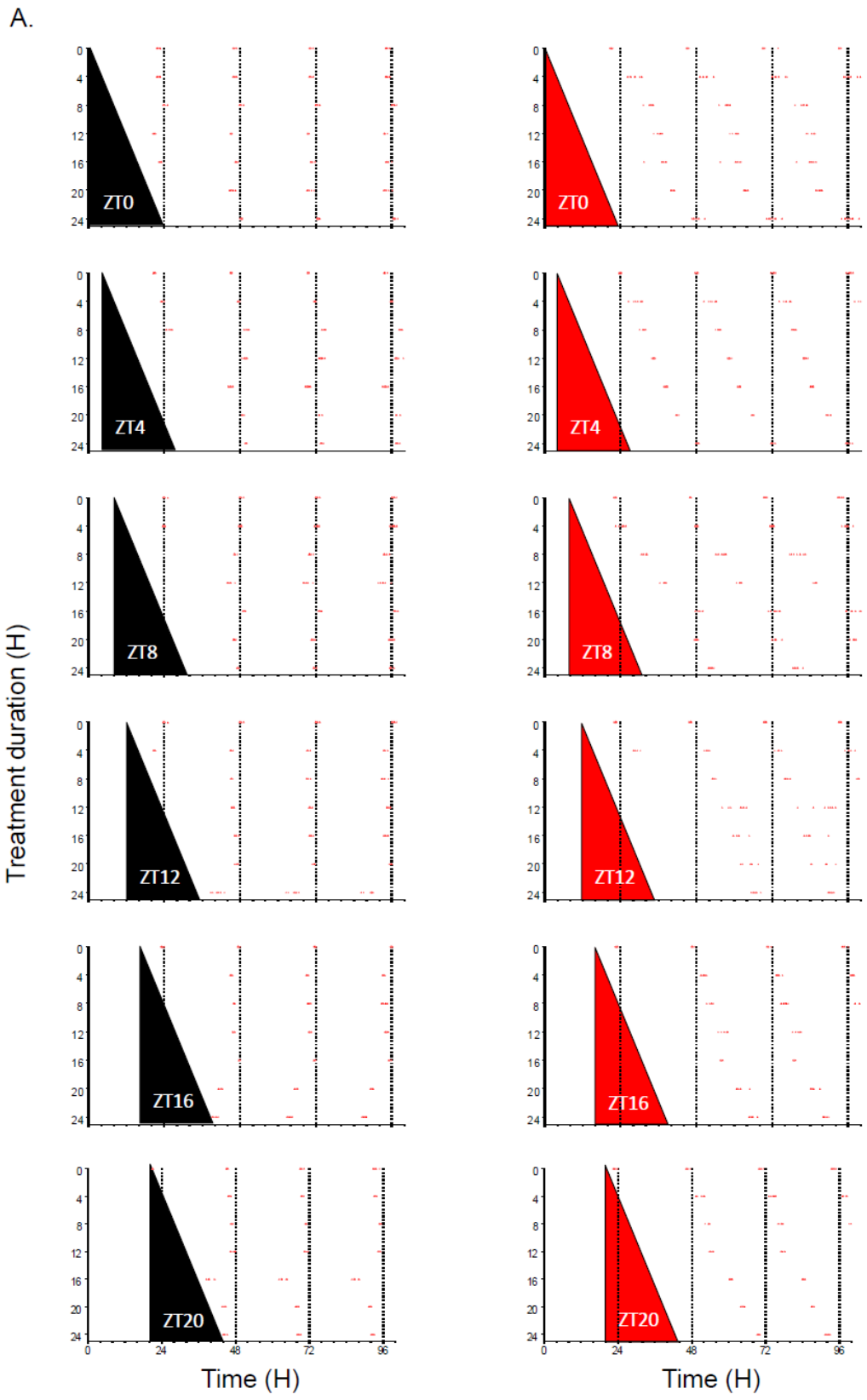
A.
ZT0
ZT0
ZT4
ZT4
ZT8
ZT8
ZT12
ZT12
ZT16
ZT16
ZT20
ZT20
Treatment duration (H)
Time (H)
Time (H)

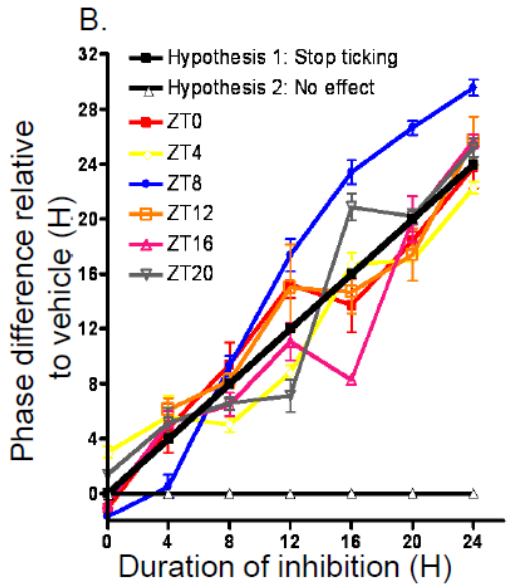

Figure 6.9: Proteasomal inhibition stops TTFL rhythmicity independent of phase
Wedge data from cells entrained in 12:12 blue light:dark cycles and released into constant red and blue light (LL) for data recording by the Topcount. A) MG132 inhibition (red wedge) or vehicle treatment (DMSO, grey wedge) were applied to cells for various (0-24) hours starting at ZT0 and ending with wash-off. The peak phase of individual wells of *CCA1*::CCA1::LUC following wash-off are shown by the black triangles. B) Summary of phase shifts relative to vehicle controls for all treatment times. Error is represented as SD, n≥6. The two hypothetical responses of either complete stopping of the oscillator (Hypothesis 1: Stop ticking) or no effect (Hypothesis 2: No effect) are shown on the graph.

6.2.6 Proteasome mediated degradation is not the only clock relevant protein degradation mechanism in O. tauri

The degradation of *CCA1::*CCA1::LUC is under circadian regulation (Figure 6.7) and the wedge analysis shows that the clock can not continue when the proteasome is not functional (Figure 6.9). However, analysis of the imaging traces indicates that the relationship between CCA1 and the proteasome is more complicated than just direct proteasomal-mediated degradation of CCA1. When either MG132 or epoximicin are applied to CCA1::LUC cells at ZT36, before the peak in CCA1 degradation but when levels of CCA1 are decreasing, no immediate effect is observed but the rhythms are not sustained (Figure 6.10A). With the application of MG132 or epoximicin following peak degradation rates, ZT38, the rhythms are lost and the levels of CCA1 does not

rise again (Figure 6.10B). This could suggest that CCA1 degradation is not directly proteasome mediated but that the proteasome is required for CCA1 levels to rise. Such a requirement implies that there is a negative regulator of CCA1, the levels of which are controlled by the proteasome and degradation of this negative regulator is required for CCA1 levels to rise.

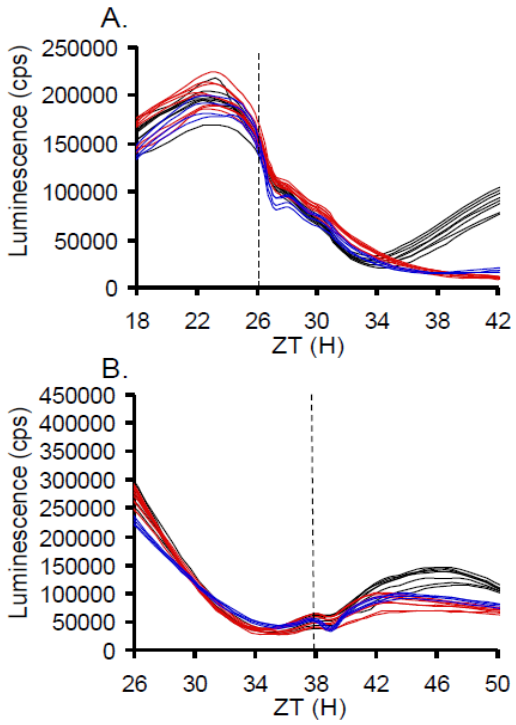

Figure 6.10: Effects of proteasomal inhibition on CCA1
O. tauri cells were entrained in 12:12 blue light:dark cycles and released into constant blue and red light for data recording by the Topcount. Saturating concentrations of epoximicin (10 μM) and MG132 (40 μM) were applied to *CCA1*::CCA1::LUC cells at either ZT 26 (A) or ZT 38 (B) indicated by the black dotted line and luminescence recorded. Vehicle (black lines), epoximicin (blue lines) and MG132 (red lines), n=5.

6.3 Discussion

With genetic modification comes the possibility to continually and non-invasively monitor molecular rhythms within cells and organisms. This allows tracking of the circadian rhythm, under different environmental conditions, as well as the manipulation and monitoring of its responses. *A. thaliana* enables this but has limitations. Most notably the high level of genetic redundancy can make interpretation of mutant phenotypes particularly hard. Also *A. thaliana* is

not very amenable to pharmacological assays, an experimental tool which has proven to be very powerful in investigating circadian rhythms in other organisms. *O. tauri,* like *A. thaliana,* can be used to continually monitor circadian rhythms in a non-invasive fashion; it is also amenable to genetic and pharmacological manipulation. Furthermore, unlike *A. thaliana, O. tauri* has a low level of genetic redundancy, specifically relating to the core TTFL circadian genes and is highly amenable for pharmacological assays [53]. *A. thaliana* offers a wealth of genetic tools, including T-DNA mutants and gene characterisation; therefore in combination with *O. tauri* they are a very powerful tool for investigating plant circadian rhythms [53, 168 and 170]. The work in this chapter further contributes and develops the use of *O. tauri* as a model organism for studying circadian rhythms.

Like *A. thaliana, O. tauri* shows circadian rhythms in delayed fluorescence (Figure 6.1). This observation could be very useful in screening for circadian mutants as it allows a high-throughput screen and requires absolutely no genetic manipulation of the cell, which could affect the circadian rhythms. It also demonstrates that the photosynthetic machinery of *O. tauri* is under circadian control.

The use of *O. tauri* also enables investigation of the circadian clocks responses to nutrient levels, something which is technically hard to achieve with *A. thaliana* due to growth condition requirements. It is common for photosynthesis to be separated from nitrate metabolism as photosynthesis produces oxygen and aspects of nitrogen metabolism require an anaerobic environment. In some multi-cellular plants this problem has been resolved through spatial separation (C4 metabolism) [279] but an obvious solution in a single celled alga is temporal. In the marine environment a number of nutrients are limiting, in particular nitrates, this is because they are usually sequestered in large complexes, much deeper in the ocean [126]. For this reason a number of dinoflagulates and alga dive during the night, and this is one of the circadian phenotypes observed in *L. polyedra* [126]. *O. tauri'*s circadian rhythm responses to varying

nitrate levels were investigated (Figures 6.5 and 6.6) and it too shows sensitivity to nitrate levels. This response is observed in the amplitude and possibly synchronisation of the rhythms (Figure 6.6). In *L. polyedra* nitrate has been identified to have an effect on the phase of a circadian clock output. In *O. tauri* nitrates were not observed to have a significant effect on the phase of the oscillations when applied at ZT0 (Figures 6.5 and 6.6). A role in phase regulation of the *O. tauri* clock can not be eliminated as it may be affecting the rhythms in a phase-specific manner, and not all phases where investigated here. A possible mechanism is that nitrate signaling is both an output and an input and could be signaling in conjunction with light signaling pathways. This would make a simple chemical based dissection of the pathway extremely hard.

This is also true for dissecting the role of photosynthate versus light signaling through the photosynthetic machinery regarding entrainment and synchronization of rhythms. Whilst the enriched carbohydrate ASW is sufficient to keep *O. tauri* cells alive it does not permit normal cellular behavior [53] making it technically hard to separate the signaling contributions from light signaling and the photosynthetic electron transport chain. Chemical analysis of this pathway through the application of DCMU indicates that a functional photosynthetic electron transport chain is very important for rhythms. The speed with which the cells respond to DCMU inhibition in constant light (Figure 6.4) in enhanced carbohydrate ASW may suggest that the function of this chain is not simply the carbohydrate output but could be linked with the reducing potentials created through a functional photosynthetic chain.

The importance of redox has previously been reported relating to circadian rhythms [280] and was further endorsed with the identification of sulphonylation of peroxiredoxins as a rhythmic marker [Appendix A, 53, 140]. The rhythms in sulphonylation of peroxiredoxin persist in the absence of transcription and translation in *O. tauri* (Appendix A and [53]) and are now being identified to occur in all taxa currently studied in circadian biology [J. O'Neill, personal communication]. This strongly suggests that post-translational mechanisms are going to be

important in the regulation of circadian rhythms. One type of post-translational mechanism which has been linked with circadian regulation is protein degradation [177]. The role of protein degradation for sustaining circadian rhythms in *O. tauri* is investigated in this chapter, sections 6.2.4 to 6.2.6.

The results in Figures 6.6 to 6.10 show that protein degradation is essential for sustaining circadian rhythms and that the clock has a role in regulation of protein degradation. It was previously considered that although protein degradation is relevant to the clock it did not need to be regulated by the clock. At a mechanistic level only one of the two central component's degradation is under strong circadian regulation, CCA1 (Figure 6.7). However, the results from Figure 6.10 suggest that it is a negative regulator of CCA1 which is the target for proteasome mediated degradation, not directly CCA1 protein. Through comparison with *A. thaliana*, DET1 is a potential candidate [109]. TOC1 protein is not directly regulated by circadian controlled degradation but through light-controlled degradation, which is photoperiod sensitive (Figure 6.7). Through comparison with *A. thaliana,* ZTL and COP1 are possible candidates for this dual circadian and dark dependent regulation [11 and 242]. In *A. thaliana,* ZTL is a blue-light photoreceptor which targets TOC1 for degradation in the dark [11]; the levels of ZTL are regulated by the clock [81]. Likewise COP1 in *A. thaliana* is a dark active ubiquitin E3-ligase which targets proteins involved in photomorphogenesis, including clock proteins such as ELF3, for degradation [85] and Chapter 5. TOC1 protein degradation in *O. tauri* is not independent of circadian regulation as an increase in degradation rate is not immediately observed with the onset of darkness in all photoperiodic conditions. Under short-day conditions the increase in degradation is gated to the second half of the dark period (Figure 6.7). The complete resetting of circadian phase observed in the wedge experiment in Figure 6.9 shows that timing information is contained regarding protein abundance, or possibly modification state. Whilst transcription is required for circadian rhythms it is not providing a significant proportion of the timing

information [53, 64]. The observation that protein degradation is required for sustaining circadian rhythms suggests that degradation control on the core clock proteins should be important for circadian timing. Both CCA1 and TOC1 show at least some circadian regulation on degradation. However, it seems that both are indirectly regulated at the level of protein degradation. In fact the close regulation of TOC1 with photoperiodic conditions and its importance in the phase of the circadian mechanism in *O. tauri* may suggest that it is more closely involved with the entrainment of the oscillator rather than the oscillator itself, an idea which is explored further in Chapter 8.

Chapter 7

Using *Ostreococcus tauri* in chemical biology

The chemical screen uses compounds from M. Tyers group and the work is in collaboration with J. Wildenhain. My thanks to Martin Beaton for help with pairing the screen results.

7.1 Introduction

As introduced in Chapters 1 and 6 *Ostreococcus tauri* has been recently sequenced [169], characterised and identified to contain a minimal plant circadian clock [170]. The development of genetic tools [170] has enabled this network to be investigated through non-destructive luminescence imaging (Chapter 6 and 8) [170, 53, 168]. This work has relied on the physiology of the cells to form aggregates at the base of 96-well plates which enables manipulation of the media without loss of cells. This method, in particular, lends itself to pharmacological studies. The identification of a plant species which is both amenable to genetic and pharmacological manipulations enables a range of experiments which were not previously possible in *Arabidopsis*. This is due to a number of factors; the robust plant cell wall means that a very high compound concentration is required to observe effects, the plant vacuole can store and denature the compounds, and due to the time taken for the compounds to enter the plant pulse treatments are impossible. Also, the screening of whole seedling to pharmacological compounds is extremely laborious due to planting, growth conditions and size of the seedlings [281, 282, 283]. The alternative is less physiologically relevant plant stem cell lines [284]. As pharmacological inhibitors often target enzyme active sites, it makes them ideal to investigate the cytosolic and enzymatic components of the circadian clock. Work detailed in [53] has used previously verified pharmacological compounds to identify that the circadian mechanism in *O. tauri* responds to these compounds in the same way as observed in other organisms, including

mammals, insects and fish. The study has re-emphasized that the post-translational mechanisms are as essential as transcription for circadian rhythms; furthermore it suggests that there could be a common mechanism to the circadian clock across taxa. Of particular interest is that transcription does not always have an essential role in the setting of circadian time as transcription can be inhibited at certain phases and have no effect on circadian timing [53]. This is consistent with the observation in mouse fibroblasts where circadian rhythms were largely unaffected by the global rates of transcription [64]. A number of publications have identified roles for post-translational and cytosolic components in circadian clocks [reviewed in 29 and 56]. Only a few of these components have been linked with the plant circadian network, such as Casein kinase II and cADPR/Ca^{2+} [10, 174] and not without controversy [285]. Others such as *tej*, which is a poly(ADP-ribose) glycohydrolase [148] and LIP1 a small GTPase [160] have not been linked into specific locations within the plant clock network.

To develop on the results of [53] and Chapter 6, a number of compounds were tested which were associated with similar biological processes as those identified in [53] or have been identified in other species to have effects on circadian rhythms. Previous pharmacological work has been conducted on *L. polyedra,* another unicellular alga, which was used as a starting guide for drug searches, along with other previously verified compounds in plants [286, 287, 288]. Through this a small number of compounds were identified to have effects on *O. tauri's* circadian rhythms, but not all of the compounds tested were effective (Table 7.1). This was mainly due to it being very hard to identify groups of compounds which will specifically target aspects of metabolism and the circadian clock and are soluble in non-toxic vehicle solutions.

As *O. tauri* could be successfully used in pharmacological assays a more systematic, high-throughput approach could be employed to identify compounds which affect circadian rhythms. Chemical screens have been used on mammalian cells to identify a number of compounds which affect the circadian clock [289, 290]. This includes the identification of a compound which

causes a short period rhythm in human U20S cells, through characterisation it was identified to be targeting the glycogen synthase kinase 3 (GSK3β) [289]. This confirmed previous reports that GSK3β was required for period control in the mammalian clock [273]. A more recent high-throughput screen has identified a novel compound, longdaysin, which extends the circadian period in animal cell lines through inhibiting PER1 degradation via action on CKIα [290]. As a single-celled plant, amenable to both genetic and pharmacological manipulation, *O. tauri* offers the potential to run a circadian screen which measures changes in the circadian regulation of clock protein as its output. Particularly the use of the *CCA1*::CCA1::LUC line, as a robust, high-amplitude rhythmic marker, provides the possibility of identifying new clock components and regulators. The screen approach aims to identify a wealth of possible compounds which have an effect on the clock network, each of which requires validation and follow-up. The approach used for *O. tauri* was to develop a semi-automated protocol to screen a 1,600 compound chemical library. This library has been collected, developed and characterised by M. Tyers group (University of Edinburgh) and has been used to screen the biological responses of *A. thaliana, S. pombe, S. cerevisea, Zebrafish, E. coli,* and mammalian cells. From the analysis of these screens the compound library has been highly enriched for bioactive compounds. The library contains a diverse array of compounds both in structure and biological target and has been clustered according to structure to enable the efficient identification of similar compounds. A number of the compounds have been fully characterised, to the level of biological target.

7.2 Results

7.2.1 Pharmacological manipulation of O. tauri

The pharmacological data presented in detail in [53 and Appendix A] will not be extensively replicated here. The work presented in this chapter develops the assays used and aims to identify a wider array of compounds which could be affecting the circadian mechanism (Table

7.1). The data presented in [53 and 140] shows that peroxiredoxin sulphonylation continues without transcriptional input and therefore indicates the involvement of post-translational based mechanism in the clock, specifically relating to redox. Work presented in Chapter 6 shows that the *O. tauri* clock is sensitive to DCMU, the photosystem II inhibitor, and data from the cyanobacteria *S. elongatus* has identified that its' clock network is entrained through the redox state of the quinone pool [75]. This suggests that other compounds which affect the redox equilibrium of the cell will also affect the clock. To investigate the role of redox further two redox-associated sugars, sorbitol and mannitol [291, 292], two redox-related enzymes, superoxide dismutase [293] and peroxidase [294] and one small molecule involved in redox signalling, hydrogen peroxide were investigated [295]. The sugars showed no effect on the circadian period which is consistent with the results presented in Chapter 6. This could be because in the low light environment used for data collection the sugars which could be transported into the cell were simply metabolised. The use of the additional sugars does have the potential to alter circadian rhythms (Chapter 8), but this was not observed, suggesting the sugars had no effect on the rhythms or that they did not enter the cells. The addition of the antioxidant enzyme superoxide dismutase (SOD) had no effect on *O. tauri* rhythms but peroxidase did, showing a period lengthening (Figure 7.1) in the translational line. These results should be interpreted with caution as the proteins were not from *O. tauri* and a lack of effect may just indicate that the protein was either unable to enter the cell, or remain in its correct tertiary structure. If the proteins remained in the media, it is very unlikely that they would be functional, mainly due to the high salinity of the ASW. As a small highly polar compound, the entry into the cell may also be variable for hydrogen peroxide. At high concentrations, 100-10 mM, rhythms were undetectable in both transcriptional and translational lines. At lower concentrations, 1 mM-10 μM, rhythms were normally the same as the vehicle (Table 7.1).

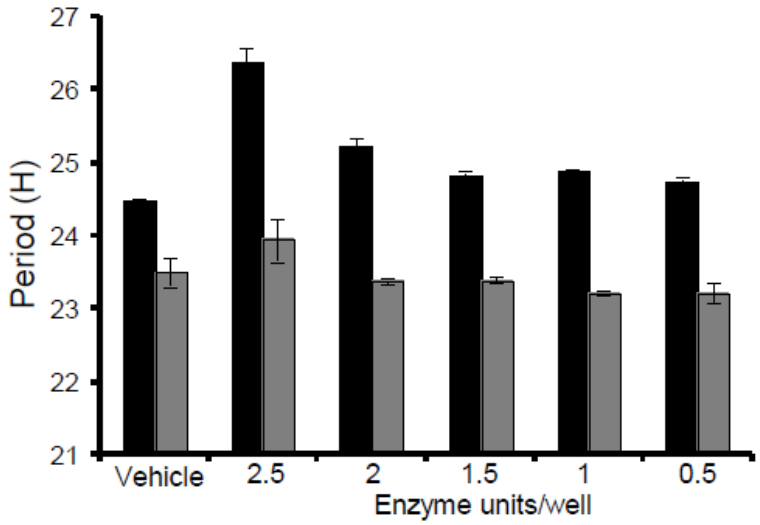

Figure 7.1: Addition of peroxidase to *O. tauri* cells
O. tauri cells were entrained under 12:12 blue light:dark cycles and then released into constant red and blue light at ZT0. Before release peroxidase was added to the cells at the enzyme units/well shown on the x-axis. Period response were determined through FFT-NLLS analysis on BRASS v3 and are shown for the transcriptional *pCCA1*::LUC (grey bars) and translational *CCA1*::CCA1::LUC (black bars) fusion reporters.

Data presented in [53] showed that alteration in the normal mechanisms of chromatin modification, through Trichostatin-A inhibition of histone deacetylation, caused significant period lengthening in the *O. tauri* clock. The importance of histone acetylation and deacetylation has also been observed for rhythms in mammalian cells and plants, both through the use of Trichostatin A [296, 21]. Two other compounds, L-ethionine and 5-Azacytidine, have also been shown to disrupt normal DNA and chromatin modification, both of these compounds target DNA methylation in animals [297, 298] but in *O. tauri* show only a very mild period lengthening (Table 7.1). This period lengthening is not significant and not near the magnitude observed by Trichostatin-A inhibition ([53], Appendix A). This suggests that either both L-ethionine and 5-Azacytidine are not effective in *O. tauri*, but as general inhibitors this seems unlikely, or that the effects on chromatin de-acetylation are very specific. This highlights one of the problems with pharmacological assays, in isolation a negative result is very hard to interpret

as it could be that the compound was ineffective in the assay or it could mean that the compound was unable to enter the cell.

FK866, an inhibitor of nicotinamide phosphoribosyl transferase, and 8-Bromo-cyclic adenosine diphosphate ribose, an analogue of cADPR have both been identified to affect the circadian mechanism in either mammalian cells or plants [299, 174]. However, neither compound, across a wide concentration range had an effect on the *O. tauri* circadian network at either the transcriptional or translational level (Table 7.1). As DCMU targeted the photosynthetic electron transport chain and had a significant effect on circadian rhythms the role of the mitochondrial transport chain was also investigated. If total cellular redox is being sensed by the circadian mechanism it is reasonable to assume the redox outputs from the mitochondria will affect this, as seen in *N. crassa* [300]. Rotenone inhibits electron transport in the mitochondria through inhibiting the transfer of electrons from the iron-sulphur centres in complex I to ubiquinone. Addition of rotenone to *O. tauri* cells caused a period lengthening, between 100-1 mM of rotenone, in the translational lines but had no effect on the transcriptional line, just like peroxidase. This suggests that the redox state of the mitochondria is also important for circadian rhythms but the effects do not feedback to the transcriptional reporters.

The importance of kinases and phosphatases in the circadian clock is relatively well documented [29]. Casein kinases have been identified to have functions in the clock network of a number of species [29]. In the plant circadian clock, Casein kinase II functions to modify one of the central morning transcription factors, CCA1 [10]. Glycogen Synthase 3 (GSK3β) has been shown to modulate the length of circadian period in mammalian cells [289]. The specific pharmacological inhibitors known to target these enzymes also function in the same way in *O. tauri* [53]. Previous work in *L. polyedra* has also identified a role for phosphatases in maintaining circadian rhythms [286]. In [286], the serine/threonine phosphoprotein phosphastases inhibitor, 6-dimethylaminopurine (DMAP), was shown to have a light-conditional effect on circadian

rhythms. In *O. tauri*, DMAP shows a dramatic effect on circadian rhythms. DMAP causes a dose dependent period lengthening in both transcriptional and translational lines (Figure 7.2).

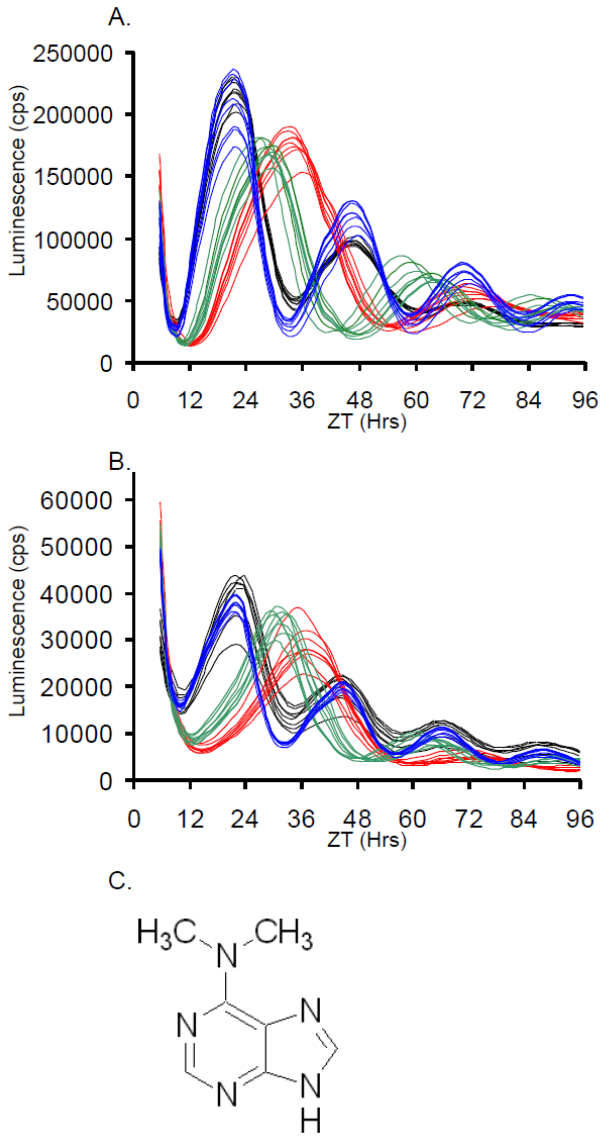

Figure 7.2: Inhibition of protein kinases with the small molecule, DMAP
O. tauri were entrained under 12:12 blue light:dark cycles and then released into either constant red and blue, red or blue light at ZT0. Inhibition by DMAP causes a dose-dependent lengthening of period in both translational, CCA1::CCA1::LUC (A) and transcriptional pCCA1::LUC (B) with example plots from release into red and blue light where vehicle control (black), 1 mM (red), 500 µM (green), 50 µM (blue). The compound structure of DMAP is shown in skeletal form in (C).

The lengthening in period was similar for both transcriptional and translational fusion markers from around 24 hours for the translational (CCA1) marker to ~43 hours at 1 mM and 38 hours at 500 μM and from ~22.5 hours for the transcriptional (pCCA1) marker to ~35 hours at 1mM and ~30 hours at 500 μM (Figure 7.2). This confirms again that phosphor-regulation is very important for the correct timing of circadian rhythms. The period lengthening observed with DMAP are the longest, still rhythmic responses observed to date with the pharmacological approach. This indicates that the post-translational mechanisms provided by kinases/ phosphatases are not necessarily essential for the maintenance of circadian rhythms but are required for their correct timing.

As the photosystem II inhibitor, DCMU, had an effect on *O. tauri* rhythms other compounds linked with light signalling and associated metabolism were tested. Norflurazon is an inhibitor of carotenoid synthesis [301]. Carotenoids are plant compounds which absorb light (normally in the blue spectrum) and protect chlorophyll from photo-damage. The addition of norflurazon across a wide concentration range (500-0.1 nM) and under red, blue and red and blue light had no significant effect on circadian rhythms in *O. tauri.* However, the cells were not observed to bleach and so it could be that the low light levels used in the Topcount recording were not sufficient to cause photo-oxidative damage, limiting the likelihood of observing an effect through norflurazon.

Compound name	Biological target	n	Effects on Period	Notes	Reference
Sorbitol	Redox and metabolism	8	Unchanged	100mM to 10μM	Shen *et al*, 1997 [291]
Sorbitol	Redox and metabolism	8	Unchanged	100mM to 10μM	Shen *et al*, 1997 [291]
Mannitol	Redox	8	Unchanged	10mM to 1μM	Shen *et al*, 1997 [291]
Mannitol	Redox	8	Unchanged	10mM to 1μM	Shen *et al*, 1997 [291]
Superoxide dismutase	Enzymes which catalyse superoxide to oxygen and hydrogen peroxide	8	Unchanged	2.5 to 0.0025 units	Alscher *et al*, 2002 [293]
Superoxide dismutase	Enzymes which catalyse superoxide to oxygen and hydrogen peroxide	8	Unchanged	2.5 to 0.0025 units	Alscher *et al*, 2002 [293]
Hydrogen Peroxide	Small signalling molecule	8	Unchanged	1mM to 10 μM	Rhee 1999 [295]
Hydrogen Peroxide	Small signalling molecule	8	Unchanged	1mM to 10 μM	Rhee 1999 [295]
Peroxidase	Redox	8	Lengthened	2.5 to 0.5 units	Yoshida *et al*, 2002 [294] , Figure 7.1
Peroxidase	Redox	8	Unchanged	2.5 to 0.5 units	Yoshida *et al*, 2002 [294], Figure 7.1
DCMU	Blocks plastoquinone binding site of PS II	8	Very low amplitude rhythm (1nM)	10 μM to 1nM	Metz *et al*, 1986 [302]
DCMU	Blocks plastoquinone binding site of PS II	8	Very low amplitude rhythm (1nM)	10 μM to 1nM	Metz *et al*, 1986 [302]
Rotanone	Blocks mitochondrial electron transport chain	8	Lengthened (100 to 1 mM)	100 mM to 10 μM	Marx and Brinkmann, 1978 [287]
Rotanone	Blocks mitochondrial electron transport chain	8	Unchanged	100 mM to 10 μM	Marx and Brinkmann, 1978 [287]
5-Azacytidine	DNA methylation	8	Mild lengthening of < 1hr	Cell death at 1mM	Christman, 2002 [298]

5-Azacytidine	DNA methylation	8	Mild lengthening by ~1hr (100μM)	Cell death at 1mM	Christman, 2002 [298]
L-ethionine	DNA methylation	8	Mild lengthening by ~1hr	100 μM	Umen *et al*, 2001 [297]
L-ethionine	DNA methylation	8	Unchanged	100μM to 100nM	Umen *et al*, 2001 [297]
FK866	Nicotinamide phosphoribosyl-transferase	8	Unchanged	100μM to 100nM	Nakahata *et al*, 2009 [299]
FK866	Nicotinamide phosphoribosyl-transferase	8	Unchanged	100μM to 100nM	Nakahata *et al*, 2009 [299]
8-Bromo-cyclic adenosine diphosphate ribose	Signalling cascades	8	Unchanged	50μM to 1μM	Dodd *et al*, 2007 [174]
8-Bromo-cyclic adenosine diphosphate ribose	Signalling cascades	8	Unchanged	50μM to 1μM	Dodd *et al*, 2007 [174]
Norflurazon	Inhibits carotenoid synthesis	8	Unchanged (red or blue light)	500nM to 0.1nM	Jung, 2004 [301]
Norflurazon	Inhibits carotenoid synthesis	8	Unchanged (red or blue light)	500nM to 0.1nM	Jung, 2004 [301]
Creatine	Metabolism and Light signalling	8	Unchanged	1mM to 500nM	Roenne-berg *et al* 1988 [303]
Creatine	Metabolism and Light signalling	8	Unchanged	1mM to 500nM	Roenne-berg *et al* 1988 [303]
DMAP (6-dimethylamino-purine)	Protein phosphatase inhibitor	8	Lengthened	1mM to 500nM	Comolli *et al*, 1996 [286] and Figure 7.2
DMAP (6-dimethylamino-purine)	Protein phosphatase inhibitor	8	Lengthened	1mM to 500nM	Comolli *et al*, 1996 [286] and Figure 7.2

Table 7.1: The effects of a selected range of pharmacological compounds on *O. tauri* rhythmicity. White rows are the effects of *CCA1*::CCA1::LUC and grey rows the effects of *pCCA1*::LUC.

7.2.2 A chemical screen on O. tauri cells

In combination the results presented in [53], Chapter 6 and above demonstrate that the use of *O. tauri* to investigate the circadian responses to pharmacological manipulation is valid. *O. tauri* cells are amenable to pharmacological assays and give highly reproducible results. However, as the results in Table 7.1 show not every compound has the expected result and sieving through all possible compounds in a pathway at a range of concentrations is expensive and laborious. Furthermore, this approach does not lend itself to the identification of new compounds which affect the clock, new target pathways or new clock components. To do this a small-scale chemical screen was conducted. This chemical screen has enabled the development of a semi-automated pipeline which could be used for a much larger screen of compounds. Trialling of a number of plate sizes enabled the development of a protocol which uses half the amount of cells used in previous pharmacological assays, therefore reducing the amount of compound and luciferin required (Figure 7.3).

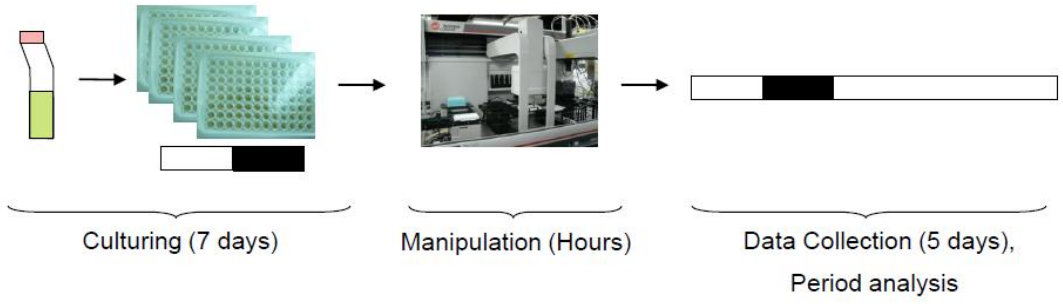

Figure 7.3: Workflow for chemical screen on *O. tauri* cells
O. tauri CCA1::CCA1::LUC cells were split to 96-well plates and entrained for 6 days in blue light:dark cycles. On day 6 media was refreshed and luciferin added. The plates were returned to entrainment. On day 7 compounds were added by a liquid handling robot and plates were moved to data collection. Data was recorded over one red and blue light:dark cycle and then four days of constant light.

Plate sizes smaller than 96-wells did not allow the cells to survive, possibly due to the light levels perceived in the smaller wells. The protocol developed allowed robust oscillations of the *CCA1*::CCA1::LUC *O. tauri* cells, with a period difference of approximately 0.5h between separate trials of control conditions, with the addition of the DMSO vehicle. Between the DMSO controls of the replicated screen batches, there was a period difference of 0.1h (Bio1-Cyto2) and 1.2h (Cyto3- Cyto12), (Table 7.2). To investigate both circadian and light signalling responses data was collected across one light:dark cycle and then into continuous light, for 96 hours. This enables the identification of compounds which affect the light signalling pathways, potentially relating to the entrainment of the clock. The screen used *CCA1*::CCA1::LUC *O. tauri* cells as these show the most robust, high amplitude rhythmic oscillations in constant conditions (Chapter 8) and enables measurement of the protein response. Initially the screen was conducted at the same compound concentration which had been identified as effective in other single-celled organisms (*S. cerevisiae* and *S. pombe*) of 20 μM. However, in *O. tauri,* which has a much thinner cell wall than yeast, this concentration was almost completely toxic, with only a few wells in a ~800 compound screen showing a luciferase output (data not included). Therefore the complete screen was conducted at 2 μM. To gain a high level of temporal resolution, data from 10 plates was collected for each screen batch, with each plate containing four control compounds, DMSO, cordycepin, cycloheximide and DCMU in quadruplicate wells. These controls were used as, at the chosen concentrations, they show the vehicle response (DMSO), period lengthening (cordycepin), period shortening (cycloheximide) and loss of viability (DCMU), ([53] and Chapter 6). To allow for controls on each plate, and for the high temporal resolution of the data collected, the compounds were split into two groups for the screen (Bio1-Cyto2 and Cyto3-Cyto12). A complete, biologically separate repeat was conducted for the entire compound library. The data collected was then analysed in BRASS v3 [182] and plots made for each well.

7.2.2.1 Viability analysis

Visual inspection for viability was conducted, to firstly identify the toxicity of the concentration used and secondly to inspect how well, qualitatively, the results replicated. The toxicity was assessed by two criteria, firstly whether the luciferase signal could be observed following 20 hours of data collection and secondly that the luminescence must have only decreased from the time of compound application. The screen showed that approximately a quarter of the compounds were toxic to *O. tauri* cells at this concentration (Figure 7.4) with 150 compounds, from 1,600, not replicating at the level of viability.

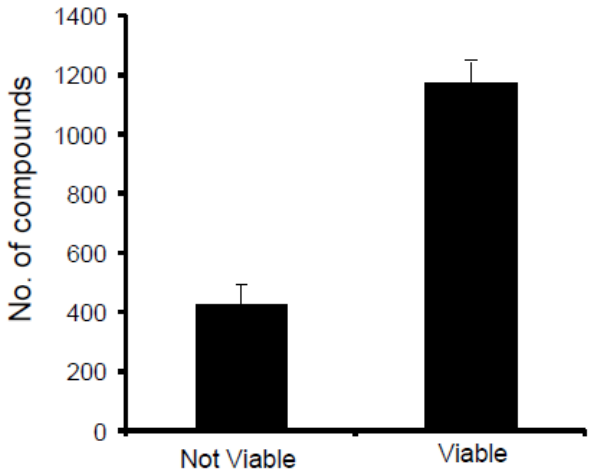

Figure 7.4: Viability of *O. tauri* cells from the chemical screen
The viability of cells was determined by the level of luminescence to be below 100 cps at ZT20 hours and that the luminescence must only have decreased from the time of compound addition. Viability has been plotted only if both replicates showed the same result and the error is the number of wells which did not show the same result between the two screens.

7.2.2.2 Rhythmicity analysis

The rhythmicity of the output was analysed in BRASS v3 using the FFT- NLLS algorithm [182]. The period of the *CCA1*::CCA1::LUC cells in DMSO vehicle was analysed over the free run, continuous light conditions (36-120 hours). Period does vary between the screen batches; this is most likely due to slight variation in cell density of starting cultures, as it is consistent for each

batch. This means that within a batch the period estimates are very similar but between the replicates the period difference is greater. For the first set of compounds, Bio1-Cyto2 the difference between replicates is not significant by Students t-test, $p>0.05$. For the second batch Cyto3-Cyto12 the difference is significant by Students t-test, $p<0.05$. As the averages and standard deviations show in Table 7.2, this is because within each batch the variability in the controls is negligible.

Screen	Average (Hrs)	StDev
Bio1-Cyto2, rep 1	21.7	0.1
Bio1-Cyto2, rep 2	21.8	0.3
Cyto3-Cyto12, rep 1	22.6	0.6
Cyto3-Cyto12, rep 2	23.8	0.3

Table 7.2: Average period estimate from BRASS v3 analysis of DMSO controls.
Each replicate (rep) contained 10 plates with each plate containing 4 DMSO control wells**.**

The average period of the two screens for Bio1-Cyto2 compounds was very similar, 0.1 h difference. However, for the Cyto3-Cyto12 screen the average period varied by about 1h, this variability is much greater than that previously observed in the control plates with just DMSO. The Bio1-Cyto2 and Cyto3-Cyto12 compounds showed the same range in periods from the averaged DMSO period (+/-0.5 h), Figure 7.5. For this analysis the compounds from the replicates were paired and only those with the replicates showing the same trend, either long or short period, included.

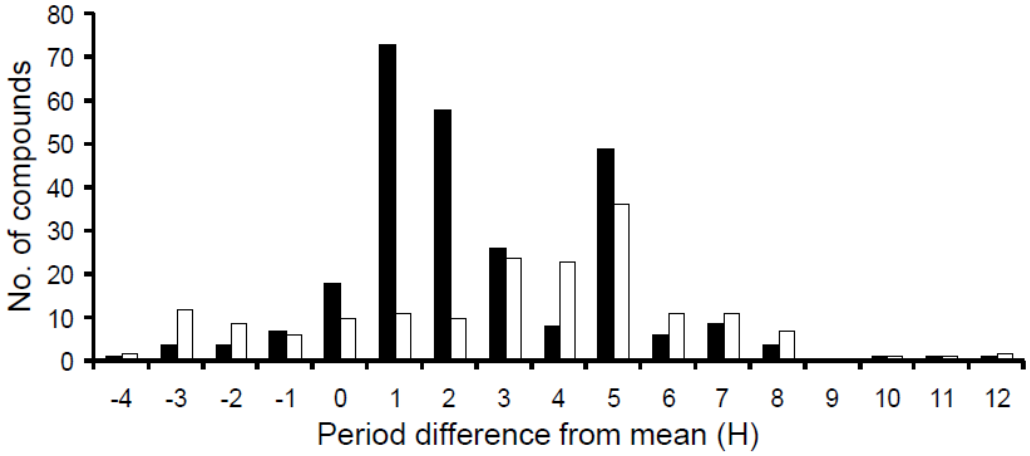

Figure 7.5: Range of periods from screen compounds
Period estimates from the replicates of Bio1-Cyto2 (black bars) and Cyto3-Cyto12 (white bars) were combined and ordered according to the difference from the average of the replicates DMSO controls (21.8 hours Bio1-Cyto2 and 23.2 hours Cyto3-Cyto12). This period difference is represented in 1 hour blocks.

Subsequent analysis has focused on the Bio1-Cyto2 compounds as the periods of the controls were best replicated. Using the analysis from the period range (Figure 7.5) compounds were identified for the replicates which showed the same trend. The range of periods from this analysis is shown in (Figure 7.6) and the compounds listed in Appendix G.

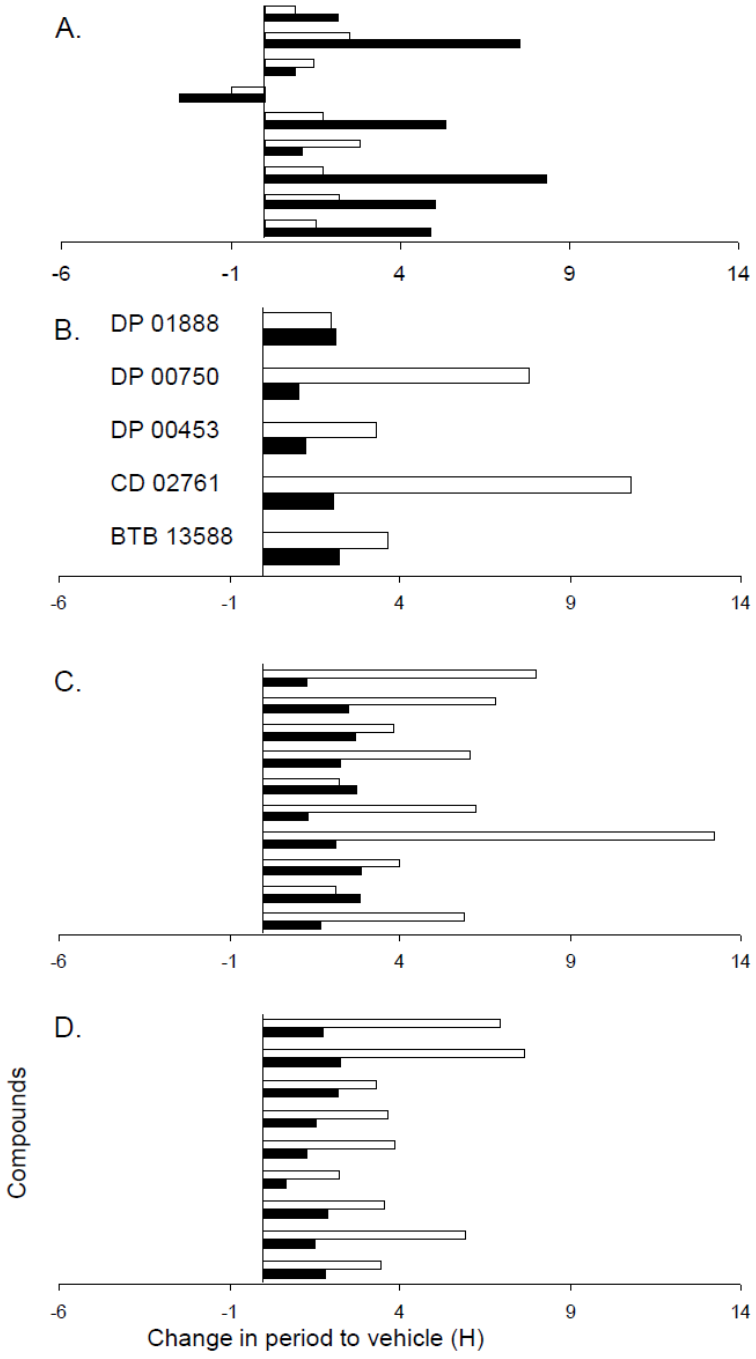
A.
-6
-1
4
9
14
B.
DP 01888
DP 00750
DP 00453
CD 02761
BTB 13588
-6
-1
4
9
14
C.
-6
-1
4
9
14
D.
-6
-1
4
9
14
Compounds
Change in period to vehicle (H)

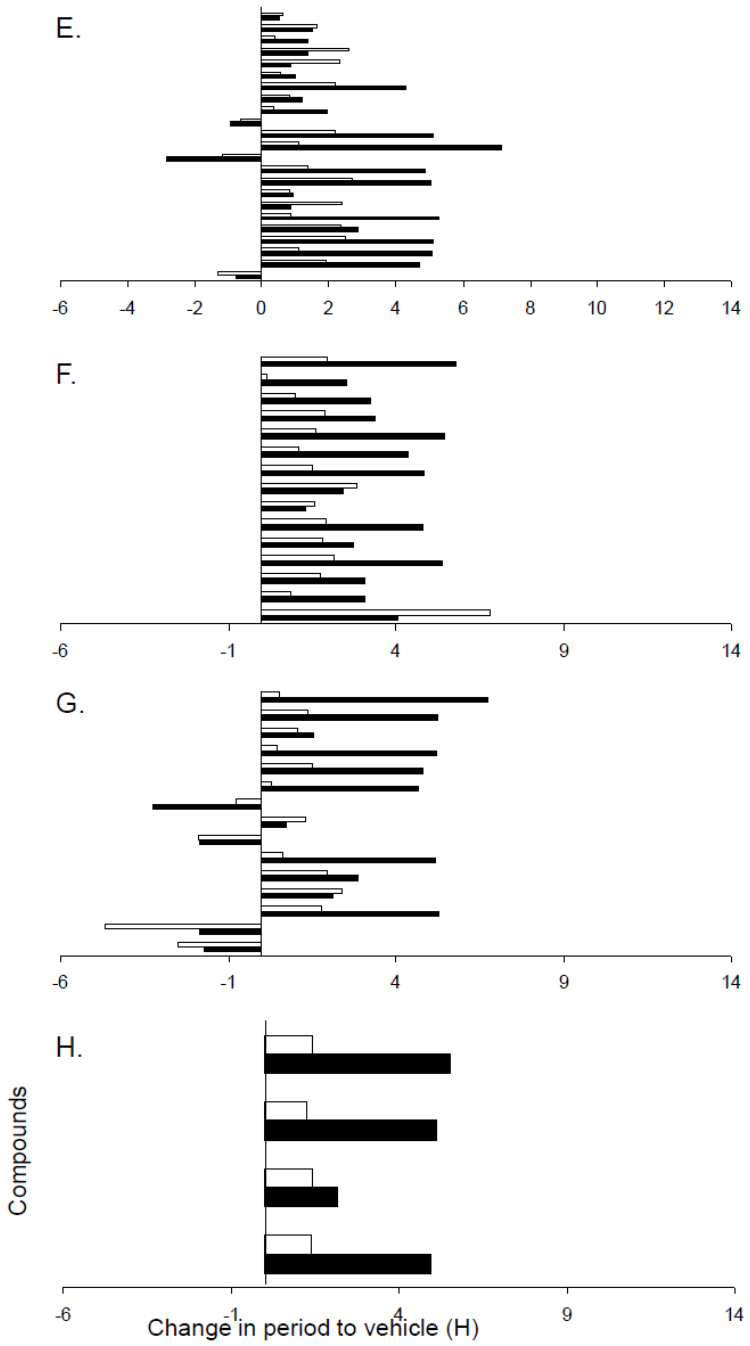
E.
-6
-4
-2
0
2
4
6
8
10
12
14
F.
-6
-1
4
9
14
G.
-6
-1
4
9
14
H.
Compounds
-6
-1
4
9
14
Change in period to vehicle (H)

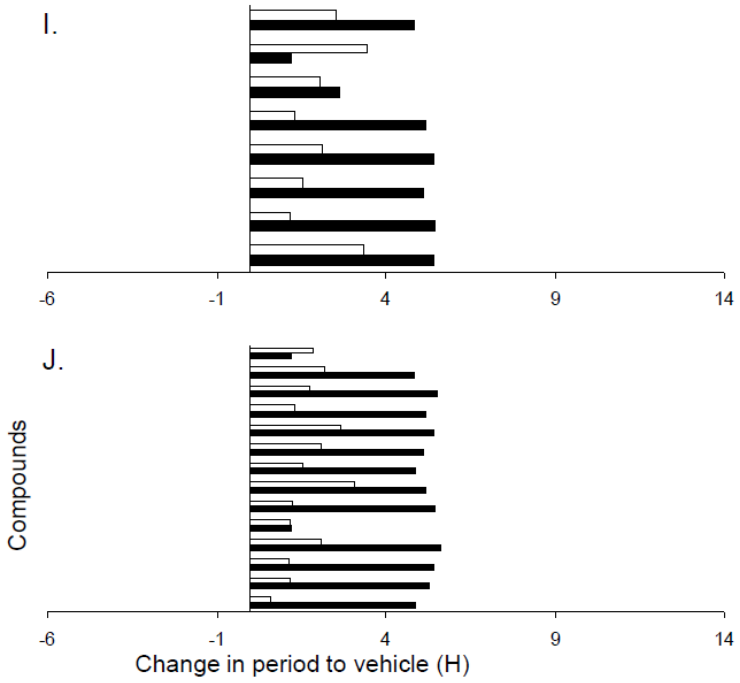

Figure 7.6: Period distribution of compound clusters
From period analysis, compounds which produced the same period effect (lengthening or shortening) in both replicates on *O. tauri CCA1*::CCA1::LUC cells were identified and the change in period from the DMSO control average calculated. This distribution is shown for each plate from the Bio1-Cyto2 screen with replicate 1 in black bars and replicate 2 in white bars. Compounds are identified in Appendix G, Table G1 with compound identification starting at the base of each graph (an example is given for Bio2 (B)). A. Bio1, B. Bio2, C. Bio3, D. Bio4, E. Bio6, F. Bio7, G. Bio8, H. Bio9, I. Cyto1 and J. Cyto2.

Due to the toxicity observed (Figure 7.4), the period analysis for the comparison of compounds is across the whole timeseries, 0-120 hours. Those results which showed the same trend and were linked to compounds were then clustered according to compound structure. From this 12 groups, of particular interest, have been identified (Appendix G, Table G2). Compound groups were chosen either because the compounds in the group show a high degree of structural similarity (Figure 7.7) or because the period difference from the average is large (Appendix G, Table G2). Some of the compounds had been characterised in other species, these included SJC 00146, BTB 06877 and SPB 00506.

A.

Plate	Well	Period difference from mean (H)	Compound	Cluster
Bio4, rep1	M	1.81	HTH 07401	300
Bio4, rep2	M	3.43	HTH 07401	300
Bio6, rep1	AF	5.13	RF 03487	300
Bio6, rep2	AF	2.49	RF 03487	300
Bio6, rep1	CL	1.51	RJF 00177	300
Bio6, rep2	CL	1.64	RJF 00177	300
Bio7, rep1	AO	3.09	S07044	300
Bio7, rep2	AO	1.76	S07044	300
Bio7, rep1	AY	5.38	S11644	300
Bio7, rep2	AY	2.14	S11644	300

B.

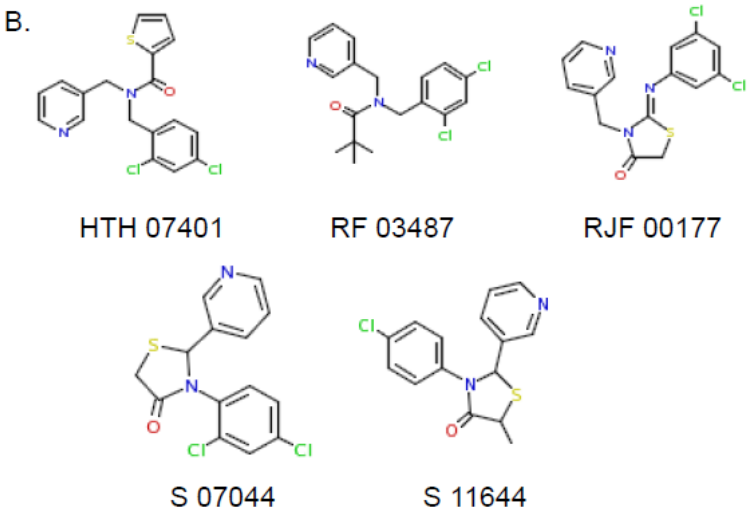

Figure 7.7: Examples of compound clusters with similar structures
From period analysis cluster 300 showed a long period trend (A). Identification of the compounds shows that they have a similar structure involving benzene rings connecting to chloride and nitrogen (B).

Of particular interest was compound BTB 06877 (Figure 7.8) which has been identified to be involved with the regulation of HIR1, involved in chromatin and cell cycle regulation in yeast [304].

A.

Plate	Well	Period difference from mean (H)	Compound	Cluster
Cyto1, rep1	CK	1.19	BTB 06877	299
Cyto1, rep2	CK	3.44	BTB 06877	299
Cyto2, rep1	CN	1.21	CD 06603	299
Cyto2, rep2	CN	1.84	CD 06603	299
Bio6, rep1	AC	5.05	RF 02465	299
Bio6, rep2	AC	1.11	RF 02465	299

B.

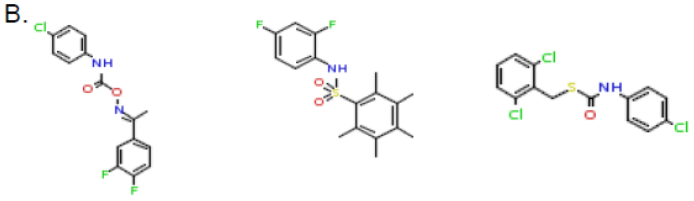

BTB 06877 CD 06603 RF 02465

Figure 7.8: Compounds in the cluster with BTB 06877
From period analysis cluster 299 showed a long period trend (A). The compounds in this cluster showed similarities in structure (B) indicating that CD 06603 and RF 02465 may have a similar function to BTB 06877.

This analysis has proved to be potentially very interesting. However, visual inspection of the screen results show that the compounds had a diverse effect on the circadian rhythms of the cells. Examples of this diversity are shown in Figure 7.9.

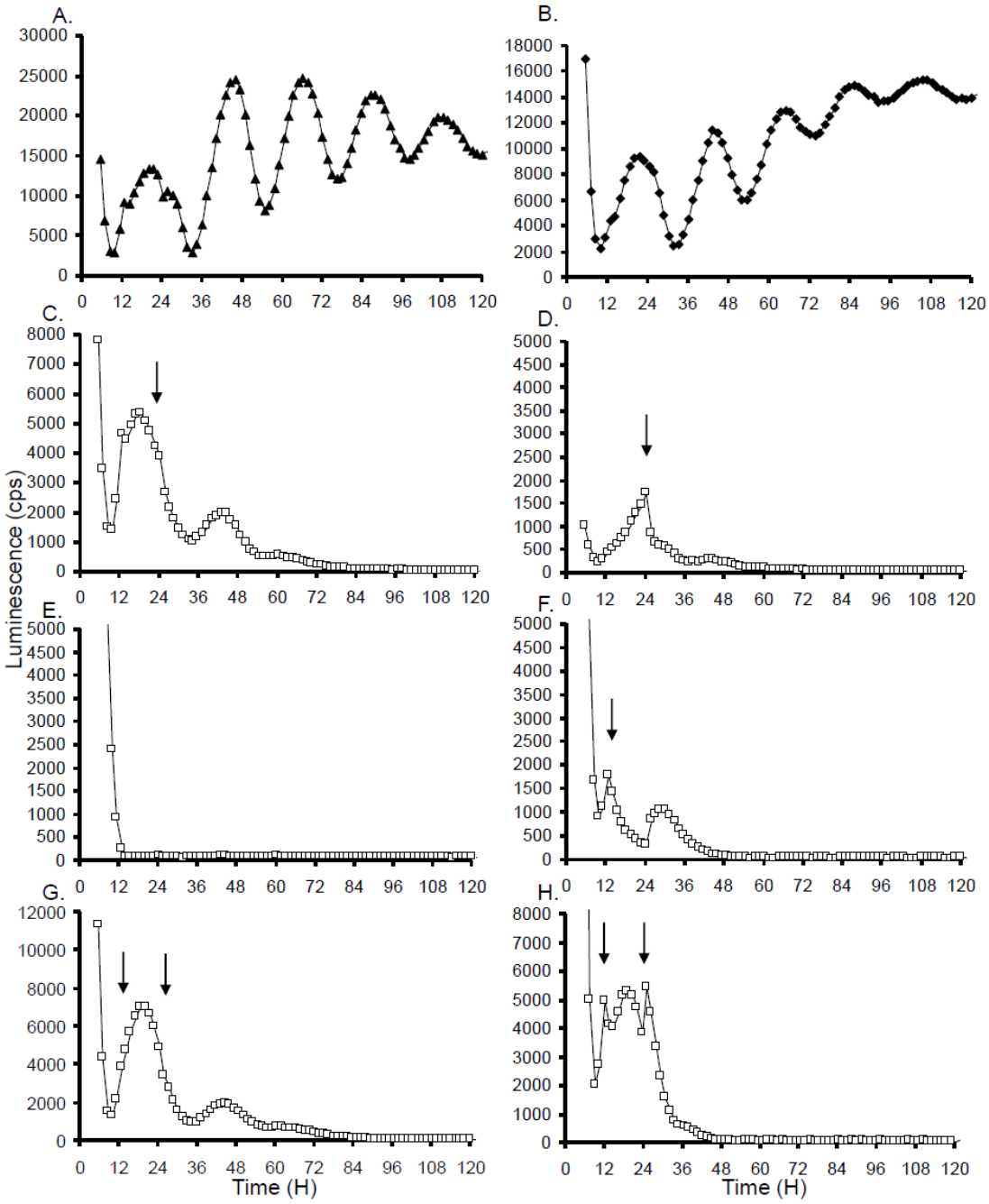

Figure 7.9: Examples of the diversity of the compound's effects on the circadian rhythms of *O. tauri*

O. tauri CCA1::CCA1::LUC cells were entrained under 12:12 blue light:dark cycles and then transferred to one red and blue light:dark cycle followed by continuous light for data collection. Data was analysed by FFT-NLLS in BRASS v3 software and example plots are presented. A) DMSO vehicle control, B) Cycloheximide control, C) F11, Bio5 D) G11, Bio5 E) E11, Bio5 F) C6, Bio5 G) H8, Bio4 and H) E7, Cyto1

Figure 7.9 demonstrates that it is not just the rhythmicity of the cells which is affected by the compounds but also the shape of the response. In Figure 7.9D the rise of CCA1 is much slower through the dark period than that of the control (Figure 7.9A) and then shows a sudden repression with the onset of light (Figure 7.9D, black arrow), as opposed to the usual acute light response (Figure 7.9A). In Figure 7.9F, CCA1 shows a total repression through the dark phase (Figure 7.9F, starting at the black arrow) followed by a strong acute light signalling response (Figure 7.9F, ZT24). The acute light signalling response is affected in a number of ways, in Figure 7.9C it is lost (Figure 7.9C, black arrow), in Figure 7.9G the transient signalling is lost at both of the light changing conditions (Figure 7.9G, black arrows) and in Figure 7.9H the light signalling response is actually greater (Figure 7.9H, black arrows). As summarised in the viability analysis (Figure 7.4) a quarter of the compounds were toxic at this concentration (an example plot is shown in Figure 7.9E). Further analysis will be required to identify and characterise these results, a process which ideally would be automated to remove human bias and to handle the large data set in a manageable and reliable form.

7.3 Discussion

This work has developed the use of *O. tauri* as a plant cell line which is both amenable and reliable for use in pharmacological studies. Pharmacological manipulation offers the possibility of identifying novel clock components and modulators not identified in previous screening methods as inhibitors can be identified to target all enzymes in a family, therefore avoiding redundancy. Furthermore, the dose control of compounds allows target functions to be reduced without causing lethality. Also as pharmacological compounds target biological processes their characterisation will enable the investigation of post-translational and cytosolic elements of the

plant circadian clock. These results could easily be transferred to other species. The initial approach of testing compounds which have been verified in other species, confirmed that a number of compounds affected the *O. tauri* clock in the same way as they affected other circadian networks [53 and Table 7.1]. However, the effects were not always as anticipated. Whilst the photosystem II inhibitor, DCMU, had a dramatic effect on circadian rhythms in a dose-dependent way, inhibitors which affected targets that feed into the photosystem, such as norfluazon did not (Table 7.1). Also, inhibition of the mitochondria electron transport chain, with rotenone, did not have such a significant effect. This could be interpreted that the effects observed through inhibition of the photosynthetic chain are more related to the metabolic consequences rather than through redox signalling. It could indicate that the contribution of redox signalling from the mitochondria in plant circadian systems may be quite minimal; this would need to be further verified with mutants. Especially when considering that mitochondrial mutants in another circadian system, *N. crassa* do affect the clock [300]. Rotenone and peroxidise both affected only the translational line (Table 7.1 and Figure 7.1), which may suggest that the redox effects are specific to the post-translational aspect of the clock. As such CCA1 may not be the best biological marker to assess their effects on circadian rhythmicity. The investigation of other compounds which affected redox signalling produced variable results. This is probably linked with the ability of the compounds or proteins to permeate through the plasma membrane either due to their high molecular weight or polar nature. Still, manipulation of the cells redox state does have effects on the circadian rhythms (Figure 7.1). As data in Table 7.1 demonstrates pharmacological manipulation can be very specific, differentiating between DNA acetylation and methylation. Also, through the targeting of serine/threonine phosphoprotein phosphastases, through the previously characterised inhibitor DMAP (Figure 7.2), it is clear that phosphatase activity is essential for determining circadian period in *O. tauri*, just as observed in mammalian cells [29]. This analysis identified a major advantage of using

pharmacological agents which have already been characterised; physiological concentrations are known, as is the vehicle and entry into a cell. Therefore the use of a characterised compound library would be advantageous, as well as offering the potential of identifying new clock components and regulators. This approach has been used, in circadian biology, in mammalian cell lines with the characterisation of compounds which target GSK3β and CKIα as well as other potential pharmaceutical compounds [305].

To enable the screening of a large number of compounds a semi-automated, 96-well plate protocol has been developed (Figure 7.3). The screening of a 1,600 compound library has validated this protocol as a high-throughput screening platform and has identified a number of potential compounds which can be investigated further experimentally (Figures 7.7 and 7.8). Analysis of the screen results shows that the compounds have a wide variety of effects on the circadian rhythms, (Figure 7.9). Generally, if the cells remain rhythmic the period of the rhythm is lengthened, as is observed in mammalian cells [305]. In the follow-up of the compounds identified in Figure 7.6 and listed in Appendix G, Table G1, the dose response curves would be required to indicate if the compounds are having a specific effect. It would also be interesting to test the compounds on the transcriptional marker lines to identify if they affect the clock in the same way. Peroxidase and rotenone were identified to affect the period of the transcriptional and translational lines in different ways (Figure 7.1 and Table 7.1). Further to this waveform analysis would enable the identification of compounds which differentially affect light signalling versus circadian responses. However, this analysis should be automated to enable the efficient, unbiased, identification of specific features.

The chemical library used for this screen lends itself to the follow-up of target compounds through investigating if other structurally similar compounds have the same effect. In one of the clusters identified the compound structure looks very similar (Figure 7.7) and therefore, it suggests that they may be targeting the same biochemical function. The compound library used

has also been screened on a number of other species and through the characterisation of the effects in other species a possible function can be inferred in *O. tauri*. The BTB 06877 compound which has been shown to target HIR1 in yeast also has a period lengthening effecting *O. tauri* (Figure 7.8). HIR1 is involved in heterochromatin and cell cycle regulation [304], both of which have been identified to be important in the regulation of the *O. tauri* clock. Cell-cycle output was one of the first biological processes to be identified as under the regulation of the *O. tauri* clock [14]. Furthermore, pharmacological investigation of chromatin regulation has identified that inhibition of de-acetylation by Trichostatin-A has a clear period lengthening effect (increase of around 10 hours). Therefore, BTB 06877 could be a possible mechanistic identification. Further characterisation of this would also require genetic modification, mutants and over-expressers, in *O. tauri* to validate the mechanism.

The viability analysis of the total screen shows that approximately a quarter of the compounds were toxic to *O. tauri*. This is expected as the library was chosen for its bioactivity. However, it is a high proportion of toxicity and suggests that at least some of these compounds will be of interest to study at lower concentrations. Therefore if the screen was to be repeated, it would be advisable to do so at a lower compound concentration.

The work presented in this chapter adds further support to the role of post-translational mechanism, particularly relating to phosphorylation, in the circadian clock. The screen protocol developed shows that *O. tauri* cells are amenable to high-throughput assays; however, caution should be taken regarding the stability of the starting circadian period. Both screens replicate well at the level of viability but the circadian period measurement is slightly harder to assess. This is due firstly to the variability in the period of vehicle controls, possibly due to cell density or different cell batches and secondly due to the rapid damping of reporter signal often observed following compound addition.

However, now this has been identified it could be more controlled for in subsequent screens. The development of *O. tauri* as a plant cell line for high-throughput chemical screens offers a number of other advantages relating to compound identification, not just regarding circadian responses. The *O. tauri* line could be used in a high-throughput screen for compounds which act as herbicides, in order to identify first hits for compounds which could replace herbicides for which plants have developed resistance, such as glyphosate [306]. *O. tauri* could also be used to test the toxicity of compounds in plant cells and as an assay for toxins in the environment. The latter would be particularly effective as *O. tauri* is sensitive to relatively low concentrations of compounds compared to other single celled organisms. The targets identified in *O. tauri* could also be easily tested in *A. thaliana,* utilising its wealth of genetic mutants in further characterisation. Therefore, this screen is not solely interesting to circadian biology but also applicable to other assays.

Chapter 8

A comparative analysis of circadian rhythm markers in *Arabidopsis thaliana* and *Ostreococcus tauri*

A. thaliana experiments and data assimilation were conducted by Sarah Hodge.

8.1 Introduction

A circadian oscillator is an endogenous signalling mechanism which maintains oscillations of approximately 24 hours under constant conditions (Chapter 1). This oscillator mechanism has been identified in a wide variety of organisms from the cyanobacteria *Synechococcus elongatus* to humans [1]. The now predictable rhythmic environment on Earth may have provided the requirement for certain physiological and biochemical events to be timed to particular points during the 24 hour cycle, such as nocturnal DNA replication. To understand a circadian oscillator's real function it must be considered in the context of this rhythmic environment, rather than the constant conditions of the laboratory. The ability of the circadian oscillator to entrain is essential and it means that the near 24 hour period of the innate oscillator becomes a 24 hour period under entrained conditions of that period [307]. This, along with changing environmental cues, allows the oscillator to control the phase of biological processes. Furthermore, it is the requirement to entrain which is believed to provide the necessity of multiple interlocking feedback loops observed in many of the circadian mechanisms [182]. Multiple loops could enable the required flexibility to track changing phases in the external cycle [308]. This is particularly relevant to seasonal changes in photoperiod and the timing of developmental transitions. However, in natural conditions there are not only changes in seasonal photoperiods, but also daily variations in light intensity which need to be considered. Total and perceived light levels change regarding duration, intensity, shading, cloud cover, and abundance and position of photoreceptors. Therefore a circadian network must be robust to these daily

perturbations which are not, believed to be, significant to the entrainment phase. A set of modelling experiments suggested that environmental noise favoured complex clocks [309] and that having a high level of flexibility in a clock network increased its robustness when exposed to environmental change [308].

Many of the properties of circadian oscillators have been studied and defined under free-running or constant conditions, as this removes complications associated with entrainment. These complications include; the introduction of transient and acute responses to the entraining stimuli, a strong entraining stimulus driving the oscillations, and the constraint of the oscillator period to that of the entraining stimuli period [310]. The transient or acute responses are observed in circadian reporters due to the requirement of the oscillator to entrain, and therefore be responsive to the external stimuli. This is important as the acute responses enable the positive light signalling input which is not only required for circadian entrainment but also for a number of physiological processes, such as photomorphogenesis, and shade avoidance [101]. However, the acute light response can hide the circadian response. This is called masking [310]. Biological oscillators are entrained by common signals or zeitgebers [310]. These include the strong zeitgeber light, as well as temperature and nutrients ([126] and Chapter 6).

Understanding how the entrainment signals feed into oscillator mechanisms and the relative importance of each of these signals in nature is important to understand the circadian mechanisms biological significance. Classic phase response curves (PRC) show that the circadian oscillator gates or regulates the phases at which entrainment is possible [311]. A light pulse applied at dawn will produce a different response to one applied at mid-day. Furthermore, it can be seen through skeleton photoperiods which have only 3 hours of light at dawn and 3 hours at dusk that this is sufficient to entrain the oscillator mechanism [311]. These observations suggest that the model of discrete entrainment proposed by Pittenridge is favoured in plants, as it

is in flies [115]. Discrete entrainment is when an oscillator mechanism can become entrained to light:dark transitions, such as the pulses in a skeleton photoperiod, as the response to these transitions is assumed to be rapid. For plants entrained in 12:12 light:dark cycles and then moved into a skeleton photoperiod the first 3 hours of light would be perceived as dawn, then 6 hours of darkness, followed by 3 hours of light which would be perceived as dusk and not a new dawn. Therefore, it is the timing of the light pulses and not the total amount of light which is driving entrainment. However, the competing theory proposed by Aschoff is that the total light intensity is important for circadian entrainment [115]. Aschoff observed that under free-running conditions increasing light intensity caused a shorter period of the innate oscillator (in non-nocturnal animals), this has become Aschoff's Rule. From this observation, and a number of photoperiod experiments, Aschoff proposed that the total light intensity was important for circadian entrainment [115]. Entrainment is most likely a combination of the two theories, with the importance of each varying under differing conditions. The oscillator mechanism can entrain to a range of periods around its innate period, but this entrainment is often not observed to be immediate. The lag in entrainment is believed to be caused by the oscillator moving between stable states of entrainment, as proposed by Eric Petterson in his limit-cycle model in 1980 [312]. A perturbation, such as a strong entraining signal, will move the oscillator away from a stable limit cycle. The movement back to the original limit cycle or to a new limit cycle is experimentally observed as a number of transient days in which circadian rhythms have moving phases before the new entrainment regime and the oscillator assume a stable phase relationship.

With the characterisation of *O. tauri* and the identification that it contained a simpler (but most probably not a single loop) plant-like clock [170], a comparison of responses to entrainment conditions between two clock networks became possible (*O. tauri* and *A. thaliana*). It has been observed that a network with many loops is flexible and robust as a property of its structure

[182]. Another mechanism through which both robustness and flexibility may be achieved is proposed in [168] where a single loop *O. tauri* clock can respond to varying photoperiods by light affecting the clock network at five different places (Figure 8.1).

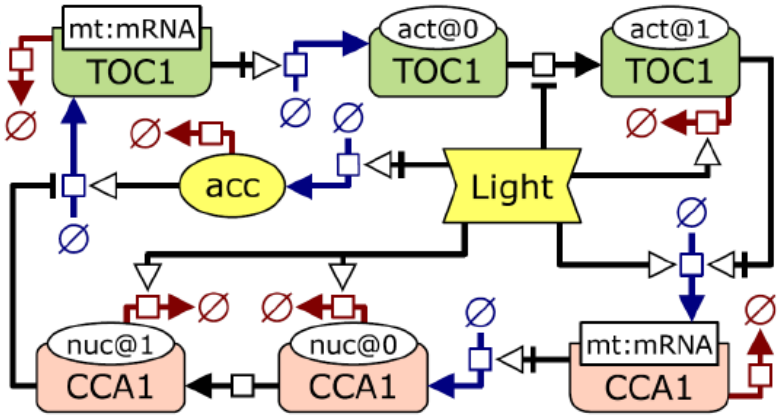

Figure 8.1: Scheme of the proposed *O. tauri* circadian network
The network is represented in Systems Biology Graphical Notation (SBGN). TOC1 (green boxes) and CCA1 (pink boxes) are connected through arrows in blue for synthesis, red for degradation and black for conversion or transport. TOC1 exists in two states, with light-regulated conversion from (act@0) to active (act@1). Degradation of TOC1 is light-induced and only acts on the active form. CCA1 protein exists in the cytosol (nuc@0) and the nucleus (nuc@1), and is subject to light-induced degradation at the same rate in both compartments. The light accumulator which regulates *TOC1* transcription links the overall gene expression levels to the amount of light received by the *O. tauri* (yellow acc) [168].

This model proposed two main mechanisms through which light is affecting the clock network. Firstly, light has a direct effect on biochemical processes such as transcription and degradation rates. Secondly, there is an accumulator function which enables the co-ordination of overall gene expression to the amount of light received by *O. tauri* and is required for the observed timing of *TOC1* expression. These mechanisms enable the behaviour of the modelled network to capture transient light responses and some of the circadian phases [168]. However, the model did not capture all of the amplitude changes and phase changes experimentally observed in photoperiod transitions [168]. This may support the existence of another potential loop, or at least the requirement for additional components in the model [53].

The clock networks in plants are extremely responsive to light (Chapter 6 and [45, 46, 47, 48]) and it is believed to be the strongest entraining signal [122]. In this chapter light has been used as the entrainment signal and the oscillator responses, in photoperiod conditions, were observed and compared after a large switch from the entrainment conditions. Through this, transient and oscillator responses could be distinguished. To complement the photoperiod switch and to enable a comparison of the relative importance of light duration versus intensity the oscillator's response to varying the light intensity was investigated. A comparison was also made, under photoperiod conditions, of the response of the oscillator to additional carbohydrate. In plants carbohydrate is a photosynthetic output, and therefore light-dependent. The amount of carbohydrate produced will depend on the amount of light-harvested through the light-harvesting chlorophyll. Normally, the levels available will vary throughout the 24 hour cycle, and metabolic regulation of carbohydrate storage has been shown to be under circadian regulation [313]. Such metabolic regulation is relevant because it links the clock with the basic physiology of the plant and indicates that through circadian regulation of metabolism the plant is able to anticipate dawn and use its carbohydrate reserves accordingly through the night [313]. Also, sucrose has been shown to provide entrainment between different plant organs [23]. Furthermore, in animals, feeding and nutrients are strong entrainment cues [1]. Therefore, it is conceivable that the oscillator responses, via light will be different with and without additional carbohydrate.

8.2 Results

The investigation is based on the use of non-invasive luciferase imaging. This technique enables the continual monitoring of responses during changes in photoperiod, with a temporal resolution much higher than that feasible through RNA measurements. Luciferase imaging also allows the monitoring of single plant and population responses, whilst RNA extraction only allows the monitoring of population responses. As such, luciferase imaging enables a relatively high-throughput method to gain a wealth of data in a variety of photoperiods.

As previously described for *O. tauri* transcriptional (*pTOC1* and *pCCA1*) and translational (TOC1 and CCA1) luciferase fusion markers have been generated [170]. In *A. thaliana* only transcriptional luciferase fusions exist for these genes and these are used in this study (Chapter 2). Due to the slightly different experimental protocols required for the luciferase imaging in *O. tauri* and *A. thaliana* (*O. tauri* in 96-well plates recorded in the Topcount, *A. thaliana* on tissue-culture plates under a low-light imaging camera) and the number and different types of markers used the results for the two species are presented differently. The power of having both transcriptional and translational markers in *O. tauri* means that the effects of transient responses from entrainment can be dissected into a transcriptional and translational response; therefore the two are viewed together. Furthermore, as *O. tauri* only has two genes tagged with luciferase the feedback of the single loop can be easily investigated.

For *A. thaliana* the clock network is believed to be much larger (Chapter 1) and so a number of the clock genes transcript profiles were investigated (*CCA1*, *LHY*, *TOC1*, *GI*, *PRR9* and *ELF3*). The time resolution for imaging *A. thaliana* is one image every 1.5 hours and so the small transients that are captured through the more frequent recording, once every 20 minutes, used with *O. tauri* are potentially lost. Importantly, plotting *O. tauri* at the same time resolution as the *A. thaliana* data is captured does not move the position of the peaks. Due to the number of

genes, the fact that all the reporters are transcriptional and the short day and long day responses have been investigated in some detail before, it seems easier to draw an immediate comparison with transient responses.

Finally, due to the different light requirements of *A. thaliana* and *O. tauri* the light intensities are not the same. In *A. thaliana* high light conditions are ~60 μE/m^2 and low light conditions are ~6 μE/m^2. In *O. tauri* high light conditions are ~10 μE/m^2 and low light conditions are ~1 μE/m^2. The main requirement for this difference is that under higher light intensities than ~10 μE/m^2 *O. tauri* cells can not survive, whilst for *A. thaliana* 10 μE/m^2 is relatively a low light intensity.

8.2.1 Ostreococcus tauri

8.2.1.1 Phase markers in entraining conditions

When circadian reporters are imaged in constant conditions the waveforms produced are very smooth, similar to those of sine or cosine waves. In *O. tauri*, imaged in constant light (LL), this is observed in both the transcriptional and translational markers (Figure 8.2). However, unlike sine and cosine waves the circadian oscillations damp or lose amplitude over time. This loss of amplitude could be due to loss of synchrony in individual oscillators between cells (observed in mammalian cells [314]) as each individual cell has an oscillator of slightly different period. Or it could be caused by the oscillators in individual cells moving from the entrainment conditions. The later is often due to the oscillator not being stably entrained.

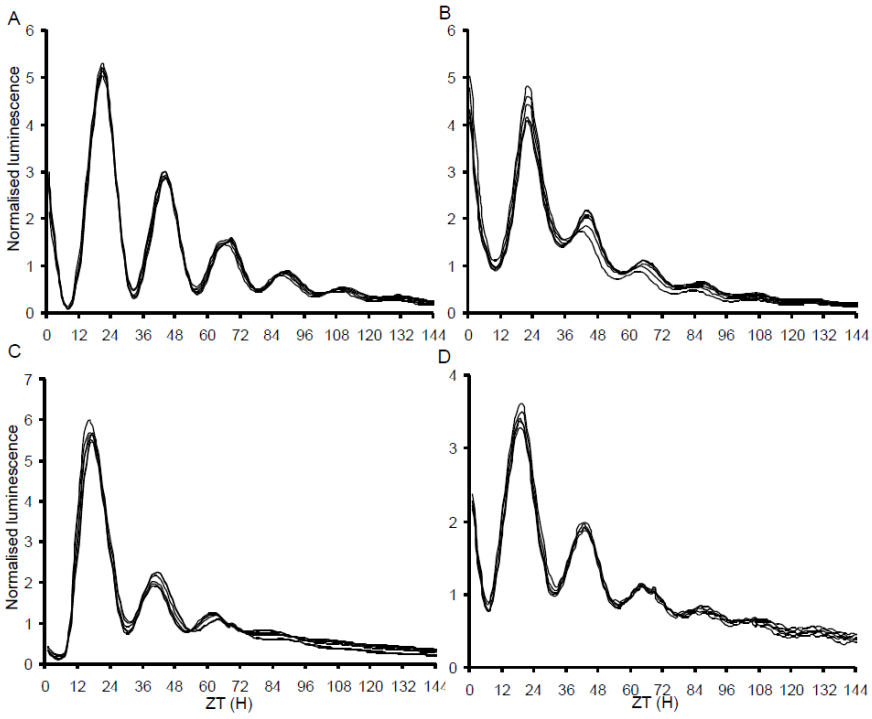

Figure 8.2: *O. tauri* rhythms in constant light
O. tauri cells entrained under 12:12 blue light and released at ZT0 to constant red and blue light. Luminescence of each marker is measured, on the Topcount, following a 2 minute delay to ensure delayed fluorescence does not interfere with readings. A) *CCA1*::CCA1::LUC, B) *pCCA1*::LUC, C) *TOC1*::TOC1::LUC and D) *pTOC1*::LUC. Traces are normalised to the average of each time series with n=8 and representative of n=48.

In *O. tauri* the various reporters show different behaviour in free-run constant light conditions. In particular, the TOC1 line shows very rapid damping, such that the oscillations are lost by ZT96 (Figure 8.2C). It has already been shown that TOC1 protein is regulated by photoperiod cycles, in particular darkness after ZT12 increases its degradation rate (Chapter 6). The absence of this cue for protein degradation may be in part responsible for the rapid damping observed in LL. Also, the TOC1 line is the only line from the *O. tauri* transformations which shows an altered period (Figure 8.3 and [170]). This line is long period (~28 hours) and therefore the entrainment conditions are not as close to the innate period as other lines, which could mean that the movement away from entrainment would be more rapid. Still, circadian oscillations can be

observed in free-running constant light conditions and these single peaks and troughs can act as phase markers when the lines are imaged under photoperiodic conditions.

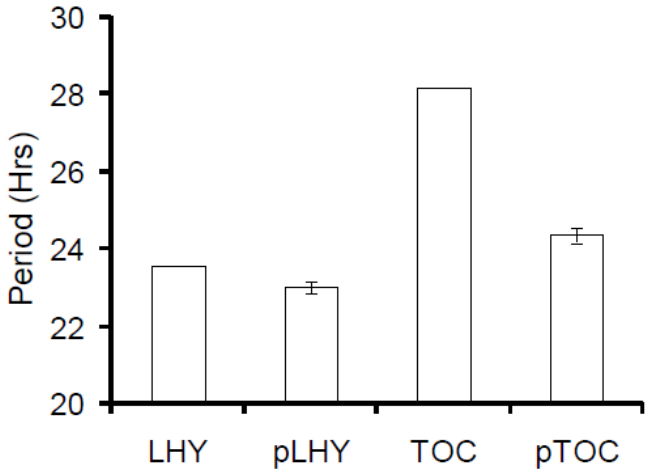

Figure 8.3: Period of *O. tauri* lines in constant light
O. tauri cells entrained in 12:12 blue light:dark cycles and released into constant red and blue light, plots shown in Figure 8.2. Period estimates made through FFT-NLLS analysis using BRASSv3 software [182] of 48 wells with error being represented as SEM.

Under long day (LD 16:8 light:dark cycles) or short day (SD 8:16 light:dark cycles) conditions the lines show different responses to those in free-running conditions and to each other. For ease of the narrative, an example of transient responses has been highlight in certain graphs by a red arrow and an example of the circadian response by a black arrow.

Both of the transcriptional reporters are very sensitive to the photoperiodic conditions, and can be considered as markers for aspects of the light condition. *pCCA1* shows an induction at dawn (Figure 8.4B, red arrow, ZT48 and Figure 8.5B red arrow, ZT72) and *pTOC* a greater acute repression in expression at dusk (Figure 8.4D, red arrow, ZT30) but also shows a small acute expression peak with dawn (Figure 8.4D, red arrow, ZT 48 and Figure 8.5D, red arrow, ZT72).

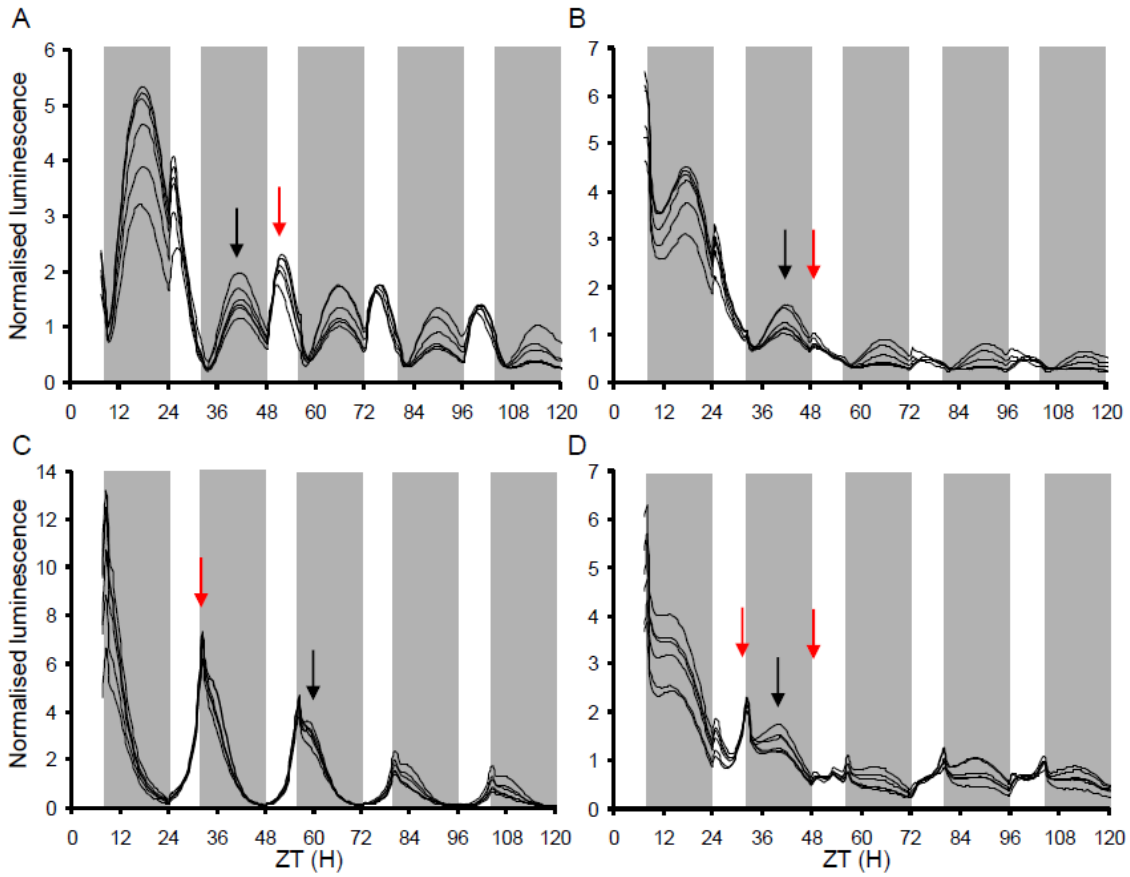

Figure 8.4: *O. tauri* rhythms under short day (SD) photoperiod
O. tauri cells are entrained under 8:16 blue light:dark cycles and transferred at ZT0 to 8:16 red and blue light:dark cycles. Luminescence of each marker is measured following a 2 minute delay to ensure delayed fluorescence does not interfere with readings. A) *CCA1*::CCA1::LUC, B) *pCCA1*::LUC, C) *TOC1*::TOC1::LUC and D) *pTOC1*::LUC. Traces are normalised to the average of each time series and then averaged across a column, so effects of light intensity do not affect the averages, with n=8 for each trace. Red arrows indicate transient responses to light and black arrows indicate the circadian responses. White (day) and Grey (night) shading represents the photoperiod.

The transient responses to changes in light conditions are clear (identified by the red arrows on Figure 8.4 and 8.5), but the amplitude of these responses may be more dramatic than those which occur naturally. This is due to the square waveform used in imaging; naturally changes in light conditions are more gradual. It is quite probable that under more natural conditions the phases of the circadian and transient waveforms would merge. This is already nearly observed for TOC1 where the circadian peak (Figure 8.4C, black arrow, ~ZT60 and Figure 8.5C, black arrow, ~ZT40) is very close to the dark-induced repression which guides the TOC1 peak (Figure 8.4C, red arrow, ZT30 and Figure 8.5C, red arrow, ZT64). The merger of circadian and acute response is also quite possible when considering the CCA1 response (Figure 8.4A black and red arrows, and 8.5A, black and red arrows).

Under LD the circadian aspect of the CCA1 waveform starts to rise in the light phase, but does not continue to rise in the dark (Figure 8.5A, black arrow, ~ZT40). However, it then recaptures its expression pattern with the following dawn (Figure 8.5A, red arrow, ~ZT74). This indicates that the circadian waveform itself is sensitive to the light conditions and that the control of the acute light signalling is linked to circadian regulation.

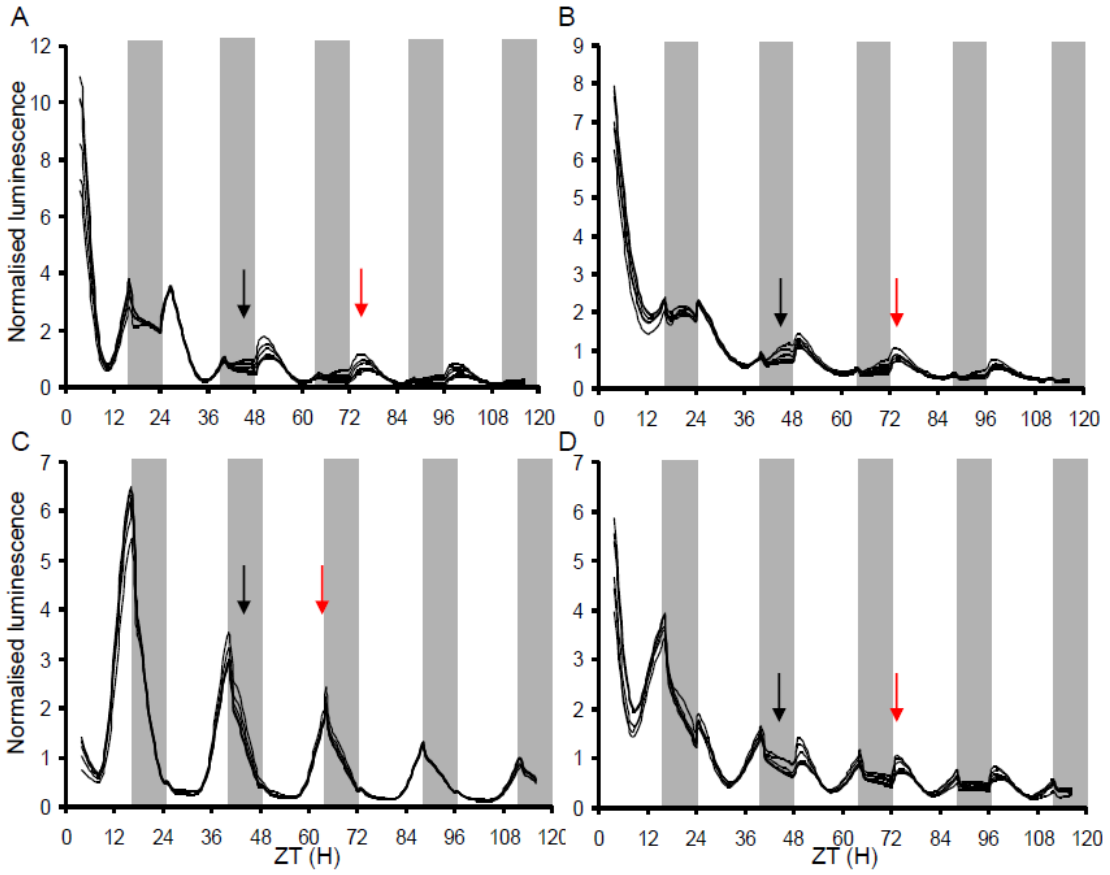

Figure 8.5: *O. tauri* rhythms under long day (LD) photoperiod
O. tauri cells are entrained under 16:8 blue light:dark cycles and transferred at ZT0 to 16:8 red and blue light:dark cycles. Luminescence of each marker is measured following a 2 minute delay to ensure delayed fluorescence does not interfere with readings. A) *CCA1*::CCA1::LUC, B) *pCCA1*::LUC, C) *TOC1*::TOC1::LUC and D) *pTOC1*::LUC. Traces are normalised to the average of each time series and then averaged per column so effects of light intensity do not affect the averages, with n=8 for each trace. Red arrows indicate transient responses of the lines to light and black arrows indicate the circadian responses. White (day) and Grey (night) shading represents the photoperiod.

8.2.1.2 Shifting photoperiods

To further dissect the transient and circadian responses and to identify how quickly the oscillator could adjust its phase to a new photoperiod condition, a single photoperiod switch was applied either at dawn or dusk. This switch was between entrained LD to SD or entrained SD to LD conditions. For the photoperiods to switch at dawn the length of the photoperiod cycle is altered for the transition cycle. To make the switch at dusk the cycle length remains the same. The dusk transitions will be discussed first.

The peak of TOC1 is dominated by its response to dusk and the translational marker makes an immediate adjustment to the changed photoperiod regarding its peak time (Figure 8.6C, ZT64 and Figure 8.7C, ZT 56). The circadian element of the TOC1 line shows a slower response as it moves phase following the photoperiodic switch, as observed in the SD to LD switch. This is plotted as phase movement relative to dawn (Figure 8.8). This response is only clearly observed in the slightly higher light wells at the edge of the plate, from the Topcount data collection. Again, this re-iterates that the circadian and light-signalling responses are closely linked. In SD to LD transition CCA1 also shows a very quick shift between photoperiod conditions with a single, high amplitude transient day (Figure 8.6, starting at ZT64) before settling into the dark repressed LD circadian response seen in constant LD's (Figure 8.6A, from ZT84 and 8.5A, black arrow). In both of the photoperiod switches the transcriptional markers follow the light conditions (Figures 8.6B and 8.7B for *pCCA1* and Figures 8.6D and 8.7D for *pTOC1*) as observed in the SD and LD entrainment (Figures 8.4B and 8.5B for *pCCA1* and Figures 8.4D and 8.5D for *pTOC1*).

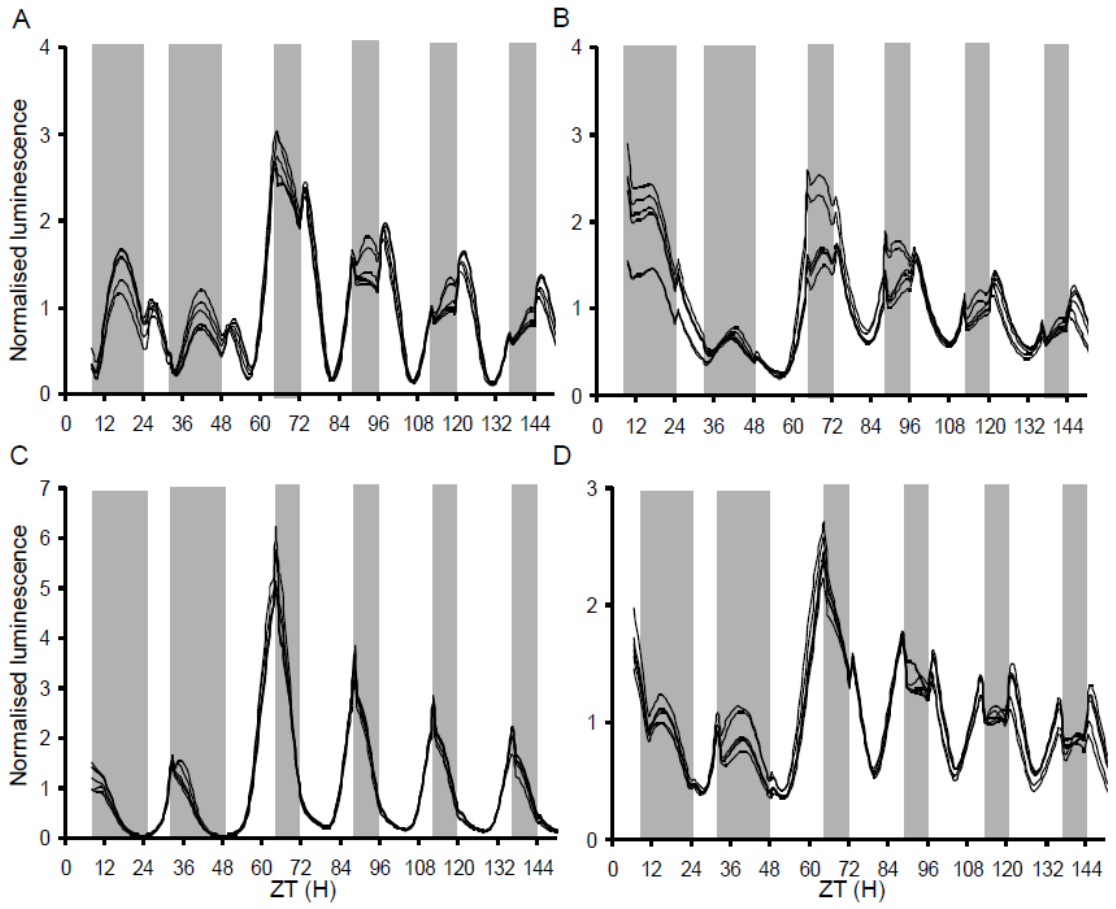

Figure 8.6: *O. tauri* rhythms under short day to long day switch of photoperiods
O. tauri cells are entrained under 8:16 blue light:dark cycles and transferred at ZT0 to 8:16 red and blue light:dark cycles for 2 cycles. Then photoperiodic conditions are switched, for the rest of the data recording, to long day 16:8 light:dark cycles at ZT48. Luminescence of each marker is measured following a 2 minute delay to ensure delayed fluorescence does not interfere with readings. A) *CCA1*::CCA1::LUC, B) *pCCA1*::LUC, C) *TOC1*::TOC1::LUC and D) *pTOC1*::LUC. Traces are normalised to the average of each time series and then averaged per column with n=8 for each trace. White (day) and Grey (night) shading represents the photoperiod.

In the LD to SD photoperiod shift *O. tauri* cells were kept on carbohydrate supplemented media [53] as following the switch to SD on non-supplemented media the cells had an extremely low amplitude rhythm where waveform features could not be identified (data not included). On carbohydrate supplemented media acute responses to changes in light conditions are greatly reduced, but can still be observed (red arrows Figure 8.7). This suggests that the level of

carbohydrate available to the cells influences the amplitude of acute light-signalling response. The transition to SD causes a reduction in oscillator amplitude for all components (Figure 8.7). This confirms the observations from the SD to LD transitions that light acts as a positive input to the amplitude of the oscillator (Figure 8.6). Expression and protein levels in the first long night are extremely low for TOC1 (Figure 8.7C for TOC1, green arrow, starting ~ZT60 and Figure 8.7D for *pTOC*, starting ~ZT60), which indicates that an early dusk, rather than a late dusk, has a greater affect on the oscillator. The low levels of TOC1 across the transition day (Figure 8.7C, green arrow, ~ZT60) only has a mild effect on the levels of *pCCA1* (Figure 8.7B, ZT72). This is significant as TOC1 is the indirect activator of *pCCA1* in the single loop clock (Figure 8.1) therefore with low TOC1, *pCCA1* and CCA1 levels should drop. This is not observed suggesting that TOC1 is not the only activator of *pCCA1*. This is proposed in a mathematical model of *O. tauri* network where a modified form of TOC1 is the direct activator of *pCCA1* [168].

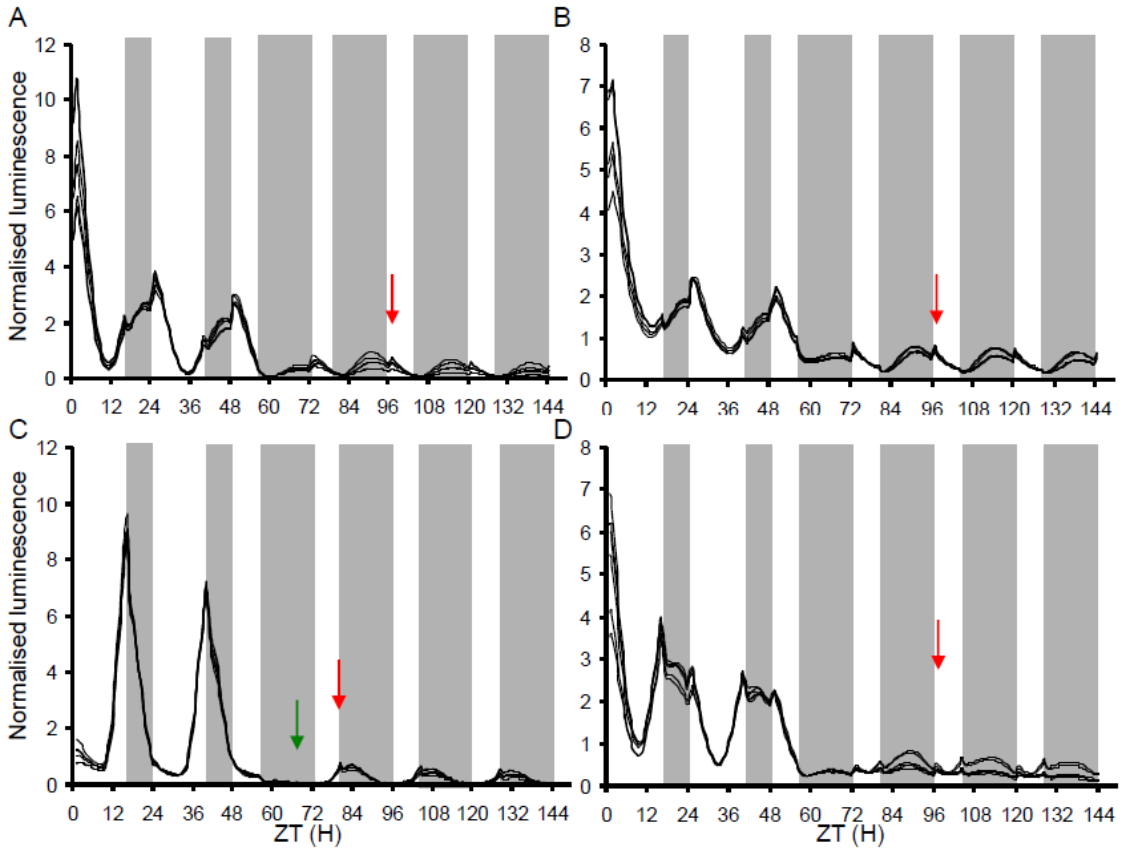

Figure 8.7: *O. tauri* rhythms under long day to short day switch photoperiods
O. tauri cells are entrained under 16:8 blue light:dark cycles and transferred at ZT0 to 16:8 red and blue light:dark cycles for 2 cycles. Then photoperiodic conditions are switched, for the rest of the recordings, to short day 8:16 light:dark cycles at ZT48. Luminescence of each marker is measured following a 2 minute delay to ensure delayed fluorescence does not interfere with readings. A) *CCA1*::CCA1::LUC, B) *pCCA1*::LUC, C) *TOC1*::TOC1::LUC and D) *pTOC1*::LUC. Traces are normalised to the average of each time series and then averaged per column with n=8 for each trace. Red arrows indicate transient responses of the lines to light and the green highlights the day of low TOC1 protein. White (day) and Grey (night) shading represents the photoperiod.

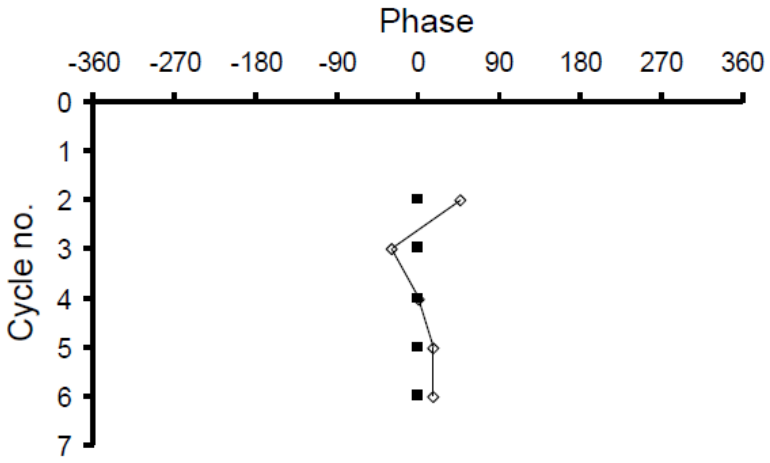

Figure 8.8: Masking effect of transient lights-off response of the TOC1 marker
When *Ostreococcus tauri* cells are moved from entrained SD to LD conditions (Figure 8.6) the phase of the circadian *TOC1*::TOC1::LUC peak changes relative to the position of the transient light to dark peak. Transient peak is represented filled squares and SD to LD circadian peak is represented as open diamonds. Phase 0, which is dusk in both photo-conditions.

For transitions at dawn either an abnormal short or long photoperiod is inserted on the transition day. For entrained SD to LD switch this is a short photoperiod cycle, such that dawn arrives 8 hours earlier than the oscillator was entrained to. The transcriptional markers and CCA1 show a transient response to this early dawn (red arrows on Figure 8.9A (CCA1, ~ZT66), 8.9B (*pCCA1*, ~ZT66) and 8.9D (*pTOC1*, ~ZT66)). CCA1 shows a high acute response (Figure 8.9A, red arrow, ZT66) followed by its standard dark repression (Figure 8.9A, black arrow, ZT84) previously observed in LD (as shown in constant LD, Figure 8.5A). However, the position of the CCA1 protein level rise does not alter, relative to the new dawn, from its entrained position in SD conditions. That is, the transient responses alter to the new LD photoperiod but the circadian response is unchanged, specifically relating to the troughs, just after ZT72, 96, 120 (Figure 8.9A). This is also true for the TOC1 protein line where, as previously discussed, the time of the peak is determined by dusk. Therefore, TOC1 shows a high amplitude cycle with the transition to LD (Figure 8.9C, red arrow, ZT80) but the trough is unchanged with the changing photoperiod (Figure 8.9C, ZT72, 96, 120). The same temporal pattern is observed for the

transcriptional lines, but the transient responses occur at both dawn and dusk (Figure 8.9B for pCCA1 and Figure 8.9D for *pTOC1*).

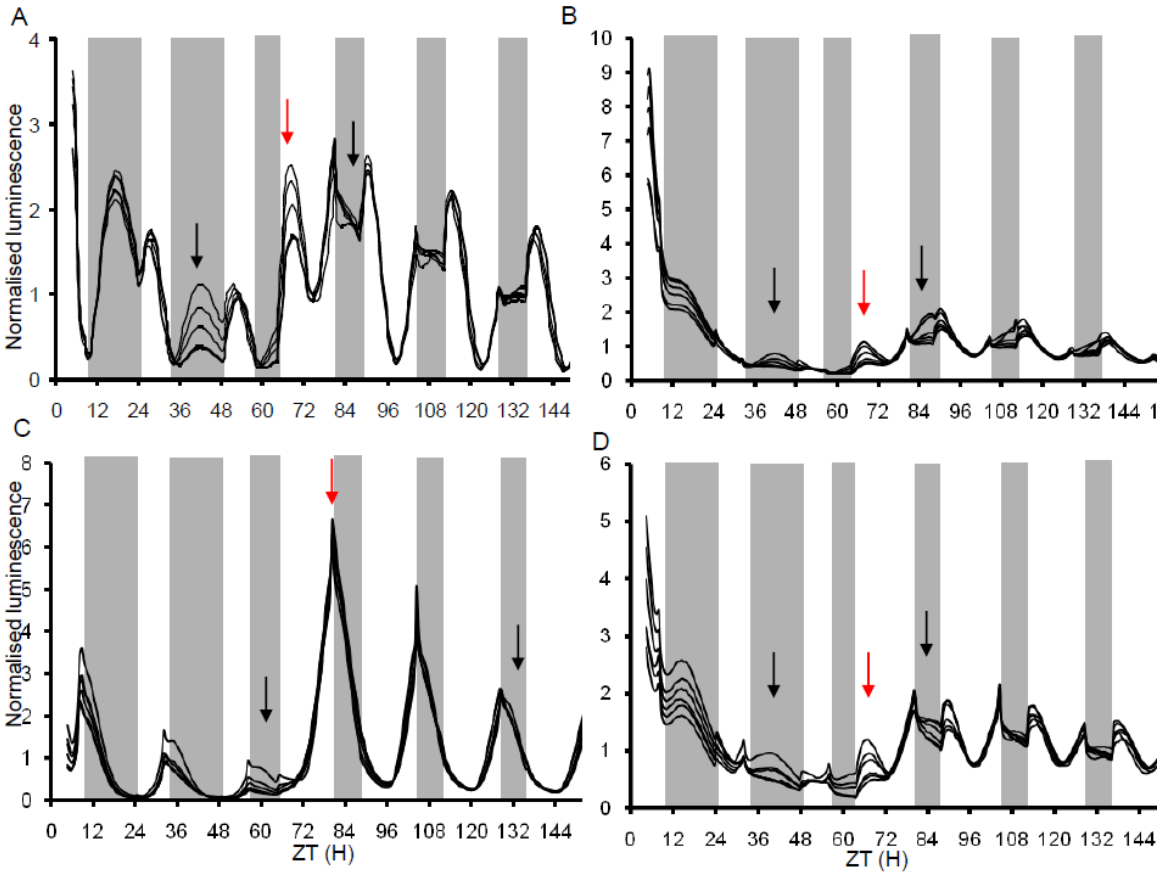

Figure 8.9: *O. tauri* rhythms under short day to long day switch photoperiods, movement of dawn
O. tauri cells are entrained under 8:16 blue light:dark cycles and transferred at ZT0 to 8:16 red and blue light:dark cycles for 2 cycles. Then photoperiodic conditions are switched, for the rest of the recordings, to long day 16:8 light:dark cycles at ZT64. Luminescence of each marker is measured following a 2 minute delay to ensure delayed fluorescence does not interfere with readings. A *CCA1*::CCA1::LUC, B) *pCCA1*::LUC, C) *TOC1*::TOC1::LUC and D) *pTOC1*::LUC. Traces are normalised to the average of each time series and then averaged per column with n=8 for each trace. White (day) and Grey (night) shading represents the photoperiod.

For the LD to SD dawn transition, for the same reasons as the evening transition, the cells are on high carbohydrate media. Following this photoperiod switch the amplitude of the response for all of the lines (Figure 8.10) is much more constant relative to LD levels than the LD to SD dusk

transition (Figure 8.7). The circadian element to all of the waveforms is maintained (Figure 8.10, black arrows) but the transient dawn responses are greatly reduced (Figure 8.10A, red arrow, ~ZT56 and Figure 10B, red arrow, ~ZT56). This again suggests that the oscillator mechanism is not responding to the alteration in dawn, it is the position of dusk which drives the circadian phases.

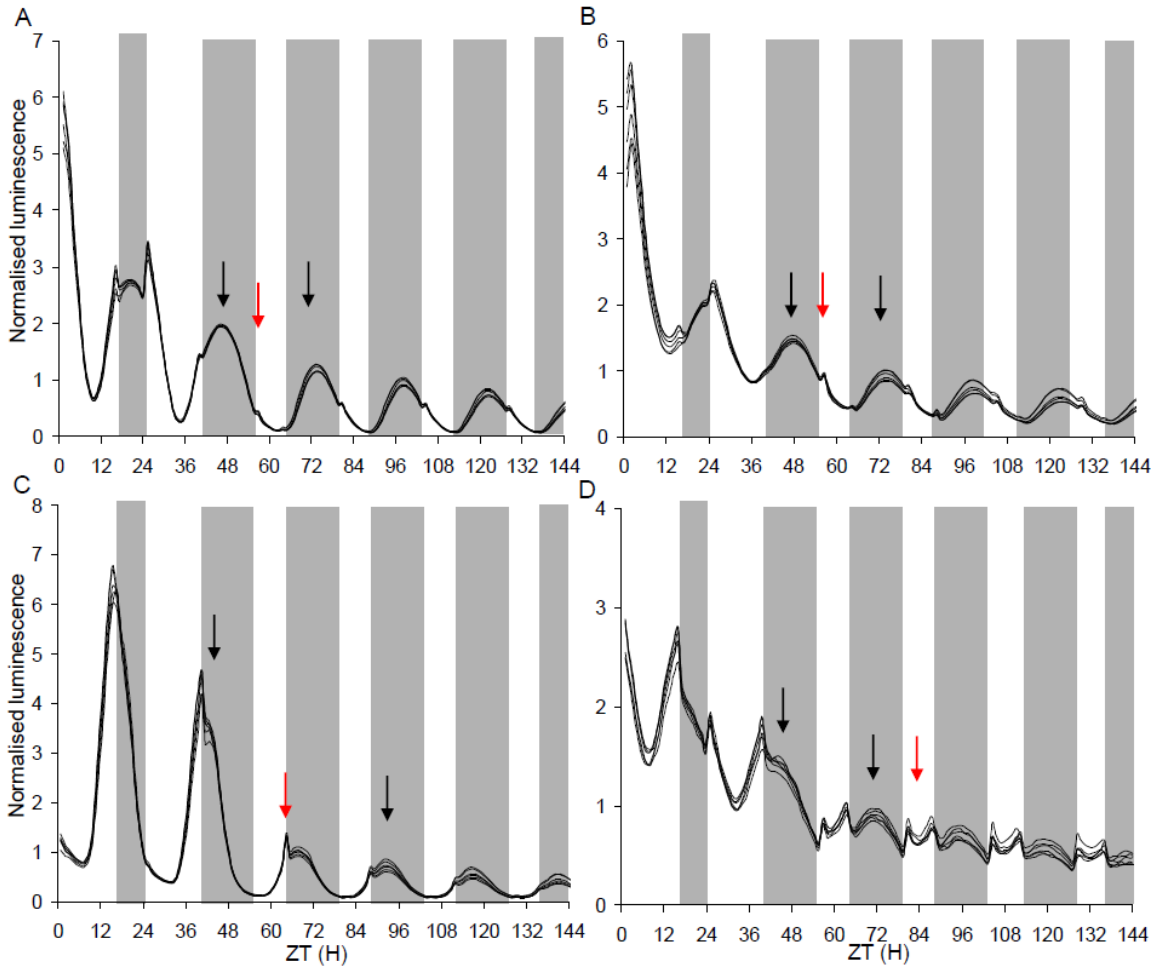

Figure 8.10: *O. tauri* rhythms under long day to short day switch photoperiods, movement of dawn

O. tauri cells are entrained under 16:8 blue light:dark cycles and transferred at ZT0 to 16:8 red and blue light:dark cycles for 2 cycles. Then photoperiodic conditions are switched, for the rest of the recordings, to short day 8:16 light:dark cycles at ZT56. Luminescence of each marker is measured following a 2 minute delay to ensure delayed fluorescence does not interfere with readings. A) *CCA1*::CCA1::LUC, B) *pCCA1*::LUC, C) *TOC1*::TOC1::LUC and D) *pTOC1*::LUC. Traces are normalised to the average of each time series and then averaged per column with n=8 for each trace. Red arrows indicate transient responses of the lines to light and the green highlights the day of low TOC1 protein. White (day) and Grey (night) shading represents the photoperiod.

8.2.1.3 Inter-peak differences

To quantify how quickly the phases moved with the new photoperiodic conditions the inter-peak difference was calculated. To gain the inter-peak difference a specific phase marker was identified (highlighted by black arrows in Figure 8.4) and the difference between the peaks measured, through an automatic peak identifying programme (Chapter 2). The measured intervals were identified from a mean of 8 replicates, from the cells in the highest light conditions in the Topcount. This measure enables the determination of how long the peak phases take to become distributed at the original (~24 hour) period following a transition and therefore how many cycles it takes for the oscillator to entrain. It is expected that phase advances cause a shortening of period whilst phase delays cause a lengthening of period over the transient day [307].

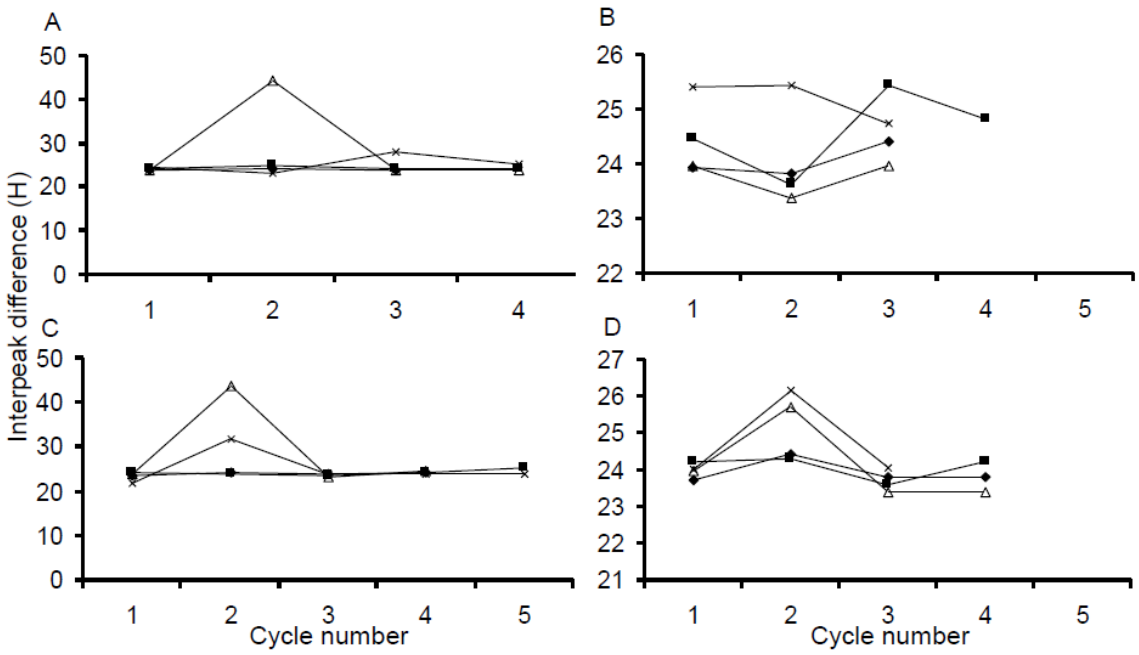

Figure 8.11: *O. tauri* inter-peak differences

Inter-peak differences were calculated for SD (filled squares (Figure 8.4)), LD (filled diamonds (Figure 8.5)), SD to LD (open triangles (Figure 8.6)) and LD to SD (crosses (Figure 8.7)) conditions. A. *CCA1*::CCA1::LUC, B) *pCCA1*::LUC, C) *TOC1*::TOC1::LUC, D) *pTOC1*::LUC

Analysis of the inter-peak difference in *O. tauri* showed that under stable photoperiod conditions, either LD or SD the inter-peak difference was constant (Figure 8.11), with the highest day-to-day variation being observed in the *pCCA1* line (Figure 8.11B). Following a photoperiod switch (Figures 8.6 and 8.7) the inter-peak difference became longer, 26 hours (*pTOC1*, Figure 8.11D) and much longer, over 40 hours (TOC1, Figure 8.11C) for both evening switches. This is due to the low amplitude cycle which is observed following LD to SD transition which means that a peak is missed. Most notable is that the transition day (day 2) is the only day which shows any alterations of inter-peak difference, the new phase of components is assumed very quickly with a new photoperiod. This indicates that the *O. tauri* clock is highly sensitive and responsive to light signals. The determination of inter-peak differences is not possible for the transitions with a movement at dawn (Figures 8.9 and 8.10) due to the abnormal photoperiod cycle.

8.2.1.4 Investigating the role of light intensity and sucrose on waveforms

Light is a very strong entraining stimulus for the *O. tauri* clock, this is not too surprising given that every transcript measured to date responds to a diurnal light:dark cycle in *O. tauri* [315]. However, light also plays another important role in the formation of the circadian waveforms. Through varying light duration (above) or light intensity (Figure 8.12) the amplitude of rhythms is altered, whilst the phase of the peaks between days of differing light intensity, remain very similar. The waveform does change following two days of low light intensity relative to the previous high light intensity conditions, but again this is mostly observed through the relative amplitudes and not changing phases. This suggests that *O. tauri* entrains mostly via discrete entrainment, an idea which is support through *O. tauri's* ability to entrain to skeleton

photoperiods [168]. The addition of D-sorbitol and glycerol [53] (Figure 8.7 and 8.10) also affects the amplitude of the oscillator. However, sucrose appears to reduce the acute light response, suggesting that there could be another layer of feedback. This could relate to the level of sucrose available to the cell influencing the amplitude of the acute response.

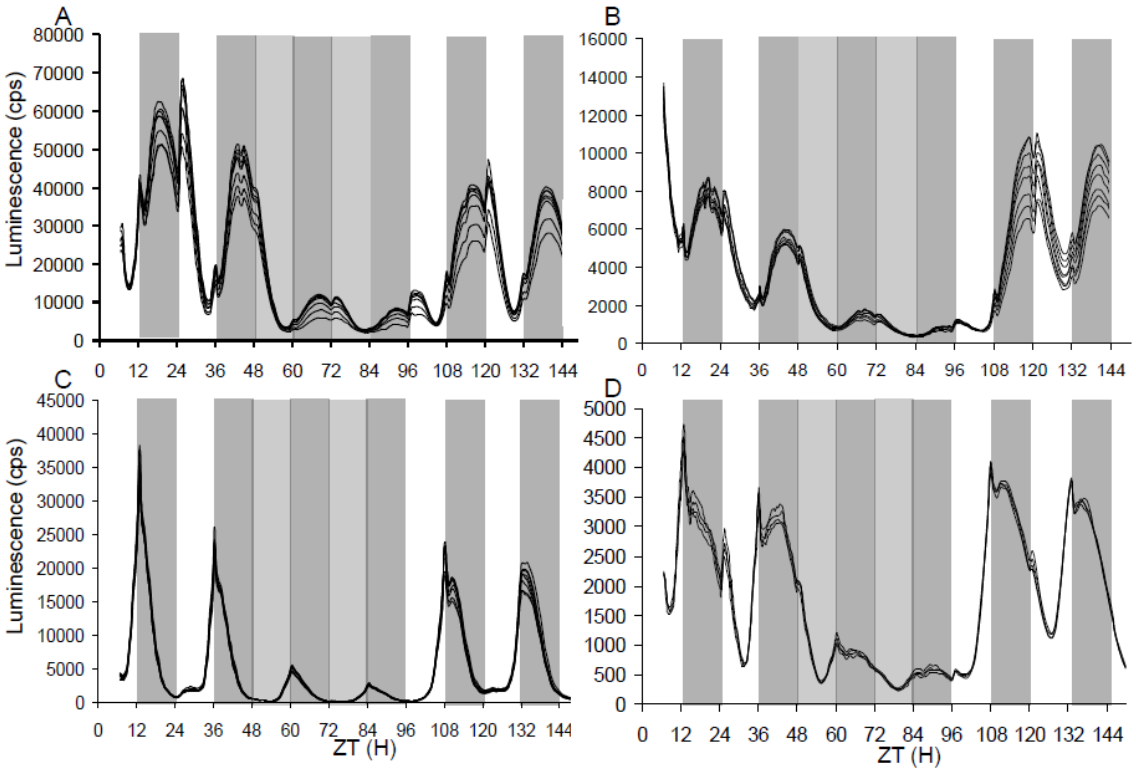

Figure 8.12: *O. tauri* rhythms under high and low light intensity
O. tauri cells were entrained under 12:12 blue light:dark cycles and transferred at ZT0 to 12:12 red and blue light:dark cycles for data recording on the Topcount. For the first two days cells were under high light intensity of ~10 μE/m^2 between ZT48 and ZT96 the days were low light intensity, depicted by light grey shading, and then the cells were returned to highlight intensity. A) *CCA1*::CCA1::LUC, B) *pCCA1*::LUC, C) *TOC1*::TOC1::LUC and D) *pTOC1*::LUC. Traces are normalised to the average of each time series and then averaged per column with n=8 for each trace. White areas represent high light and grey areas represent low light and dark grey represents darkness.

8.2.2 *Arabidopsis thaliana*

8.2.2.1 Phase markers in entraining conditions

Unlike *O. tauri*, the markers used to track the responses of the *A. thaliana* clock network peak throughout the 24 hour cycle and not all of the markers show transient responses to changing light conditions. This confirms that the regulation of the luciferase protein itself is not the major output being measured. By comparing the SD, LD and photoperiod switches the markers used can be classified into two main groups, those which are predominantly responding to light signalling (this classification does not exclude circadian regulation being important) and those which predominantly show a circadian response.

The reporters which are predominantly responding to light signalling are *TOC1* and *ELF3*. The *TOC1* response is very similar to that observed with the transcriptional *pTOC1* marker in *O. tauri* such that under LD conditions it can be considered to be a reporter for the changes in light conditions (Figure 8.13B) and in SD it shows a very low level of expression (Figure 8.14B). *ELF3* also tracks the light conditions and shows very low levels of expression after a switch from LD into SD (Figure 8.14F). This low level of expression in *ELF3* may be significant regarding the changing of other circadian genes phases to new photoperiods as *ELF3* has been proposed to have zeitnehmer function [106]. For the markers showing a predominantly circadian response (*CCA1*, *GI* and *PRR9*) the speed of entrainment is different depending on the direction of the switch, this has previously been observed in *Drosophila* [307]. Following a SD to LD transition (Figure 8.13C (*CCA1*), 8.13D (*GI*) and 8.13A (*PRR9*)) the shift in the waveform from SD characteristics to LD characteristics is much slower than compared to a LD to SD switch where the waveform shift is almost immediate (Figure 8.14C (*CCA1*), 8.14D (*GI*) and

8.14A (*PRR9*)). Under SD conditions, components which peak early in the day seem to be particularly slow to respond to the change in dusk position. For *PRR9* a large peak phase shift and waveform change is required to move the peak from the light responsive dawn SD peak to the split waveform of small dawn light response and a larger later circadian response in LD (Figures 8.13A). This trend does not seem to be reflected in the SD to LD transition with a change in the time of dawn, most probably due to the immediate coincidence of the new light phase with the peak expression times (Figure 8.15A).

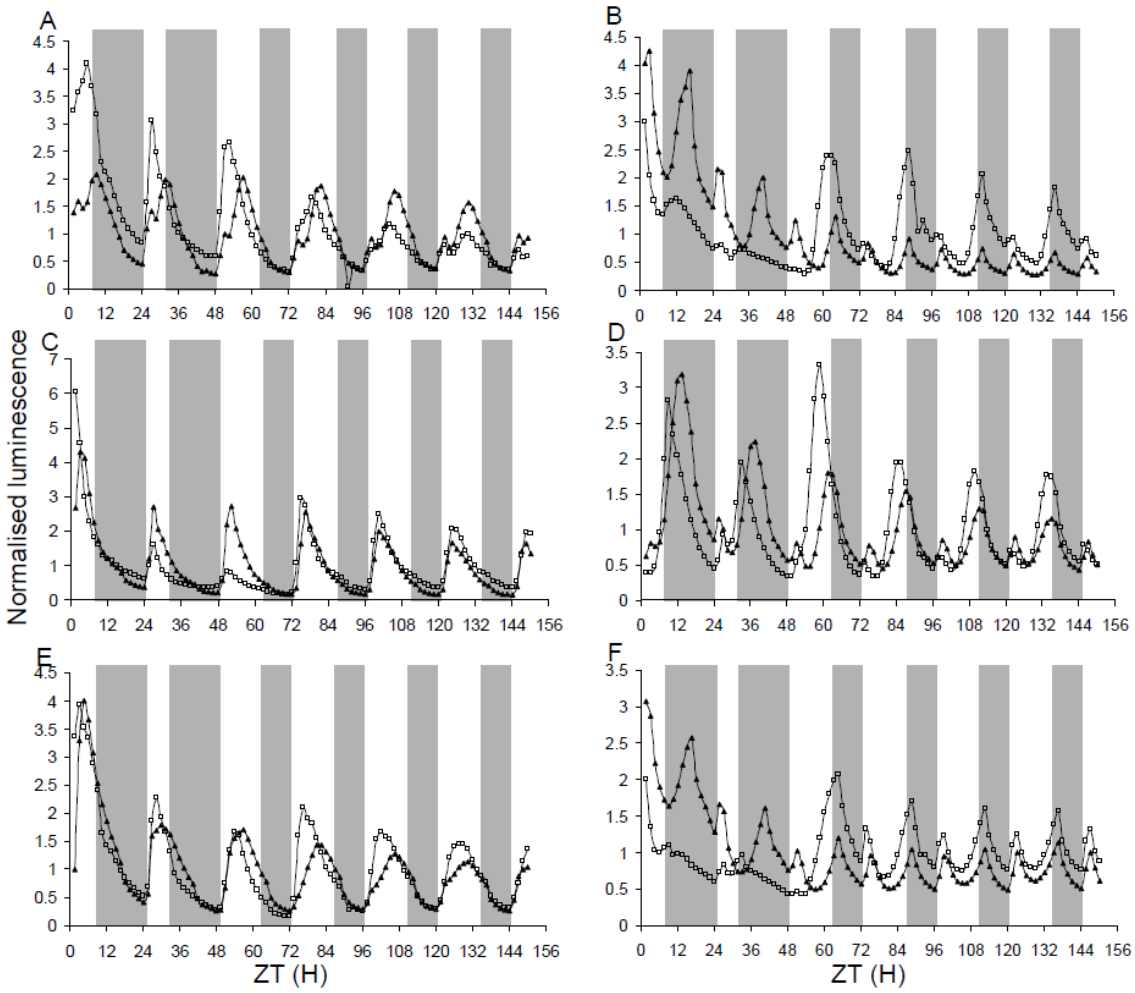

Figure 8.13: *A. thaliana* rhythms under long day photoperiod and short day to long day transition

A. thaliana plants were entrained under white light ~70 μE/m^2 in the starting imaging condition and imaging started on 6 day-old seedlings. Closed triangles show the imaging profile from continuous long day (16:8 blue and red light:dark cycles) and the open squares from short day (8:16 blue and red light:dark cycles) for 48 hours to long day (16:8 blue and red light:dark cycles). A) *PRR9::LUC*, B) *TOC1::LUC*, C) *CCA1::LUC*, D) *GI::LUC*, E) *CAB2::LUC* and F) *ELF3::LUC*. White (day) and Grey (night) shading represents the photoperiod. Each trace is an average which have been normalised within each experiment to enable comparison between photoperiodic conditions.

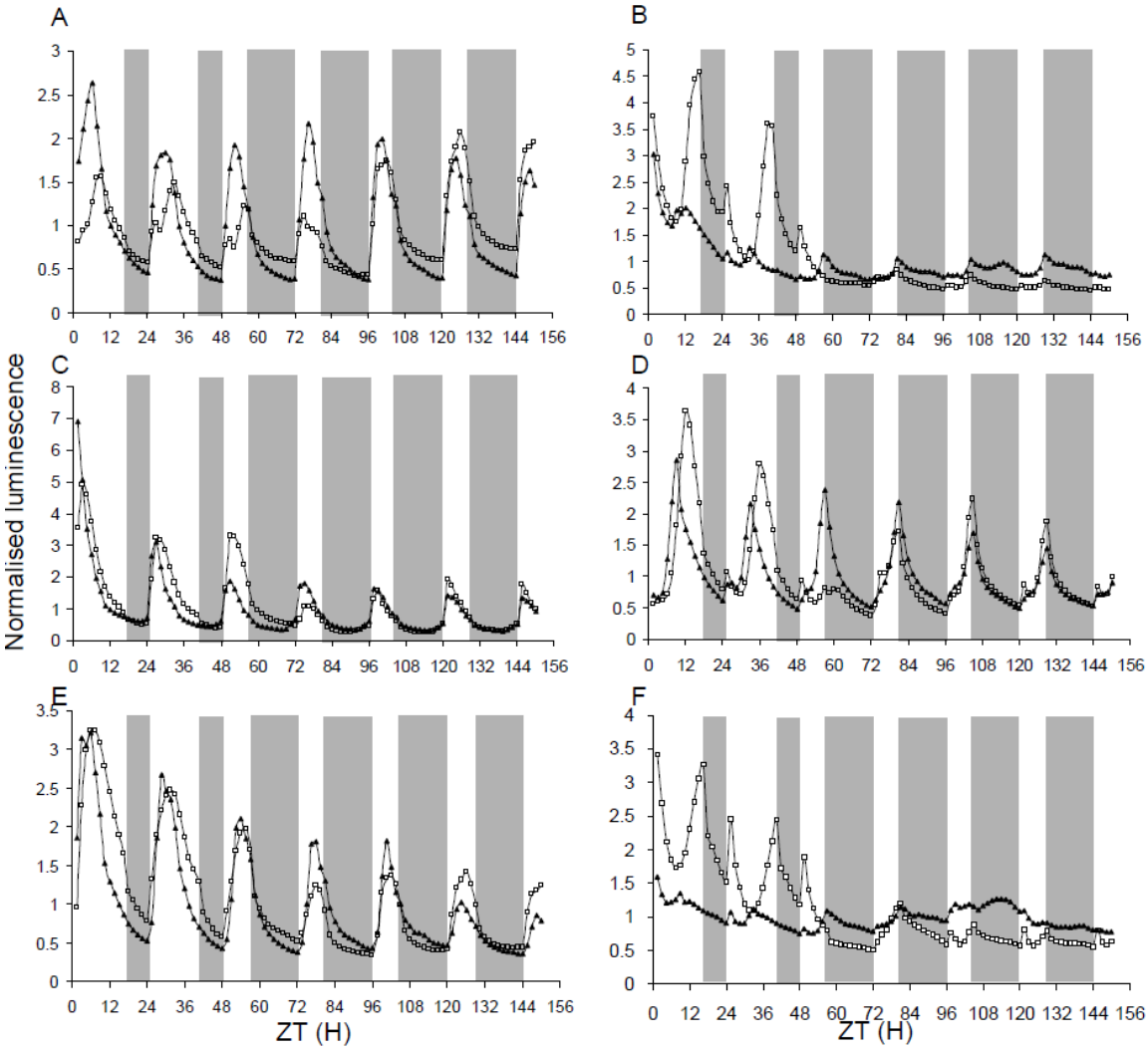

Figure 8.14: *A. thaliana* rhythms under short day photoperiod and long day to short day transition

A. thaliana plants were entrained under white light of ~70 μE/m^2 in the starting imaging condition and imaging began on 6 day-old seedlings. Closed triangles show the imaging profile from continuous short day (8:16 blue and red light:dark cycles) and the open squares from long day (16:8 blue and red light:dark cycles) for 48 hours to short day (8:16 blue and red light:dark cycles). A) *PRR9::LUC*, B) *TOC1::LUC*, C) *CCA1::LUC*, D) *GI::LUC*, E) *CAB2::LUC* and F) *ELF3::LUC*. White (day) and Grey (night) shading represents the photoperiod. Each trace is an average which have been normalised within each experiment to enable comparison between photoperiodic conditions.

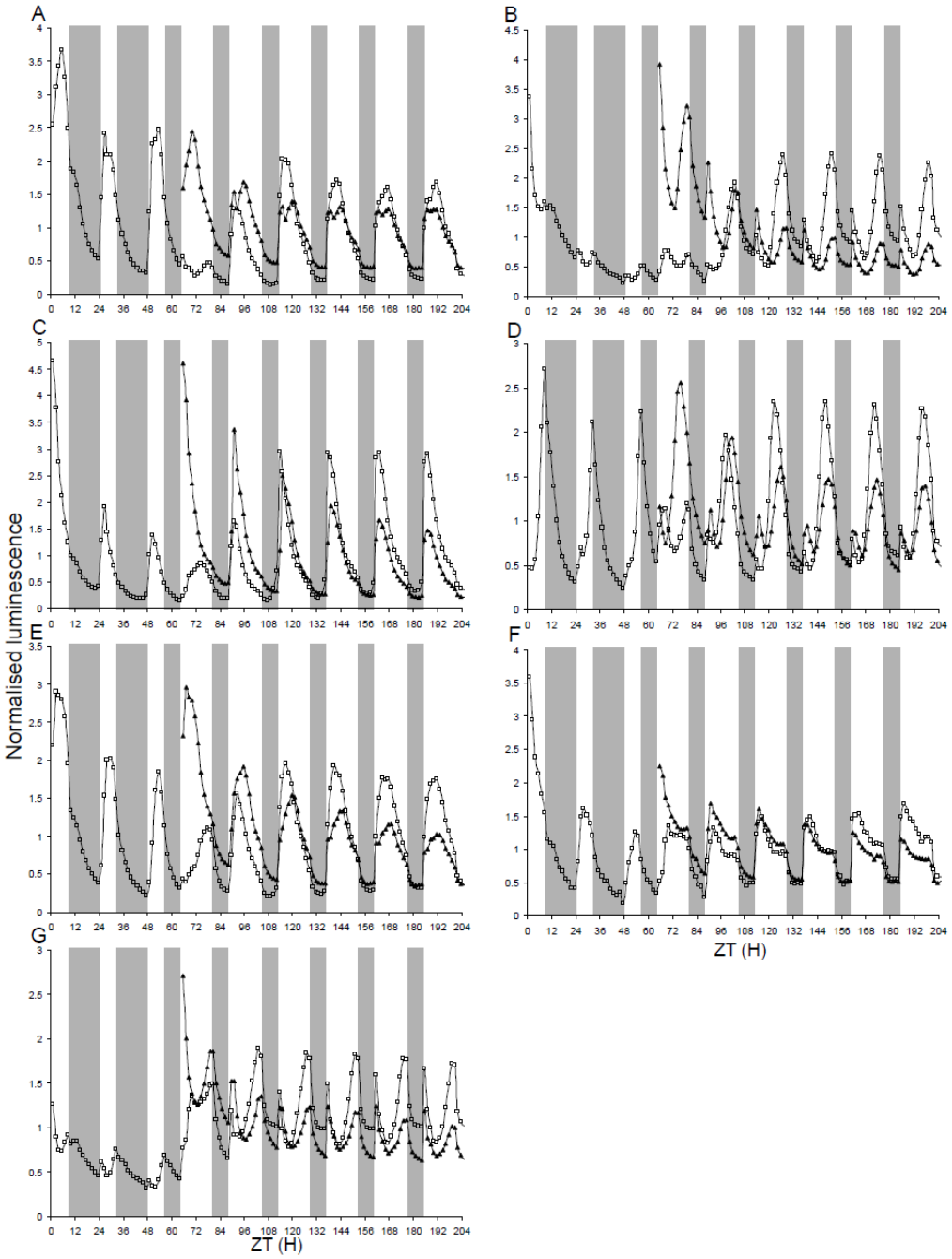

Figure 8.15: *A. thaliana* rhythms under short day to long day switch photoperiods, movement of dawn

A. thaliana cells are entrained under 8:16 white light:dark cycles and transferred at ZT0 to 8:16 red and blue light:dark cycles for 2 cycles. Closed triangles show the imaging profile from continuous long day (16:8 blue and red light:dark cycles) and the open squares from short day (8:16 blue and red light:dark cycles) to long day (16:8 blue and red light:dark cycles) from ZT64. A) *PRR9::LUC*, B) *TOC1::LUC*, C) *CCA1::LUC*, D) *GI::LUC*, E) *CAB2::LUC*, F) *LHY::LUC* and G) *ELF3::LUC*. Traces are normalised to the average of each time series and

then averaged with n= for each trace. White (day) and Grey (night) shading represents the photoperiod.

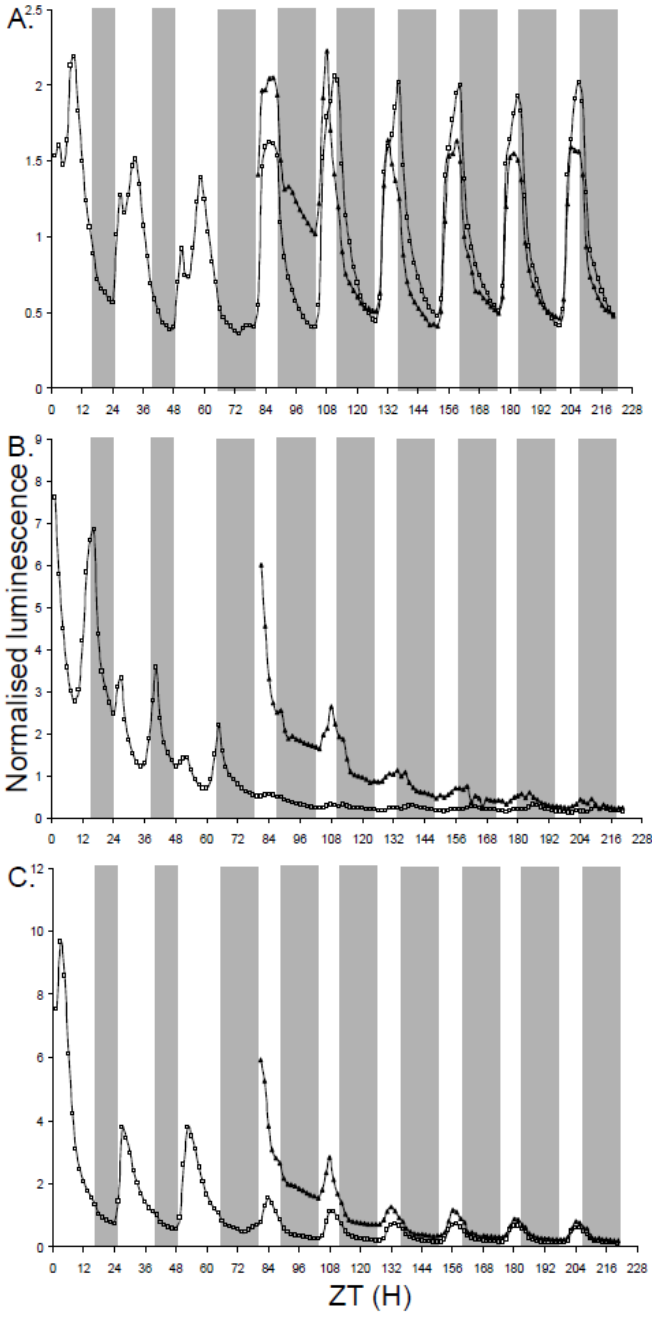
A.
B.
C.
Normalised luminescence
ZT (H)

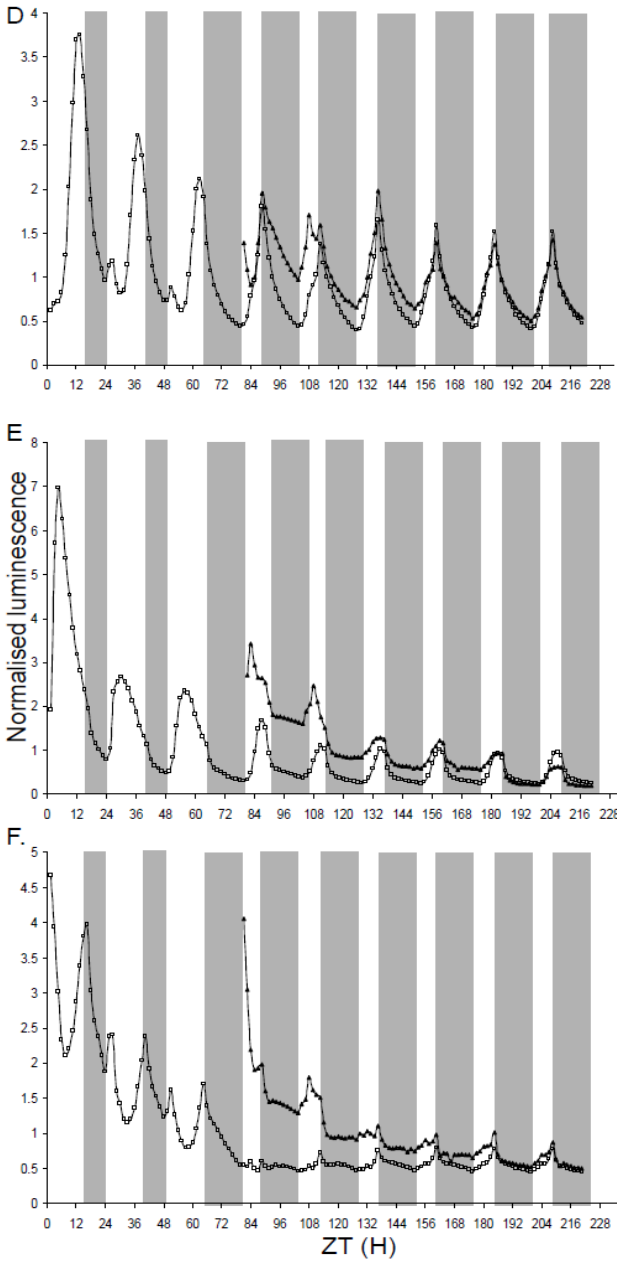

Figure 8.16: *A. thaliana* rhythms under long day to short day switch photoperiods, movement of dawn

A. thaliana cells are entrained under 16:8 white light:dark cycles and transferred at ZT0 to 16:8 red and blue light:dark cycles for 2 cycles. Then photoperiodic conditions are switched, for the rest of the recordings, to short day 8:16 light:dark cycles at ZT56 (open squares) plotted against constant short day conditions 8:16 (closed triangles) A) *PRR9::LUC,* B) *TOC1::LUC,* C) *CCA1::LUC,* D) *GI::LUC,* E) *CAB2::LUC* and F) *ELF3::LUC.* Traces are normalised to the average of each time series and then averaged with n= for each trace. White (day) and Grey (night) shading represents the photoperiod.

As the waveforms show two different types of response (light-signalling and moving circadian phase), the nature of the oscillator responses under different conditions can also be analysed. GI shows a classic circadian response. Inter-peak difference analysis identifies it has the anticipated pattern for the two transitions; phase advances showing a shortening in period and phase delays a lengthening in period (Figure 8.17C).

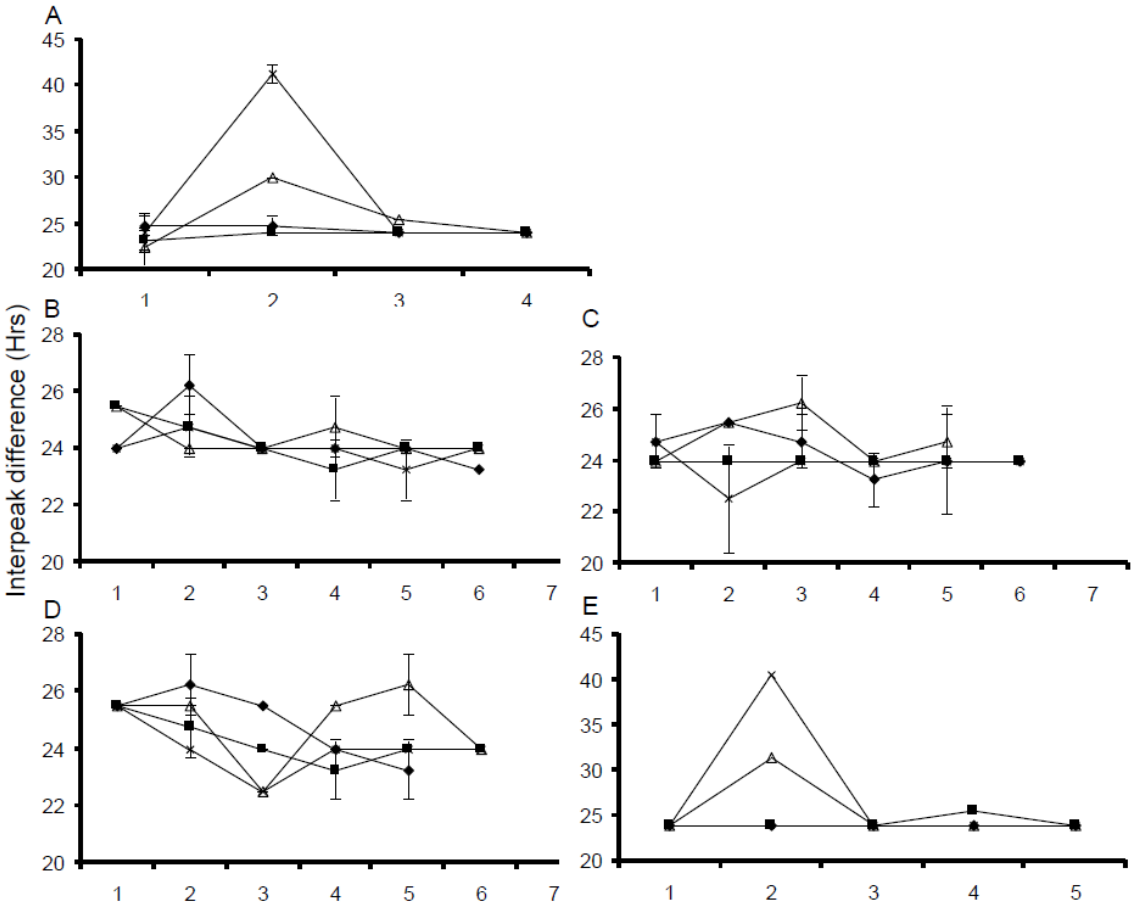

Figure 8.17: *A. thaliana* inter-peak differences
Inter-peak differences were calculated for SD (filled squares (Figure 8.14)), LD (filled diamonds (Figure 8.13)), SD to LD (open triangles (Figure 8.13)) and LD to SD (crosses (Figure 8.14)) conditions. A) *TOC1::LUC*, B) *CCA1::LUC*, C) *GI::LUC*, D) *CAB2::LUC* and E) *ELF3::LUC* with the error being the StDev between two replicates.

It is clear from Figures 8.13D and 8.14D that the peak of *GI* expression moves following the photoperiod switches. Through plotting the individual waveforms for each day under LD, *GI* shows a small dawn peak and a broad dusk peak which has a slight variation in its timing, peaking between ZT13-16 (Figure 8.18A). Where as under SD conditions the *GI* peak is very narrow and falls reliably just after dusk at around ZT9 (Figure 8.18B). Following both SD to LD and LD to SD dusk transitions there is a dramatic change in amplitude. In the SD to LD transition there is a marked increase (Figure 8.18C). With the LD to SD transition there is a clear decrease in amplitude, re-enforcing the idea that light and most probably the subsequent metabolites are controlling clock response amplitude of *GI* (Figure 8.18D). These changes in amplitude also support the limit-cycle model of the oscillator as they could be interpreted as the oscillator is moving between two stable states. It also suggests that the timing of dusk strongly influences the peak phase of *GI* transcript. It would be interesting to understand whether this shift affects the timing of GI protein levels as GI protein levels have been shown to oscillate even with constant transgenic expression of GI ([164] and Chapter 5).

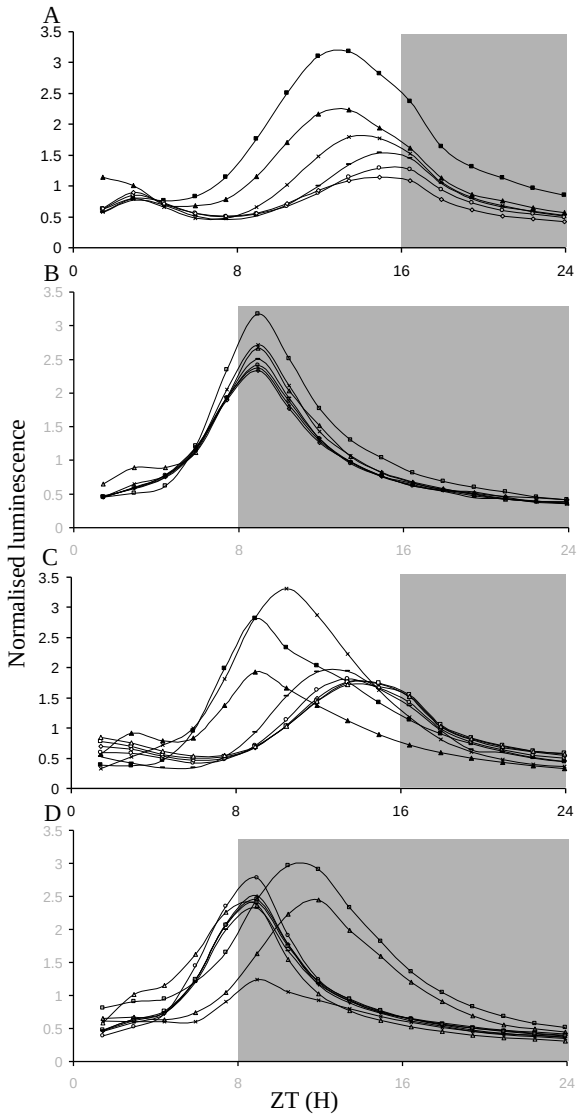

Figure 8.18: Comparison of individual days of *GI*::LUC
Individual day traces for the *GI::*LUC marker from Figures 8.13 and 8.14 are plotted for phase comparison. A) Long day photoperiod: Day 1 (Filled squares), Day 2 (Filled triangles), Day 3 (Crosses), Day 4 (Dash), Day 5 (Open circles), Day 6 (Open diamonds). B) Short day photoperiod: Day 1 (Filled squares), Day 2 (Filled triangles), Day 3 (Crosses), Day 4 (Dash), Day 5 (Filled circles), Day 6 (Upright dash) and Day 7 (Filled diamonds). C) Entrained SD to LD photoperiod: Day 1 (Filled squares), Day 2 (Filled triangles), Day 3 (Crosses), Day 4 (Dash), Day 5 (Open circles), Day 6 (Open diamonds), Day 7 (Open squares) and Day 8 (Open triangles). And D) Entrained LD to SD photoperiod: Day 1 (Filled squares), Day 2 (Filled triangles), Day 3 (Crosses), Day 4 (Open triangles), Day 5 (Open circles), Day 6 (Upright dash), Day 7 (Open diamonds), Day 8 (Open squares), Day 9 (Dash). Photoperiod conditions shown for the final condition in B and D.

In *O. tauri* the response of the oscillator to the dawn transitions was much less than to the evening transitions. In *A. thaliana* this is also observed (Figures 8.15 and 8.16), but the oscillator does respond. With the transition from SD to LD at dawn the more light responsive elements respond immediately (*TOC1* and *ELF3*) and like the evening transition the more circadian-regulated components take longer to settle to a new phase (Figure 8.13B & F for evening and Figure 8.15B & F for morning). Both *GI* and *PRR9* take about 4 cycles to find the same waveform as entrained LD plants and whilst *CCA1* finds this phase much faster, its anticipation of dawn, following the movement of dawn, is different to standard LD conditions (Figure 8.13C).

8.2.2.2 A. thaliana inter-peak differences

Under constant light:dark cycle conditions both *TOC1* and *ELF3* waveforms are very stable. This is mainly due to the responses being driven by the light conditions (Figure 8.17A and 8.17E). Both show the same inter-peak lengthening following the LD to SD switch as *O. tauri* TOC1, due to the loss of marker amplitude. *GI, CCA1* and *CAB* all show more variation in their responses to the photoperiodic transition (Figure 8.17C, 8.17B and 8.17D). GI shows the more classical lengthening and shortening of inter-peak difference expected of an oscillator mechanism, described in section 8. 2. 2.1. *CCA1* does not show a clear pattern in its response. This may be linked with the conditions used for imaging. All of the photoperiodic transitions where conducted on media without sucrose, whilst *CCA1* shows better anticipation, and therefore a more circadian-like response, on media with sucrose (discussed in next section, 8. 2. 2. 3). This may mean that the responses measured on media without sucrose represent only part of *CCA1* function. The idea that different elements of the clock require different metabolic

states to function is not unreasonable as the role of metabolism is increasingly understood to be important in all clock systems studied [316].

8.2.2.3 Investigating the role of light intensity and sucrose on waveforms

According to Aschoff's rule, the higher the light intensity the faster the oscillator runs. A change in light intensity should cause a change in the phase of components under the control of the clock, although the period is constrained to the entrainment conditions. This was not observed in *O. tauri* where a change in light intensity simply affected the clock markers expression levels (Figure 8.12). In *A. thaliana* the change in expression levels is also observed (Figure 8.19) with all components measured showing a high amplitude in high light intensity and a low amplitude in low light intensity. However, the *A. thaliana* clock also shows a change in waveform. Most notably the anticipation of *CCA1* before dawn (Figure 8.19C) and *GI* before dusk (Figure 8.19D) is increased under high light conditions. The waveform of the evening components (*TOC1* and *GI*) is also altered with the transition between light intensities (Figure 8.19B and 8.19D). The first exposure to a low light intensity dawn (ZT48, filled squares) causes a small dawn response where previously there was not a response at dawn, suggesting that part of the mechanism which represses the expression of the evening components at dawn is under photo-perception control. All of the markers measured in low light conditions following high light show a later phase, but getting a quantified delay, through FFT-NLLS, is not possible due to the low amplitude of the response. Under constant high or low light the markers are stable and so this change in phase is in response to a change in light intensity. *TOC1* shows a particularly low amplitude response in low light intensities which indicates that light perception of a certain intensity is essential for

TOC1 expression as opposed to total light levels. Following a transition from low light to high light intensities the *TOC1* peak seems to shift to just after dusk.

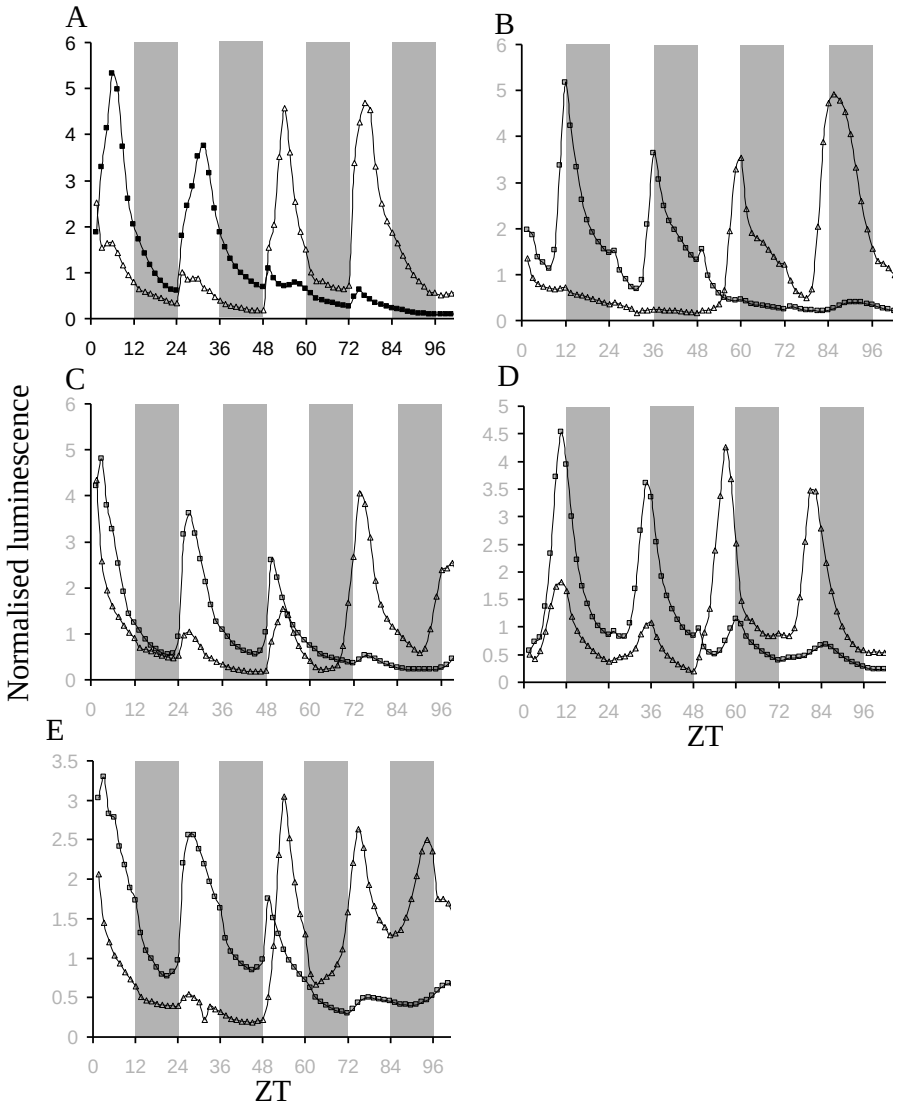

Figure 8.19: *A. thaliana* rhythms following transitions between high and low light intensity
A. thaliana seedlings were entrained under 12:12 white light:dark cycles ~70 μE/m^2 for 6 days and then transferred to red and blue light 12:12 light:dark cycles for imaging. Imaging for 48 hours under either high light intensity, 60 μE/m^2 (squares) or low light intensity 6 μE/m^2 (triangles) light conditions were then switched for the next 48 hours. A) *PRR9::LUC*, B) *TOC1::LUC*, C) *CCA1::LUC*, D) *GI::LUC*, E) *LHY::LUC*.

The effect of sucrose on circadian rhythms was also tested, not through using sucrose as an entraining cue but by measuring the global responses. In *TOC1*, the combination of high light and sucrose produced a shoulder in expression throughout the night, which is not otherwise observed (Figure 8.20B). This is significant as all previous luciferase imaging of *TOC1* has been conducted under high sucrose, high light conditions which suggests that the waveforms measured are only a reflection of a specific light condition which does not represent the most common, or naturally likely, *TOC1* profile. Both of the morning transcription factors, *CCA1* and *LHY*, showed different anticipation when measured on high sucrose media. On high sucrose media *CCA1* and *LHY* anticipate dawn sooner, irrespective of the light intensity (Figure 8.20C and 8.20F). For *LHY* the absence of sucrose causes a broader waveform during the light period (ZT24-36 and ZT48-60). Interestingly, the effects of sucrose and the alterations in phase of *CCA1* and *LHY* do not have subsequent effects on the phase or patterns of expression of other clock components. *GI, PRR9* and the clock output *CAB2* appear not to have any significant alteration in expression profiles with different levels of sucrose (Figure 8.19 D, 8.19A and 8.19E respectively).

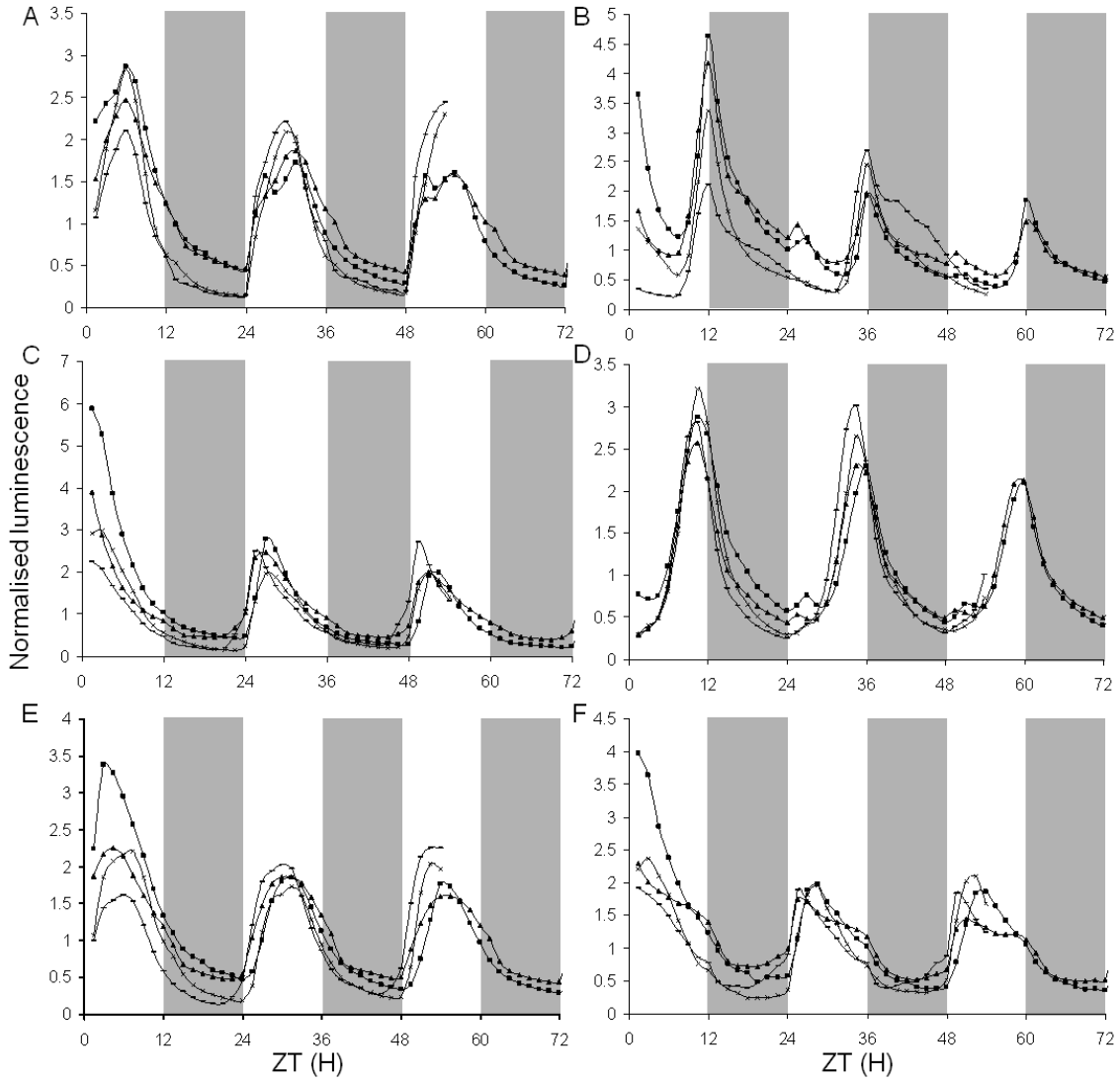

Figure 8.20: *A. thaliana* rhythms comparing light intensity responses on different levels of sucrose

A. thaliana seedlings were entrained under 12:12 white light:dark cycles ~70 μE/m^2 for 6 days and then transferred to red and blue light 12:12 light:dark cycles for imaging. Imaging was either under high light intensity, 60 μE/m^2 or low light intensity 6 μE/m^2 on either no sucrose media or 3% sucrose media. No sucrose low light (Closed squares), 3% sucrose low light (Closed triangles), no sucrose high light (crosses) and 3% sucrose high light (dashes) A) *PRR9::LUC*, B) *TOC1::LUC*, C) *CCA1::LUC*, D) *GI::LUC*, and E) *CAB2::LUC* and F)*LHY::LUC*.

This could suggest that the components form a separate clock or that sucrose only affects the input pathways to the clock without this then influencing the clock network. Interestingly, the clock network is known to be affected differentially by sucrose regarding tissue specificity [23]. The profiles measured in the imaging presented here are from whole plants, but the luminescence is largely localised to the cotyledons and first leaves. As such any tissue specific information is lost and so more subtle effects will not have been identified.

8.3 Discussion

The common topology of circadian clock networks is that of interlocking loops [1]. This is believed to provide the circadian network with both flexibility and robustness to respond to entrainment signals without being oversensitive to natural variations in entraining stimuli, such as dull days or bright moonlight [308]. The identification of a plant clock network which contains a more minimal transcriptional/translational feedback loop network, in *O. tauri*, offered the possibility to test whether multiple loops are required for more complex circadian responses.

The use of light entrainment is common in circadian biology for a number of reasons. Firstly, light is considered the strongest entrainment signal to the oscillator network and so entrainment is often faster. Secondly, it is very easy to manipulate (Chapter 3) and control in the laboratory. Light pulses have been successfully used in skeleton photoperiods and in the gradual movement of dawn and dusk. However, light regimes which require pulses of less than 1.5 hours are not currently possible for *A. thaliana* due to the experimental reporters used. Luciferase imaging is the collection of light and therefore the sample has to enter darkness. For *O. tauri* cells being imaged in 96-well plates on the Topcount this takes approximately five minutes each recording, for *A. thaliana* being imaged under CCD-cameras this takes 30 minutes each image. Therefore, the experimental set-up does not permit a reliable measure for short light pulses during the

blocks of photoperiod (either day or night). However, through careful timing, the times of dawn and dusk transitions were maintained in the data presented here. Therefore, measuring responses to changing the position of dawn and dusk is both possible and reliable in both experimental designs.

Both clock networks were responsive to changes in photoperiodic conditions, and showed changes in the phase of peak times with evening transitions (Figures 8.6, 8.7, 8.13 and 8.14), as observed in [182, 168]. The *O. tauri* clock quickly changed with the evening transition, such that following the transient day the clock markers were adjusted to the new photoperiodic condition. This is partly due to the high degree of light responsiveness both CCA1 and TOC1 show (Figure 8.4 and 8.5). TOC1 protein has its peak phase locked to dusk, irrespective of its previous entrainment condition. This feature is caused through the dark-mediated degradation of TOC1 protein (Chapter 6). The circadian element of the marker is often masked by this light:dark response. However, tracking the small circadian peak, or shoulder in the waveform (Figure 8.4C and 8.5C, black arrows), a circadian response in TOC1 protein can be identified following changes in photoperiod (Figure 8.8). This circadian response is not observed in the transcriptional fusion lines, either pTOC1 or pCCA1 (Figure 8.6B and 8.6D and Figure 8.7B and 8.7D), but both lines do show elements of circadian gating as the transient responses at dawn and dusk are not of equal amplitude. CCA1 shows a very distinct pattern of circadian followed by acute light response (Figure 8.4A). Unlike its *A. thaliana* counterpart, the *O. tauri* CCA1 and pCCA1 lines show a peak which is falling by the arrival of dawn. That is CCA1 does not anticipate dawn. In *O. tauri* the dawn phased response is a transient acute light response, which raises the question as to whether the separate responses now observed through *LHY* and *CCA1* in *A. thaliana,* of *LHY* seeming to be more light responsive (Figure 8.19E) and *CCA1* more circadian (Figure 8.19C), may have once been combined into the same gene. Such observations

would need to be confirmed through measurement of mRNA as the luciferase reporter does show a delay in its response, as luciferase protein is formed [182].

The regulation of *TOC1* also shows a number of similarities between *O. tauri* and *A. thaliana* even through the overall clock responses regarding the transitions are not the same. The responses observed in *TOC1* along with the experimental data already collected for TOC1 in *A. thaliana* [11, 158] and presented in Chapter 6 for *O. tauri*, strongly suggest that TOC1 plays an important role in clock entrainment. In both organisms *TOC1* peak expression is locked to dusk (Figure 8.4D, 8.5D, 8.6D, 8.7D, 8.13B and 8.14B) and this regulation is mirrored in TOC1 protein regulation in *O. tauri* (Figure 8.4D, 8.5D, 8.6D and 8.7D). TOC1 levels and expression is also acutely sensitive to light intensity and duration such that under low light or short periods of light *TOC* expression and therefore protein is hardly observed (Figure 8.4, 8.6 and 8.14). This very low amplitude rhythm is observed to quickly regain amplitude with transfer into higher light conditions (both intensity and duration), Figure 8.13B and 8.19B [182]. Interestingly in the one-loop *O. tauri* network the very low amplitude, hardly rhythmic expression observed in *TOC1* is, arguably, not reflected in *CCA1* levels in the following day suggesting that this simple-loop is not sufficient for the photoperiodic responses observed. This is also supported through the evidence for *O. tauri* in constant light where TOC1 amplitude rapidly damps but the oscillator is capable of continuing past 96 hours in constant light. However, it would need to be confirmed that other clock markers were oscillating in the TOC1 line and observed for native TOC1 protein, before this conclusion can be firmly made. Through comparison with the *A. thaliana* TOC1 protein which is directly regulated through its interaction with the putative blue-light photoreceptor ZTL [11], it suggests that TOC1 is extremely important for the entrainment of the oscillator.

This study, in agreement with the conclusions drawn by Corelleu *et al* [170], indicates that the *O. tauri* clock can not be functioning as a single one-loop feedback mechanism. The expression and protein profiles do not show an anti-phasic relationship between TOC1 and CCA1 as both components show circadian peaks in the middle of the dark period (Figure 8.4 and 8.5). The low amplitude in TOC1 with its transition to SD conditions and the absence of reciprocal regulation on pCCA1 suggests that these two components do not both directly regulate each other.

The photoperiodic analysis of the *A. thaliana* clock has highlighted a number of features. Firstly that re-entrainment from LD to SD is much faster than that of SD to LD. This observation links to the limit-cycle model that in one direction the oscillator takes longer to find a new stable limit cycle. This is also confirmed through the changes in amplitude of *GI* response on the transient day. Movement from LD to SD conditions shows a single day of very low amplitude response, as the oscillator finds its stable limit-cycle. Secondly, it has identified that some of the markers used to understand the circadian responses are, under more realistic photoperiodic conditions, much more closely linked to following the light responses. Two of the considered central clock components *TOC1* and *LHY* both seem to predominantly track the light conditions. This can also be observed for the *LHY* waveform following release into constant light [182]. Both *TOC1* and *LHY* have been linked with mechanisms which enable direct light control, TOC1 at the protein level [11] and LHY at the level of translation [108]. *ELF3* also tracks the light conditions and has recently been identified to be linking to the clock network via *PRR9* (Chapter 4).

The data presented in this chapter highlights that the circadian response is not simply relating to the period, amplitude and peak phase of waveforms. The whole waveform shape is often observed to change between different conditions, such as in *A. thaliana PRR9* (Figure 8.13A), *TOC1* (Figure 8.13B, 8.14B and 8.19B) and *LHY* (Figure 8.20F) and in *O. tauri* CCA1's

different repression responses during darkness (Figure 8.4A and 8.5A). This indicates that to further understand these responses another layer of analysis would be required which measures the shape and changes in shape of the waveforms. To conduct such analysis in a rigorous and reliable fashion wave fitting software would be required, as highlighted in Chapter 7.

The analysis conducted in this chapter does indicate that the *O. tauri* clock is more responsive to photoperiodic conditions, as it switches rapidly between the photoperiodic cycles, whereas *A. thaliana* has both a rapid and a delayed response. This may suggest that the additional loops of the *A. thaliana* clock do enable more subtle responses to changing photoperiodic conditions.

Chapter 9

Discussion

The work presented in this thesis investigates the endogenous rhythms of the plant circadian clock. The effects of these rhythms are observed at all levels of plant physiology. As introduced in Chapter 1, the identified clock network is formed of interlocking transcriptional/translational feedback loops but there is also substantial evidence which suggests that metabolic and post-translational components are involved in its regulation. Whilst the canonical clock components identified appear not to be conserved across taxa the modulators and regulators of these components, the kinases and phosphatases are. This has raised the question as to whether the kinases and phosphatases have a more predominant function in circadian timing.

This thesis has taken a number of approaches to investigate the mechanism and entrainment of the circadian clock. It has combined molecular biology and mathematical modelling to enable known components which affect clock regulation to be linked with the network. The work has also developed a platform for the identification of new clock components and regulatory mechanisms. The study has utilised three model organisms, *S. cerevisiae, A. thaliana* and *O. tauri.*

9.1 Synthetic biology

S. cerevisiae provided the framework for the investigation and characterisation of photoreceptors. Photoreception is involved in the entrainment of the circadian clock [71] and through the careful characterisation of photoreceptors in yeast they can now also be used in the entrainment of a synthetic clock network in *S. cerevisiae*. An entrainable synthetic clock would provide a mechanism to test the basic principles of entrainment of circadian rhythms, including the importance of directly coupling light signalling to the clock [75]. A number of synthetic

oscillator mechanisms have already been developed, but only one of these is in eukaryotic (mammalian) cells [317]. Most of the synthetic oscillators are based on a transcriptional/translational regulation mechanism. The simplest, and first, is the Goodwin oscillator which is formed of a single gene [318]. Whilst this mechanism can produce oscillations, when models are constrained to biologically relevant parameters the oscillations rapidly damp, this is because a one gene oscillator is highly sensitive to biological noise. More robust and reliable oscillations were observed with the designing, building and characterisation of the repressilators [319], gene networks which repress each components expression, and the repressilators with a positive feedback [318]. However, amplitude, period and the proportion of the bacterial population which showed oscillations varied. Currently the most robust bacterial oscillator is the Smolen oscillator [318], due to its feedback mechanism of having a two gene network with one gene promoting its own expression and that of the other gene and the second gene repressing its own expression and that of the other gene. This network structure has strong similarities to the plant circadian network with CCA1 functioning as a repressor [42]. The only eukaryotic oscillator is the Fussenegger oscillator [317] which is formed of sense-antisense transcript regulation. Notably no oscillator has yet been developed in yeast. This is relevant as yeast is a key tool in molecular biology due to its eukaryotic nature and relatively high level of simplification. Only one synthetic oscillator has been developed to incorporate metabolism [175]. This metabolic oscillator shows temperature compensation, a quality also identified in circadian clocks [176]. Yeast cells have also been identified to contain an oscillating mechanism based on metabolism [320] and so it may be easier to use this feature for the basis of a synthetic yeast oscillator.

Not many of the oscillator networks have been synchronised through external stimuli. One of the synthetic oscillator networks has been synchronised through quorum sensing [321]. Furthermore, most of the photoreceptor uses in synthetic biology has focused on phytochromes,

due to their light-switchability [197]. Again this characterisation has largely focused on bacterial hosts and linking light regulation to biochemical processes, such as light-controlled protein degradation. A BLUF-domain protein from *Rhoderbacter sphaeroides* has also been characterised for synthetic applications [322]. In mammalian cells it has been shown that the period of each cell is quite variable [314] and so synchronisation of a synthetic circadian oscillator would be essential for replication of the synchronised biological mechanism. The easiest mechanism of entrainment is through light treatment and therefore the suite of characterised photoreceptors detailed in Chapter 3 is of use to achieve this in synthetic networks.

9.2 *Arabidopsis thaliana*

Whilst it is known that the clock network entrains to light pulses the mechanism and pathways involved are unclear. EARLY FLOWERING 3 (ELF3) is part of one of the entrainment pathways and has been suggested to function as a zeitnehmer; repressing the action of light to the clock network in the evening [106]. A direct interaction with PHYB and ELF3 had been identified [80] but ELF3 also activated the expression of the light-inducible morning transcription factors *CCA1* and *LHY* [178]. Therefore, the pathway and function of ELF3 in the clock was ambiguous. Through experimentation and mathematical modelling the function of ELF3 was investigated (Chapter 4 and 5). It is proposed that ELF3 functions as a repressor to clock gene expression through its function as a modulator in the regulation of protein degradation. In particular, ELF3 associates with the promoter of *PRR9* and represses its expression, producing a double negative effect on the activation of *CCA1* and *LHY* (Chapter 4). However, this is not the only point of entry ELF3 has into the circadian mechanism as the work by Yu *et al* demonstrated [85]. ELF3 is regulated by the ubiquitin E3-ligase COP1 and both COP1 and ELF3 appeared to have a function in the regulation of GI protein stability.

This regulation was investigated through the comparison of a number of mathematical models and these support ELF3 having a central role in the regulation of GI. The model also suggests that ELF3 requires a higher rate of degradation than GI and that the peak time of GI is controlled through its interaction with ELF3 and COP1, rather than its interaction with ZTL. Interestingly, the observation that GI and COP1 do not form a dimer is supported through this analysis (Chapter 5). The model networks formed are simplifications of the biological processes. If the networks were to be developed further, rather than adding more protein species, it may be interesting to include more cellular dynamics, such as the sub-cellular localisation of the proteins. The modelling investigation strongly supports a role for ELF3 in protein degradation. This was tested experimentally through the inhibition of the 26S-proteasome with MG132. Without an active proteasome ELF3 formed a much less distinct speckle pattern within the nucleus and became more diffuse across the nuclear area (Chapter 5). This suggests that ELF3 is associating with an active proteasome when it forms the speckle structures and that this may be linked with ELF3's biological function in protein degradation.

The protein profile obtained for ELF3 levels from confocal microscope imaging are also of interest. This technique has a lot of potential as it will enable the continual imaging of protein levels over time. The timecourse obtained for ELF3 showed that the protein levels fluctuate more around the light:dark transition than anticipated from the lower time-resolution protein blots ([80] and Chapter 5). This could be interpreted that the regulation of ELF3 protein involves a number of factors including the light:dark cycle and circadian clock. The investigation of ELF3 function re-iterated that mathematical modelling is a powerful technique in understanding biological mechanisms. The ability to compare networks has given insight into the topology required for ELF3 and GI regulation which is not yet possible at the experimental level. Furthermore, the modelling of a protein only network in the plant circadian clock is unusual but will become more important for the understanding of the inherent complexity of the

post-translational clock network. Mathematical modelling has also been employed in the study of the circadian clock to help understand the increasing complexity associated with the *A. thaliana* interlocking feedback loops [45, 46, 47, 48]. However, this increasing complexity is also inhibiting the understanding of the clock network as it is easy to become lost in fine detail. Therefore, a simpler clock network was utilised; that found in the unicellular alga *Ostreococcus tauri*.

9.3 *Ostreococcus tauri*

The *O. tauri* circadian network was identified and initially characterised as the CCA1/TOC1 feedback loop [170]. From this its ease for genetic and pharmacological manipulation has made *O. tauri* a particularly useful tool in the study of clock mechanisms [53]. *O. tauri's* responses to pharmacological compounds, which have been verified in other species, have been tested and surprisingly, these compounds often had the same effects on the clock [53]. Further to this *O. tauri* could be used in the classical wedge experiments where it was shown that rhythmic transcription is not the driving force of cellular oscillations [53] and that protein degradation is essential for the maintenance of these rhythms, Chapter 6.

Using pharmacological and photoperiod manipulations it was identified that the protein degradation of one of the central clock components TOC1 is under a very low level of regulation by the clock network; its regulation is predominated by light to dark transitions (Chapter 6). This work supports the role of a more protein and metabolic dominated clock network such as that observed in *Synechococcus elongatus* [66, 67, 68]. In *S. elongatus* one of the central clock proteins, KaiC, total abundance is not under circadian regulation but is under light:dark control. Furthermore, the circadian rhythmicity is observed through the phosphorylation of this protein, as well as protein complex formation and ATP hydrolysis [323]. Phosphoylation regulation is quite possible for TOC1 and would be interesting to test.

In the *O. tauri* circadian network, the measured components, CCA1 and TOC1, do not always appear to be anticipating entrained conditions, at either the transcriptional or translational level (Chapter 8 and [168]). In fact, the clock network is responsive to changes in light condition and the oscillator changes phase accordingly (Chapter 8). This is unusual for circadian mechanism, and not observed for a number of the components in the *A. thaliana* network (Chapter 8). However, in the *A. thaliana* network some of the component's transcription do acutely respond to light:dark signals under photoperiodic conditions and so provides the clock network directly with light-signalling information (Chapter 8). This identifies that under photoperiodic conditions, the components measured in the two clock networks respond differently, most likely due to the different species requirements. *O. tauri* is an obligate photoautotroph whilst *A. thaliana* can survive for a period without light and requires seasonal information for the correct timing of flowering transition. It will be interesting to see if this is observed when post-translational markers are measured.

Work presented in [53] and Appendix A identifies an aspect of the circadian oscillator that is conserved from alga to mammals [140]. This is peroxiredoxin sulphonylation and strongly suggests that redox is an important mechanism for the regulation of the clock. This is supported by the effects of mitochondrial mutants on the *Neurospora* circadian clock [300]. To further investigate this, other redox-related compounds were tested and indeed, a number of them have effects on the clock network; as did the inhibition of phosphatases, histone acetylation and the photosynthetic chain (Chapter 7, Table 7.1). Together this indicates that the post-translational and cytosolic regulation of clock components is very important for the maintenance and regulation of rhythms.

One of the long-standing conceptual and practical problems relating to circadian oscillations is how the biological mechanism creates a 24 hour period. Transcription and translation of proteins could achieve this if some of the proteins were very stable, became spatially separate

from their downstream targets or went though many intermediate targets before affecting the circadian gene. That is for a transcriptional/translational loop to have a 24 hour period a mechanism of delay is required. This is reiterated by the short period oscillations observed in all transcriptional/translational synthetic oscillators built [318]. Phosphorylation in the cyanobacterial clock has been identified to occur with a ~24 hour periodicity and as a secondary modification phosphorylation is known to be kinetically tuneable, such as the rapid signalling phosphorylation (example [200]) and the long-term phosphorylation of proteins which is associated with memory [324]. In the *O. tauri* clock the inhibition of phosphatases significantly slowed the clock mechanism (Chapter 6), indicating that phosphorylation markers are strongly involved in the regulation of circadian period. Likewise, the inhibition of chromatin acetylation also dramatically slowed the clock [53] again suggesting this modification also has a role in controlling circadian period. Secondary modifications to the transcriptional/translational loops could be controlling clock period, and ultimately rhythmicity, in a more indirect manner than the phosphorylation of proteins.

To try and identify mechanisms which are involved in the regulation of the circadian clock in *O. tauri* a chemical screen of 1,600 compounds was conducted (Chapter 7). Initial analysis of this has identified a compound which targets chromatin regulation in yeast cells and potentially could be acting in the same pathway in *O. tauri* (Chapter 7).

Chemical screens in *O. tauri* have a number of features which are widely applicable. The protocol developed is semi-automated and enables the collection of quantitative data. This is not always possible with phenotype collection in plants and greatly increases the number of compounds available for screening. As a single-cell, with a thin cell wall, the compounds show effects very rapidly and at low doses. Therefore, *O. tauri* can be used in toxicity assays which have particular applications to the environment. Also, the effects of the pharmacological compounds in *O. tauri* are not complicated by cell-type specificity which is the case for multi-

cellular plant screens and for plant stem cell lines. Relating to this reduction in complexity, the subsequent characterisation and biological understanding may be easier in *O. tauri* as a compound which inhibits a specific type of enzyme in plants may be targeting a large protein family whereas in *O. tauri* the family is likely to be much smaller and therefore, theoretically, quicker to identify the target. However, the large genetic resources of *A. thaliana* will be useful in transferring this understanding to land plants. Characterisation in *A. thaliana* can then investigate cell and organ specificity as well as light signalling and environmental associated phenotypes. Linking to this the *O. tauri* cells are powerful in analysing biomolecular processes, such as the circadian clock, but not as useful for investigating processes which involve intercellular signalling, such as hormone trafficking [283]. The dose specificity, which is possible with chemical application, enables phenotypes to be identified in pathways where the genetic mutants are lethal. For the development of the chemical screen pipeline in *O. tauri* the data processing would need to become automated as this would not only enable the efficient identification of trends and hit compounds but also would remove bias in the selection of targets.

9.4 Circadian biology

The deduction of a network in plants which is sufficient for circadian oscillations remains a big challenge. At the time of the identification of the first clock mutants a molecular revolution was occurring which enabled the creation of transgenic organisms. With this the focus naturally became related to understanding the DNA/protein level of regulation. In plants the first clock mutants were identified through mutant screens for abnormal flowering patterns or gene expression. As such the genes identified are not only going to be related to the circadian mechanism but also to these particular outputs. Furthermore, in *A. thaliana* there is a high level of genetic redundancy where other similar proteins can assume the function of the mutated gene. Interestingly in other species these early screens identified a number of metabolic mutants, such

as the *tau* mutation in mice which is in Casein kinase II [1] and the mitochondrial and lipid synthesis mutations in *Neurospora* [300]. Through these genetic screens a large number of proteins involved in the plant clock mechanism were identified and characterised (Chapter 1). However, protein function remains largely unclear; it is still unknown, for example, how TOC1 functions or what the biochemical roles of GI or ELF4 are. From the large number of genes which have been identified to be involved with the generation of the circadian clock rhythm, linking them together to form an oscillating network has proved even more of a challenge. Currently, a three-loop model exists which incorporates post-translational regulation of TOC1 [48]. This model captures many of the experimental phenotypes (Chapter 1).

In all organisms studied the oscillator mechanism comprises of at least one negative feedback loop; however, only in *Synechococcus elongatus* has this been proven to be sufficient [66, 67, 68]. Furthermore, the sufficiency of this loop is at the level of orchestrated and controlled phosphorylation [67]. This is relevant as, in the *A. thaliana* network, total levels of transcript and more recently protein are measured to understand the circadian network. However, it may be the modifications to these proteins which are more revealing regarding circadian function. This is highlighted through the phosphorylational regulation in cyanobacteria [67] as well as the peroxiredoxin sulphonylation modification in *O. tauri* and human red blood cells [53, 140]. Certain 'central' components of the plant clock lack an identified biochemical mechanism (TOC1, ELF4, GI and PRR's), with their function possibly being at the level of protein regulation and phospho-carries. This is particularly relevant to the TOC1 and the PRR's which have homology to the bacterial his-asp phosphorelay signalling mechanisms, but the PRR's lack the phosphor accepting aspartate site [99]. It is already known that the PRR's become phosphorylated and this phosphorylation is important for their stability [156] but it may have another role in clock function.

The TTFL's are still important; from the breadth and depth of data it is clear that they have a substantial role in many aspects of circadian biology and the identification of a post-translational/ cytosolic oscillator would not render the transcriptional/translational oscillator obsolete. The inter-regulation could be similar to the regulation observed in cyanobacteria where the transcriptional/translational mechanism forms a slave oscillator to the protein post-translational oscillator [323]. Without the protein post-translational oscillator the transcriptional/ translational oscillator rapidly damps. However, the total levels of protein are obviously required for the post-translational oscillator. Therefore research into, splice variants [325], chromatin modification [21] and miRNA's [111] all provide important regulatory mechanisms to the clock.

In fact the identification of a post-translational/cytosolic oscillator may simply aid the understanding of the TTFL's as it may address some of the outstanding experimental observations. These include the resilience of TTFL to clamping expression of central genes and the lack of arrhythmia in a number of clock mutants [1]. The post-translational/cytosolic oscillator may also address some of the outstanding experimental results relating to metabolic mutants, such as the lipid mutants and the FRQ-less oscillators from *N. crassa* [300] as well as LIP1 and *tej* from *A. thaliana* [160, 148]. Coupling between the TTFL and post-translational/metabolic oscillator may also aid in the understanding of clock organisation. This includes the two clocks identified in the single cell of *L. polyedra* [131] as well as cell-specificity and co-ordination in *A. thaliana* [23, 130].

The identification of biochemical mechanisms involved with clock networks is increasingly suggesting that there are common processes involved in the generation of circadian rhythms. These included histone modification (CLOCK in mammals [31], JMJD5 in plants [149]), small metabolites (cAMP in mammals [173], cADPR in plants [174]), phosphorylation (BMAL in mammals [29], CCA1 in plants [10]), sulphonylation (peroxiredoxins in mammals and plants

[53, 140]) as well as the known transcription factors, detailed in Chapter 1. This evidence suggests the existence of a conserved aspect to the oscillator, originating from a common ancestor. As detailed above this conserved component appears to be more closely linked with metabolism, particularly redox, and protein regulation and will be an area of great research interest in the coming years.

Finally, understanding how the clock mechanism is entrained is important. Without this knowledge applying understanding of the clock network to practical situations is extremely hard as the phases of biological processes are guided through the entrainment of the clock. Light has a very important role in entrainment [70] but may not be exclusively acting through photoreceptor signalling mechanisms [75]. The high level of redundancy and the fact that a quadruple mutant in *phyA phyB cry1 cry2* [119] and the quintet mutant in *phyA phyB phyC phyD phyE* can still entrain [120], may suggest that other light-dependent mechanisms also link to the clock. Specifically this could be through the photosynthetic chain and redox state of plastoquinone. The relative importance of the entrainment signals, such as light, temperature and nutrients, is also an aspect which requires further investigation.

In plant circadian biology it will be important to understand how the oscillations are organised at the tissue and cell level and how they co-ordinate. Understanding this is, again, fundamental with respect to biological application. How does timing start? How is timing co-ordinated between different organs of different ages? Is this timing linked to senescence? And does the clock network remain the same in different aged tissues?

The work presented in this thesis has used a variety of techniques with the aim of adding to the understanding of the mechanism and entrainment of the plant circadian clock. As outlined above the work has added to the understanding of the function of ELF3 as well as further developed the use of *O. tauri* as a model organism in circadian biology. Through this, the work presented details an important role for a number of post-translational mechanisms in circadian

regulation. These post-translational mechanisms and integrating the role of metabolism to the circadian clock will be important in further understanding the clock mechanism.

Chapter 10

Bibliography

1. M. H. Hastings, E. S. Maywood, J. S. O'Neill. (2008). Cellular circadian pacemaking and the role of cytosolic rhythms. Current Biology 18, R805-R815
2. J. J. de Mairan. (1729). Observation botanique. Histoire de l'Academie Royale de Sciences (Paris), p. 35 (see Sleep, 2, 155-160, 1979, for English translation)
3. Z. Ni, E.-D. Kim, M. Ha, E. Lackey, J. Liu, Y. Zhang, Q. Sun, Z. J. Chen. (2009). Altered circadian rhythms regulate growth vigor in hybrids and allopolyploids. Nature 457, 327-331
4. R. Schaffer, N. Ramsay, A. Samach, S. Corden, J. Putterill, I. A. Carre, G. Coupland. (1998). The *late elongated hypocotyl* Mutation of *Arabidopsis* Disrupts Circadian Rhythms and the Photoperiodic Control of Flowering. Cell 93, 1219-1229
5. M. T. Zagotta, S. Shannon, C. I. Jacobs, D. R. Meeks-Wagner. (1992). Early-flowering mutants of *Arabidopsis thaliana.* Australian Journal of Plant Physiology, 19 411-418
6. T. P. Michael, C. R. McClung. (2003). Enhancer Trapping Reveals Widespread Circadian Clock Transcriptional Control in Arabidopsis. Plant Physiology 132, 629-639
7. S. L. Harmer, J. B. Hogenesch, M. Staume, H.-S. Chang, B. Han, T. Zhu, X. Wang, J. A. Kreps, S. A. Kay. (2000). Orchestrated Transcription of Key Pathways in *Arabidopsis* by the Circadian Clock. Science 290, 2110-2113
8. A. J. Millar and S. A. Kay (1991). Circadian control of CAB gene transcription and mRNA accumulation in *Arabidopsis.* Plant Cell 3, 541-550
9. A. J. Millar, I. A. Carre, C. A. Strayer, N.-H. Chua, S. A. Kay. (1995). Circadian clock mutants in *Arabidopsis* identified by luciferase imaging. Science 267, 1161-1163
10. X. Daniel, S. Sugano, E. M. Tobin. (2004). CK2 phosphorylation of CCA1 is necessary for its circadian oscillator function in *Arabidopsis.* PNAS 101, 3293-3297
11. P. Mas, W. Y. Kim, D. E. Somers, S. A. Kay. Targeted degradation of TOC1 by ZTL modulates circadian function in *Arabidopsis thaliana*. (2003) Nature 426, 567-570
12. P. S. Kerr, T. W. Rufty, S. C. Huber. (1985). Endogenous rhythms in photosynthesis, sucrose phosphate synthase activity, and stomatal resistance in leaves of soybean (*Glycine max* [L.] Merr.) Plant Physiology 77, 275-280
13. M. Brunner and M. Merrow. The green yeast uses its plant-like clock to regulate its

animal-like tail. (2008) Genes and Development 22, 825-831

14. M. Moulager, A. Monnier, B. Jesson, R. Bouvet, J. Mosser, C. Schwartz, L. Garnier, F. Corellou, F.-Y. Bouget. Light-Dependent Regulation of Cell Division in *Ostreococcus*: Evidence for a Major Transcriptional Input. (2007) Plant Physiology 144, 1360-1369
15. N. Sauerbrunn and N. L.Schlaich. (2004). PCC1: a merging point for pathogen defence and circadian signalling in Arabidopsis. Planta 18, 552-61
16. S. A. Finlayson, I.-J. Lee, P. W. Morgan. (1998). Phytochrome B and the regulation of circadian ethylene production in sorghum. Plant Physiology 116, 17-25
17. G. Ievinsh and O. Kreicbergs. (1992). Endogenous rhythmicity of ethylene production in growing intact cereal seedlings. Plant Physiology 100, 1389-1391
18. L. Jouve, T. Gaspar, C. Kevers, H. Greppin, R. D. Agosti. (1999). Involvement of indole-3-acetic acid in the circadian growth of the first internode of *Arabidopsis*. Planta 209, 136-42
19. L. Jouve, H. Greppin, R. D. Agosti. (1998). *Arabidopsis thaliana* floral stem elongation: evidence for an endogenous circadian rhythm. Plant Physiol. Biochem. 36, 469-72
20. M. F. Covington and S. L. Harmer. (2007). The Circadian Clock Regulates Auxin Signalling and Responses in *Arabidopsis.* PLoS Biology 5(8) DOI: 10.1371
21. M. Perales and P. Mas. (2007). A Functional Link between Rhythmic Changes in Chromatin Structure and the *Arabidopsis* Biological Clock. Plant Cell 19, 2111-2123
22. S. C. Thain, A. Hall, A. J. Millar. (2000). Functional independence of circadian clocks that regulate plant gene expression. Current Biology 10, 951-956
23. A. B. James, J. A. Monreal, G. A. Nimmo, C. L. Kelly, P. Herzyk, G. I. Jenkins, H. G. Nimmo. (2008). The Circadian Clock in *Arabidopsis* Roots Is a Simplified Slave Version of the Clock in Shoots. Science 322, 1832-183
24. www.wistep.wisc.edu for *A. thaliana* image
25. J. Love, A. N. Dodd, A. A. R. Webb. (2004). Circadian and Diurnal Calcium Oscillations Encode Photoperiodic Information in Arabidopsis. Plant Cell 16, 956-966
26. S. L. Harmer. The circadian system in higher plants. (2009) Annual Review of Plant Biology 60, 357-77
27. C. S. Pittendrigh. (1961). Circadian rhythms and circadian organisation of living systems. Cold Spring Harbour Symp. Quant. Biol. 25, 159
28. C. S. Pittendrigh. (1967). Circadian Systems I. the Driving Oscillation and Its Assay in *Drosophila pseudoobscura.* PNAS 58, 1762-1767

29. M. Gallego and D.M. Virshup. (2007). Post-translational modifications regulating the ticking of the circadian clock. Nature Reviews 8, 139-148
30. J. P. Etchegaray, C. Lee, P. A. Wade, S. M. Reppert. (2003). Rhythmic histone acetylation underlies transcription in the mammalian clock. Nature 421, 177-182
31. J. A. Ripperger, U. Schibler. (2006). Rhythmic CLOCK-BMAL binding to multiple E-box motifs drives circadian Dbp transcription and chromatin transitions. Nature Genetics 38, 369-374
32. W. Yu, H. Zheng, J. H. Houl, B. Dauwalder, P. E. Hardin. (2006). PER-dependent rhythms in CLK phosphorylation and E-box binding regulate circadian transcription. Genes and Development 20, 723-733
33. E. Malzahn, S. Ciprianidis, K. Kaldi, T. Schafmeier, M. Brunner. (2010). Photoadaptation in *Neurospora* by Competitive Interaction of Activating and Inhibitory LOV Domains. Cell 142, 762-772
34. M. H. Vitaterna, D. P. King, A. M. Chang, J. M. Kornhauser, P. L. Lowrey, J. D. McDonald, W. F. Dove, L. H.Pinto, F. W. Turek, J. S. Takahashi. (1994). Mutagenesis and mapping of a mouse gene, Clock, essential for circadian behaviour. Science 264, 719-725
35. R.Allada, N. E. White, W. V. So, J. C. Hall, M. Rosbash. (1998). A mutant *Drosphia* homolg of mammalian *clock* disrupts circadian rhythms and transcription of *period* and *timeless.* Cell 93, 791-804
36. M. A. Collett, J. C. Dunlap, J. J. Loros. (2001). Circadian clock-specific roles of the light response protein WHITW COLLAR-2. Mol Cell Biol 21, 2619-2628
37. J. P. DeBruyne, D. R. Weaver, S. M. Reppert. (2007). CLOCK and NPAS2 have overlapping roles in the suprachiasmatic circadian clock, Nature Neuroscience 10, 543-545
38. J. P. DeBruyne, D. R. Weaver, S. M. Reppert. (2007). Peripheral circadian oscillators require CLOCK. Current Biology 17, R538-539
39. J. P. Debruyne, E. Noton, C. M. Lambert, E. S. Maywood, D. R. Weaver, S. M. Reppert. (2006). A clock shock: mouse CLOCK is not required for circadian oscillator function. Neuron 50, 465-477
40. T. K. Sato, R. G. Yamada, H. Ukai, J. E. Baggs, L. J. Miraglia, T. J. Kobayashi, D. K. Welch, S. A. Kay, H. R. Ueda, J. B. Hogenesch. (2006). Feedback repression is required for mammalian circadian clock function. Nature Genetics 38, 312-319

41. B. Aronson, K. Johnson, J. J. Loros, J. C. Dunlap. (1994). Negative feedback defining a circadian clock: autoregulation in the clock gene frequency. Science 263, 1578-1584
42. Z.-Y. Wang and E. M. Tobin. (1998) Constitutive Expression of the *CIRCADIAN CLOCK ASSOCIATED 1(CCA1)* Gene Disrupts Circadian Rhythms and Suppresses Its Own Expression. Cell 93, 1207-1217
43. D. Alabadi, T. Oyama, M. J. Yanovsky, F. G. Harmon, P. Mas, S. A. Kay. (2001). Reciprocal Regulation between *TOC1* and *LHY/CCA1* within the *Arabidopsis* Circadian Clock. Science 293, 880-883
44. D. Somers, A. Webb, M. Pearson, S. A. Kay. (1998). The short period mutant, toc1-1, alters circadian clock regulation of multiple outputs throughout development in *Arabidopsis thaliana.* Development 125, 485-494
45. J. C. W. Locke, M. M. Southern, L. Kozma-Bognár, V. Hibberd, P. E. Brown, M. S. Turner, A. J. Millar. (2005). Extension of a genetic network model by iterative experimentation and mathematical analysis. Molecular Systems Biology, 1:13
46. J. C. W. Locke, L. Kozma-Bognar, P. D. Gould, B. Feher, E. Kevei, F. Nagy, M. S. Turner, A. Hall, A. J. Millar. (2006). Experimental validation of a predicted feedback loop in the multi-oscillator clock of Arabidopsis thaliana. Molecular Systems Biology, 2:59.
47. M. N. Zeilinger, E. M. Farre, S. R. Taylor, S. A. Kay, F. J. Doyle 3rd (2006). A novel computational model of the circadian clock in Arabidopsis that incorporates PRR7 and PRR9. Molecular Systems Biology, 2:58.
48. A. Pokhilko, S. K. Hodge, K. Stratford, K. Knox, K. D. Edwards, A. W. Thomson, T. Mizuno, A. J. Millar. (2010). Data assimilation constrains new connections and components in a complex, eukaryotic circadian clock model. Molecular Systems Biology, 6: 416
49. International Conference of Arabidopsis Research, 2010, Presentation.
50. S. P. Hazen, T. F. Schultz, J. L. Pruneda-Paz, J. O. Borevitz, J. R. Ecker, S. A. Kay. (2005). *LUX ARRHYTHMO* encodes a Myb domain protein essential for circadian rhythms. PNAS, 102 10387-10392
51. M. R. Doyle, S. J. Davis, R. M. Bastow, H. G. McWatters, L. Kozma-Bognar, F. Nagy, A. J. Millar, R. M. Amasino. (2002). The *ELF4* gene controls circadian rhythms and

flowering time in *Arabidopsis thaliana.* Nature 419, 74-77

52. L. Busino, F. Bassermann, A. Maiolica, C. Lee, P. M. Nolan, S. I. H. Godinho, G. F. Draetta, M. Pagano. (2007). SCF^{Fbxl3} Controls the Oscillation of the Circadian Clock by Directing the Degradation of Cryptochrome Proteins. Science 316, 900-904
53. J. S. O'Neill, G. van Ooijen, L. E. Dixon, C. Troein, F. Corellou, F. Bouget, A. B. Reddy, A. J. Millar. (2011). Circadian rhythms persist without transcription in a eukaryote. Nature 469, 554-558
54. A. Sehgal. (2008) Ac-ing the Clock. Neuron 57, 8-10
55. P. Mas. (2008). Circadian clock function in *Arabidopsis thaliana*: time beyond transcription. Trends in Cell Biology 18, 273-281
56. A. Mehra, C. L. Baker, J. J. Loros, J. C. Dunlap. (2009) Post translational modifications in circadian rhythms. Trends Biochemistry Sci 34, 483-490
57. C.-T. Tang, S. Li, C. Long, J. Cha, G. Huang, L. Li, S. Chen, Y. Liu. (2009). Setting the pace of the *Neurospora* circadian clock by multiple independent FRQ phosphorylation events. PNAS 106, 10722-10727
58. E. Y. Kim, K. Bae, F. S. Ng, N. R. J. Glossop, P. E. Hardin, I. Edery. (2002). *Drosophila* CLOCK protein is under posttranscriptional control and influences light-induced activity. Neuron 34, 69-81
59. Z. Yang and A. Sehgal. (2001). Role of molecular oscillations in generating behaviour rhythms in *Drosophila*. Neuron 29, 453-467
60. Y. Fujimoto, K. Yagita, H. Okamura. (2006). Does mPER2 protein oscillate without its coding mRNA cycling? Post-transcriptional regulation by cell clock. Genes Cells 11, 525-530
61. I. Yamanaka, S. Koinuma, Y. Shigeyoshi, Y. Uchiyama, K. Yagita. (2007). Presence of robust circadian clock oscillation under constitutive over-expression of mCry1 in rat-1 fibroblasts. FEBS Letters 581, 4098-4102
62. M. K. Christensen, G. Falkeid, J. J. Loros, J. C. Dunlap, C. Lillo, P. Ruoff. (2004). A Nitrate-Induced frq-Less Oscillator in Neurospora crassa. J Biol Rhythms 19, 280-286
63. P. L. Lakin-Thomas. (2006). Transcriptional Feedback Oscillators: Maybe, Maybe Not… Journal of Biological Rhythms 21, 83-92
64. C. Dibner, D. Sage, M. Unser, C. Bauer, T. d'Eysmond, F. Naef, U. Schibler. (2008). Circadian gene expression is resilient to large fluctuations in overall transcription rates. EMBO Journal 28, 123-134

65. T. V. Driessche. (1966). The role of the nucleus in the circadian rhythms of *Acetabularia mediterranea.* Biochimica et Biophysica Acta (BBA) 126, 456-470
66. M. J. Rust, J. S. Markson, W. S. Lane, D. S. Fisher, E. K. O'Shea. (2007). Ordered Phosphorylation Governs Oscillations of a Three-Protein Circadian Clock. Science 318, 809-812
67. M. Nakajima, K. Imai, H. Ito, T. Nishiwaki, Y. Murayama, H. Iwasaki, T. Oyama, T. Kondo. (2005). Reconstruction of circadian oscillation of cyanobacterial KaiC phosphorylation *in vitro.* Science 308, 414-415
68. J. Tomita, M. Nakajima, T. Kondo, H. Iwasaki. (2005) No transcription-translation feedback in circadian rhythm of kaiC phosphorylation. Science 307, 251-254
69. J. L. Pruneda-Paz, S. A. Kay. (2010). An expanding universe if circadian networks in higher plants. Trends in Plant Sciences 15, 259-265
70. P. A. Salome and C. R. McClung. (2005). What makes the Arabidopsis clock tick on time? A review on entrainment. Plant, Cell and Environment 28, 21-38
71. D. E. Somers, P. F. Devlin, S. A. Kay. (1998). Phytochromes and cryptochromes in the entrainment of the Arabidopsis circadian clock. Science 282, 1488-1490
72. P. F. Devlin and S. A. Kay. (2000). Crytochromes are required for phytochrome signalling to the circadian clock but not for rhythmicity. Plant Cell 12, 2499-2510
73. M. J. Yanovsky, M. A. Mazzella, G. C. Whitelam, J. J. Casal. (2001). Resetting of the circadian clock by phytochromes and cryptochromes in Arabidopsis. Journal of Biological Rhythms 16, 523-530
74. D. E. Somers, T. F. Schultz, M. Milnamow, S. A. Kay. (2000). *ZEITLUPE* encodes a novel clock-associated PAS protein from *Arabidopsis*. Cell 101, 319-329
75. N. B. Ivleva, T. Gao, A. C. LiWang, S. S. Golden. (2006). Quinone sensing by the circadian input kinase of the cyanobacterial circadian clock. PNAS 103, 17468-17473
76. C. Lin. (2000). Plant blue-light receptors. Trends in Plant Science 5, 337-42
77. D. E. Somers, W. Y. Kim, R. Geng. (2004). The F-Box protein ZEITLUPE confers dosage-dependent control on the circadian clock, photomorphogenesis, and flowering time. Plant Cell 16, 769-782
78. T. F. Schultz, T. Kiyosue, M. Yanovsky, M. Wada, S. A. Kay. (2001). A Role for LKP2 in the circadian clock of *Arabidopsis.* Plant Cell 13, 2659-2670
79. D. C. Nelson, J. Lasswell, L. E. Rogg, M. A. Cohen, B. Bartel. (2000). FKF1, a clock-controlled gene that regulates the transition to flowering in *Arabidopsis.* Cell 101, 331-

340

80. X. L. Liu, M. F. Covington, C. Fankhauser, J. Chory, D. R. Wagner. (2001). ELF3 Encodes a Circadian Clock-Regulated Nuclear protein That Functions in an Arabidopsis PHYB Signal Transduction Pathway. Plant Cell 13, 1293-1304
81. W.-Y. Kim, S. Fujiwara, S.-S. Suh, J. Kim, Y. Kim, L. Han, K. David, J. Putterill, H.G.Nam, D. E. Somers. (2007). ZEITLUPE is a circadian photoreceptor stabilized by GIGANTEA in blue light. Nature 449, 356-360
82. M. Sawa, D. A. Nusinow, S. A. Kay, T. Imaizumi. (2007). FKF1 and GIGANTEA Complex Formation Is Required for Day-Length Measurement in *Arabidopsis.* Science 318, 261-265
83. K. A. Oliverio, M. Crepy, E. L. Martin-Tryon, R. Milich, S. L. Harmer, J.Putterill, M. J. Yanovsky, J. J. Casal. (2007). GIGANTEA Regulates Phytochrome A-Mediated Photomorphogenesis Independently of Its Role in the Circadian Clock. Plant Physiology 144, 495-502
84. T. Kiba, R. Henriques, H. Sakakibara, N.-H. Chua. (2007). Targeted degradation of PSEUDO-RESPONSE REGULATOR 5 by an SCFZTL complex regulates clock function and photomorphogenesis in *Arabidopsis thaliana.* Plant Cell 19, 2516-2530
85. J.-W. Yu, V. Rubio, N.-Y. Lee, S. Bai, S.-Y. Lee, S.-S. Kim, L. Liu, Y. Zhang, M. L. Irigoyen, J. A. Sullivan, Y. Zhang, I. Lee, Q. Xie, N.-C. Paek, X. W. Deng. (2008). COP1 and ELF3 Control Circadian Function and Photoperiodic Flowering by Regulating GI Stability. Molecular Cell 32, 617-630
86. H. Wang, L-G Ma, J-M Li, H-Y Zhao, X. W. Deng (2001) Direct Interaction of *Arabidopsis* Cryptochromes with COP1 in Light Control Development. Science 294, 154-158
87. A. Baudry, S. Ito, Y. H. Song, A. A. Strait, T. Kiba, S. Lu, R. Henriques, J. L. Pruneda-Paz, N. H. Chua, E. M. Tobin, S. A. Kay, T. Imaizumi. (2010). F-Box Proteins FKF1 and LKP2 Act in Concert with ZEITLUPE to Control *Arabidopsis* Clock Progression. Plant Cell 22, 606-622
88. L. Han, M. Mason, E. P. Risseeuw, W. L. Crosby, D. E. Somers. (2004). Formation of an SCF^{ZTL} complex is required for proper regulation of circadian timing. Plant Journal 40, 291-301
89. R. Toth, E. Kevei, A. Hall, A. J. Millar, F. Nagy, L. Kozma-Bognar. (2001). Circadian clock regulated expression of phytochrome and cryptochrome genes in *Arabidopsis*

thaliana. Plant Physiology 127, 1607-1616

90. A. Hall, L. Kozma-Bognar, R. Toth, F. Nagy, A. J. Millar. (2001). Conditional circadian regulation of PHYTOCHROME A gene expression. Plant Physiology 127, 1808-1818
91. R. A. Sharrock, T. Clark. (2002). Patterns of expression and normalised levels of the five *Arabidopsis* phytochromes. Plant Physiology 130, 442-456
92. G. Toledo-Ortiz, E. Huq, P. H. Quail. (2003). The Arabidopsis basic/helix-loop-helix transcription factor family. Plant Cell 15, 1749-1770
93. F. Nagy, E. Schafer. (2000).Nuclear and cytosolic events of light-induced, phytochrome-regulated signalling in higher plants. EMBO Journal 19, 157-163
94. J. F. Martinez-Garcia, E. Huq, P. H. Quail. (2000). Direct targeting of light signals to a promoter-element bound transcription factor. Science 288, 859-863
95. B. Al-Sady, W. Ni, S. Kircher, E. Schafer, P. H, Quail. (2006). Photoactive Phytochrome induces rapid PIF3 phosphorylation prior to proteasome-mediated degradation. Molecular Cell 23, 439-446
96. H. Shen, L. Zhu, A. Castillon, M. Majee, B. Downie, E. Huq. (2008). Light-induced phosphorylation and degradation of the negative regulator PHYTOCHROME INTERACTING FACTOR 1 from *Arabidopsis* depend upon its direct physical interactions with photoactive phytochromes. Plant Cell 20, 1586-1602
97. Y. Shen, R. Khanna, C. M. Carle, P. H. Quail. (2007). Phytochrome induces rapid PIF5 phosphorylation and degradation in response to Red-light activation. Plant Physiology 145, 1043-1051
98. B. Al-Sady, E. A. Kikis, E. Monte, P. H. Quail. (2008). Mechanistic duality of transcription factor function in phytochrome signalling. PNAS 105, 2232-2237
99. E. M. Farre, S. L. Harmer, F. G. Harmon, M. J.Yanovsky, S. A. Kay. (2005). Overlapping and distinct roles of PRR7 and PRR9 in the Arabidopsis circadian clock. Current Biology 15, 47-54
100. E. M. Farre, S. A. Kay. (2007). PRR7 protein levels are regulated by light and the circadian clock in Arabidopsis. Plant Journal 52, 548-560
101. K. A. Franklin and G. C. Whitelam. (2005). Phytochromes and Shade-avoidance Responses in Plants. Annals of Botany 96, 169-175
102. E.-M. Josse, K. J. Halliday. (2010). Skotomophogenesis: The Dark Side of Light Signalling. Current Biology R1144-R1147
103. T. Yamashino, A. Matsushika, T. Fujimori, S. Sato, T. Kato, S. Tabata, T.

Mizuno. (2003). A link between circadian-controlled bHLH factors and the APRR1/TOC1 quintet in *Arabidopsis thaliana*. Plant Cell and Physiology 44, 619-629

104. A. Viczian, S. Kircher, E. Fejes, A. J. Millar, E. Schafer, L. Kozmar-Bognar, F. Nagy. (2005). Functional characterisation of *PHYTOCHROME INTERACTING FACTOR* 3 for the *Arabidopsis* circadian clockwork. Plant Cell Physiology 46, 1591-1602

105. T. Allen, A. Koustenis, G. Theodorou, D. E. Somers, S. A. Kay, G. C. Whitelam, P. F. Devlin. (2006). *Arabidopsis* FHY3 Specifically Gates Phytochrome Signalling to the Circadian Clock. Plant Cell 10, 2506-2516

106. H. G. McWatters, R. M. Bastow, A. Hall, A. J. Millar. (2000). The ELF3 *zeitnehmer* regulates light signalling to the circadian clock. Nature 408, 716-720

107. D. Staiger, L. Allenbach, N. Salathia, V. Fiechter, S. J. Davis, A. J. Millar, J. Chory, C. Frankhauser. (2003). The Arabidopsis SRR1 gene mediates phyB signalling and is required for normal circadian clock function. Genes and Development 17, 256-68

108. J.-Y. Kim, H.-R. Song, B. L. Taylor, I. A. Carre. (2003). Light-regulated translation mediates gated induction of the *Arabidopsis* clock protein LHY. EMBO Journal 22, 935-944

109. H. R. Song and I. A. Carre. (2005). DET1 regulates the proteosomal degradation of LHY, a component of the *Arabidopsis* circadian clock. Plant Molecular Biology 57, 761-771

110. E. Yakir, D. Hilman, M. Hassidim, R. M. Green. (2007). *CIRCADIAN CLOCK ASSOCIATED 1* Transcript Stability and the Entrainment of the Circadian Clock in Arabidopsis. Plant Physiology 145, 925-932

111. C. Sire, A. B. Moreno, M. Garcia-Chapa, J. J. Lopez-Moya, B. S. Segundo. (2009). Diurnal oscillation in the accumulation of *Arabidopsis* microRNAs, miR167, miR168, miR171 and miR398. FEBS Letters 583, 1039-1044

112. A. N. Dodd, J. Love, A. A. R. Webb. (2005). The plant clock shows its metal: circadian regulation of cytosolic free Ca^{2+}. Trends in Plant Sciences 10, 15-21

113. M. F. Covington, S. Panda, X. L. Liu, C. A. Strayer, D. R. Wagner, S. A. Kay. (2001). ELF3 Modulates Resetting of the Circadian Clock in Arabidopsis. Plant Cell 13, 1305-1315

114. E. L. Martin-Tryon, J. A. Kreps, S. L. Harmer. (2007). *GIGANTEA* Acts in Blue Light Signalling and Has Biochemically Separable Roles in Circadian Clock and

Flowering Time Regulation. Plant Physiology 143, 473-486

115. S. Daan. (1998) Colin Pittenridgh, Jurgen Aschoff, and the Natural Entrainement of Circadian Systems. Journal of Biological Rhythms 15, 195-207

116. E. Monte, J. M. Alonso, J. R. Ecker, Y. Zhang, X. Li, J. Young, S. Austin-Philips, P. H. Quail. (2003). Isolation and characterisation of phyC mutants in *Arabdiopsis* reveals complex crosstalk between phytochrome signalling pathways. Plant Cell 15, 1962-1980

117. M. Ahmad, J. A. Jarillo, O. Smirnova, A. R. Cashmore. (1998). The CRY1 Blue Light Photoreceptor of *Arabidopsis* Interacts with Phytochrome A In Vitro. Cell 1, 939-948

118. P. Mas, P. F. Devlin, S. Panda, S. A. Kay. (2000). Functional interaction of phytochrome B and cryptochrome 2. Nature 408, 207-211

119. M. J. Yanovsky, M. A. Mazzella, J. J. Casal. (2000). A quadruple photoreceptor mutant still keeps track of time. Current Biology 10, 1013-101

120. B. Strasser, M. Sanchez-Lamas, M. J. Yanovsky, J. J. Casal, P. D. Cerdan. (2010). *Arabidopsis thaliana* life without phytochromes. PNAS 107, 4776-4781

121. W.-Y. Kim, R. Geng, D. E. Somers. (2003). Circadian phase-specific degradation of the F-box protein ZTL is mediated by the proteosome. PNAS 100, 4933-4938

122. M. J. Gardner, K. E. Hubbard, C. T. Hotta, A. N. Dodd, A. A. R. Webb. (2006). How plants tell the time. Biochemical Journal 397, 15-24

123. N. A. Eckardt. (2005). Temperature Entrainment of the Arabidopsis Circadian Clock. Plant Cell 17, 645-647

124. P. A. Salome, D. Weigel and C. R. McClung. (2010) The Role of the Arabidopsis Morning Loop Components CCA1. LHY, PRR7 and PRR9 in Temperature Compensation. Plant Cell 22, 3650-3661

125. K. A. Kaczorowski and P. H. Quail. (2003). *Arabidopsis PSEUDO-RESPONSE REGULATOR 7* is a signalling intermediate in phytochrome-regulated seedling deetiolation and phasing of the circadian clock. Plant Cell 15, 2654-2665

126. T. Roenneberg and J. Rehman. Nitrate, a nonphotic signal for the circadian system. FASEB 10, 1443-1447

127. O. E. Blasing, Y. Gibbon, M. Gunther, M. Hohne, R. Morcuende, D. Osuna, O. Thimm, B. Usadel, W.-R. Scheible, M. Stitt. (2005). Sugars and Circadian Regulation

Make Major Contributions to the Global Regulation of Diurnal Gene Expression in *Arabidopsis*. Plant Cell 17, 3257-3281

128. H. Fukuda, N. Nakamichi, M. Hisatsune, H. Murase, T. Mizuno. (2007). Synchronization of Plant Circadian Oscillators with a Phase Delay Effect of the Vein Network. Physical Review Letters 99, 098102

129. J. Sai and C. H. Johnson (1999). Different circadian oscillators control Ca^{2+} fluxes and *Lhcb* gene expression. PNAS 96, 11659-11663

130. T. P. Michael, P. A. Salome, C. R. McClung. (2003). Two *Arabidopsis* circadian oscillators can be distinguished by differntial temperature sensitivity. PNAS 100, 6878-6883

131. T. Roenneberg, D. Morse. (1993). Two circadian oscillators in one cell. Nature 362, 362-364

132. C. Ramalho, J. Hastings, P. Colepicolo. Circadian Oscillation of Nitrate Reductase Activity in *Gonyaulax polyedra* Is Due to Changes in Cellular Protein Levels. (1995) Plant Physiology 107, 225-231

133. B. Wenden, L. Kozma-Bognar, K. D. Edwards, A. J. W. Hall, J. C. W. Locke, A. J. Millar. (2011). Light inputs shape the Arabidopsis circadian system. Plant Journal DOI: 10.1111

134. R. Rawat, J. Schwartz, M. A. Jones, I. Sairanen, Y. Cheng, C. R. Andersson, Y. Zhao, K. Ljung, S. L. Harmer. (2009). REVEILLE1 a Myb-like transcription factor, integrates the circadian clock and auxin pathways. PNAS 106, 16883-16888

135. F. C. Robertson, A. W. Skeffington, M. J. Gardner, A. A. R. Webb. (2008). Interactions between circadian and hormonal signalling in plants. Plant Molecular Biology 69, 419-427

136. A. N. Dodd, N. Salathia, A. Hall, E. Kevei, R. Toth, F. Nagy, J. M. Hibberd, A. J. Millar, A. A. R. Webb. (2005) Plant Circadian Clocks Increase Photosynthesis, Growth, Survival, and Competitive Advantage. Science 309, 630-633

137. R. M. Green, S. Tingay, Z.-Y. Wang, E. M. Tobin. (2002). Circadian Rhythms Confer a Higher Level of Fitness to Arabidopsis Plants. Plant Physiology 129, 576-584

138. N. Nakamichi, M. Kita, S. Ito, T. Yamashino, T. Mizuno. (2005). PSEUDO-RESPONSE REGULATORS, PRR9, PRR7 and PRR5, Together Play Essential Roles Close to the Circadian Clock of *Arabidopsis thaliana.* Plant Cell Physiology 46, 686-698

139. I. S. Booij-James, W. M. Swegle, M. Edelman, A. K. Mattoo. (2002). Phosphorylation of the D1 Photosystem II Reaction Center Protein Is Controlled by an Endogenous Circadian Rhythm. Plant Physiology 130, 2069-2075

140. J. S. O'Neill and A. B. Reddy. Circadian Clocks in Human Red Blood Cells. (2010) Nature 469, 498-503

141. A. R. Cashmore, J. A. Jarillo, Y. J. Wu, D. Liu. (1999). Cryptochromes: Blue Light Receptors for Plants and Animals. Science 284, 760-765

142. J. C. Dunlap, J. J. Loros, Y. Liu, S. K. Crosthwaite. (1999). Eukaryotic circadian systems: cycles in common. Genes to Cells 4, 1-10

143. M. W. Young, S. A. Kay. (2001). Time Zones: A Comparative Genetics of Circadian Clocks. Nature Reviews 2, 702-715

144. S. DasSarma, S. P. Kennedy, B. Berquist, W. V. Ng, N. S. Baliga, J. L. Spudich, M. P.Krebs, J. A. Eisen, C. H. Johnson, L. Hood. (2001). Genomic perspective on the photobiology of *Halobacterium* species NRC-1, a phototrophic, photoactive, and UV-tolerant haloarchaeon. Photosynthesis Research 70, 3-17

145. C. H. Johnson and S. S. Golden. (1999). Circadian programs in cyanobacteria: adaptiveness and mechanism. Annual Review of Microbiology 53, 389-409

146. V. Dvornyk, O. Vinogradova, E. Nevo. (2003). Origin and evolution of circadian clock genes in prokaryotes. PNAS 100, 2495-2500

147. M. Murakami, Y. Tago, T. Yamashino, T. Mizuno. (2007). Comparative overviews of clock-associated genes of *Arabidopsis thaliana* and *Oryza sativa*. Plant Cell Physiology 48, 110-121

148. S. Panda, G. G. Poirier, S. A. Kay. (2002). *tej* Defines a Role for Poly(ADP-Ribosyl)ation in Establishing Period Length of the *Arabidopsis* Circadian Oscillator. Cell 3, 51-61

149. M. A. Jones, M. F. Covington, L. DiTacchio, C. Vollmers, S. Panda, S. L. Harmer. (2010) Jumonji domain protein JMJD5 functions in both the plant and human circadian systems. PNAS 107, 21623-21628

150. J. Kim, Y. Kim, M. Yeom, J.-H. Kim, H. G. Nam. (2008) FIONA1 Is Essential for Regulating Period Length in the *Arabidopsis* Circadian Clock. Plant Cell 20, 307-319

151. Y. H. Song, S. Ito, T. Imaizumi. (2010). Similarities in the circadian clock and photoperiodism in plants. Current Opinion in Plant Biology 13, 594-603

152. A. Hall, R. M. Bastow, S. J. Davis, S. Hanano, H. G. McWatters, V. Hibberd, M. R. Doyle, S. Sung, K. J. Halliday, R. M. Amasino, A. J. Millar. (2003). The TIME FOR COFFEE Gene Maintains the Amplitude and Timing of Arabidopsis Circadian Clocks. Plant Cell 15, 2719-2729

153. L. E. Dixon, K. Knox, L. Kozma-Bognar, M. M. Southern, A. Pokhilko, A. J. Millar. (2011). Temporal repression of Core Circadian Gens is Mediated through EARLY FLOWERING 3 in Arabidopsis. Current Biology 21, 120-125

154. A. Helfer, D. A. Nusinow, B. Y. Chow, A. R. Gehrke, M. L. Bulyk, S. A. Kay. (2011). *LUX ARRHYTHMO* Encodes a Nighttime Repressor of Circadian Gene Expression in the *Arabidopsis* Core Clock. Current Biology 21, 126-133

155. Nakamichi, N., Kiba, T., Henriques, R., Mizuno, T., Chua, N.-H., Sakakibara, H., (2010). PSEUDO-RESPONSE REGULATORS 9, 7, and 5 Are Transcriptional Repressors in the *Arabidopsis* Circadian Clock. Plant Cell 22, 594-605

156. S. Fujiwara, L. Wang, L. Han, S. S. Suh, P. A. McClung, D. E. Somers. (2008). Post-translational regulation of the *Arabidopsis* circadian clock through selective proteolysis and phosphorylation of Pseudo-Response Regulator proteins. Journal Biological Chemistry 283, 23073-23083

157. A. Matsushika, S. Makino, M. Kojima, T. Mizuno. (2000). Circadian waves of expression of the APPR1/TOC1 family of pseudo-response regulators: Insight into the plant circadian clock. Plant Cell Physiology 41, 1002-1012

158. A. Para, E. M. Farre, T. Imaizumi, J. L. Pruneda-Paz, F. G. Harmon, S. A. Kay. (2007). PRR3 Is a Vascular regulator of TOC1 Stability in the *Arabidopsis* Circadian Clock. Plant Cell 19, 3462-3473

159. J. L. Pruneda-Paz, G. Breton, A. Para and S. A. Kay. (2009). A Functional Genomics Approach Reveals CHE as a Component of the *Arabidopsis* Circadian Clock. Science 323, 1481-1485

160. E. Kevei, P. Gyula, B. Feher, R. Toth, A. Viczian, S. Kircher, D. Rea, D. Dorjgotov, E. Schafer, A. J. Millar, L. Kozma-Bognar, F. Nagy. (2007). *Arabidopsis thaliana* Circadian Clock Is Regulated by the Small GTPase LIP1. Current Biology 17, 1456-1464

161. M. Murakami-Kojima *et al* (2002). The APRR3 component of the clock-associated APRR1/TOC1 quintet is phosphorylated by a novel protein kinase belonging

to the WNK family, the gene for which is also transcribed rhythmically in *Arabidopsis thaliana*. Plant Cell Physiology 43, 675-683

162. B. Xu, J. M. English, J. L. Willsbcher, S. Stippec, E. J. Goldsmit, M. H. Cobb. (2000). WNK1, a novel mammalian serine/threonine protein kinase lacking the catalytic lysine in subdomain II. Journal of Biological Chemistry 275, 16795-16801

163. N. Nakamichi, M. Murakami-Kojima, E. Sato, Y. Kishi, T. Yamashino, T. Mizuno. Compilation and Characterisation of a Novel WNK Family of Protein Kinases in *Arabidopsis thaliana* with Reference to Circadian Rhythms. Biosci. Biiotechnol. Biochem. 66, 2429-2436

164. K. David, U. Armbruster, N. Tama, J. Putterill (2006) *Arabidopsis* GIGANTEA protein is post-transcriptionally regulated by light and dark. FEBS Letters 580, 1193-1197

165. E. M. Farre and S. A. Kay. (2007). PRR7 protein levels are regulated by light and the circadian clock in *Arabidopsis*. Plant Journal 52, 548-560

166. S. Ito, N. Nakamichi, T, Kiba, T. Yamashino, T.Mizuno. (2007). Rhythmic and light-inducible appearance of clock-associated pseudo-response regulator protein PRR9 through programmed degradation in the dark in *Arabidopsis thaliana.* Plant Cell Physiology 48, 1644-1651

167. C. J. Doherty and S. A. Kay. (2010). Circadian Control of Global Gene Expression Patterns. Annual Review of Genetics 44, 419-44

168. C. Troein, F. Corellou, L. E. Dixon, G. Van Ooijen, J. S. O'Neill, F.-Y. Bouget, A. J. Millar. (2011). Multiple light inputs to a simple clock circuit allow complex biological rhythms. Plant Journal 66, 375-385

169. E. Derelle, C. Ferraz, S. Rombaauts, P. Rouze *et al.* Genome analysis of the smallest free-living eukaryote *Ostreococcus tauri* unveils many unique features. (2006) PNAS 103, 11647-11652

170. F. Corellou, C. Schwartz, J.-P. Motta, E. B. Djouani-Tahri, F. Sanchez, F.-Y. Bouget. Clocks in the Green Lineage: Comparative Functional Analysis of the Circadian Architecture of the Picoeukaryote *Ostreococcus*. (2009) Plant Cell 21, 3436-3449

171. Q. Thommen, B. Pfeuty, P.-E. Morant, F. Corellou, F.-Y. Bouget, M. LeFranc. (2010). Robustness of Circadian Clocks to Daylight Fluctuations: Hints from the Picoeucaryote *Ostreococcus tauri*. PLoS Computational Biology 6(11): e1000990

172. F. Zhang, L.-P. Wang, E. S. Boyden, K. Deisseroth. (2006). Channelrhodopsin-2 and optical control of excitable cells. Nature Methods 3, 785-792

173. J. S. O'Neill, E. S. Maywood, J. E. Chesham, J. S. Takahashi, M. H. Hastings. (2008). cAMP-Dependent Signalling as a Core Component of the Mammalian Circadian Pacemaker. Science 320, 949-953

174. A. N. Dodd, M. J. Gardner, C. T. Hotta, K. E. Hubbard, N. Dalchau, J. Love, J. M. Assie, F. C. Robertson, M. K. Jakobsen, J. Goncalves, D. Sanders, A. A. Webb. (2007). The Arabidopsis circadian clock incorporates a cADPR-based feedback loop. Science 318, 1789-92

175. E. Fung, W. W. Wong, J. K. Suen, T. Butler, S. Gu Lee, J. C. Liao. (2005). A synthetic gene-metabolic oscillator. Nature 435, 118-122

176. S. Portoles and P. Mas. (2010). The functional interplay between protein kinase CK2 and CCA1 transcriptional activity is essential for clock temperature compensation in Arabidopsis. PLoS Genet 6(11):e1001201

177. A. Mehra, M. Shi, C. L. Baker, H. V. Colot, J. J. Loros, J. C. Dunlap. (2009). A role for casein kinase 2 in the mechanism underlying circadian temperature compensation. Cell 137, 749-760

178. E. A. Kikis, R. Khanna, and P. H. Quail. (2005). ELF4 is a phytochrome-regulated component of a negative-feedback loop involving the central oscillator components CCA1 and LHY. Plant Journal 44, 300-313

179. R. Yoshida, R. Fekih, S. Fujiwara, A. Oda, K. Miyata, Y. Tomozoe, M. Nakagawa, K. Niinuma, K. Hayashi, H. Ezura, G. Coupland, T. Mizoguchi. (2009). Possible role of EARLY FLOWERING 3 (ELF3) in clock-dependent floral regulation by SHORT VEGETATIVE PHASE (SVP) in *Arabidopsis thaliana*. New Phytologist, 182 838-850

180. T. Murashige and F. Skoog. (1962). A revised medium for rapid growth and bioassays with tobacco tissue cultures. Physiological Plant 15(3): 473-497.

181. H. G. McWatters, E. Kolmos, A. Hall, M. R. Doyle, R. M. Amasino, P. Gyula, F. Nagy, A. J. Millar, S. J. Davis. (2007). *ELF4* Is Required for Oscillatory Properties of the Circadian Clock. Plant Physiology 144, 391-401

182. K. D. Edwards, O. E. Akman, K. Knox, P. J. Lumsden, A. W. Thomson, P. E. Brown, A. Pokhilko, L. Kozma-Bognar, F. Nagy, D. A. Rand, A. J. Millar. (2010).

Quantitative analysis of regulatory flexibility under changing environmental conditions. Molecular Systems Biology 6, 424 DOI: 10.1038

183. K. Richardson, S. Fowler, C. Pullen, C. Skelton, B. Morris, J. Putterill. (1998). T-DNA tagging of a flowering-time gene and improved gene transfer by *in planta* transformation of *Arabidopsis.* Austrailian Journal of Plant Physiology 25, 125-130

184. S. Fowler, K. Lee, H. Onouchi, A. Samach, K. Richardson, B. Morris, G. Coupland, J.Putterill. (1999). *GIGANTEA*: a circadian clock-controlled gene that regulates photoperiodic flowering in *Arabidopsis* and encodes a protein with several possible membrane-spanning domains. EMBO Journal 18, 4679-4688

185. K. A. Hicks, T. A. Albertson, D. R. Wagner. (2001). EARLY FLOWERING 3 Encodes a Novel Protein That Regulates Circadian Clock Function and Flowering in Arabidopsis. Plant Cell 13, 1281-1292

186. M. M. Southern, A. J. Millar. (2005). Circadian genetics in the model higher plant, *Arabidopsis thaliana.* Methods Enzymology 393, 23-35

187. W. S. Rasband. ImageJ, U. S. National Institutes of Health, Bethesda, Maryland, USA, http://rsb.info.nih.gov/ij/, 1997-2009

188. J. Sambrook and D. W. Russell. Molecular Cloning, A Laboratory Manual. Third Edition, CSHL Press

189. O. J. Marshall. (2004). PerlPrimer: cross-platform, graphical primer design for standard, bisulphite and real-time PCR. Bioinformatics 20, 2471-2472

190. R. R. L. Guillard. (1975). Culture of phytoplankton for feeding marine invertebrates. pp 26-60. *In* W. L. Smith and M. H. Chanley (Eds.) *Culture of Marine Invertebrate Animals*. Plenum Press, New York, USA.

191. R. R. L. Guillard and J. H. Ryther. (1962). Studies of marine planktonic diatoms. I. *Cyclotella nana* Hustedt and *Detonula confervacea* Cleve. Canadian Journal of Microbiology 8, 229-239.

192. M. D. Keller and R. R. L. Guillard. (1985). Factors significant to marine diatom culture. pp. 113-6. *In* D. M. Anderson, A. W. White and D. G. Baden. (eds.) *Toxic Dinoflagellates*. Elsevier, New York.

193. M. D. Keller, R. C. Selvin, W. Claus and R. R. L. Guillard. (1987). Media for the culture of oceanic ultraphytoplankton. Journal of Phycology 23, 633-638.

194. E. Rosato, V. Codd, G. Mazzotta, A. Piccin, M. Zordan, R. Costa, C. P. Kyriacou. (2001) Light-dependent interaction between Drosophila CRY and the clock protein PER mediated by the carboxy terminus of CRY. Current Biology 11, 909-917

195. S. Alberti, A. D. Gitler, S. Lindquist. (2007). A suite of gateway cloning vectors for high-throughput genetic analysis in *Saccharomyces cerevisiae.* Yeast 24, 913-919

196. D. Dimberger and K. Seuwen. (2007) Signaling of Human Frizzled Receptors to the Mating Pathway in Yeast. PLOS One 2, 9

197. O. Sorokina, A. Kapus, K. Terecskei, L. E. Dixon, L. Kozma-Bognar, F. Nagy, A. J. Millar. (2009). A switchable light-input, light-output system modelled and constructed in yeast. Journal of Biological Engineering 3, 15

198. A. J. W. Hall and H. G.McWatters (Eds), (2005). Endogenous Plant Rhythms. Annual Plant Reviews, Volume 21, Wiley-Blackwell

199. S. Fields and O. Song. (1989). A novel genetic system to detect protein-protein interactions. Nature 340, 245-246

200. B. Kofahl and E. Klipp. (2004). Modelling the dynamics of the yeast pheromone pathway. Yeast 21, 831-850

201. S. Rupp. (2003). *LacZ* assays in yeast. Methods in Enzymology 350, 112-131

202. Biobricks Foundation www.bbf.openwetware.org (Correct 25/01/11)

203. N. C. Rockwell, Y. S. Yu, J. C. Lagarias. (2006). Phytochrome structure and signalling mechanisms. Annual Review of Plant Biology 57, 837-858

204. A. Castillon, H. Shen, E. Huq. (2007). Phytochrome Interacting Factors: central players in phytochrome-mediated light signalling networks. Trends in Plant Sciences 12, 514-521

205. A. Hiltbrunner, A. Viczian, E. Bury, A. Tscheuschler, S. Kircher, R. Toth, A. Honsberger, F. Nagy, C. Fankhauser, E. Schafer. (2005). Nuclear accumulation of the phytochrome A photoreceptor requires FHY1. Current Biology 15, 2125-2130

206. A. Hiltbrunner, A. Tscheuschler, A. Viczian, T. Kunkel, R. S. Kircher, E. Schafer. (2006). FHY1 and FHL act together to mediate nuclear accumulation of the phytochrome A photoreceptor. Plant Cell and Physiology 47, 1023-1034

207. S. Shimizu-Sato, E. Huq, J. M. Tepperman, P. H. Quail. (2000). A light-switchable gene promoter system. Nature Biotechnology 20, 1041-1044

208. D. W. Leung, C. Otomo, J. Chory, M. K. Rosen. (2008). Genetically encoded photoswitching of actin assembly through the Cdc42-WASP-Arp2/3 complex pathway. PNAS 105, 12797–12802.

209. C. Lin and T. Todo. (2005). The Cryptochromes. Genome Biology 6, 220

210. H. S. Seo, E. Watanabe, S. Tokutomi, A. Nagatani, N. H. Chua. (2004). Photoreceptor ubiquitination by COP1 E3 ligase desensitizes phytochrome A signalling. Genes and Development 18, 617-622

211. G. Ladds, A. Goddard, J. Davey. (2005). Functional analysis of heterologous GPCR signalling pathways in yeast. Trends in Biotechnology 23, 7

212. I. Provencio, G. Jiang, W. J. De Grip, W. P. Hayes, M. D. Rollag. (1998). Melanopsin: An opsin in melanophores, brain and eye. PNAS 95, 340-345

213. X. Qui, T. Kumbalasiri, S. M. Carlson, K. Y. Wong, V. Krishna, I. Provencio, D. Berson. (2005). Induction of photosensitivity by heterologous expression of melanopsin. Nature 433, 745-749

214. S. Panda, T. K. Sato, A. M. Castrucci, M. D. Rollag, W. J. DeGrip, J. B. Hogenesch, I. Provencio, S. A. Kay. (2002). Melanopsin (Opn4) Requirement for Normal Light-Induced Circadian Phase Shifting. Science 298, 2213-2216

215. S. Panda, S. K. Nayak, B. Campo, J. R. Walker, J. B. Hogenesch, T. Jegla. (2005). Illumination of the Melanopsin Signalling pathway. Science 307, 600-604

216. A. J. Brown, S. L. Dyos, M. S. Whiteway, J. H. M. White, M.-A. E. A. Watson, M. Marzioch, J. J. Clare, D. J. Cousens, C. Paddon, C. Plumpton, M. A. Romanos, S. J. Dowell. (2000). Functional coupling of mammalian receptors to the yeast mating pathway using novel yeast/mammalian G protein α-subunit chimeras. Yeast 16, 11-22

217. G. Nagel, D. Ollig, M. Fuhrmann, S. Kateriya, A. M. Musti, E. Bamberg, P. Hegemann. (2002). Channelrhodopsin-1: A Light-Gated Proton Channel in Green Algae. Science 296, 2395-2398

218. G. Nagel, T. Szellas, W. Huhn, S. Kateriya, N. Adeishvili, P. Berthold, D. Ollig, P. Hegemann, E. Bamberg. (2003). Channelrhodopsin-2, a directly light-gated cation-selective membrane channel. PNAS 100, 13940-13945

219. J. Y. Lin. (2010). A User's Guide to Channelrhodopsin Variants: Features, Limitations and Future Developments. Exp Physiol doi:10.1113

220. O. P. Ernst, P. A. Sanchez Murcia, P. Daldrop, S. P. Tsunoda, S. Kateriya, P. Hegemann. (2008). Photoactivation of Channelrhodopsin. Journal of Biological Chemistry 283, 1637-1643

221. N. L. Novère, M. Hucka, H. Mi, S. Moodie, F. Schreiber, A. Sorokin, E. Demir, K. Wegner, M. I. Aladjem, S. M. Wimalaratne *et al.* (2009). The Systems Biology Graphical Notation. Nature Biotechnology. 27, 735-741.

222. S. Madathil, G. Furlinski, K. Fahmy. (2006). Structure and pH sensitivity of the transmembrane segment 3 of rhodopsin. Biopolymers 82, 329-333

223. L. Li, J. C. Lagarias. (1994). Phytochrome assembly in the living cells of the yeast *Saccharomyces cerevisiae.* PNAS 91, 12535-12539

224. V. Sineschchekov, L. Hennig, T. Lamparter, J. Hughes, W. Gartner, E. Schafer. (2001). Recombinant Phytochrome A in Yeast Differs by its Spectroscopic and Photochemical Properties from the Major phyA' and is close to the Minor phyA'': Evidence for Posttranslational Modification of the Pigment in Plants. Photochemistry and Photobiology 73, 692-696

225. L. Hennig and E. Schafer. (2001). Both subunits of the dimeric plant photoreceptor phytochrome require chromophore for Pfr stability. Journal of Biological Chemistry 276, 7913-7918

226. T. Kunkel, G. Neuhaus, A. Batschauer, N.-H. Chua, E. Schafer. (1996). Functional analysis of yeast-derived phytochrome A and B phycocyanobilin adducts. Plant Journal 10, 625-636

227. T. Kunkel, V. Speth, C. Buche, E. Schafer. (1995). In vivo characterisation of Phytochrome-Phycocyanobilin Adducts in Yeast. Journal of Biological Chemistry 270, 20193-20200

228. D. A. Drubin, J. C. Way, P. A. Silver. (2007). Designing biological systems. Genes and Development 21, 242-254

229. K. A. Hicks, A. J. Millar, I. A, Carre, D. E. Somers, M. Straume, D. R. Meeks-Wagner, S. A. Kay. (1996). Conditional Circadian dysfunction of the Arabidopsis early-flowering 3 Mutant. Science, 274 790-792

230. M. T. Zagotta, K. A. Hicks, C. I. Jacobs, J. C. Young, R. P. Hangarter, D. R. Meeks-Wagner. (1996). The *Arabidopsis* ELF3 gene regulates vegetative photomorphogenesis and the photoperiodic induction of flowering. Plant Journal, 10 691-702

231. M. P. Coluccio, S. E. Sanchez, L. Kasulin, M. J. Yanovsky, J. F. Botto. (2010). Genetic mapping of natural variation in a shade avoidance response: *ELF3* is the candidate gene for a QTL in hypocotyls growth regulation. Journal of Experimental Botany doi 10.1093/jxb/erq253

232. J. M. Jimenez-Gomez, A. D. Wallace, J. N. Maloof. Network Analysis Identifies *ELF3* as a QTL for the Shade Avoidance Response in Arabidopsis. PLoS Genetics 6:9

233. B. Thines and F. G. Harmon. (2010). Ambient temperature response establishes ELF3 as a required component of the core *Arabidopsis* circadian clock. PNAS 107, 3257-3262

234. B. Stasser, M. J. Alvarez, A. Califano, P. D. Cerdan. (2009). A complementary role for ELF3 and TFL1 in the regulation of flowering time by ambient temperature. Plant Journal 58, 629-640

235. M. J. Dowson-Day and A. J. Millar. (1999). Circadian dysfunction causes aberrant hypocotyls elongation patterns in Arabidopsis. Plant Journal 17, 63-71

236. P. D. Gould, P. Diaz, C. Hogben, J. Kusakina, R. Salem, J. Hartwell, A. Hall. (2009). Delayed fluorescence as a universal tool for the measurement of circadian rhythms in higher plants. Plant Journal 58, 893-901

237. T. Mizoguchi, L. Wright, S. Fujiwara, F. Cremer, K. Lee, H. Onouchi, A. Mouradov, S. Fowler, H. Kamada, J. Putterill, G. Coupland. (2005). Distinct Roles of GIGANTEA in Promoting Flowering and Regulating Circadian Rhythms in Arabidopsis. Plant Cell 17, 2255-2270

238. Y. Niwa, S. Ito, N. Nakamichi, T. Mizoguchi, K. Niinuma, T. Yamashino, T. Mizuno. (2007). Genetic Linkages of the Circadian Clock-Associated Genes, TOC1, CCA1 and LHY, in the Photoperiodic Control of Flowering Time in Arabidopsis thaliana. Plant and Cell Physiology 48: 925-937

239. S. Fujiwara, A. Oda, R. Yoshida, K. Niinuma, K. Miyata, Y. Tomozoe, T. Tajima, M. Nakagawa, K. Hayashi, G. Coupland, T. Mizoguchi. (2008). Circadian Clock Proteins LHY and CCA1 Regulate SVP Protein Accumulation to Control Flowering in *Arabidopsis.* Plant Cell 20, 2960-2971

240. J. D. Salazar, T. Saithong, P. E. Brown, J. Forman, J. C. W. Locke, K. J. Halliday, I. A. Carre, D. A. Rand, A. J. Millar. (2009). Prediction of Photoperiodic Regulators from Quantitative Gene Circuit Models. Cell 139, 1170-1179

241. C. J. Tomlin and J. D. Axelrod. (2007). Biology by numbers: mathematical modelling in developmental biology. Nature Review Genetics 8, 331-340

242. R. J. Deshaies and X.-W. Deng. (2000). COP1 patrols the night beat. Nature Cell Biology 2, E102-E104

243. C. S. Hardtke and X.-W. Deng. (2000). The cell biology of COP/DET/FUS proteins: Regulating proteolysis in photomorphogenesis and beyond? Plant Physiology 124, 1548-1557

244. J. A. Kreps, Y. Wu, H.-S. Chang, T. Zhu, X. Wang, J. F. Harper. (2002). Transcriptome Changes for Arabidopsis in Response to Salt, Osmotic, and Cold Stress. Plant Physiology 130, 2129-2141

245. C. Strayer, T. Oyama, T. F. Schultz, R. Ramen, D. E. Somers, P. Mas, S. Panda, J. A. Kreps, S. A. Kay. (2000). Cloning of the *Arabidopsis* Clock Gene *TOC1*, an Autoregulatory Response Regulator Homolog. Science 289, 768-771

246. R. Yamaguchi, M. Nakamura, N. Mochizuki, S. A. Kay, A. Nagatani. (1999). Light-dependent Translocation of a Phytochrome B-GFP Fusion Protein to the Nucleus in Transgenic *Arabidopsis.* Journal of Cell Biology 145, 437-445

247. L, Kim, S. Kircher, R. Toth, E. Adam, E. Schafer, F. Nagy. (2000). Light induced nuclear import of phytochrome A-GFP fusion proteins is differentially regulated in transgenic tobacco and *Arabidopsis.* Plant Journal 22, 125-133

248. D. Bauer, A. Viczian, S. Kircher, T. Nobis, R. Nitschke, T. Kunkel, K. C. S. Panigrahi, E. Adam, E. Fejes, E. Schafer, F. Nagy. (2004). Constitutive Photomorphogenesis 1 and Multiple Photoreceptors Control Degradation of Phytochrome Interacting Factor 3, a Transcription Factor Required for Light Signaling in Arabidopsis. Plant Cell 16, 1433-1445

249. M. Chen, R. M. Galvao, M. Li, B. Burger, J. Bugea, J. Bolado, J. Chory. (2010). *Arabidosis HEMERA/pTAC12* initiates photomorphogenesis by phytochromes. Cell 141, 1230-1240

250. L.-H. Ang, S. Chattopadhyay, N. Wei, T. Oyama, K. Okada, A. Batschauer, X.-W. Deng. (1998). Molecular Interaction between COP1 and HY5 Defines a Regulatory Switch for Light Control of *Arabidopsis* Development. Cell 1, 213-222

251. M. G. Stacey, S. N. Hicks, A. G. von Arnim. (1999). Discrete Domains Mediate the Light-Responsive Nuclear and Cytoplasmic Localisation of Arabidopsis COP1. Plant Cell 11, 349-363

252. S. Datta, G. H. C. M. Hettiarachchi, X.-W. Deng, M. Holm. (2006). *Arabidopsis* CONSTANS-LIKE3 Is a Positive Regulator of Red Light Signaling and Root Growth. Plant Cell 18, 70-84

253. P. Leivar, E. Monte, B. Al-Sady, C. Carle, A. Storer, J. M. Alonso, J. R. Ecker, P. H. Quail. (2008). The *Arabdiopsis* Phytochrome-Interacting Factor PIF7, Together with PIF3 and PIF4, Regulates Responses to Prolonged Red Light by Modulating phyB Levels. Plant Cell 20, 337-352

254. S. H. Hong, H. J. Kim, J. S. Ryu, H. Choi, S. Jeong, J. Shin, G. Choi, H. G. Nam (2008). CRY1 inhibits COP1-mediated degradation of BIT1, a MYB transcription factor, to activate blue light-dependent gene expression in Arabidopsis. Plant Journal 55, 361-371

255. X. Yu, R. Sayegh, M. Maymon, K. Warpeha, J. Klejnot, H.Yang, J. Huang, J. Lee, L. Kaufman, C. Lin. (2009). Formation of Nuclear Bodies of *Arabidopsis* CRY2 in Response to Blue Light Is Associated with Its Blue Light-Dependent Degradation. Plant Cell 21, 118-130

256. S. Datta, H. Johansson, C. Hettiarachchi, M. L. Irigoyen, M. Desai, V. Rubio, M. Holm. (2008). LZF1/SALT TOLERANCE HOMOLOG3, an *Arabidopsis* B-Box Protein Involved in Light-Dependent Development and Gene Expression, Undergoes COP1-Mediated Ubiquitination. Plant Cell 20, 2324-2338

257. S. Datta, C. Hettiarachchi, H. Johansson, M. Holm. (2007). SALT TOLERANCE HOMOLOG2, a B-Box Protein in *Arabidopsis* That Activates Transcription and Positively Regulates Light-Mediated Development. Plant Cell 19, 3242-3255

258. K. Marrocco, Y. Zhou, E. Bury, M. Dieterle, M. Funk, P. Genschik, M. Krenz, T. Stolpe, T. Kretsch. (2006). Functional analysis of EID1, an F-box protein involved in phytochrome A-dependent light signal transduction. Plant Journal 45, 423-438

259. M. Ballesteros, C. Bolle, L. M. Lois, J. M. Moore, J.-P. Vielle-Calzada, U. Grossniklaus, N.-H. Chua. (2001). LAF1, a MYB transcription activator for phytochrome A signalling. Genes and Development 15, 2613-2625

260. X. C. Zhang and S. M. Mount. (2009). Two Alternatively Spliced Isoforms of the Arabidopsis SR45 Protein Have Distinct Roles during Normal Plant Development. Plant Physiology 150, 1450-1458

261. O. A. Koroleva, G. Calder, A. F. Pendle, S. H. Kim, D. Lewandowska, C. G. Simpson, I. M. Jones, J. W. S. Brown, P.J. Shaw. (2009). Dynamic Behaviour of *Arabidopsis* elF4A-III, Putative Core Protein of Exon Junction Complex: Fast Relocation to Nucleolus and Splicing Speckles under Hypoxia. Plant Cell 21, 1592-1606

262. I. C. Jang, J. Y. Yang, H. S. Seo, N. H. Chua. (2005) HFR1 is targeted by COP1 E3 ligase for post-translational proteolysis during phytochrome A signaling. Genes and Development 19, 593-602

263. S. Laubinger, K. Fittinghoff, U. Hoecker. (2004) The SPA quartet: a family of WD-repeat proteins with a central role in suppression of photomorphogenesis in Arabidopsis. Plant Cell 16, 2293-2306

264. D. Bauer, A. Viczián, S. Kircher, T. Nobis, R. Nitschke, T. Kunkel, K. C. Panigrahi, E.Adám, E. Fejes, E. Schäfer, F. Nagy. (2001) Constitutive photomorphogenesis 1 and multiple photoreceptors control degradation of phytochrome interacting factor 3, a transcription factor required for light signaling in Arabidopsis. Plant Cell 16, 1433-1445

265. X. Yu, J. Klejnot, X. Zhao, D. Shalitin, M. Maymon, H. Yang, J. Lee, X. Liu, J. Lopez, C. Lin. (2007) *Arabidopsis* Cryptochrome 2 Completes its Posttranslational Life Cycle in the Nucleus. Plant Cell 19, 3146-3156

266. J. A. Jarillo, J. Capel, R. H. Tang, H. Q. Yang, J. M. Alonso, J. R. Ecker, A. R. Cashmore. (2001) An Arabidopsis circadian clock component interacts with both CRY1 and phyB. Nature 410 487-490

267. E. Kevei, P. Gyula, A. Hall, L. Kozma-Bognar, W.-Y. Kim, M. E. Eriksson, R.Toth, S.Hanano, B. Feher, M.M. Southern, R. M. Bastow, A. Viczian, V. Hibberd, S. J. Davis, D. E. Somers, F. Nagy, A. J.Millar. (2006). Forward genetic analysis of the circadian clock separates the multiple functions of *ZEITLUPE*. Plant Physiology 140, 933-945

268. T. S. Tseng, P.A. Salome, C. R. McClung, N. E. Olszewski. (2004). SPINDLY and GIGANTEA interact and act in Arabidopsis thaliana pathways involved in light responses, flowering, and rhythms in cotelydon movement. Plant Cell 16, 1550-1563

269. J.-H. Lee, D. G. Skalnik. (2002). CpG-binding protein Is a Nuclear Matrix- and Euchromatin-associated Protein Localized to Nuclear Speckles Containing Human Trithorax. Journal of Biological Chemistry 277, 42259-42267

270. D. K. Welsh and S. A. Kay. Bioluminescence imaging in live organisms. (2005) Current Opinion in Biotechnology 16, 73-78

271. J. Lee, Y. Lee,M. J. Lee, E. Park, S. H. Kang, C. H. Chung, K. H. Lee, K. Kim. Dual modification of BMAL1 by SUMO2/3 and ubiquitin promotes circadian activation of the CLOCK/BMAL1 complex. (2008) Molecular Cell Biology 28, 6056-6065

272. B. Maier, S. Wendt, J. T. Vaneslow, T. Wallach, S. Reischl, S. Oehmke, A. Schlosser, A. Kramer. A large-scale functional RNAi screen reveals a role for CK2 in the mammalian circadian clock. (2009) Genes and Development 23, 708-718

273. C. Iitaka, K. Miyazaki, T. Akaike, N. Ishida. A role for glycogen synthase kinase-3 beta in the mammalian circadian clock. (2005) Journal of Biological Chemistry 280, 29397-29402

274. E. J.Eide, M. F. Woolf, H. Kang, P. Woolf, W. Hurst, F. Camacho, E. L. Vielhaber, A. Giovanni, D. M. Virshup. Control of mammalian circadian rhythms by CKIepsilon-regulated proteasome mediated PER2 degradation. (2005) Molecular Cell Biology 25, 2795-2807

275. M. Merrow, G. Mazzotta, Z. Chen, T. Roenneberg. The right place at the right time: regulation of daily timing by phosphorylation. (2006) Genes and Development 20, 2629-2623

276. T. Roenneberg and M. Mittag. The Circadian program of algae. (1996) Cell and Developmental Biology 7, 753-763

277. C. Lillo, C. Meyer, P. Ruoff. The Nitrate Reductase Circadian System. The Central Clock Dogma Contra Multiple Oscillatory Feedback Loops.(2001) Plant Physiology 125, 1554-1557

278. M. L. Pilgrim, T. Caspar, P. H. Quail, C. R. McClung. Circadian and light-regulated expression of nitrate reductase in Arabidopsis. (1993) Plant Molecular Biology 23, 349-364

279. R. T. Furbank. (2001). Molecular Engineering of C4 Photosynthesis. Annual Review Plant Biology 52, 297-314

280. M. Merrow and T. Roenneberg. Circadian Clocks: Running on Redox. (2001) Cell 106, 141-143

281. Y. Zhao, T. F. Chow, R. S. Puckrin, S. E. Alfred, A. K. Korir, C. K. Larive, S. R. Cutler. (2007). Chemical genetic interrogation of natural variation uncovers a molecule that is glycoactivated. Nature Chemical Biology 3, 716-721

282. K. Schreiber, W. Ckurshumova, J. Peek, D. Desveaux. (2008). A high-throughput chemical screen for resistance to *Pseudomonas syringae* in Arabidopsis. Plant Journal 54, 522-531

283. Y. Tsuchiya, D.Vidaurre, S. Toh, A. Hanada, E. Nambara, Y. Kamiya, S. Yamaguchi, P. McCourt. (2010). A small-molecule screen identifies new functions for the plant hormone strigolactone. Nature Chemical Biology 6, 741-749

284. G. R. Hicks and N. V. Raikhel. (2009). Opportunities and challenges in plant chemical biology. Nature Chemical Biology 5, 268-272

285. X. Xu, R. Graeff, Q. Xie, K. L. Gamble, T. Mori, C. H. Johnson. (2009). Comment on "The Arabidopsis circadian clock incorporates a cADPR-based feedback loop". Science 326, 230

286. J. Comolli, W. Taylor, J. Rehman, J. W. Hastings. (1996). Inhibitors of Serine/Threonine Phosphoprotein Phosphastases Alter Circadian Properties in *Gonyaulax polyedra*. Plant Physiology 111, 285-291

287. R. Marx and K. Brinkmann. (1978) Characteristics of Rotenone-Insensitive Oxidation of Matrix-NADH by Broad Bean Mitochondria. Planta 142, 83-90

288. T.Roenneberg and T.-S. Deng. (1997). Photobiology of the *Gonyaulax* circadian system. I. Different phase response curves for red and blue light. Planta 202, 494-501

289. T. Hirota, W. G. Lewis, A. C. Liu, J. W. Lee, P. G. Schultz, S. A. Kay (2008) A chemical biology approach reveals period shortening of the mammalian circadian clock by specific inhibition of GSK-3β. PNAS 105, 20746-20751

290. T. Hirota, J. W. Lee, W. G. Lewis, E. E. Zhang, G. Breton, X. Liu, M. Garcia, E. C. Peters, J.-P. Etchegaray, D. Traver, P. G. Schultz, S. A. Kay. (2010) High-Throughput Chemical Screen Identifies a Novel Potent Modulator of Cellular Circadian Rhythms and Reveals CKIα as a Clock Regulatory Kinase. PLoS Biol 8(12): e1000559

291. B. Shen, R. G. Jenson, H. J. Bohnert. (1997). Increased resistance to Oxidative Stress in Transgenic Plants by Targeting Mannitol Biosynthesis to Chloroplasts. Plant Physiology 113, 1177-1183

292. N. Smirnoff and Q. J. Cumbes. (1998). Hydroxyl radical scavenging activity of compatible solutes. Phytochemistry 28, 1057-1060

293. R. G. Alscher, N. Erturk, L. S. Heath. (2002). Role of superoxide dismutases (SODs) in controlling oxidative stress in plants. Journal of Experimental Botany 53, 1331-1341

294. K.Yoshida, P. Kaothien, T. Matsui, A. Kawaoka, A. Shinmyo. (2003). Molecular biology and application of plant peroxidase genes. Appl Microbiol Biotechnol 60, 665-670

295. S. G. Rhee. (1999). Redox signalling: hydrogen peroxide as intracellular messenger. Exp Mol Med 31, 53-59

296. Y. Naruse, K. Oh-hashi, N. Iijima, M. Naruse, H. Yoshioka, M. Tanaka. (2004). Circadian and Light-Induced Transcription of Clock Gene *Per1* Depends on Histone Acetylation and Deacetylation. Molecular Cell Biology 24, 6278-6287

297. J. G. Umen and U.W. Goodenough. (2001). Chloroplast DNA methylation and inheritance in *Chlamydomonas.* Genes and Development 15, 2585-2597

298. J. K. Christman. (2002). 5-Azacytidine and 5-aza-2'-deoxycytidine as inhibitors of DNA methylation: mechanistic studies and their implications for cancer therapy. Oncogene 21, 5483-5495

299. Y. Nakahata, S. Sahar, G. Astarita, M. Kaluzova, P. Sassone-Corsi. (2009). Circadian Control of the NAD^+ Salvage Pathway by CLOCK-SIRT1. Science 324, 654-657

300. S. Brody, K. Oelhafen, K. Schneider, S. Perrino, A. Goetz, C. Wang, C. English. (2010). Circadian rhythms in *Neurospora crassa:* Downstream effectors. Fungal Genetics and Biology 47, 159-168

301. S. Jung. (2004). Effect of chlorophyll reduction in Arabidopsis thaliana by methyl jasmonate nor norflurazon on antioxidant systems. Plant Physiology and Biochemistry 42, 225-231

302. J. G. Metz, H. B. Pakrasi, M. Seibert, C. J. Arntzer. (1986). Evidence for a dual function of the herbicide-binding D1 protein in photosystem II. FEBS Letters 205, 269-274

303. T. Roenneberg, H. Nakamura and J. W. Hastings. (1988). Creatine accelerates the circadian clock in a unicellular alga. Nature 334, 432-434

304. P. Prochasson, L. Florens, S. K. Swanson, M. P. Washburn, J. L. Workman. (2005). The HIR corepressor complex binds to nucleosomes generating a distinct protein/DNA complex resistant to remodelling by SWI/SNF. Genes and Development 19, 2534-2539

305. T. Hirota, S. A .Kay (2009) High-Throughput Screening and Chemical Biology: New Approaches for Understanding Circadian Clock Mechanisms. Cell Press Chemistry and Biology crosstalk 16 921- 927

306. L. Comai, L. C. Sen, D. M. Stalker. (1983). An Altered aroA Gene Product Confers Resistance to the Herbicide Glyphosate. Science 221, 370-371

307. C. H. Johnson, J. A. Elliott, R. Foster. (2003). Entrainment of Circadian Programs. Chronobiology International 20, 741-774

308. C. Troein, J. C. Locke, M. S. Turner, A. J. Millar. (2009). Weather and seasons together demand complex biological clocks. Current Biology 19, 1961-1964

309. O. E. Akman, D.A. Rand, P.E.Brown, A. J. Millar. (2010). Robustness from flexibility in the fungal circadian clock. BMC Systems Biology 4, 88

310. T. Roenneberg, Z. Dragovic, M. Merrow. (2005) Demasking biological oscillators: Properties and principles of entrainment exemplified by the *Neurospora* circadian clock. PNAS 102, 7742-7747

311. M. Kawato and R. Suzuki. (1981). Analysis of entrainment of circadian oscillators by skeleton photoperiods using phase transition curves. Bio Cybern. 40, 139-149

312. E. L. Petterson and D. S. Saunders. (1980). The circadian eclosion rhythm in *Sarcophaga argyrostoma*: A limit cycle representation of the pacemaker. Journal of Theoretical Biology 2, 265-277

313. A. Graf, A. Schlereth, M. Stitt, A. M. Smith. (2010). Circadian control of carbohydrate availability for growth in Arabidopsis in plants at night. PNAS 107, 9458-9463

314. D. K. Welsh, S.-H. Yoo, A. C. Liu, J. S. Takahashi, S. A. Kay. (2004). Bioluminescence Imaging of Individual Fibroblasts Reveals Persistent, Independently Phased Circadian Rhythms of Clock Gene Expression. Current Biology 14, 2289-2295

315. A. Monnier, S. Liverani, R. Bouvet, B. Jesson, J. Q. Smith. J. Mosser, F. Corellou, F. Y. Bouget. Orchestrated transcription of biological processes in the marine picoeukaryote *Ostreococcus* exposed to light/dark cycles. (2010) BMC Genetics 11, 192

316. O. Froy. (2011). The circadian clock and metabolism. Clin Sci 120, 65-72

317. M. Tigges, T. T. Marquez-Lago, J. Stelling, M. Fussenegger. (2009). A tuneable synthetic mammalian oscillator. Nature 457, 309-31

318. O. Purcell, N. J.Savery, C. S. Grierson, M. di Bernardo. (2010). A comparative analysis of synthetic genetic oscillators. Journal of the Royal Society, Interface DOI 10. 1098

319. M. B. Elowitz and S. Leibler. (2000). A synthetic oscillatory network of transcriptional regulators. Nature 403, 335-338

320. Z. Eelderink-Chen, G. Mazzotta, M. Sturre, J. Bosman, T. Roenneberg, M. Merrow. (2010). A circadian clock in *Saccharomyces cerevisiae.* PNAS 107, 2043-2047

321. J. Garcia-Ojalvo, M. B. Elowitz, S. H. Strogatz. (2004). Modeling a synthetic multicellular clock: repressilators coupled by quorum sensing. PNAS 101, 10955-10960

322. J. Hendriks, M. Avila Perez, F. Bruggeman, K. J. Hellingwerf. (2007). Photosensory Proteins as a Tool in Synthetic Biology: Bridging Computational Biophysics and Systems Biology. Computational Biophysics to Systems Biology, Proceedings of the NIC Workshop 2007 36, 149-153

323. X. Qin, M. Byrne, Y. Xu, T. Mori, C. H. Johnson. (2010). Coupling of a Core Post-Translational Pacemaker to a Slave Transcription/Translation Feedback Loop in a Circadian System. PLoS Biology 8:6 e1000394

324. A. L. Purcell, T. J. Carew. (2003). Tyrosine kinases, synaptic plasticity and memory: insights from vertebrates and invertebrates. Trends in Neuroscience 26, 625-630

325. S. E. Sanchez, E. Petrillo, E. J. Beckwith, X. Zhang, M. L. Rugnone, E. Hernando, J. C. Cuevas, M. A. G. Herz, A. Depetris-Chauvin, C. G. Simpson, J. W. S. Brown, P. D. Cerdan, J. O. Borevitz, P. Mas, M. F. Ceriani, A. R. Kornblihtt, M. J. Yanovsky. (2010). A methyl transferase links the circadian clock to the regulation of alternative splicing. Nature 468, 112-116

326. T. Mockler, H. Yang, X. H. Yu, D. Parikh, Y. C. Cheng, S. Dolan, C. Lin. (2003) Regulation of photoperiodic flowering by *Arabidopsis* photoreceptors. PNAS 100 2140-2145

Appendix A

“Circadian rhythms persist without transcription in a eukaryote”

Appendix B

“Temporal repression of Core Circadian Gens is Mediated through EARLY FLOWERING 3 in *Arabidopsis*”

Appendix C

“Multiple light inputs to a simple clock circuit allow complex biological rhythms”

Appendix D

“A switchable light-input, light-output system modelled and constructed in yeast”

Appendix E

Model Simulations

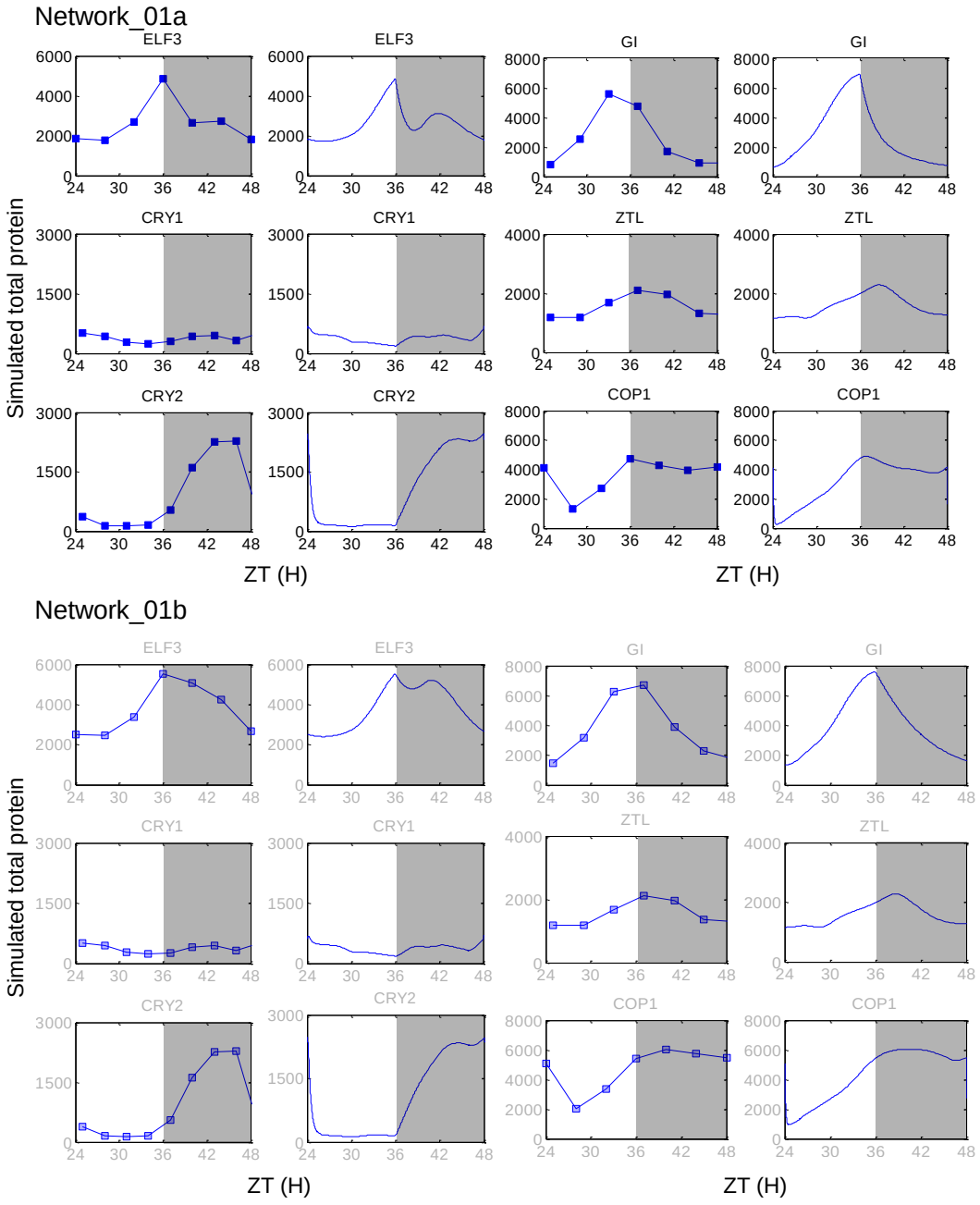

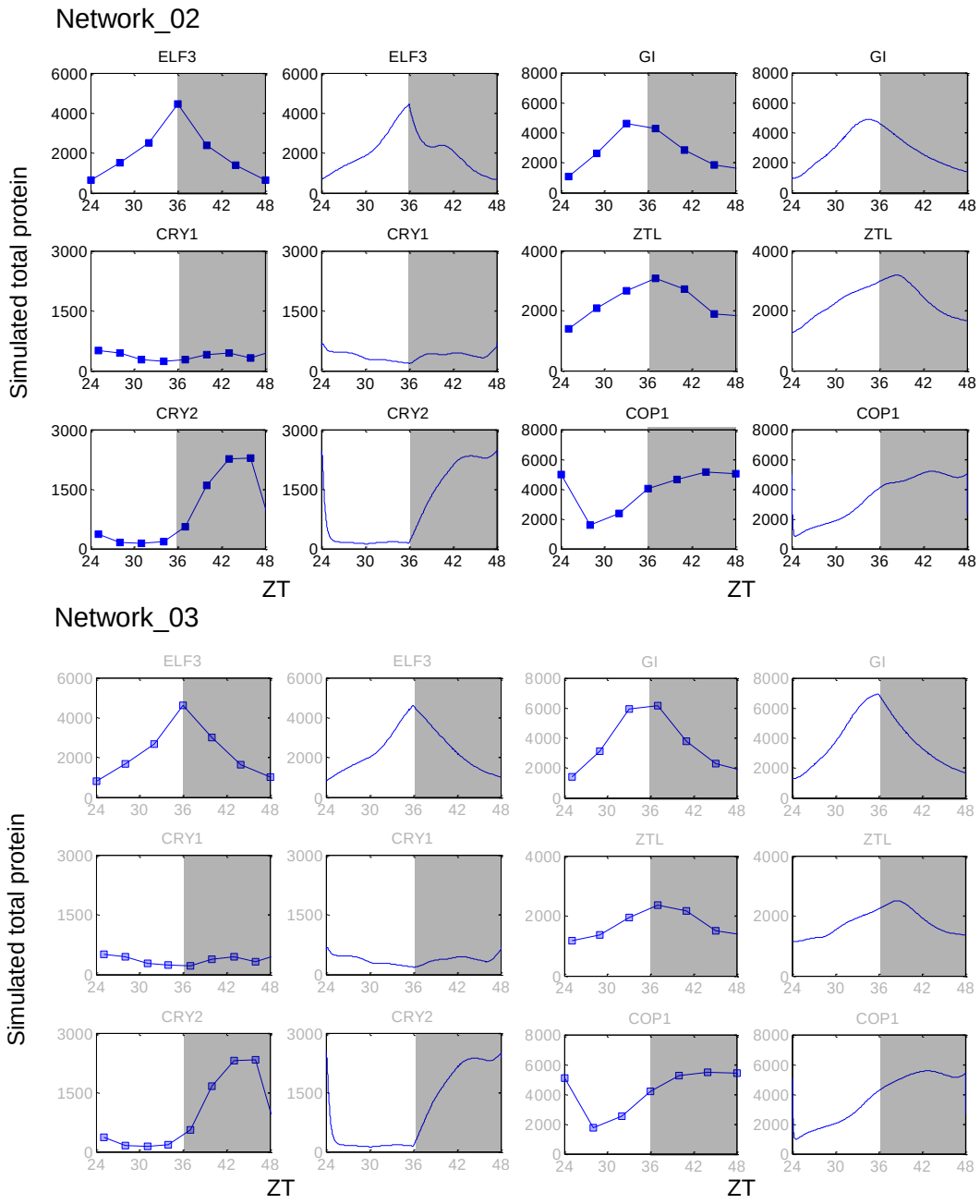

Figure E21: Simulations showing experimental sampling time points and continual sampling

Sampling with the same frequency as in experimental data (Chapter 5) is shown with the blue squares. Continual sampling is shown with a smooth blue line in adjacent panels.

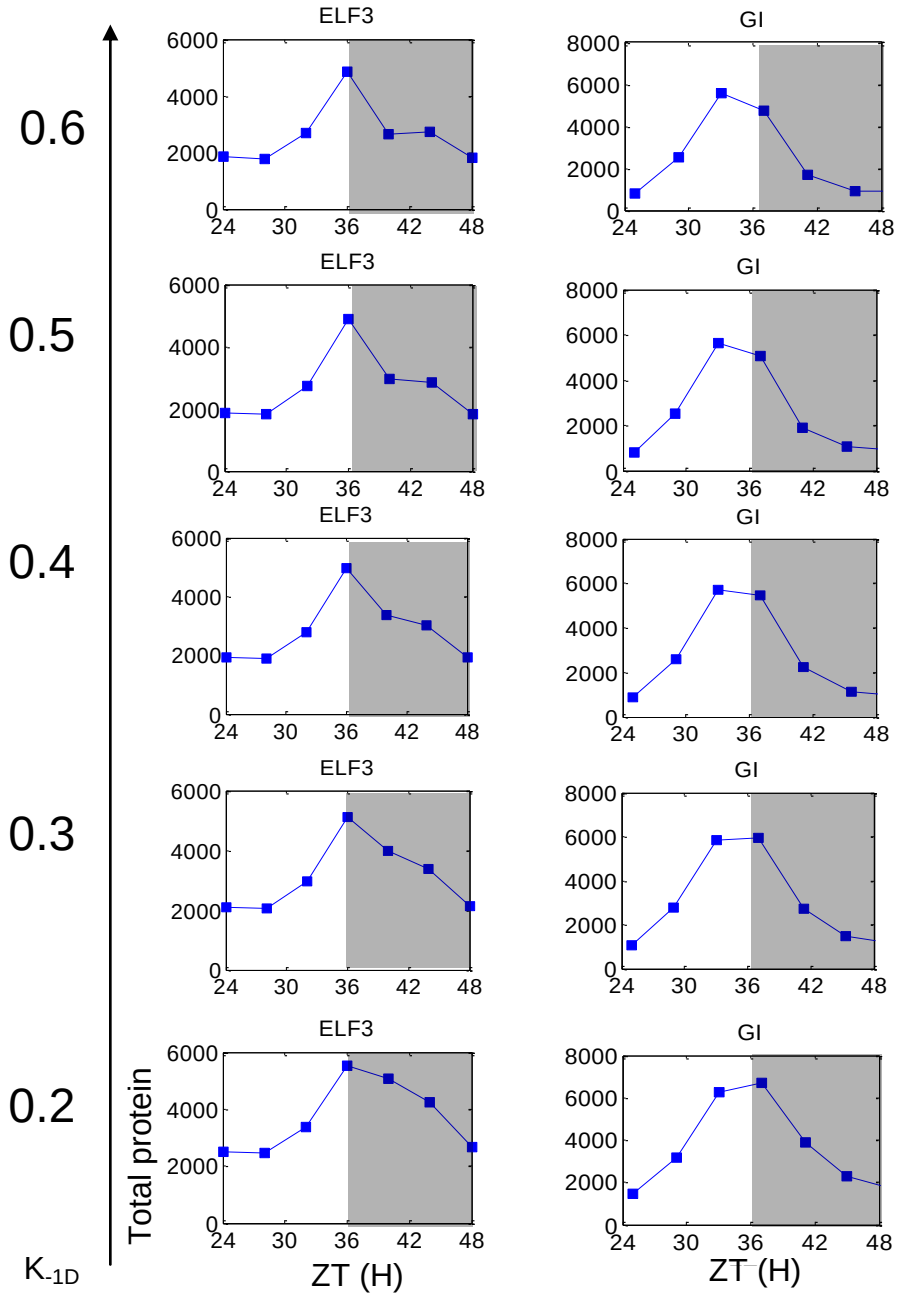

Figure E22: Simulation showing the effects of changing trimer degradation rates in Network_01

Appendix F

“Proteasome function is required to generate a post-translational circadian rhythm”

Appendix G

Chemical screen cluster analysis

	Brass ID	Period (H)	Period effects	Compound	Cluster	Average Period (H)	difference between average
						21.7	
BIO1	P_.001	26.6	L	AW00475	218		4.9
	P_.001	23.2	L				1.5
	Q_.001	26.72	L	AW00480	218		5.02
	Q_.001	23.9	L				2.2
	Y_.001	30	L	BTB 00693	197		8.3
	Y_.001	23.43	L				1.73
	AG_.001	22.83	L	BTB 01594	73		1.13
	AG_.001	24.51	L				2.81
	AV_.001	27.05	L	BTB 05066	183		5.35
	AV_.001	23.44	L				1.74
	BS_.001	19.18	S	BTB 08363	212		-2.52
	BS_.001	20.7	S				-1
	BU_.001	22.6	L	BTB 08512	199		0.9
	BU_.001	23.14	L				1.44
	CA_.001	29.22	L	BTB 10320	46		7.52
	CA_.001	24.21	L				2.51
	CE_.001	23.84	L	BTB 10705	26		2.14
	CE_.001	22.59	L				0.89
BIO2	M_.001	23.92	L	BTB 13588	243		2.22
	M_.001	25.35	L				3.65
	AR_.001	23.74	L	CD 02761	81		2.04
	AR_.001	32.49	L				10.79
	CF_.001	22.93	L	DP 00453	110		1.23
	CF_.001	24.99	L				3.29
	CH_.001	22.73	L	DP 00750	291		1.03
	CH_.001	29.47	L				7.77
	CM_.001	23.8	L	DP 01888	209		2.1
	CM_.001	23.7	L				2
BIO3	R_.001	23.37	L	FM 00281	87		1.67
	R_.001	27.6	L				5.9
	AI_.001	24.53	L	HAN 00332	71		2.83
	AI_.001	23.82	L				2.12
	AQ_.001	24.54	L	HTS 01021	172		2.84

	AQ_.001	25.69	L				3.99
	AS_.001	23.81	L	HTS 01365	146		2.11
	AS_.001	34.93	L				13.23
	AU_.001	23.01	L	HTS 01570	115		1.31
	AU_.001	27.9	L				6.2
	AZ_.001	24.44	L	HTS 01888	285		2.74
	AZ_.001	23.93	L				2.23
	BA_.001	23.95	L	HTS 02290	270		2.25
	BA_.001	27.77	L				6.07
	BG_.001	24.39	L	HTS 03642	261		2.69
	BG_.001	25.53	L				3.83
	BJ_.001	24.2	L	HTS 03658	261		2.5
	BJ_.001	28.51	L				6.81
	BY_.001	22.99	L	HTS 05534	235		1.29
	BY_.001	29.68	L				7.98
	CA_.001	22.23					0.53
	CA_.001	21.47					-0.23
	CG_.001	22.59	L	HTS 06168	152		0.89
	CG_.001	29.21	L				7.51
BIO4	M_.001	23.51	L	HTS 07401	300		1.81
	M_.001	25.13	L				3.43
	P_.001	23.2	L	HTS 07816	217		1.5
	P_.001	27.61	L				5.91
	AA_.001	23.59	L	JFD 00972	214		1.89
	AA_.001	25.27	L				3.57
	AC_.001	22.37	L	JFD 01208	73		0.67
	AC_.001	23.92	L				2.22
	AS_.001	22.97	L	JFD 03196	125		1.27
	AS_.001	25.55	L				3.85
	AU_.001	23.24	L	JFD 03446	236		1.54
	AU_.001	25.36	L				3.66
	BW_.001	23.86	L	KM 04031	291		2.16
	BW_.001	25.02	L				3.32
	BY_.001	23.97	L	KM 04177	261		2.27
	BY_.001	29.35	L				7.65
	CG_.001	23.42	L	KM 05872	29		1.72
	CG_.001	28.65	L				6.95
BIO6	R_.001	20.95	S	RDR 03443	212		-0.75
	R_.001	20.39	S				-1.31
	U_.001	26.42	L	RDR 03804	280		4.72
	U_.001	23.62	L				1.92
	AC_.001	26.75	L	RF 02465	299		5.05
	AC_.001	22.81	L				1.11
	AF_.001	26.83	L	RF 03487	300		5.13

	AF_.001	24.19	L				2.49
	AN_.001	24.57	L	RF 05472	104		2.87
	AN_.001	24.06	L				2.36
	AT_.001	26.97	L	RH 00590	178		5.27
	AT_.001	22.57	L				0.87
	BD_.001	22.58	L	RH 01646	311		0.88
	BD_.001	24.12	L				2.42
	BE_.001	22.63	L	RH 01669	201		0.93
	BE_.001	22.53	L				0.83
	BF_.001	26.74	L	RH 01676	173		5.04
	BF_.001	24.41	L				2.71
	BL_.001	26.56	L	RH02128	45		4.86
	BL_.001	23.07	L				1.37
	BN_.001	18.85	S	RJC 00155	221		-2.85
	BN_.001	20.54	S				-1.16
	BS_.001	28.86	L	RJC 00588	8		7.16
	BS_.001	22.8	L				1.1
	BT_.001	26.83	L	RJC 00807	130		5.13
	BT_.001	23.86	L				2.16
	BV_.001	20.78					-0.92
	BV_.001	21.06					-0.64
	BW_.001	23.63	L	RJC 01539	157		1.93
	BW_.001	22.04	L				0.34
	BX_.001	22.91	L	RJC 01734	54		1.21
	BX_.001	22.51	L				0.81
	CD_.001	26	L	RJC 03423	191		4.3
	CD_.001	23.87	L				2.17
	CF_.001	22.7	L	RJC 03734	221		1
	CF_.001	22.24	L				0.54
	CG_.001	22.56	L	RJC 04020	202		0.86
	CG_.001	24.03	L				2.33
	CI_.001	23.08	L	RJC 04107	55		1.38
	CI_.001	24.28	L				2.58
	CK_.001	23.07	L	RJF 00101	31		1.37
	CK_.001	22.06	L				0.36
	CL_.001	23.21	L	RJF 00177	300		1.51
	CL_.001	23.34	L				1.64
	CN_.001	22.21	L	RFJ 00692	212		0.51
	CN_.001	22.33	L				0.63
BIO7	AD_.001	25.75	L	S 03463	288		4.05
	AD_.001	28.51	L				6.81
	AM_.001	24.77	L	S 04777	73		3.07
	AM_.001	22.56	L				0.86
	AO_.001	24.79	L	S 07044	300		3.09
	AO_.001	23.46	L				1.76

	AY_.001	27.08	L	S11644	300		5.38
	AY_.001	23.84	L				2.14
	BA_.001	24.43	L	S11729	282		2.73
	BA_.001	23.51	L				1.81
	BF_.001	26.49	L	S13644	243		4.79
	BF_.001	23.6	L				1.9
	BN_.001	23.01	L	S15517	143		1.31
	BN_.001	23.28	L				1.58
	BV_.001	24.13	L	SEW 01297	252		2.43
	BV_.001	24.51	L				2.81
	BW_.001	26.53	L	SEW 01395	128		4.83
	BW_.001	23.23	L				1.53
	BX_.001	26.06	L	SEW 01771	212		4.36
	BX_.001	22.8	L				1.1
	CA_.001	27.14	L	SEW02447	82		5.44
	CA_.001	23.3	L				1.6
	CC_.001	25.09	L	SEW 02609	138		3.39
	CC_.001	23.59	L				1.89
	CE_.001	24.92	L	SEW 02680	279		3.22
	CE_.001	22.7	L				1
	CF_.001	24.22					2.52
	CF_.001	21.86					0.16
	CM_.001	27.47	L	SEW 03247	186		5.77
	CM_.001	23.63	L				1.93
BIO8	Q_.001	19.99	S	SEW 04443	205		-1.71
	Q_.001	19.2	S				-2.5
	V_.001	19.86	S	SEW 05288	138		-1.84
	V_.001	17.04	S				-4.66
	AU_.001	26.96	L	SJC 00146	73		5.26
	AU_.001	23.5	L				1.8
	AX_.001	23.82	L	SJC 00209	154		2.12
	AX_.001	24.09	L				2.39
	AY_.001	24.57	L	SJC 00210	154		2.87
	AY_.001	23.67	L				1.97
	BJ_.001	26.88	L	SP 01325	270		5.18
	BJ_.001	22.34	L				0.64
	BP_.001	19.86	S	SPB 00414	230		-1.84
	BP_.001	19.83	S				-1.87
	BQ_.001	22.44	L	SPB 00429	230		0.74

	BQ_.001	23.03	L				1.33
	BS_.001	18.47	S	SPB 00506	182		-3.23
	BS_.001	20.91	S				-0.79
	BW_.001	26.37					4.67
	BW_.001	21.98					0.28
	BZ_.001	26.5	L	SPB 01018	172		4.8
	BZ_.001	23.22	L				1.52
	CA_.001	26.9					5.2
	CA_.001	22.16					0.46
	CD_.001	23.26	L	SPB 02109	213		1.56
	CD_.001	22.74	L				1.04
	CE_.001	26.95	L	SPB 02129	185		5.25
	CE_.001	23.07	L				1.37
	CI_.001	28.44	L	SPB 02722	276		6.74
	CI_.001	22.21	L				0.51
BIO9	R_.001	26.64	L	SPB03924	304		4.94
	R_.001	23.06	L				1.36
	S_.001	23.87	L	SPB 04439	163		2.17
	S_.001	23.14	L				1.44
	U_.001	26.83	L	SPB 05487	210		5.13
	U_.001	22.95	L				1.25
	AX_.001	27.23	L	XAX 00043	261		5.53
	AX_.001	23.13	L				1.43
	BA_.001	26.67	L	NF			4.97
	BA_.001	23.27	L				1.57
	BC_.001	22.85	L	NF			1.15
	BC_.001	22.97	L				1.27
	BD_.001	27.22	L	NF			5.52
	BD_.001	23	L				1.3
	BF_.001	24.42	L	NF			2.72
	BF_.001	23.64	L				1.94
	BG_.001	26.73	L	NF			5.03
	BG_.001	23.26	L				1.56
	BI_.001	22.43	L	NF			0.73
	BI_.001	23.13	L				1.43
	BM_.001	27.03	L	NF			5.33
	BM_.001	23.55	L				1.85
	BN_.001	26.8	L	NF			5.1
	BN_.001	23.12	L				1.42
	BO_.001	25.23	L	NF			3.53
	BO_.001	23.82	L				2.12
	BP_.001	22.86	L	NF			1.16
	BP_.001	23.46	L				1.76
	BQ_.001	22.19	L	NF			0.49
	BQ_.001	23.08	L				1.38

	BR_.001	28.71	L	NF			7.01
	BR_.001	22.8	L				1.1
	BV_.001	27.35	L	NF			5.65
	BV_.001	22.92	L				1.22
	BX_.001	24.3	L	NF			2.6
	BX_.001	22.21	L				0.51
	CE_.001	33.65	L	NF			11.95
	CE_.001	22.26	L				0.56
	CF_.001	24.42					2.72
	CF_.001	21.68					-0.02
	CG_.001	28.44	L	NF			6.74
	CG_.001	24.01	L				2.31
	CI_.001	26.61					4.91
	CI_.001	21.93					0.23
	CJ_.001	26.65	L	NF			4.95
	CJ_.001	22.67	L				0.97
	CL_.001	26.77	L	NF			5.07
	CL_.001	22.64	L				0.94
	CM_.001	24.6	L	NF			2.9
	CM_.001	22.38	L				0.68
CYTO1	S_.001	27.11	L	AW 00837	135		5.41
	S_.001	25.06	L				3.36
	AL_.001	27.16	L	BTB 02164	301		5.46
	AL_.001	22.86	L				1.16
	BO_.001	26.78	L	BTB 05131	271		5.08
	BO_.001	23.24	L				1.54
	BW_.001	27.11	L	BTB 05417	182		5.41
	BW_.001	23.81	L				2.11
	BX_.001	26.89	L	BTB 05434	182		5.19
	BX_.001	23.03	L				1.33
	CI_.001	24.3	L	BTB 06671	7		2.6
	CI_.001	23.75	L				2.05
	CK_.001	22.89	L	BTB 06877	299		1.19
	CK_.001	25.14	L				3.44
	CL_.001	26.52	L	BTB 06908	237		4.82
	CL_.001	24.23	L				2.53
CYTO2	N_.001	26.55	L	BTB 07256	304		4.85
	N_.001	22.29	L				0.59
	R_.001	26.98	L	BTB 08347	33		5.28
	R_.001	22.86	L				1.16
	S_.001	27.11	L	BTB 08378	157		5.41
	S_.001	22.83	L				1.13
	Y_.001	27.32	L	BTB 10696	238		5.62
	Y_.001	23.79	L				2.09

	AC_.001	22.91	L	BTB 11110	85		1.21
	AC_.001	22.86	L				1.16
	AL_.001	27.16	L	BTB 12669	212		5.46
	AL_.001	22.94	L				1.24
	BC_.001	26.87	L	BTBG 00139	184		5.17
	BC_.001	24.75	L				3.05
	BF_.001	26.56	L	CD 00352	227		4.86
	BF_.001	23.26	L				1.56
	BO_.001	26.78	L	CD 02154	272		5.08
	BO_.001	23.78	L				2.08
	BW_.001	27.11	L	CD 03380	191		5.41
	BW_.001	24.36	L				2.66
	BX_.001	26.89	L	CD 03470	204		5.19
	BX_.001	23.02	L				1.32
	CF_.001	27.19	L	CD 04220	87		5.49
	CF_.001	23.46	L				1.76
	CL_.001	26.52	L	CD 05196	301		4.82
	CL_.001	23.87	L				2.17
	CN_.001	22.91	L	CD 06603	299		1.21
	CN_.001	23.54	L				1.84

Table G3: Compound identities which showed period effects Bio1- Cyto2
Compound identities from Chemical database (M. Tyers group) where NF indicates not found. L=long period and S=short period

Plate	Well	Average period (Hrs)	Compound	Cluster
Bio1	P	24.95	AW00475	218
Bio1	Q	25.31	AW00480	218

Plate	Well	Average period (Hrs)	Compound	Cluster
Bio1	AG	23.67	BTB 01594	73
Bio7	AM	23.67	S 04777	73
Bio8	AU	25.23	SJC 00146	73
Bio4	AC	23.15	JFD 01208	73

Plate	Well	Average period (Hrs)	Compound	Cluster
Cyto1	CK	24	BTB 06877	299
Cyto2	CN	23.23	CD 06603	299
Bio6	AC	24.78	RF 02465	299

Plate	Well	Average period (Hrs)	Compound	Cluster
Bio4	M	24.32	HTH 07401	300
Bio6	AF	25.51	RF 03487	300
Bio6	CL	23.3	RJF 00177	300
Bio7	AO	24.11	S07044	300
Bio7	AY	25.46	S11644	300

Plate	Well	Average period (Hrs)	Compound	Cluster
Bio6	L	25	RJC 03423	191
Cyto2	BW	25.7	CD 03380	191

Plate	Well	Average period (Hrs)	Compound	Cluster
Bio7	BF	25	S 13644	243
Bio2	M	24.6	BTB 13588	243

Plate	Well	Average period (Hrs)	Compound	Cluster
Bio8	AX	24	SJC 00209	154
Bio8	AY	24.12	SJC 00210	154

Plate	Well	Average period (Hrs)	Compound	Cluster
Bio8	BJ	24.61	SP 01325	270
Bio3	BA	25.86	HTS 02290	270

Plate	Well	Average period (Hrs)	Compound	Cluster
Bio9	AX	25.18	XAX 00043	261
Bio3	BG	25	HTS 03642	261
Bio3	BY	26.4	HTS 03658	261
Bio4	BY	26.6	KM 04177	261

Plate	Well	Average period (Hrs)	Compound	Cluster
Cyto1	AL	25.01	BTB 02164	301
Cyto2	CL	25.2	CD 05196	301

Plate	Well	Average period (Hrs)	Compound	Cluster
Bio2	CH	26.1	DP 00750	291
Bio4	BW	24.4	KM 04031	291

Plate	Well	Average period (Hrs)	Compound	Cluster
Bio8	BZ	24.9	SPB 01018	172
Bio3	AQ	25	HTS01021	172

Table G4: Selected clusters from Bio1-Cyto 2 analysis